

**GENCORP**  
**AEROJET**

**AD-A253 786**



1

---

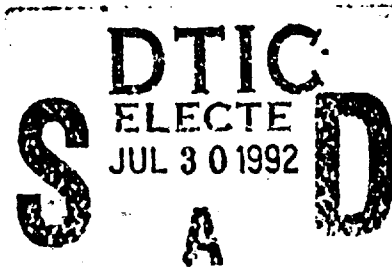
## **Orbital Transfer Rocket Engine Technology**

---

Contract NAS 3-23772  
Advanced Engine Study  
Task D.6 Final Report

NASA CR-187216

June 1992



Prepared For:  
National Aeronautics and Space Administration  
Lewis Research Center  
21000 Brookpark Road  
Cleveland, Ohio 44135

This document has been approved  
for public release and sale; its  
distribution is unlimited.

**92 7 19 005**

**Propulsion Division**

**92-20651**



NASA CR 187216  
Aerojet 2459-31-1

NASA

ORBITAL TRANSFER ROCKET ENGINE TECHNOLOGY

ADVANCED ENGINE STUDY  
TASK D.6 FINAL REPORT

Prepared By:

Warren R. Hayden

Prepared For:

National Aeronautics and Space Administration  
NASA Lewis Research Center

Contract No. NAS 3-23772

June 1992

Accession For	
NTIS CRA&I	<input checked="checked" type="checkbox"/>
DTIC TAB	<input type="checkbox"/>
Unannounced	<input type="checkbox"/>
Justification	
By	
Distribution /	
Availability Codes	
Dist	Avail and / or Special
A-1	

DTIC QUALITY INSPECTED 2



National Aeronautics and  
Space Administration

## REPORT DOCUMENTATION PAGE

1. Report No. NASA CR 187216		2. Government Accession No.		3. Recipient's Catalog No.	
4. Title And Subtitle Orbital Transfer Rocket Engine Technology Advanced Engine Study Final Report Task D.6				5. Report Date June 1992	
				6. Performing Organization Code	
7. Author(s) Warren R. Hayden				8. Performing Organization Report No.	
				10. Work Unit No.	
9. Performing Organization Name and Address  Org. 9962, Bldg. 2019 Aerojet TechSystems Sacramento, CA 95813				11. Contract or Grant No. NAS 3-23772	
				13. Type of Report and Period Covered Final Oct 1988 to Mar 1990	
12. Sponsoring Agency Name and Address  NASA Lewis Research Center Cleveland, Ohio 44135				14. Sponsoring Agency Code	
15. Supplementary Notes					
16. Abstract <p>This report documents an advanced LOX/LH2 engine study for the use of NASA and vehicle prime contractors in developing concepts for manned missions to the Moon, Mars, and Phobos. Parametric design data was obtained at five engine thrusts from 7.5K lbf to 50K lbf. Also, a separate task evaluated engine throttling over a 20:1 range and operation at a mixture ratio of <math>12 \pm 1</math> versus the <math>6 \pm 1</math> nominal. Cost data was also generated for DDT&amp;E, first unit production, and factors in other life cycle costs. The major limitation of the study was lack of contact with vehicle prime contractors to resolve the issues in vehicle/engine interfaces. The baseline Aerojet dual propellant expander cycle was shown capable of meeting all performance requirements with an expected long operational life due to the high thermal margins. The basic engine design readily accommodated the 20:1 throttling requirement and operation up to a mixture ratio of 10 without change. By using platinum for baffled injector construction the increased thermal margin allowed operation up to mixture ratio 13. An initial engine modeling with an Aerojet transient simulation code (named MLETS) indicates stable engine operation with the baseline control system. A throttle rate of 4 to 5 seconds from 10% to 100% thrust is also predicted. Performance predictions are 483.1 sec at 7.5K lbf, 487.3 sec at 20K lbf, and 485.2 sec at 50K lbf with a mixture ratio of 6 and an area ratio of 1200. Engine envelopes varied from 120 in. length/53 in. exit diameter at 7.5K lbf to 305 in. length/136 in. exit diameter at 50K lbf. Packaging will be an important consideration. Continued work is recommended to include more vehicle prime contractor/engine contractor joint assessment of the interface issues.</p>					
17. Key Words (Suggested by Author(s))  Rocket Engine, Lunar Mission, Cryogenic Propellants, Throttling Engine, Moon Mining, Space Transfer Vehicles			18. Distribution Statement  Unclassified - Unlimited		
19. Security Classif. (of this report) Unclassified		20. Security Classif. (of this page) Unclassified		21. No. of pages 277	
				22. Price	

## FOREWORD

This report documents an engine parametric study expected to generate useful planning and design information for the vehicle prime contractors developing concepts for manned missions to the moon, Phobos, and Mars. The baseline engine uses some form of a hydrogen expander cycle within the thrust range of 7.5K lbf to 50K lbf. The data base for starting the study was the 7.5K lbf OTV engine preliminary design. an expander cycle engine was mandated. There was no comparison or tradeoffs with other engine cycles. These constraints on the study served to focus it within a limited design range highly dependent on the technology developed over the past decade by the Orbital Transfer Vehicle (OTV) engine technology program sponsored by NASA Lewis Research Center.

The terms Chemical Transfer Propulsion (CTP) engine and OTV engine are used interchangeably in this report although the OTV engine may be just one of several engines developed under the CTP program. The specific application of a CTP engine for the Lunar return mission is designated as a LTV/LEV engine. The Lunar Transfer Vehicle (LTV) and Lunar Excursion Vehicles (LEV) are expected to use the same basic engine.

Interaction with and feedback from the vehicle prime contractors was very limited. Interface requirements were gleaned primarily from the NASA-MSFC sponsored Phase A Vehicle Studies plus direction from NASA-LeRC.

This study was initially directed by Jerry Pieper. The work was continued through the Design and Parametric Subtask under the direction of Judy Schneider. Completion of the study and preparation of the final report was done by Warren Hayden who served as senior Project Engineer throughout the period of performance.

The period of performance for this study was October 1988 to May 1990.

## TABLE OF CONTENTS

<u>Section</u>	<u>Title</u>	<u>Page</u>
1.0	Summary	1
2.0	Introduction and Background	3
2.1	Background	3
2.2	Scope	9
2.3	Relevance to Current Rocket Engine Technology	14
2.4	Significance of the Program	16
3.0	Discussion	18
3.1	Design and Parametric Analysis	18
3.1.1	Engine and Cycle Definition	20
3.1.2	Power Balance	42
3.1.3	Performance, Mass and Envelope Parameters	71
3.2	Engine Requirement Variation Studies	92
3.2.1	Design for 20:1 Throttling	92
3.2.2	High Mixture Ratio Operation	108
3.3	Vehicle/Engine Study Coordination	135
3.3.1	Engine Design, Development, Test and Engineering (DDT&E) Cost Estimates	135
3.3.2	Engine Production Cost	145
3.3.3	Mission Related Costs	145
3.3.4	In-Space Maintenance and Servicing	155
3.3.5	Engine Requirements for the Lunar Mission	159
3.3.6	Issues in Engine Throttling	160
3.3.7	Weight Penalties for Space Basing	166
3.3.8	Parametric Data Requests	166
3.4	Engine Baseline Design Update	171
3.4.1	Dual Propellant Expander Cycle	171
3.4.2	Engine Control Baseline	171
3.4.3	Engine Components	176
3.5	Identification of Critical Technologies	179
3.5.1	Thrust Chamber Technology	179
3.5.2	Turbopump Technology	186

## TABLE OF CONTENTS (cont.)

<u>Section</u>	<u>Title</u>	<u>Page</u>
3.5.3	Heat Exchanger Technology	188
3.5.4	Proportioner Valve Technology	190
3.5.5	Oxygen Cooled Nozzle	190
3.5.6	Extendible/Retractable Nozzle	191
3.5.7	Integrated Control and Health Monitoring System	191
3.5.8	Engine/Vehicle Synergisms	191
4.0	Conclusions and Recommendations	192
4.1	Conclusions	192
4.2	Recommendations	193
5.0	References	195
Appendices		
A.	Detailed Engine Thermal Analysis	A-1
B.	Power Balance at High Mixture Ratio	B-1
C.	Chug Stability of OTV 20K lbf Advanced Engine	C-1

## LIST OF TABLES

<u>Table No.</u>		<u>Page</u>
2.1-1	Technology Goals for the New OTV Engine	5
2.2-1	Engine System Requirements and Goals	10
3.1-1	Advanced Engine Study Thrust Selection Rationale	20
3.1-2	Expected Results of the Parametric Study	21
3.1-3&4	CTP Engine Materials Selection, Thrust Chamber Assembly in a High Radiation Environment	23 & 24
3.1-5	Advanced Engine Study Turbopump Design Point - Pump Section	46
3.1-6	Advanced Engine Study Turbopump Design Point - Turbine Section	47
3.1-7	CTP Engine Power Balance, Thrust = 20K lbf, MR = 5	56
3.1-8	CTP Engine Power Balance, Thrust = 20K lbf, MR = 6	57
3.1-9	CTP Engine Power Balance, Thrust = 20K lbf, MR = 7	58
3.1-10	CTP Engine Power Balance, Thrust = 50K lbf, MR = 5	59
3.1-11	CTP Engine Power Balance, Thrust = 50K lbf, MR = 6	60
3.1-12	CTP Engine Power Balance, Thrust = 50K lbf, MR = 7	61
3.1-13	Performance Loss Accounting for Various Thrust Levels (7.5K lbf, 20K lbf, and 50K lbf)	74
3.1-14	LTV/LEV Engine Propellant Flowrates	77
3.1-15	7.5K lbf Preliminary Engine Weight Estimate	78
3.1-16	7.5Klbf Thrust Preliminary Engine Weight Estimate Complete Engine	80
3.1-17	Preliminary Nozzle System Weight Estimates, 7.5K lbf Engine	80
3.1-18	Advanced Flight Engine Weight Estimates	82
3.1-19	Advanced Engine Design Study Engine Contour Normalized by the Throat Radius	88
3.1-20	Advanced Engine Design Study Normalized Nozzle Contour	89
3.1-21	Advanced Engine Design Study Basic Engine Dimensions	91
3.2-1	Study Baseline - Engine Requirements Variation	93
3.2.1-1	Advanced Expander Engine Turbopump Design Specification	98
3.2.2-1	Engine Power Balance at 20:1 Throttle Down Condition	105
3.3.1-1	LTV/LEV Engine DDT&E Cost	137
3.3.3-1	CTP Engine Removal Operations	153

## LIST OF TABLES (Cont)

<u>Table No.</u>		<u>Page</u>
3.3.4-1	CTP Engine Space Maintainable Components 7.5K lbf Thrust Engine	156
3.3.4-2	Space-Based CTP Engine Maintenance Functions	157
3.3.4-3	CTP Servicing Operational Functions	158
3.3.8-1	Representative Engine Electrical Power Requirements, Watts	167
3.4-1	CTP Engine Valves and Sensors for Engine Control	172
3.4-2	Engine Operation Sequence	173
3.4-3	Component State During Engine Operation	175

## LIST OF FIGURES

<u>Figure No.</u>		<u>Page</u>
2.1-1	Dual Expander Cycle Schematic (Parallel Flow Version)	7
2.2-1	Start Cycle-Space Transfer Vehicle Engine	11
2.2-2	Task Order D.6 - Advanced Engine Study Activities	12
3.1-1	OTV Engine Dual Expander Cycle, Series Flow Schematic, 7.5K lbf Thrust Engine	19
3.1-1A	Our Regeneratively Cooled Baffles Provide a Dual Function As An Added Heat Transfer Surface as Well as a Combustion Stability Damping Device	25A
3.1-2	7.5K lbf OTV Injector/Baffle Flow Circuit	28
3.1-3	OTV Engine TCA Sketch Showing Can and Gimbal Attachments	29
3.1-4	3.0K lbf Design: Fuel Cooled Nozzle Extension Concept	31
3.1-5	7.5K lbf Thrust OTV Engine (Top View)	33
3.1-6	OTV Engine Preliminary Design Layout Drawing - Turbopump Side	35
3.1-7	Advanced Engine Study - Regenerator Channel Details	37
3.1-10	7.5K lbf Thrust Preliminary Design Engine Operating Envelope	44
3.1-11	Component Modeling	45
3.1-12	Oxygen Power Balance - Combined TPA Efficiency	48
3.1-13	Hydrogen Power Balance - Combined TPA Efficiency	49
3.1-14	Logic Path in Computerizing a Power Balance	51
3.1-15	The Oxidizer Side is Balanced First	52
3.1-16	The Fuel Side Uses Results from OX Side Balance	53
3.1-17	7.5K lbf Thrust OTV Engine Preliminary Design Power Balance	54
3.1-18	Power Balance Results for 20K lbf Engine at MR = 6	55
3.1-19	CTP Engine Model for MLETS Analysis	64
3.1-20	Dual Expander Cycle Advanced Engine Study Alternate Schematic	66
3.1-21	Advanced Engine Study Stability at Rated Thrust	68
3.1-22	Predicted Response to 10% Throttle Up Command	69
3.1-23	Predicted Response to 10% Throttle Down Command	70
3.1-24	Advanced Engine Performance	72
3.1-25	Performance Loss Accounting	73
3.1-26	Space Transfer Vehicle Propellant Flowrate vs Engine Thrust	76

## LIST OF FIGURES (Cont)

<u>Figure No.</u>		<u>Page</u>
3.1-27	Delta Payload vs Nozzle Percent Bell	81
3.1-28	Advanced Engine Study Parametric Weight Summary	84
3.1-29	Engine Thrust/Weight Ratio vs Thrust	85
3.1-30	Advanced Engine Study Thrust Versus Weight	86
3.1-31	Change in Engine Length with Thrust	87
3.1-32	Engine Half Section	90
3.2.1-1	Predicted OTV Off-Design Performance Meets 10:1 Throttling Operating Requirements	95
3.2.1-2	Estimated Head Loss Due to Cavitation	97
3.2.1-3	Advanced Engine Study - Engine Operating Range	100
3.2.1-4	NARloy-Z, Wrought, Properties	101
3.2.1-5	Hydrogen Circuit Enthalpy Pickup	102
3.2.1-6	Enthalpy Pickup - Oxygen Circuit	104
3.2.2-1	NARloy-Z Exposed to Oxidizing/Reducing Environments	110
3.2.2-2	Blanching and Cracking	111
3.2.2-3	Uncoated NASA-Z Cylinder After Oxidation and Reduction Test Cycle - 26 Slot Area (1.8% Strain)	113
3.2.2-4	Uncoated NASA-Z Cylinder After Oxidation and Test - Center Area (>2.7% Strain)	114
3.2.2-5	Variation of Combustion Gas Species with MR and Temperature	116
3.2.2-6	Variation in Specific Impulse with Mixture Ratio for Oxygen/Hydrogen Propellants - 7.5K lbf Thrust Engine	118
3.2.2-7	Variation in Specific Impulse with Mixture Ratio for Oxygen/Hydrogen Propellants - 20,000 lbf Thrust Engine	119
3.2.2-8	Variation in Specific Impulse with Mixture Ratio for Oxygen/Hydrogen Propellants - 50,000 lbf Thrust Engine	120
3.2.2-9	Advanced Engine Study - Mixture Ratio Versus LOX Flowrate and Thrust	122
3.2.2-10	Engine Maximum Wall Temperature for $P_c = 2000$ psia, $MR = 12$	123
3.2.2-11	Engine $H_2$ Bulk Temperature Rise for $P_c = 2000$ psia, $MR = 12$	124
3.2.2-12	Engine Maximum Wall Temperature for $P_c = 2000$ psia, $MR = 12$	126
3.2.2-13	Advanced Engine Study - Mixture Ratio Versus Hydrogen Flowrate and Hydrogen Temperature at Maximum Thrust	127

## LIST OF FIGURES (Cont)

<u>Figure No.</u>		<u>Page</u>
3.2.2-14	Engine Hydrogen Bulk Temperature Rise - $P_c = 1917$ psia, MR = 10	128
3.2.2-15	Engine Maximum Wall Temperature - $P_c = 1917$ psia, MR = 10	129
3.2.2-16	Engine Pressure Drops - $P_c = 1917$ psia, MR = 10	130
3.2.2-17	Engine Maximum Wall Temperature for $P_c = 1500$ psia, MR = 12	132
3.2.2-18	Engine Maximum Hydrogen Temperature for $P_c = 1500$ psia, MR = 12	133
3.2.2-19	Engine Pressure Drop for $P_c = 1500$ psia, MR = 12	134
3.3.1-1	LTV/LEV Engine Development - Design	138
3.3.1-2	LTV/LEV Engine Development - Fab	139
3.3.1-3	LTV/LEV Engine Development - Test	140
3.3.1-4	LTV/LEV Engine Development - Total Program Cum Costs	141
3.3.1-5	LTV/LEV Propulsion System Program Schedule	142
3.3.2-1	LTV/LEV Engine at Complexity = $1.1 \times RL$ -10 Engine Nth Unit Production Cost	146
3.3.2-2	LTV/LEV Engine at Complexity = $1.2 \times RL$ -10 Engine Nth Unit Production Cost	147
3.3.2-3	LTV/LEV Engine at Complexity = $1.3 \times RL$ -10 Engine Nth Unit Production Cost	148
3.3.2-4	LTV/LEV Engine at Complexity = $1.4 \times RL$ -10 Engine Nth Unit Production Cost	149
3.3.2-5	LTV/LEV Engine at Complexity = $1.5 \times RL$ -10 Engine Nth Unit Production Cost	150
3.3.5-1	LTV/LEV Reference Concepts	161
3.3.5-2	LTV Initial Weight in LEO (1 Burn) Versus Isp at Fixed P/L (26.2 MT)	162
3.3.5-3	Lunar Mission Profile	163
3.3.6-1	CTP Engine Dual Propellant Expander Cycle	165
3.3.8-1	0.030-in. Columbium Nozzle Wall Temperature vs Position	169
3.3.8-2	0.050-in. Carbon-Carbon Nozzle Wall Temperature vs Position	170
3.4.2-1	Control Effectiveness-Parallel Flow Dual Expander Cycle Engine	177

## LIST OF FIGURES (Cont)

<u>Figure No.</u>		<u>Page</u>
3.5-1	Microchannel Test Specimen (Based on 7.5K lbf Thrust Load Design)	182
3.5-2	Modified I-Triplet Injector Elements	183
3.5-3	Modified Injector Element Pattern	184
3.5-4	Water Flow Patterns for I-Triplet Element	185
3.5-5	Structural Property Variation with Temperature	187
3.5-6	Dual Spool Hydrogen Turbopump	189

## 1.0 SUMMARY

The objective of the study was to develop advanced engine system descriptions and parametric data for use by space transfer vehicle prime contractors and the NASA. Parametric design data was obtained for a LOX/LH<sub>2</sub> advanced expander cycle engine at five engine thrusts ranging from 7.5K lbf to 50K lbf. In addition, the study included an evaluation of engine throttling over a 20:1 range (2000 psia to 100 psia chamber pressure) and operation at mixture ratios from a nominal  $6 \pm 1$  to  $12 \pm 1$ . The two variation studies were done at the 20,000 lbf thrust level.

The study was expanded to assist in preparation of the NASA response to President Bush's space initiative. The Aerojet input included some parametric performance data plus DDT&E and first unit production costs. One limitation of the study was the lack of contact with vehicle primes to assess various vehicle/engine interface issues. This is recommended as a follow-on task.

Aerojet and NASA LeRC have an eight year history in the development of the dual propellant expander cycle engine. This cycle uses heated (400°F) oxygen to drive the oxygen turbopump. This allows a design free of the need for a helium purge gas system and reduces pressure demands on the hydrogen circuit for higher chamber pressure operation. During this study a cycle variant, splitting the hydrogen flow between the chamber and the baffled injector assembly, was examined and accepted as the design baseline. This cycle can maintain a 2000 psia chamber pressure over the 7.5K lbf to 50K lbf thrust range, can throttle over a 20:1 range, and can operate at the high mixture ratios needed for efficient use of lunar oxygen as a supplement to earth origin propellants. Based on an analysis with the Aerojet Modified Liquid Engine Transient Simulation (MLETS) code, this cycle is predicted to be stable at thermal equilibrium, and the basic engine control valve operation is expected to be nearly linear over the throttling range. A throttle rate of 4 to 5 seconds from 10% to 100% of thrust was predicted using the TUTSIM dynamics code.

Performance as measured by delivered specific impulse at MR = 6 and an area ratio of 1200 is 483.1 seconds at 7.5K lbf, 484.3 seconds at 20K lbf, and 485.2 seconds at 50K lbf. Predicted engine dry weight excluding gimbal and thrust takeout structure is 291.8 lbm at 7.5K lbf, 486.3 lbm at 20K lbf, and 1362 lbm at 50K lbf using available

## 1.0, Summary, (cont)

technology. Engine envelopes for a 1200:1 area ratio nozzle using one extendible/retractable section varies from 120 inches length/58 inch exit diameter at 7.5K lbf thrust to 304.8 inches length/137 inches diameter at the 50K lbf thrust with the nozzle extended. These are large engines in terms of envelope. Packaging will be an important consideration.

The DDT&E cost data was generated using a costing methodology found to be well accepted on the Advanced Launch System (ALS) program. The program as costed used assumptions typical of engine fabrication numbers and tests in a NASA MSFC program. The total DDT&E cost was about \$950M with a program start in FY91 and first flight in 1999. First unit production costs are based on production numbers, learning curve, engine thrust, and a complexity factor based on an RL-10 engine as the reference. For the lunar return mission, Nth unit engine cost is expected to be in the \$6M to \$12M range. As references, the current RL-10 cost is \$3M to \$4M and an OMS engine is about \$6M. Generation of life cycle costs was not feasible as they are dependent on the mission life and maintenance scenarios which are still incompletely defined.

The latest version of the dual expander cycle holds promise as a long-life engine capable of meeting all mission performance requirements including 20:1 throttling and MR = 12 operation. All major technical questions such as the 400°F oxygen turbine drive are being evaluated under NASA LeRC sponsored programs. The platelet heat exchanger technology is in qualification for space shuttle flight operations as this is written, and a vigorous program start has been made to develop the integrated control and health monitoring system (ICHM) capability under the OTV engine technology program. A continuation of this work is recommended, but the scope should be broadened to include more vehicle prime/engine contractor joint assessment of the interface issues.

## 2.0 INTRODUCTION AND BACKGROUND

### 2.1 BACKGROUND

#### 2.1.1 Orbit Transfer Vehicle (OTV) Engine Technology

The NASA has had some concept for a vehicle to move payloads and people beyond low earth orbit (LEO) since the inception of the United States space program. Over the years, the vehicle has had a number of names and many configurations, but the basic concept of a general purpose vehicle for a variety of tasks beyond LEO has persisted. Since 1982, this concept has been developed as part of the Orbit or Orbital Transfer Vehicle (OTV) technology program. NASA-Marshall Space Flight Center has been responsible for the vehicle studies while NASA Lewis Research Center has directed main engine development. The work reported herein was completed under a contract with NASA LeRC.

Over the seven years of this contract there has been an evolution in the mission model from an emphasis on LEO-to-GEO payload delivery missions to the current interest in the Lunar Return mission and a manned Mars mission. The effect on the engine development has been to emphasize the reliability and redundancy requirements for a man-rated propulsion system. Also, space basing and multimission capability place a premium on performance as measured by specific impulse and engine throttling. The very long service life goal (500 starts, 20 hours) mandates a sophisticated integrated health monitoring and control system. The engine resulting from these stringent requirements will be the most technically advanced and highest performing liquid oxygen/liquid hydrogen propellant engine developed in this century. It could serve as the basic upper stage main engine for both manned and unmanned missions until the middle of the next century.

The first phase of the NASA-LeRC sponsored program consisted of study efforts to generate and evaluate innovative technology concepts at the subcomponent, component, and engine system levels for an advanced  $O_2/H_2$  propulsion system. Pratt & Whitney, Rocketdyne, and Aerojet TechSystems were each awarded contracts in 1982 for this phase of the work. Aerojet initiated several new concepts during this work of which the most notable was the dual propellant expander cycle. This cycle

### **2.1.1, Orbit Transfer Vehicle (OTV) Engine Technology, (cont)**

improves the conventional hydrogen expander cycle by heating both hydrogen and oxygen for use as working fluids with consequent improvement in operating flexibility and higher chamber pressure.

The Phase II program, which is the current contract, builds on the Phase I work by evaluating through analysis, fabrication, and testing the concepts critical to the success of the proposed engine. The Aerojet technology focus has been on the oxygen turbopump (successfully tested), the thrust chamber, oxygen/materials compatibility, an engine preliminary design, and an Integrated Control Health Monitor System (ICHM). Design and development work has been in accordance with NASA-LeRC established technology goals. Table 2.1-1 summarizes the technology goals and gives the existing RL-10 engine technology as a comparison. The 1988 requirements will undergo some changes as the Lunar return mission is better defined.

The change in emphasis from an OTV for the LEO-to-GEO mission to a vehicle capable of landing on the moon or other bodies in the inner solar system will impact several of the engine requirements. The one most likely to change is engine thrust. This study was planned to generate parametric data for engines ranging in thrust from 7.5K lbf to 50K lbf as the actual mission thrust is very likely to fall within that range. An important design selection factor affecting baseline engine thrust is the number of engines per vehicle. For a man-rated vehicle at least two engines will be required, but three or four engines may be optimum when such factors as length constraints are considered. As will be discussed later in this report, the current baseline vehicles for the Lunar mission use a set of four engines each. An unmanned vehicle for LEO-to-GEO missions may very well use only one or two of these engines. The lunar mission requirements set the engine thrust once the number of engines in the propulsion set is established.

Work on the Advanced Engine Study began in November 1988 and concluded in the Spring of 1990 with this final report.

TABLE 2.1-1

## TECHNOLOGY GOALS FOR THE NEW OTV ENGINE

Parameters	RL-10	October 1986	1988
	System	NASA	Updated
	<u>Characteristics</u>	<u>Goals and/or Requirements</u>	<u>Goals or Requirements</u>
Basing	Earth	Not Specified	Space
Human-rating	No	Not Specified	Yes
Safety Criteria	Not Specified	Not Specified	Fail Operational, Fail Safe
Propellants - Fuel	Hydrogen	Hydrogen	Hydrogen
- Oxidizer	Oxygen	Oxygen	Oxygen
Vacuum Thrust (Design Point)	15,000 lbF	10,000 - 25,000 lbF*	7500 lbF (per engine)
Number of Engines per Vehicle		Not Specified	2 Minimum
Engine Mixture Ratio, O/F (Design Point)	5.0	6.0	6.0
Engine Mixture Ratio Range, O/F	4.4 to 5.6	5 - 7	5 - 7
Propellant Inlet Temperature - Hydrogen	38.3°R	37.8°R	37.8°
Oxygen	175.3°R	162.7°R	162.7°R
Gimbal	±4.0 Degrees	±6.0 Degrees (Sq. Pattern)	±20 degrees Pitch & Yaw
Aerobraking Design Criteria	The engine must be compatible with aeroassist return of the vehicle to low-earth orbit.		
Vacuum Specific Impulse	444 lbF-sec/lbm	520 lbF-sec/lbm	490 lbF-sec/lbm
Vacuum Thrust Throttling Ratio	No Throttling	30:1	10:1
Net Positive Suction Head (NPSH) - Hydrogen	133.0 ft-lbf/lbm	0	15 ft-lbf/lbm
Oxygen	16.7 ft-lbf/lbm	0	2 ft-lbf/lbm
Weight	290 lbm	360 lbm	360 lbm (2 engines)
Length	70.1 in.	40	TBD (Assume 60", Stowed)
Reliability (90% Confidence Level)	0.9982	1.0	.9975 Single engine, .99958 Dual engine**
Operational Life	3 Starts, 4000 sec	500 Starts, 20 Hours	500 Starts, 20 Hours
Service Free-Life		100 Starts, 4 Hours	100 Starts, 4 Hours
Start Cycle		Chilldown with propulsive dumping of propellants, tankhead start, pumped idle operation, autogenous tank pressurization required	

Updated 4 January 1989

\* Vehicle engine set total thrust must be in this range

\*\* MSFC/Boeing Vehicle Studies

RPT/417.55-1.T

## 2.1, Background, (cont)

### 2.1.2 Aerojet Dual Propellant Expander Cycle Engine

In a conventional expander cycle engine, hydrogen is routed through passages in the combustion chamber wall where it both cools the wall and acquires sufficient thermal energy to power the turbine drives of pumps for both the hydrogen and oxygen flow circuits. It is then routed to the injector for combustion. This cycle is fairly simple, plumbing is straight forward, it offers good performance potential, and, as all propellant is burned in the combustion chamber, it does not have the losses associated with open cycles. Its limitations are related to dependence on only one propellant as a turbine drive fluid which, in turn, requires interpropellant seals and a purge gas in the oxygen turbopump. To obtain the needed power, the hydrogen must be heated to a temperature very near to the design limit for the copper based alloys employed for the chamber liner. With the added limits imposed by high cycle life, long operating times without maintenance, and 10:1 or greater throttling requirement, the basic hydrogen expander cycle is capable of only a modest improvement over the current production expander cycle engine, the RL-10.

The Aerojet dual propellant expander cycle alleviates these limitations by using oxygen as a working fluid as well as hydrogen. This reduces the demands on the hydrogen circuit as the oxygen turbopump is driven by heated oxygen. It also eliminates the need for an interpropellant seal and the associated helium purge requirement. The gasified oxygen is also needed for the I-triplet gas-gas injector element which provides high (~100%) energy release efficiency and excellent combustion stability over a wide throttling range. The oxygen is heated to a maximum of 400°F by flowing through a LOX/GH<sub>2</sub> heat exchanger and then through the regeneratively cooled nozzle extension. The flow schematic is shown in Figure 2.1-1. This is the schematic used for the advanced engine study. The hydrogen used to heat the cold oxygen in the heat exchanger is the effluent from the hydrogen TPA turbine and provides the thermal energy to the oxygen at an efficiency cost of some pressure drop across the heat exchanger.

This cycle has proven more efficient than originally expected considering results of the 7.5K lbf thrust engine preliminary design. That design had cold hydrogen routed from the pump outlet to the regenerator, to the regeneratively cooled



### 2.1.2, Aerojet Dual Propellant Expander Cycle Engine, (cont)

chamber and then through the baffle circuit before powering the hydrogen turbine drive. This series flow generated high hydrogen temperatures, but was temperature limited by the copper walls of the chamber and baffles. Pressure drops were also high. The combination of wall temperature and pressure drops limited the power and flexibility of the cycle. A very effective remedy was to split the flow between the baffled injector circuit and the regeneratively cooled chamber as shown in Figure 2.1-1. This split or parallel flow version is capable of a 21:1 throttle range at the 20,000 lbf thrust design point (1000 lbf thrust to 21,000 lbf thrust). Chamber and baffle wall temperatures are well within design limits over the range of thrust.

Two key components in the engine are the hydrogen regenerator and the LOX/GH<sub>2</sub> heat exchanger (HEX). Both are NASA-Z copper structures fabricated from copper platelets using the same technology recently demonstrated on the Space Shuttle Main Engine (SSME) heat exchanger program, and expected to be operational in 1990. They are very compact and thermally efficient heat exchangers. The regenerator functions as a pre-heater for the hydrogen in the baffle circuit. It will be used to trim the engine output by the setting of its bypass valve. The HEX provides approximately 65% of the enthalpy gain in the oxygen circuit with the balance acquired in the oxygen cooled nozzle extension. The HEX bypass valve modulates to keep the oxygen entering the turbine at or below 400°F.

An integral part of the engine thermal design are the hydrogen cooled baffles. Baffles on an injector face are commonly used to enhance combustion stability. Generally they are transpiration cooled with fuel passing through the baffle directly into the chamber. In this engine the baffle is still designed to enhance stability but, more importantly, it provides surface area for heat input to the hydrogen. From 40 to 60% of the total hydrogen enthalpy change comes from the baffle flow circuits where hydrogen is passed down one side and back up the opposite side of the baffle to be collected and mixed with the regen chamber hydrogen prior to powering the hydrogen turbopump. The baffles allow the thrust chamber to be relatively short compared to a non-baffled hydrogen cooled thrust chamber of equivalent hydrogen heating capability. They require, however, a significant percent of the chamber barrel section volume. The

### 2.1.2, Aerojet Dual Propellant Expander Cycle Engine, (cont)

chamber diameter is increased to compensate giving an unusually high contraction ratio (chamber injector area divided by throat area). Where storable propellant engines commonly have contraction ratios of 2 to 4 this engine has a ratio of 15.3.

## 2.2 SCOPE

### 2.2.1 Objective

The objective of the study is to develop advanced engine system descriptions and parametric data for use by space transfer vehicle primes and NASA planners.

### 2.2.2 Requirements

The advanced engine continues the liquid oxygen/liquid hydrogen propellant engine technology developed under the OTV engine technology program. Specific engine system requirements and goals are given in Table 2.2-1. The baseline engine start cycle and autogenous tank pressurization requirements are given in Figure 2.2-1

### 2.2.3 Program Description

The Advanced Engine Study is a 15-month activity with five subtasks. The subtasks and their interrelationships are presented in Figure 2.2-2.

#### 2.2.3.1 Subtask 2 - Design and Parametric Analysis

The subtask objective is to develop the specific design and parametric data on advanced engines over a thrust range of 7.5K lbf to 50K lbf. The baseline for the design is the 7.5K lbf thrust OTV engine design developed under NASA LeRC Contract NAS 3-23772. This task generates at a minimum, the following:

- Needed engine cycle changes over the thrust range.
- Identification and assessment of advanced technologies needed for the advanced engine cycle.

**TABLE 2.2-1.  
Engine System Requirements and Goals**

<b>Propellants:</b>	Liquid Hydrogen Liquid Oxygen
<b>Vacuum Thrust:</b>	7,500 lbf to 50,000 lbf (Study Range)
<b>Vacuum Thrust Throttling Ratio:</b>	10:1
<b>Vacuum Specific Impulse:</b>	*
<b>Engine Mixture Ratio:</b>	6.0 (Design Point at Full Thrust) 5.0 – 7.0 (Operating Range at Full Thrust)
<b>Chamber Pressure:</b>	*
<b>Drive Cycle:</b>	Expander
<b>Dimensional Envelope:</b>	
Length (Stowed/Extended)	*
Diameter (Maximum)	*
<b>Mass:</b>	*
<b>Nozzle Type:</b>	Bell With Not More Than One Extendible/ Retractable Section
<b>Nozzle Expansion Ratio:</b>	End of Regen Section to 1200 (Study Range)
<b>Propellant Inlet Temperatures:</b>	
Hydrogen	37.8 R
Oxygen	162.7 R
<b>Inlet Net Positive Suction Head:</b>	
Hydrogen	15 ft-lbf/lbm at Full Thrust
Oxygen	2 ft-lbf/lbm at Full Thrust
<b>Design Criteria:</b>	Human Rated Aeroassist Compatible Space Based
<b>Service Life Between Overhauls:</b>	500 Starts/20 Hours Operation (Goal)
<b>Service Free Life:</b>	100 Starts/4 Hours Operation (Goal)
<b>Maximum Single Run Duration</b>	**
<b>Maximum Time Between Firings:</b>	**
<b>Minimum Time Between Firings:</b>	**
<b>Maximum Storage Time in Space:</b>	**
<b>Gimbal Requirement:</b>	
Yaw Angle	**
Acceleration (Maximum)	**
Velocity (Maximum)	**
<b>Start Cycle</b>	(Figure 2.2-1)
* Engine Parametric Study Result	
**Vehicle/Mission Study Result	

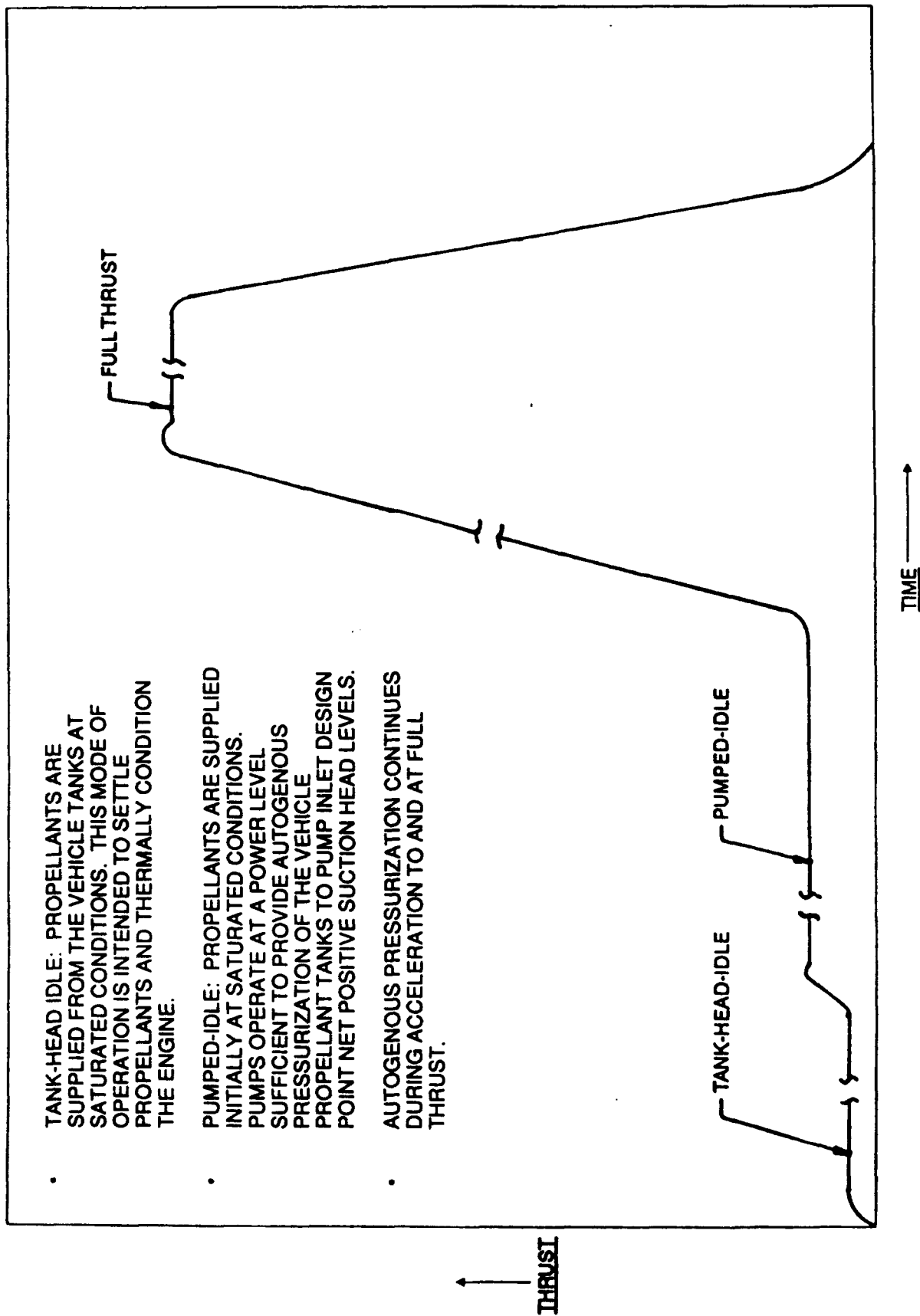


**Figure 2.2-1. Start Cycle-Space Transfer Vehicle Engine**

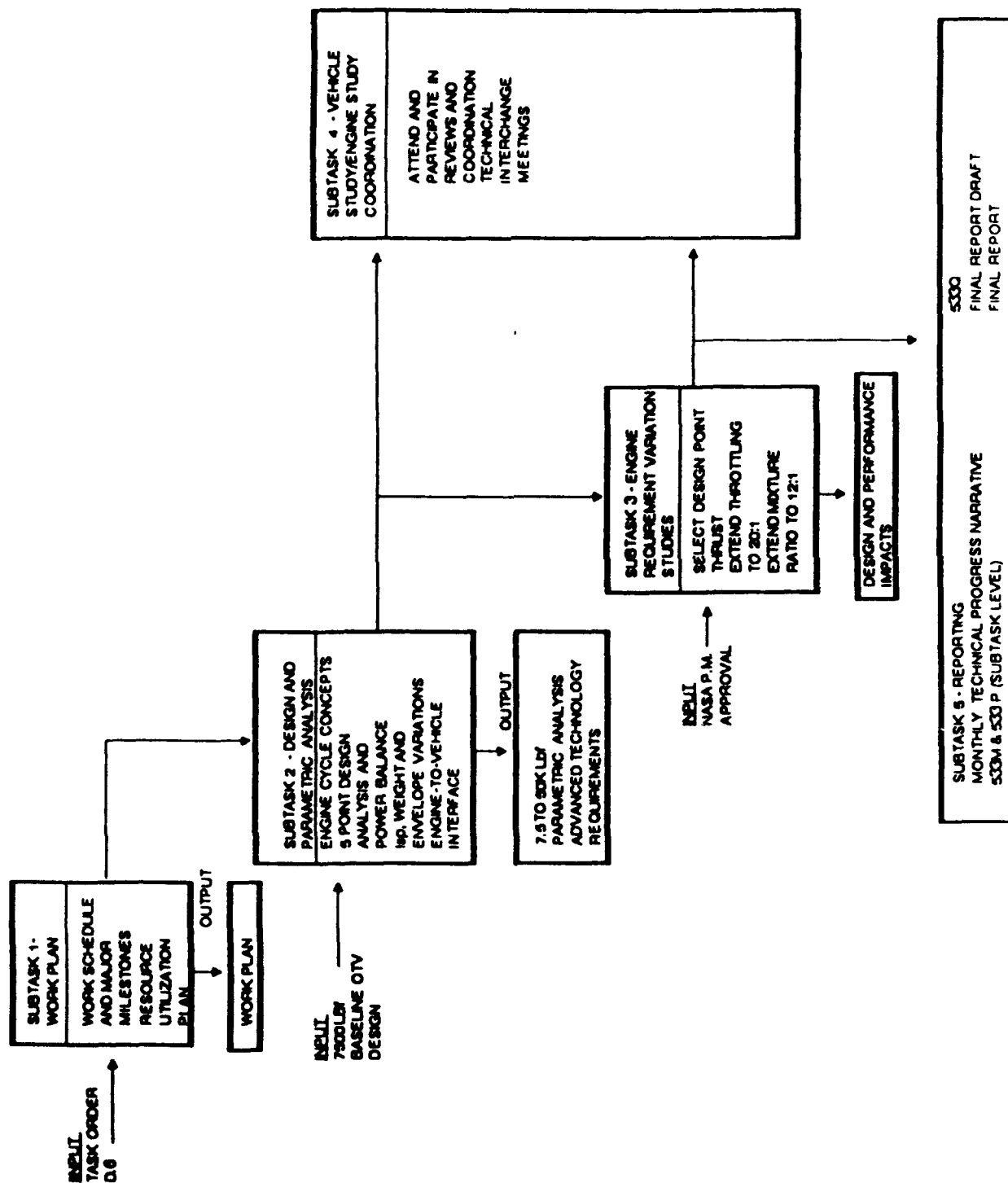


Figure 2.2-2. Task Order D6 - Advanced Engine Study Activities

### 2.2.3, Program Description, (cont)

- Obtainable design point chamber pressure for each thrust studied.
- Appropriate thermal, performance, turbopump, and power balance data for each thrust. Power balance data is obtained at mixture ratios of 5 and 7 as well as the design MR of 6, and at a thrust of 0.1X nominal (10 to 1 throttle point).
- Plots are generated for such control related factors as percent turbine bypass versus thrust.
- Estimates of delivered specific impulse, engine mass, and engine envelope.
- A preliminary definition of the engine-to-vehicle interfaces including liquid oxygen and liquid hydrogen inlet location and line sizes, thrust takeout structure, and gimbal system.

#### 2.2.3.2 Subtask 3 - Engine Requirement Variation Studies

Defines the effect of increased throttling range (up to 20:1) and very oxygen rich operation ( $MR = 12 \pm 1$ ) on the design and engine performance. A single thrust point selected by the contractor but approved by NASA LeRC, is used for this subtask.

#### 2.2.3.3 Subtask 4 - Vehicle Study/Engine Study Coordination

Discussion with and data supplied by the vehicle prime contractors shall be used to generate the following:

- Engine maximum single run duration.
- Maximum time between firings.
- Minimum time between firings.
- Maximum storage time in space.
- Gimbal requirements.

### 2.2.3, Program Description, (cont)

This information was to be supplied for each thrust level. NOTE: There was insufficient contact with the vehicle primes to define the requirements for any of these items during the course of the study.

## 2.3 RELEVANCE TO CURRENT ROCKET ENGINE TECHNOLOGY

There are three major program areas currently developing new chemical propulsion system technology: the National Aerospace Plane (NASP), the Advanced Launch System (ALS), and the Chemical Transfer Propulsion (CTP) program under Project Pathfinder. This advanced engine study supports the CTP work. The engines under development in all three programs use LOX/LH<sub>2</sub> propellants to meet program performance requirements. All share a common technical base in copper alloy chambers, pressurization by high speed turbopumps, and a need for an integrated control and health monitoring system.

The engine cycles under development include variations of the hydrogen expander cycle and gas generator cycles. The dual propellant expander cycle is arguably the most sophisticated of the cycles, but variants abound even among the gas generator cycles. Expander cycles have the merit of increased efficiency compared to gas generator cycles, but other considerations, such as engine thrust, may rule out an expander cycle. Results of the current study, however, support extending the thrust range for an expander cycle beyond 100K lbf. A modern expander cycle should be considered in any trade study for a LOX/LH<sub>2</sub> engine development up to 500K lbf thrust. Also, engine innovations by Aerojet, Rocketdyne, and Pratt & Whitney developed under the NASA LeRC contracts have demonstrated a number of ways of enhancing engine components to increase the effectiveness of the expander cycle. Examples are the Rocketdyne ribbed chamber work to improve chamber heat transfer by about 40-50%, and the Aerojet platelet heat exchangers that are used to increase the throttle range and engine control capability. This recent improvement in expander cycle technology has left even fairly recent texts on rocket propulsion obsolete concerning expander cycle capabilities. (Ref. 1, p 156).

The most important rocket engine development trend in the last third of the 20th century is the reduction of the theoretical advantages of a LOX/LH<sub>2</sub> engine to practise. The development of the RL-10 engines was a major achievement as was the

### 2.3, Relevance to Current Rocket Engine Technology, (cont)

Space Shuttle Main Engine (SSME). Both of these engines will see service in the United States Space program for several decades. The OTV engine/CTP engine will be the single most important space engine development of the next several decades, and a version of this engine will likely be in use for the first half of the 21st century. The results of this advanced engine study support several statements that help define its relevance to current rocket engine technology:

- 1) A high performance ( $>480$  seconds specific impulse) expander cycle engine can be produced.
- 2) A LOX/LH<sub>2</sub> engine capable of 20:1 throttling can be developed for the Lunar Excursion Vehicle or other vehicles requiring engine throttling.
- 3) Oxygen cooling of nozzles and hot oxygen turbine drive for turbopumps are now practical.
- 4) Operation of a LOX/LH<sub>2</sub> engine is practical at mixture ratios greater than stoichiometric (7.94:1) if the copper chamber is given a protective coating.
- 5) Current copper alloy combustion chamber technology is acceptable for an advanced engine, but some increased capability can be expected with continued materials development.
- 6) Chamber thermal design and manufacturing techniques give confidence that a chamber/injector will survive 500 starts and 100 hours of operation given a modern integrated control and health monitoring system (ICHM).
- 7) Current state-of-the-art in electronics and controls makes possible a control and health monitoring system that will greatly reduce engine operation risks and extend engine life.
- 8) Recently proven turbopump technologies such as self-aligning hydrostatic bearings and sub-critical operating speed designs help meet a 500 start 100 hour engine operation requirement.

### 2.3, Relevance to Current Rocket Engine Technology, (cont)

- 9) Platelet heat exchanger technology can be used to improve chamber thermal margins.
- 10) The Chemical Transfer Propulsion program within Project Pathfinder can now define realistic performance and operating goals for the main engine for Lunar Transfer and Lunar Excursion Vehicles.

### 2.4 SIGNIFICANCE OF THE PROGRAM

The NASA-LeRC directed LOX/LH<sub>2</sub> engine technology programs have successfully positioned the propulsion industry for a low risk development of the engine needed for Lunar Transfer Vehicle and Lunar Excursion Vehicle. The study results reported herein are based on eight years of study, analysis, design, hardware fabrication and testing. The relatively moderate cost of this extended technology work should be amply repaid by the reduction in risk for a full scale engine development program. The major significance of the program, then, is its direct applicability to propulsion requirements for the Lunar Transfer Vehicle and Lunar Excursion Vehicle.

The engine design baseline presented in this report represents a real advance in the state-of-the-art. The Soviets and the Japanese have now demonstrated successful LOX/LH<sub>2</sub> engines. The Japanese have already held discussions with American companies on licensing their engine technology. Without this program the United States would have no high technology counter to the economic inducement presented by a flight qualified Japanese engine. This program substantiates the position that the United States is still the leader in LOX/LH<sub>2</sub> engine technology. If the development does not continue, however, its significance will be that of potential wasted and opportunity lost. This engine has great significance for the survivability of the United States liquid rocket industry at a time when defense related development is vanishing and NASA has conflicting priorities for a limited budget.

A third area of significance is the general upgrading of design tools in the form of computer models and the increased sophistication of control and health monitoring capability. The design tools can better assess what is practical or possible when approaching theoretical limits as the OTV engine does. This gives higher confidence in

#### 2.4, Significance of the Program, (cont.)

designs prior to reducing them to testable hardware. The new control sophistication can readily deal with the complexity and interactions of a modern expander cycle engine while new sensors and a variety of software algorithms can be integrated into a health monitoring/management system that will greatly increase the safety of engine operation over a service life previously unobtainable in a rocket engine. Without these advances this engine could not be developed beyond drawings.

### 3.0 DISCUSSION

#### 3.1 DESIGN AND PARAMETRIC ANALYSIS

This task began with a re-evaluation of the results of the 7.5K lbf thrust engine preliminary design (Ref. 2). The cycle schematic work for that design is the dual expander series flow version as given in Figure 3.1-1. A concern in the evaluation was the high chamber and baffle wall temperatures at full thrust (2000 psia chamber pressure, mixture ratio of 6) and at the tank head idle condition (200 psia chamber pressure, mixture ratio of 5). The flow of hydrogen from the pump to the regenerator, to the baffles, and then to the TPA turbine section produced high hydrogen temperatures but had penalties in system pressure drop and wall temperature. This was corrected by going to the split or parallel flow schematic shown in Figure 2.1-1. When initial analysis proved that temperatures were lowered with no performance penalty, the parallel flow version was adopted for the study.

A hydrogen proportioner valve had to be added to the system to control the hydrogen split to each circuit. This has proven a worthwhile addition as it can be used to optimize the wall temperature of both the baffles and the regeneratively cooled chamber. This has important implications for chamber life. The regenerator now functions on just the hydrogen stream directed to the baffles. The chamber is always cooled with hydrogen directly from the pump. Also, the injector manifolding was modified as the baffle circuit is now independent of the chamber flow circuit. In all other respects the components retain their function in the engine cycle.

At the outset of the study, an arbitrary decision was made to baseline a design nominal thrust chamber pressure for each engine as 2000 psia. This was justified by a concern that a 20:1 throttle range would lead to system pogo type instabilities if the low thrust chamber pressure had to be extended below 100 psia. Also, 2000 psia was well within current thermal design capabilities. High chamber pressure engines do have greater development risk. This selection worked out very well for a 10:1 throttling requirement over all the thrusts studied (see Table 3.1-1) and accommodated a 20:1 throttling design for a 20,000 lbf thrust engine.

The task assignment bounded the engine thrust range between 7.5K lbf and 50K lbf. The intermediate points used in the study are given in Table 3.1-1. The 20,000

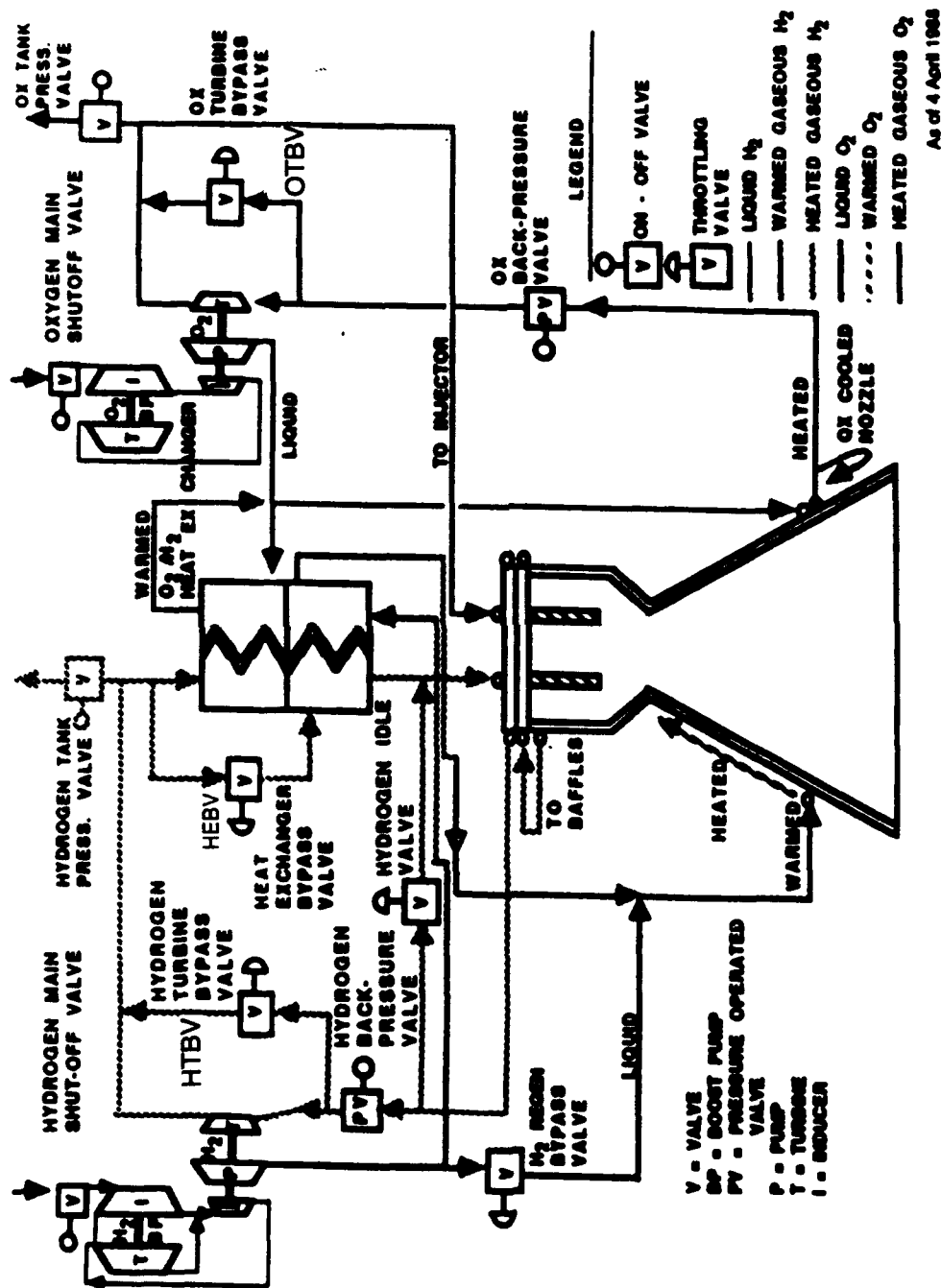


Figure 3.1-1. OTV Engine Dual Expander Cycle, Series Flow Schematic, 7.5K lbf Thrust Engine

### 3.1, Design and Parametric Analysis, (cont)

lbf thrust point was also selected for the engine requirements variation tasks after consultation and direction from the NASA-LeRC program monitor. With a baseline engine schematic, chamber pressure, and the five thrusts, the actual study results (see Table 3.1-2) could be generated.

#### 3.1.1 Engine and Cycle Definition

TABLE 3.1-1

##### ADVANCED ENGINE STUDY THRUST SELECTION RATIONALE

- 7.5K lbf OTV Program baseline; results available.
- 20K lbf Minimum thrust for a 4 engine Lunar Transfer Vehicle and Lunar Excursion Vehicle with 40 to 50,000-lb of payload.
- 25K lbf Provides a 100K lbf total thrust for a 4 engine LTV/LEV for minimum gravity losses.
- 35K lbf Nominal thrust for three engine LEO-to-moon orbit transfer vehicle (LTV)
- 50K lbf Nominal thrust for two engine LTV. This is also half the thrust of the baseline engine for the LEO-to-Mars transfer stage, and results could be extrapolated to that thrust.

#### 3.1.1.1 Thrust Chamber Assembly

a. Chamber Liner — The chamber liner is a copper alloy billet machined to final dimensions with milled coolant channels on the backside. The baseline alloy is GLIDCOP AL15 manufactured by the SCM Company using powder metallurgy techniques. This is pure copper with 0.15% aluminum oxide ( $Al_2O_3$ ) dispersed throughout the metal matrix. The small amount of aluminum oxide greatly improves the machining capability over pure copper and enhances the low cycle fatigue life of the material. An alternate material is the NASA-Z alloy which was selected for the 3.0K TCA

**TABLE 3.1-2**

**EXPECTED RESULTS OF THE PARAMETRIC STUDY**

- **Weight, Envelope and Performance Predictions for Engines at 7.5K and at three intermediate points plus a 50K maximum.**
- **Power Balance Results at Each Thrust**
- **Changes in Cycle and/or Components on Scale-Up**
- **Assessment of 20:1 Throttling at a Selected Thrust Level**
- **Assessment of high mixture ratio performance (MR of 12) at a selected thrust level**
- **Identification of Critical Technologies**
- **Preliminary Engine/Vehicle Interface Requirements**
- **Innovative Design Solutions or Technologies**
- **Interchange with vehicle primes at NASA-MSFC Conferences**
- **Preliminary DDT&E costs for a common engine for the Lunar Transfer Vehicle (LTV) and Lunar Excursion Vehicle (LEV)**
- **Propulsion analysis for various mission and operational scenarios**
- **Final report suitable for use by vehicle primes in assessing propulsion requirements**

### 3.1, Design and Parametric Analysis, (cont)

design. GLIDCOP is a dispersion hardened material less sensitive to the high radiation environment of space than NASA-Z as yield strength and volume changes are negligible for expected mission radiation doses. See Tables 3.1-3 and 3.1-4.

The low cycle fatigue life and chamber thermal performance are improved through use of a microchannel design for the coolant channels. A conventional channel design would use 30 mil channels in the throat with channel widening in the chamber converging, diverging, and barrel sections. The temperature variation using the 30 mil channels appreciably shortens chamber life due to higher induced stresses. The small temperature variation in the micro-channel design (11 mil channels, 10 mil lands) reduces stresses and improves reliability as adjacent channels can adequately cool the material around a blocked coolant channel. Channel geometry varies in both width and depth for most effective cooling with lowest pressure drop. The basic channel design was demonstrated in the NASA LeRC funded cooled throat program. (See Reference 8)

b. Liner Closeout — The liner closeout utilizes technology developed under NASA LeRC contract for electroforming with two metals simultaneously. A nickel cobalt (NiCo) electroformed closeout was demonstrated on the hydrogen cooled throat for the 3.0K lbf TCA program. This bimetal alloy has 3 times the strength of a nickel electroform, allowing a thinner closeout and improved cycle life. Alternatives to the NiCo closeout that could be used are Nickel-Manganese and Nickel-Chromium. Strength would be about the same, but there could be an improvement in the electroforming process that would give higher yields of finished liners. This could be an important consideration given the high value of the machined copper liners.

c. Dimensions and Manifolds — The 20,000 lbf thrust TCA chamber has a throat diameter of 2.5 inches, a barrel diameter of 10 inches, and a length (L') of 12 inches. The contraction ratio is 15.3. The hydrogen inlet manifold will be attached at a position equivalent to a 28:1 area ratio. A platelet filter will be designed as an integral part of the manifold to protect the microchannels from any debris that could cause a flow blockage. The manifold will be designed for even flow distribution, and

**Table 3.1-3  
CTP Engine Materials Selection**

**• THRUST CHAMBER ASSEMBLY IN A HIGH RADIATION ENVIRONMENT**

**Swelling of Neutron Irradiated Copper Alloys**

Material	Volume % Increase After Irradiation	
	3 dpa <sup>1*</sup>	15 dpa <sup>2*</sup>
Copper:		
Marz**grade (99.999%)	1.8	6.8
OF grade (99.95%)	2.1	6.6
DS Copper:		
C15720	0.8	0.9
C15760	1.1	0.6
Precipitation Hardened:		
Cu-Zr	nil	3.6
Cu-Mg-Zr-Cr	nil	nil

1. 3 dpa corresponds to fluence of  $0.4 \times 10^{26}$  n/m<sup>2</sup> (En > 0.1 MeV)
2. 15 dpa corresponds to fluence of  $0.4 \times 10^{26}$  n/m<sup>2</sup> (En > 0.1 MeV)

\* dpa = displacements per atom

\*\* Trade Name  
SCM Metal Products  
Cleveland, Ohio

**Table 3.1-4**  
**CTP Engine Materials Selection**  
**• THRUST CHAMBER ASSEMBLY IN A HIGH RADIATION ENVIRONMENT**  
**Tensile Properties of Neutron Irradiated Copper Alloys**

Material/Condition	YS (MPa)	UTS (MPa)	Elongation (%)	Reduction in Area (%)
Copper: Marz*: Control 3 dpa 15 dpa	31 33 41	152 155 149	24 25 17	89 80 48
OF: Control 3 dpa 15 dpa	26 51 49	196 200 185	27 30 24	90 59 46
DS Copper: C15720: Control 3 dpa 15 dpa	337 353 343	395 411 395	14 14 20	48 51 50
C15760: Control 3 dpa 15 dpa	397 402 379	466 468 449	12 10 11	56 43 50
Precipitation-Hardened: Cu-Zr: Control 3 dpa 15 dpa	271 274 71	334 317 226	9 9 34	70 73 44
Cu-Mg-Zr-Cr: Control 3 dpa 15 dpa	431 379 284	458 437 354	10 13 17	61 56 57

• Trade Name  
SCM Metal Products  
Cleveland, Ohio

### 3.1, Design and Parametric Analysis, (cont)

each channel will be flow checked and compared for acceptable uniformity. The coolant hydrogen is collected in a manifold at the top of the chamber for routing to the hydrogen turbopump.

d. Injector — The injector is unusual in that it incorporates inlet and collection manifolds for the hydrogen flow to the baffles (Figure 3.1-1A) as well as the usual inlets for hydrogen and oxygen for combustion. There are also flow circuits for the two GOX/GH<sub>2</sub> igniters and their laser ignition source. The dome of the injector also has a structure for attaching the gimbal actuators for the pitch and yaw gimbal (as illustrated in Figure 3.1-3).

(1) Element Design - The highest performing oxygen/hydrogen injector element is the I-triplet. It delivers very nearly 100% energy release efficiency in a chamber length of eight inches. The high energy release in such a short combustion length poses a chamber compatibility problem. Aerojet has addressed this in Task C.4 of the OTV engine contract by tailoring the element performance and energy release for element position in relation to chamber or baffle walls. The injector will have five versions of the element for maximum chamber compatibility and performance. This element is designed for gas-gas mixing. The oxygen phase change is accomplished in the LOX/GH<sub>2</sub> heat exchanger (HEX) and all oxygen entering the chamber is in the gas phase. Combustion stability with gas-gas elements is excellent over a very wide range of chamber pressures. This is needed for a throttling range of 20:1 without excluded thrust bands or potential mixture ratio fluctuations as the oxygen transits the two-phase region. (See Ref. 3).

(2) Face Bleed - The injector has precise etched flow passages for hydrogen face bleed for cooling the face, the chamber wall, and the baffle plates near the injector. This increases injector and chamber life at some cost to energy release efficiency. The precise percentage of hydrogen used for face bleed will be determined in the detail design, but should not exceed 6%. A means of reducing face bleed is to construct the injector and baffle plates of platinum instead of nickel and copper as was baselined in the 7.5K lbf thrust engine design. Recent extensive development of platinum series metal technology for rocket engine thrust chambers has reduced the risk of such an approach and made it consistent with an ultra-high performance engine design. (See Ref. 4)

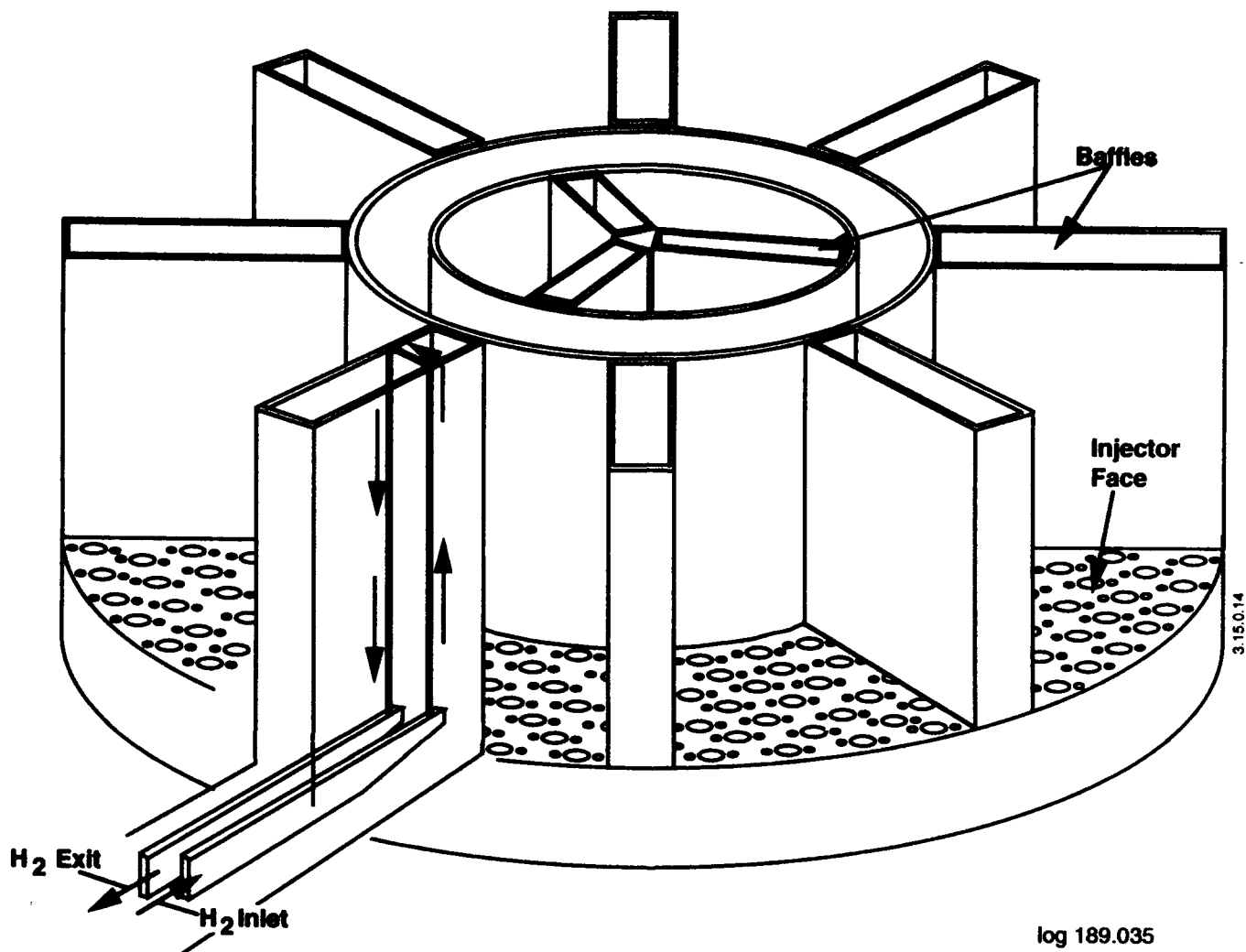


**Figure 3.1-1A Our Regeneratively Cooled Baffles Provide a Dual Function as an Added Heat Transfer Surface as Well as a Combustion Stability Damping Device**

### 3.1, Design and Parametric Analysis, (cont)

(3) Injector Concept - The spoke and hub baffle design breaks the injector face into several independent sections. These small injector areas are readily constructed using Aerojet's well developed platelet technology. The approximately 1/4 inch thick sections will be electron beam welded and/or brazed to the inconel injector body to form the hydrogen circuit. Oxygen posts pierce the hydrogen manifold and are centered in each element opening to complete the element. The dome of the injector covers the oxygen compartment. Oxygen posts are welded to the base of this compartment which also divides the hydrogen and oxygen manifolds. This is a substantial structural part with all welded joints to assure there will be no internal hydrogen and oxygen mixing. Both the oxygen and hydrogen compartments are partially segmented to accommodate the hydrogen flow passages into and out of the baffles. They are also tailored to accommodate the two ignitor ports.

(4) Baffle Construction - The baffle flow circuits are independent of injector flow circuits as their function is to increase the heat input to the hydrogen. A secondary function is combustion stability. The baffles divide the injector into small compartments to maintain a high proportion of wall area in close proximity to combustion gas. From 40 to 60% of the total heat transferred to the hydrogen is due to the baffles. The hydrogen is distributed to the baffle compartments by two semi-circular manifolds that are welded to the manifold used to collect hydrogen flowing from the regen cooled chamber. This weld line forms the mechanical connection between the injector and the regen cooled chamber. The hydrogen flows down into the baffles, around the tip, and up the back side to a separate collector system terminating in two semi-circular manifolds that are welded to the top side of the baffle inlet manifold. The basic injector design has three separate manifolds which are stacked to form the hydrogen flow circuits. The baffle inlet and outlet manifolds are divided in two sections to allow the igniter ports the necessary space to function.

The actual baffle plates extend above and below the injector face. They are built up as discrete sections. They are welded to the inlet and outlet collectors a section at a time. The sealing surface between the inlet and outlet collector may have to be brazed as there is no convenient means of welding the joint. The collectors are constructed of nickel 200. The baffles are NASA-Z copper in the baseline

### 3.1, Design and Parametric Analysis, (cont)

design, but may be constructed of platinum or platinum alloy depending on the assembly techniques and thermal margins required. Both the copper/nickel system and the nickel/platinum system have a common liquids so welding is possible. The baffles are formed from platelets with chemically etched passages for the hydrogen flow which are diffusion bonded into a unit. The rounded baffle end is finish machined to the correct dimensions after bonding. See Figure 3.1-2 for a cutaway of the 7.5K lbf TCA baffle plate.

The injector segments are welded or brazed to the portion of the injector body used as a hydrogen compartment. The dome of this compartment is pierced by the oxygen posts that must be centered in the elements. The complete element is formed when the injector segments are fitted into place with the respective oxygen post inside. Hydrogen is fed to the compartment from a passage adjacent to one of the ignitor ports. A similar passage adjacent to the ignitor port on the opposite side of the engine feeds the oxygen compartment. The oxygen compartment dome is welded onto the hydrogen dome with a circumferential fusion weld. At the top center of the oxygen dome is a cylindrical extension used as an attachment point for the  $\pm 6^\circ$  pitch and yaw gimbal system. This injector assembly is slipped into the conforming openings in the baffle assembly and manifolds. Final assembly requires the injector segments to be welded to the baffle plates and the oxygen dome to be welded to the baffle outlet manifold structure. The injector body will be an inconel or monel alloy that forms a good braze and/or weld joint with the nickel injector face plates, and that can be used for both oxygen and hydrogen service. Manifolds will be of the same alloy. Differences in thermal coefficients of expansion must be kept within bonded joint material limits for the expected thermal cycling. The injector assembly will operate at fairly low temperatures as the baffle circuit is fed by liquid hydrogen and the hydrogen stream to the injector has cooled considerably from heat given up in the LOX/GH<sub>2</sub> heat exchanger and regenerator.

e. Stress Relief and Component Mounting Structure — The throat area of the chamber must be protected from damaging stress or side loads. This is accomplished by using a "can" structure and extends to the hydrogen inlet manifold. The connection to the inlet manifold is a sliding joint that allows for thermal expansion of the chamber in the longitudinal direction but acts as a rigid stress takeout structure for side loads (See Figure 3.1-3).

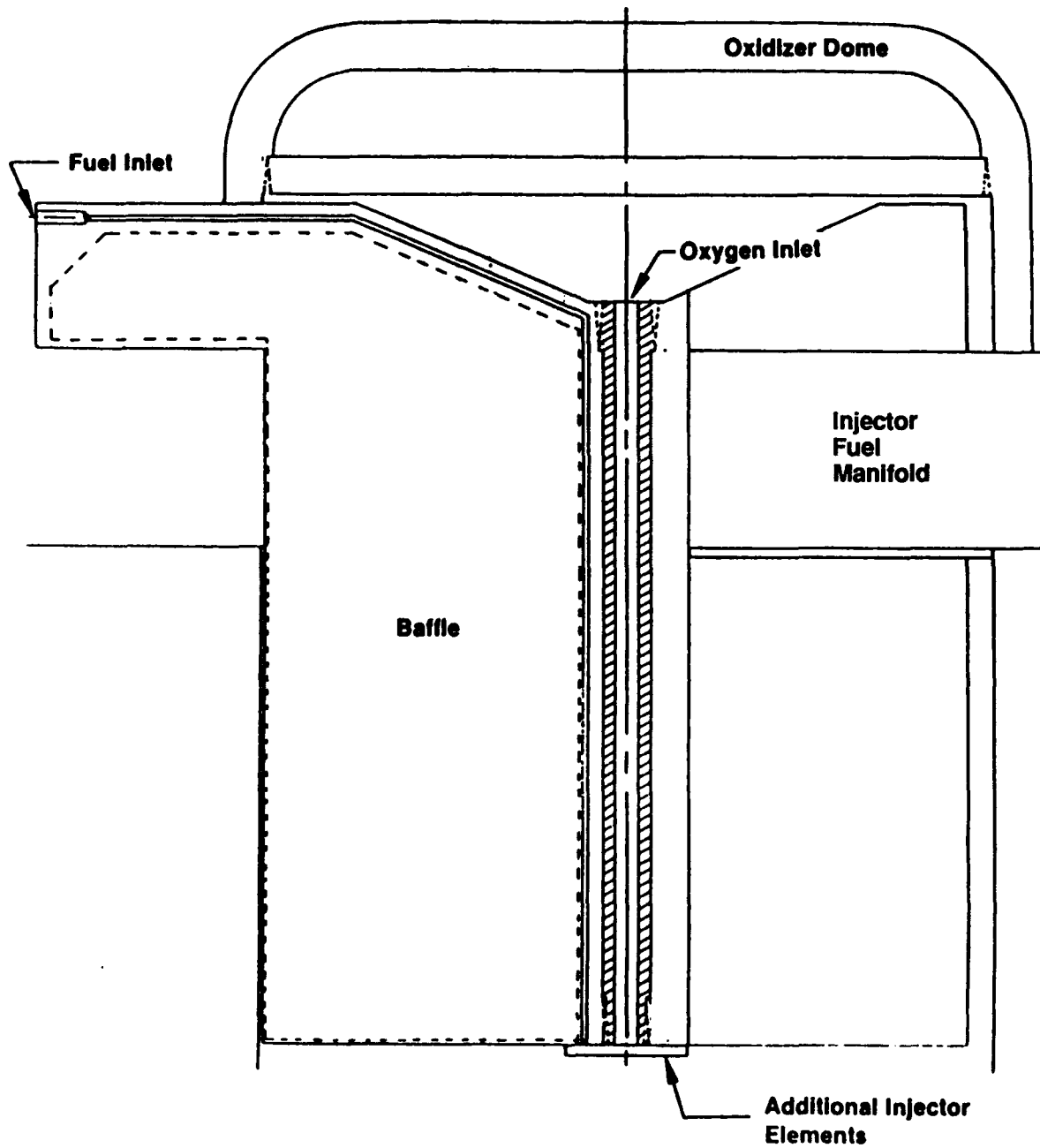


**Figure 3.1-2. 7.5K lbf OTV Injector/Baffle Flow Circuit**

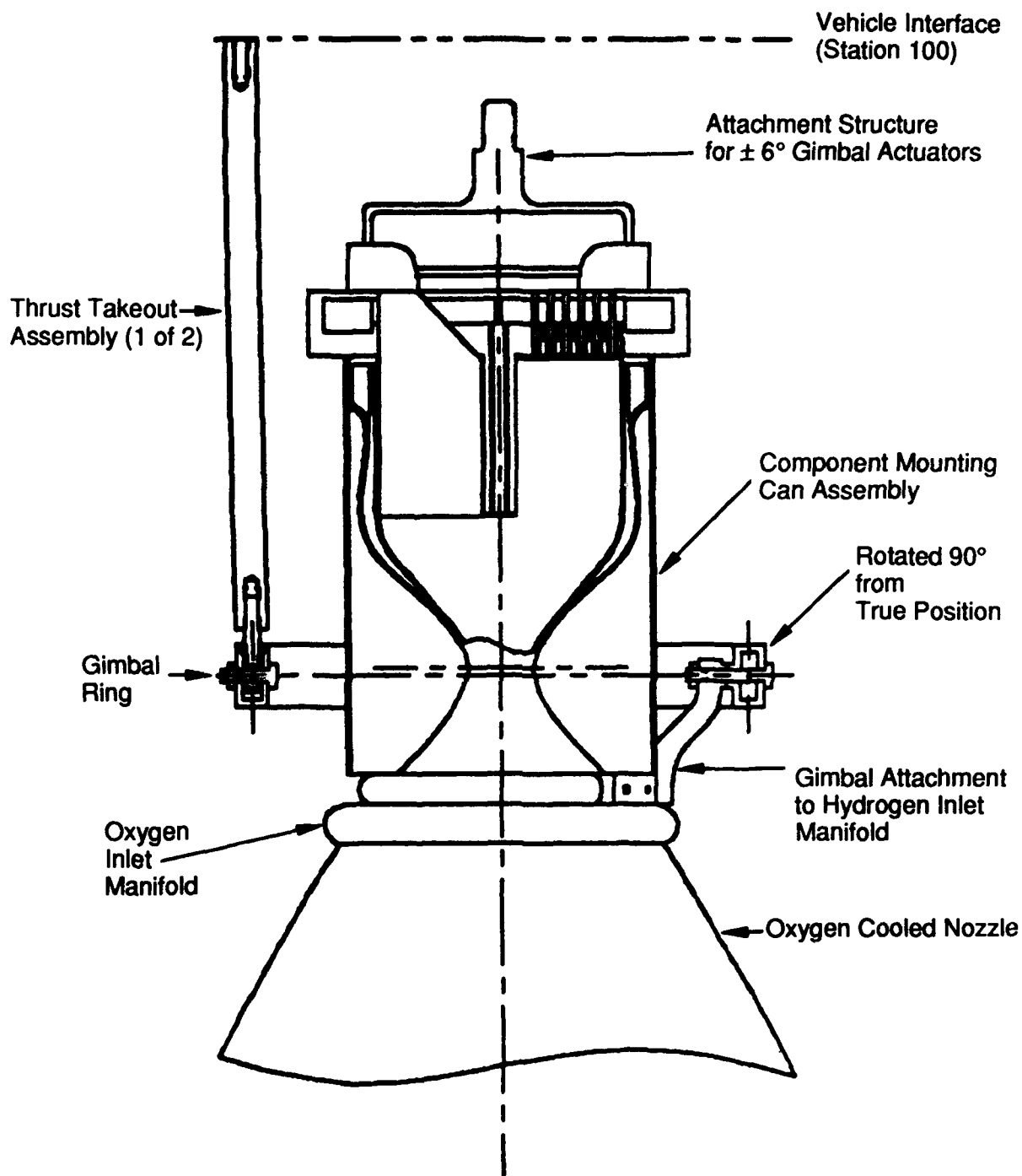


**Figure 3.1-3. OTV Engine TCA Sketch Showing Can and Gimbal Attachments**

### 3.1, Design and Parametric Analysis, (cont)

This "can" serves as a convenient mounting structure for various engine components. In particular, the two turbopumps will be mounted on it. Bracketry extending from the can will be used to mount the various valves and to stabilize the many lines and electrical wire bundles.

f. Gimbal Structure — The throat gimbal system must also serve as a thrust takeout structure. This requires that the flanges connecting the circular box gimbal structure to the hydrogen inlet manifold be of fairly robust construction. The gimbal structure is located near the throat plane for a true throat gimbal. The actuators, however, are located on the structure above the engine. They are placed 90° apart and are connected to the cylindrical top of the injector oxidizer dome. Movement of the actuator rods pivots the engine about the throat gimbal point in any combination of  $\pm 6^\circ$  pitch and yaw change from a centered thrust vector. Actual thrust takeout is accomplished where the throat gimbal system attaches to the engine mounting structure. The actuator rods see only the inertia loads related to moving this engine mass.

#### 3.1.1.2 Oxygen Cooled Nozzle

a. Concept — No detailed design has been completed for the oxygen cooled nozzle. The baseline concept is a copper alloy swaged tube bundle that is welded and then contoured on a mandrel. The inlet manifold is at area ratio 35. All tubes extend to the practical limit for forming and are then bifurcated. The bifurcations extend to area ratio of 600:1. They are then doubled back for half the length of the nozzle where they are terminated at the outlet ring manifold.

An alternative to the swaged and brazed tube bundle is a copper platelet structure that would be formed in sections that are then welded into a conical structure that would be formed to the final contour on a mandrel. A third possibility is a structure formed from two copper sheets that are explosively welded together with flow passages formed by material that could be removed by melting or solution. A design trade study is needed to select the best configuration. Figure 3.1-4 shows the three concepts that have received some study.



### 3.1, Design and Parametric Analysis, (cont)

#### 3.1.1.3 Radiation Cooled Nozzle

Material selection governs the design configuration. The candidate materials are a 2 directional wound carbon-carbon composite, and columbium. The joint temperatures are compatible with either material. The carbon-carbon will be lighter but does not have the established reliability of the columbium. The columbium requires a silicide or other coating to prevent oxidation. The carbon-carbon would require a silicon carbide impregnated layer to control both erosion and oxidation. The columbium nozzle would have two stiffening rings. The carbon-carbon nozzle would have a thicker section at the nozzle exit and where the pads for the retraction/extension assembly attach. Both would have sections of varying thickness to reduce weight. Both would be contoured for optimum performance.

The retraction/extension mechanism uses three jackscrews driven by 28 volt DC electric motors. The three motors are mechanically connected by a steel cable drive shaft inside a circular tube. This shaft assures synchronized motor operation and gives a doubly redundant capability to the mechanism as any one motor can operate all three jackscrews. The reliability of such a mechanism is demonstrated by the millions of garage door openers that are of a similar design. The motors and cable way are attached to the gimbal structure at the top of the engine. See Figure 3.1-5.

The attachment to the nozzle and the seal are critical design elements. The seal is a double finger leaf seal that can readily make and break the seal many times without significant wear or an increased leak rate. With the seal at an area ratio of 600, the gas pressure across the seal is only about 0.3 psia. This simplifies the sealing problem. The design intent is to have a rugged seal capable of many nozzle movements without an over emphasis on leakage rates.

#### 3.1.1.4 Oxygen Boost Pump

The low propellant tank pressures pose a very difficult turbopump design problem. Aerojet has determined that two separate units give the best performance potential. The first is a low head rise, low speed four stage boost pump that takes the oxygen at vapor pressure and boosts it to 55 psia for feed to the high speed turbopump. The boost pump turbine is driven by a portion of the first stage TPA pump

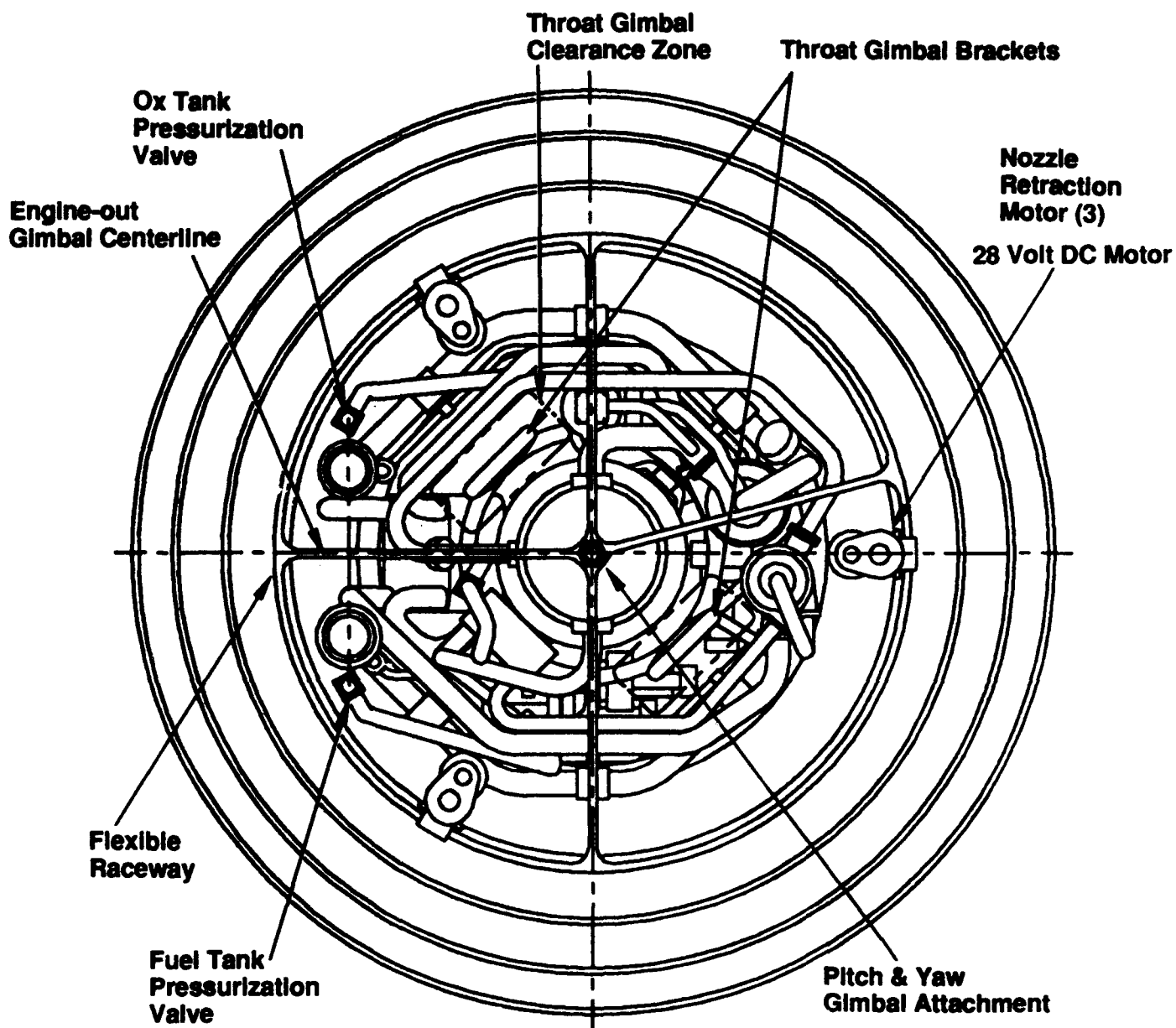


**Figure 3.1-5. 7.5K lbf Thrust OTV Engine (Top View)**

### 3.1, Design and Parametric Analysis, (cont)

output. Turbine outlet flow is combined with the pump output. The low speed operation allows a conventional ball bearing design for the rotating elements. This boost pump is installed just below the dual, in-series vortex generation flowmeters. Flexible line sections needed for gimbal motion connect it to the high speed turbopump.

#### 3.1.1.5 Oxygen Turbopump Assembly

The oxygen TPA is of the design lineage of the 3.0K lbf thrust oxygen TPA developed and partially tested in the NASA LeRC funded OTV engine program. (See Ref. 5 and 6). It has an inducer section, two pump stages, and a full admittance turbine to be driven by 400°F (maximum) gaseous oxygen (GOX) (current testing limited to ambient temperature GOX). The rotating assembly operates with a hydrostatic bearing assembly. There is no need for an interpropellant seal or a purge system. Materials selected for the TPA are copper and nickel in low stress areas, and monel 400 and K-500 where material strength is demanded. These materials were selected for best compatibility with oxygen, but the potential rub or friction areas are further protected by silver plating on the non-moving surfaces and a newly developed diamond film coating on the moving elements. This diamond film has the hardness of diamond, the slickness of teflon, and a thermal conductivity several times greater than pure copper. With this selection of materials and coatings the GOX driven LOX TPA is capable of full service life and all the required unassisted (i.e., rubbing) bearing starts required in the tank head start operation.

#### 3.1.1.6 Hydrogen Boost Pump

The low speed hydrogen boost pump is very similar in design to the low speed oxygen boost pump. It is a four stage pump driven by hydrogen from the first stage of the hydrogen TPA. Rated pressure at full thrust is 55 psia. It is located in the line just below the hydrogen flowmeters and is separated from the hydrogen TPA by flexible line sections that accommodate the gimbal motion requirements. Both low speed boost pumps are in an area that can be reached by an astronaut in a space suit. Component changeout will be possible with suitable line disconnects. The high speed TPAs, however, are packaged in a restricted area that would likely require engine removal for access. (See Figure 3.1-6).

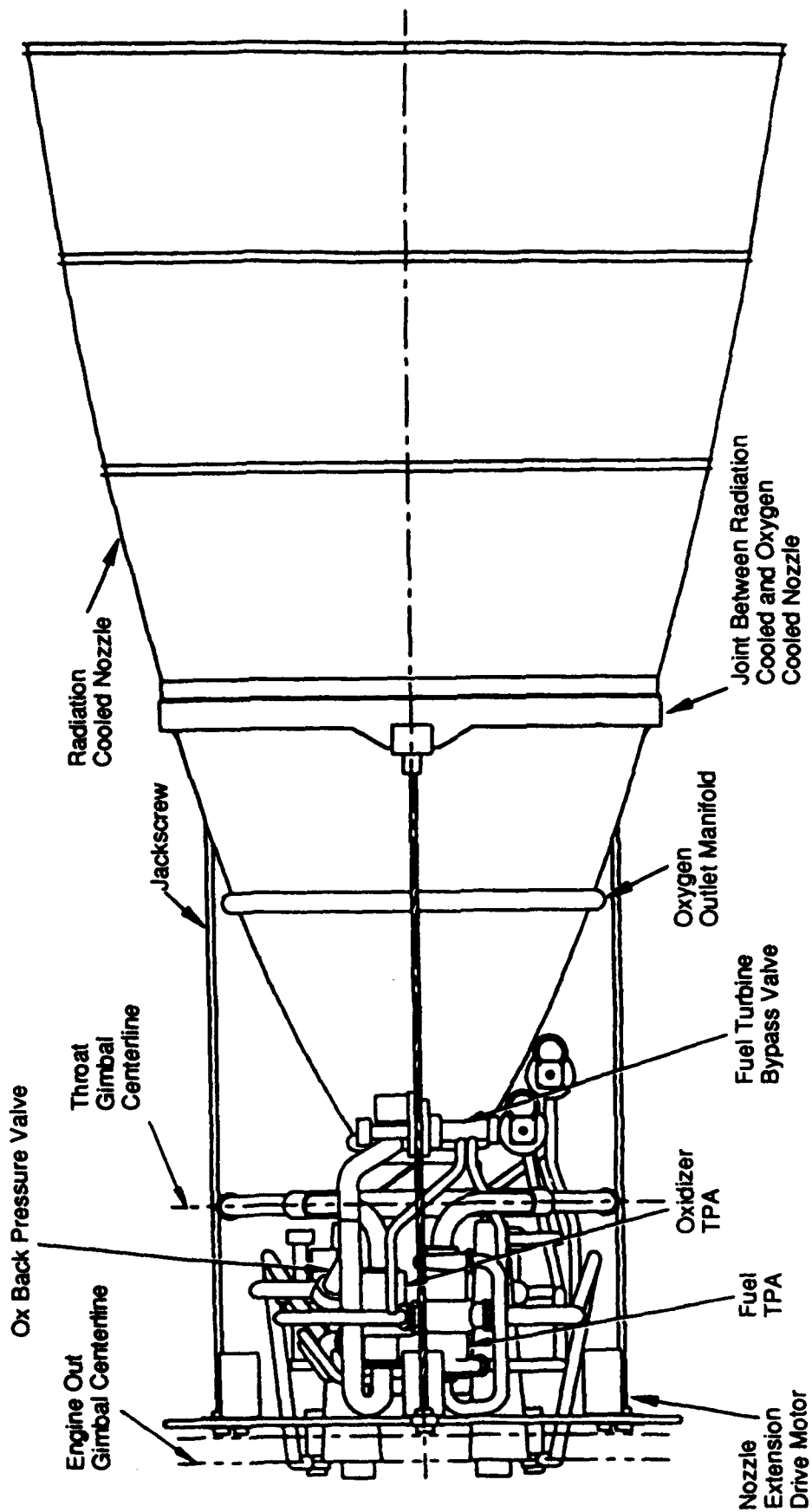


Figure 3.1-6. OTV Engine Preliminary Design Layout Drawing - Turbopump Side

### 3.1, Design and Parametric Analysis, (cont)

#### 3.1.1.7 Hydrogen Turbopump Assembly

Aerojet has developed a hydrogen TPA very similar in concept to that needed for the CTP engine. This TPA is used on the Air Force XLR-134 engine which is a low thrust LOX/LH<sub>2</sub> engine. That engine design features six pump stages and two turbines divided between separate contra-rotating shafts contained in the same housing. This double shaft system provides for a stout rotating assembly which does not exceed the critical speed over the normal operating range. For the CTP Engine, the design provides for an easier assembly and balance procedure. Each shaft will rotate at whatever speed is needed for the output requirements, but maximum speed at rated thrust is about 190,000 rpm. All bearings are hydrostatic to meet operating life requirements. The very tight clearances with a hydrostatic bearing system require careful materials selection so that expansion and contraction over the wide temperature range needed for cryogenic operation do not either bind the assembly or produce unacceptably high flow around the bearing. Materials must also lack susceptibility to hydrogen embrittlement.

#### 3.1.1.8 Hydrogen Regenerator

A regenerator is a heat exchanger used to transfer heat from the hydrogen gas exiting the turbine section of the TPA to the hydrogen stream directed through the baffle flow circuit. This converts what was waste heat into usable energy for driving the turbopump. The regenerator is downstream from the LOX/GH<sub>2</sub> heat exchanger and immediately upstream from the engine injector. One effect of the regenerator is to cool the hydrogen stream going into the injector. The result is a lowered overall injector temperature. The regenerator is an example of the Aerojet platelet technology originally developed for injectors but finding wide application in various flow devices. In appearance, it is a short block of metal shaped much like a dogbone with rounded structures at the ends being used for hydrogen inlet and outlet line connections. The very fine, close proximity flow passages characteristic of platelet design give an exceptionally efficient heat transfer structure. (See Figure 3.1-7). High  $\Delta T$ 's are maintained by counter-flowing the two streams. The baseline materials for the regenerator are zirconium copper platelets with either a silver or nickel bonding aid used in the brazing. A proposed light weight alternative is to use beryllium platelets.

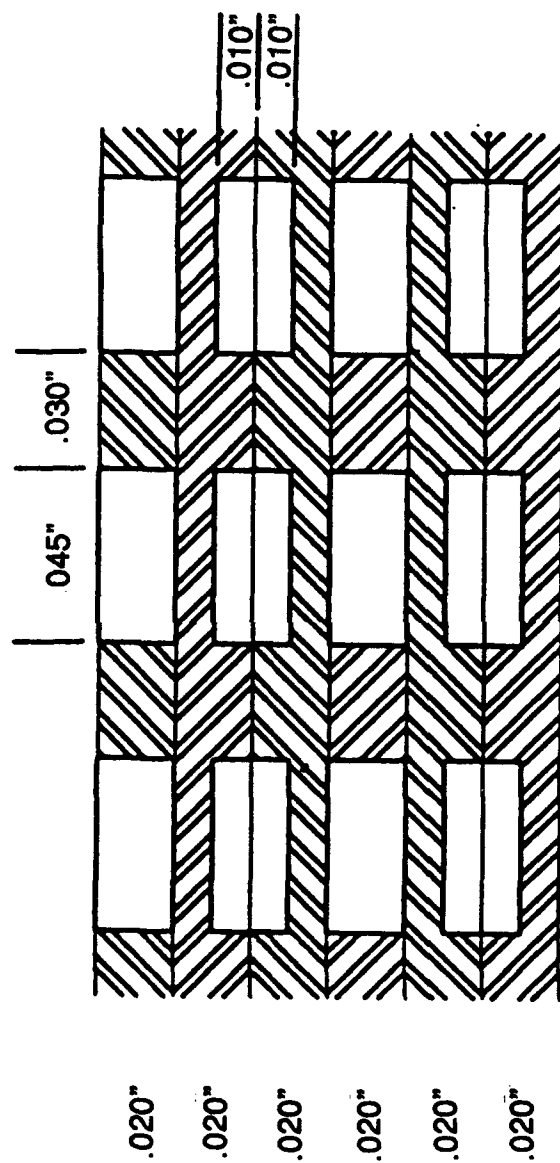


Figure 3.1-7. Advanced Engine Study -Regenerator Channel Details

### 3.1, Design and Parametric Analysis, (cont)

#### 3.1.1.9 Liquid Oxygen/Gaseous Hydrogen Heat Exchanger (HEX)

The HEX is a critical element in the operation of the dual expander engine. The engine cycle depends on the efficient heating of oxygen for turbine drive gas for the oxygen turbopump. The HEX provides one-half to two thirds of the enthalpy change needed with the balance gained in the oxygen cooled nozzle. The oxygen out of the high pressure pump is counter flowed with hydrogen coming from the hydrogen TPA turbine outlet. This gives a very high  $\Delta T$  for efficient heat transfer despite the poor heat transfer characteristics of oxygen. The HEX is similar in appearance and general construction to the regenerator. It is larger, with more flow passages to minimize pressure drop with the high flowrate of oxygen. The oxygen flow passages will depart from the straight rectangular flow passage design used on the hydrogen side in that they will include turbulence generating devices/geometries to prevent unmixed two phase flow. Two phase flow is caused by rapid film boiling as the oxygen changes from a liquid to a gas and is only a problem at low pressure operation. At rated thrust the oxygen traversing the HEX is supercritical and the phase change should take place uneventfully. The HEX is the preferred site of the phase change as the exiting stream next enters the oxygen cooled nozzle. The oxygen must be homogeneous to have predictable heat transfer characteristics for a critical cooling task. The materials for the HEX are zirconium copper or NASA-Z platelets with monel and/or inconel tubing for propellant inlet/outlet.

#### 3.1.1.10 Engine Valves and Basic Engine Control

The flight engine requires a set of 12 valves for normal operation. See Figure 2.1-1 for the valve position in the schematic. The major control valves and their functions are described below:

a. Hydrogen Flow Proportioner Valve — This valve is used to divide the cold hydrogen stream from the pump into two streams feeding the regen cooled chamber and the engine baffle plates. Its neutral position is at a 50-50 split. It can be commanded to adjust the flow  $\pm 25\%$  of total flow to either circuit. There is no existing design for this valve and several mechanisms are possible. It will be a 28 volt DC motor driven valve with separate drive coils with independent power sources for reliability. The dominant failure mode is to fail safe to a centered flow split. The valve

### 3.1, Design and Parametric Analysis, (cont)

is commanded to a particular position representing a flow-split that the engine controller has computed will optimize the hydrogen stream temperature going to the TPA turbine. This must be done in conjunction with the regenerator bypass valve position which sets the flow split for the hydrogen going through the regenerator or directly to the baffles. Any missetting of these two valves is compensated by an adjustment of the hydrogen turbine bypass valve which has its own independent feedback loop. At low thrust operation the proportioner will direct more flow through the chamber to control the bulk temperature rise while the regenerator bypass valve will go to full bypass. At full thrust a larger portion of the hydrogen flow will be directed to the baffle circuit with maximum flow through the regenerator. This gives the greatest thermal energy to the hydrogen TPA.

b. Hydrogen Regenerator Bypass Valve — This valve can direct all but 25% of the hydrogen baffle flow through the regenerator. The 25% is reserved as a control margin and can be reduced during overthrust or other abnormal operation. When the valve is fully open it is pressure balanced with the regenerator so that some flow always goes through the regenerator. The regenerator line may have to be orificed to assure that the minimum flow needed for low chamber pressure operation is attained. As noted above, the turbine bypass valve accommodates minor missettings of this valve by changing the amount of hydrogen bypassed around the turbine. The failure mode of this valve is fail-in-place with fail-full-open as an alternative. The valve will be powered by redundant 28 volt DC motors with independent power supplies.

c. Hydrogen Idle Valve — This valve is designed to provide mixture ratio control during tank head start. On start it is fully open to provide a low pressure drop passage to the injector. On light off the valve modulates between full open and closed to assist in setting the mixture ratio until the hydrogen turbine bypass valve becomes effective. Mixture ratio is computed from total hydrogen and oxygen flow rates. With the main shutoff valves designed for simple open or closed operation, the only possible mixture ratio control is to change the pressure drop in either the oxygen or hydrogen circuit. The oxygen has the lowest tank pressure but the hydrogen circuit has more components adding pressure drops. The hydrogen idle valve is positioned to open a low pressure drop path for some of the hydrogen. With the circuits balanced for a tank head start condition, the relatively small idle line is capable of the control needed

### 3.1, Design and Parametric Analysis, (cont)

using a modulating valve. The valve is designed to close at line pressures of 200 psia so that normal system pressurization can continue under increased output from the hydrogen TPA. A "close" signal should also be given by the controller when the hydrogen turbine bypass valve can assume responsibility for mixture ratio control. Unlike the other modulating valves, the idle valve must make a tight, leak free seal on closing. Its failure position is closed. Electrical redundancy is also needed for this valve.

d. Hydrogen Turbine Bypass Valve — This valve is in a line paralleling the circuit through the hydrogen TPA turbine. Closing the valve directs all hydrogen through the turbine. With the valve full open there will still be some flow through the turbine as the circuits will be pressure balanced. It is a modulating valve capable of stabilizing at any position from closed to full open. At nominal thrust it should be at the 10% bypass position for normal control authority. This control margin can be invaded for overthrust or other abnormal engine operation. The controller will direct the valve to a particular position corresponding to the commanded thrust and mixture ratio. It will then modulate based on feedback as to actual operation. When a thrust or mixture ratio change is commanded the oxygen turbine bypass will start the movement to the new position. The hydrogen turbine bypass valve will follow so that the change is synchronized. After the oxygen turbine bypass valve has stabilized, the hydrogen turbine bypass valve will make the final position change for mixture ratio tuning. The bypass valve will also compensate for any initial missetting of the regenerator bypass and hydrogen proportioner valves as reflected by the hydrogen temperature and pressure to the turbine. This compensation will be automatic up to the 10% bypass minimum. The controller uses flowmeter readings for the hydrogen and oxygen circuits to derive both thrust and mixture ratio information. This is correlated with thrust calculated from chamber pressure. Flowmeter readings are also compared with flowrate calculated from turbopump speed and output pressure. This is particularly useful at low thrust operation where flowmeter readings have the greatest errors.

e. HEX Bypass Valve — The temperature of the oxygen entering the turbine is controlled by the HEX bypass valve. This valve is on the hydrogen side as it was judged better to route all oxygen through the HEX to assure the phase change is completed prior to entering the oxygen cooled nozzle. The hot hydrogen from the

### 3.1, Design and Parametric Analysis, (cont)

TPA turbine discharge is counterflowed with the liquid oxygen just discharged from the oxygen TPA to give the oxygen about two thirds of the enthalpy change needed to power the oxygen TPA turbine. The bypass valve adjusts the hydrogen flow based on feedback from the oxygen turbine inlet temperature for a not-to-exceed maximum of 400°F and from the controller for an initial positioning corresponding to the commanded engine thrust. This valve and the oxygen turbine bypass valve will be closely synchronized so that there is no controls "hunting" during thrust changes. For instance, on receiving a throttle up command the oxygen HEX bypass valve will go to the 25% bypass position until the oxygen to the turbine approaches 400°F. At that point, the turbine bypass valve will modulate to hold the selected thrust and the HEX bypass will hold a stable temperature. This adds stability to the hydrogen circuit as the hydrogen temperature to the regenerator will stay within a narrow range. The regenerator bypass valve, then, has only a small amount of movement related to temperature compensation. The valve will operate from 25% bypass to about 100% bypass (based on power balance runs) to cover the engine operating range. Specifications for this valve will be very similar to the hydrogen turbine bypass valve.

f. Oxygen Turbine Bypass Valve — This valve is used for engine thrust control. The controller commands it to move to a designated position corresponding to the desired thrust. After the move is made, feedback information on total propellant flowrate and chamber pressure is used to trim the position to a setting corresponding to actual engine thrust. The hydrogen turbine bypass valve moves in step with the oxygen turbine bypass valve until the designated position is reached. At that time the hydrogen turbine bypass valve will modulate to establish commanded engine mixture ratio. The oxygen turbine bypass valve was selected for thrust control as percent bypass is very linear with thrust. It is the master control valve for the engine. The technique of commanding a modulating valve to a specific position in a "look-up table" for setting thrust requires both well established valve operating characteristics and a position indicator of high reliability and accuracy.

The oxygen turbine bypass valve must be fabricated from materials found compatible with hot oxygen. Copper, nickel, several of the monels, and various ceramic materials are good candidates.

### 3.1, Design and Parametric Analysis, (cont)

g. Ignitor Valves — Simple poppet type valves are suitable for use on the one quarter inch ignitor propellant lines. The hydrogen valve will have a calibrated leak path around the seat to allow hydrogen flow through the ignitor cavities for cooling. Each valve will have dual redundant electrical actuation coils for reliability. Ignitor flow is routed to two separate ignitors. These ignitors use laser ignition with two lasers in each ignitor and two separate power supplies for reliability. The valves must close at high (>300 psia) line pressures.

#### 3.1.1.11 Engine Controller

Aerojet has developed an engine controller for the Advanced Launch System (ALS) engine that can be readily modified to CTP engine requirements.

#### 3.1.1.12 Health Monitoring System

This CTP Advanced Engine was designed with an integrated control and health monitoring (ICHM) system baselined. All engine components will have designed-in sensors selected to meet overall system requirements. Sensor data is evaluated by health monitor algorithms in a computer. Selected data streams and computed information are used for immediate action by the engine controller, or stored for later maintenance decisions. As an example, during throttle-down operation the lower flowrate of hydrogen through the regen chamber reduces cooling effectiveness. Should throat temperature approach 800°F the health monitor system will signal the engine controller that continued operation at the selected thrust load will require a mixture ratio change to increase hydrogen flow (and chamber cooling) or a change in the proportioner valve setting to direct more hydrogen to the chamber circuit. This is decision-making to protect hardware and extend its life. More pressing failure indications would lead to a shutdown prior to a catastrophic failure. The fact that this is a decision-making system supports some software development using expert systems and artificial intelligence techniques.

#### 3.1.2 Power Balance

A rocket engine power balance is an energy and mass balance computed at a particular point within the engine operating envelope. If a computation does

### 3.1, Design and Parametric Analysis, (cont)

balance (i.e., there is a solution within the capability of the engine components), then the point is, by definition, within the engine operating envelope. If there is no balance (generally indicated by a failure to close on a solution after a defined number of iterations), the selected point is outside of the engine operating envelope. An array of balance points on a plot of chamber pressure versus mixture ratio is used by Aerojet to define the engine operating envelope. Thrust or total propellant flowrate could be substituted for chamber pressure to generate similar operating envelopes. As an example, Figure 3.1-10 is the operating envelope for the series flow dual expander cycle used in the 7.5K lbf thrust engine design.

#### 3.1.2.1 Power Balance Development

A power balance can be hand calculated from the basic equations through 3 or 4 iterations in about 4 hours. The Aerojet OTV engine power balance program from data input to printout takes about 15 minutes. This time savings was achieved at a heavy input of programming hours in developing the code. It is now in its fifth generation with the most recent modeling required to change from a series flow to a parallel flow dual expander cycle.

Each active component must be modeled for a look-up table within the program. Figure 3.1-11 gives some examples of the algorithms used for various components. For this study actual preliminary designs had to be defined at each of the five selected thrusts for accurate component modeling. This was particularly true of the turbopumps and the thrust chamber injectors. The initial design point for each turbopump was determined (See Tables 3.1-5 and 3.1-6) and performance curves calculated (Figures 3.1-12 and 3.1-13). An equation is then developed for each curve, or points on the curves are converted to an array of numbers for use in a lookup table. The thrust chamber/injector was thermally modeled so that hot gas side wall temperatures at rated thrust/design thrust were below the maximum. Also, preliminary configuration studies were completed to determine baffle geometry and length. Very early in the study a common 2000 psia chamber pressure was selected for each thrust as the rated or nominal full thrust point (100% thrust). A worst case design point of 2000 psia and  $MR = 5$  was selected for the thermal maximum expected operating point (MEOP). The chamber design was adjusted so that hot gas side wall temperature would not exceed

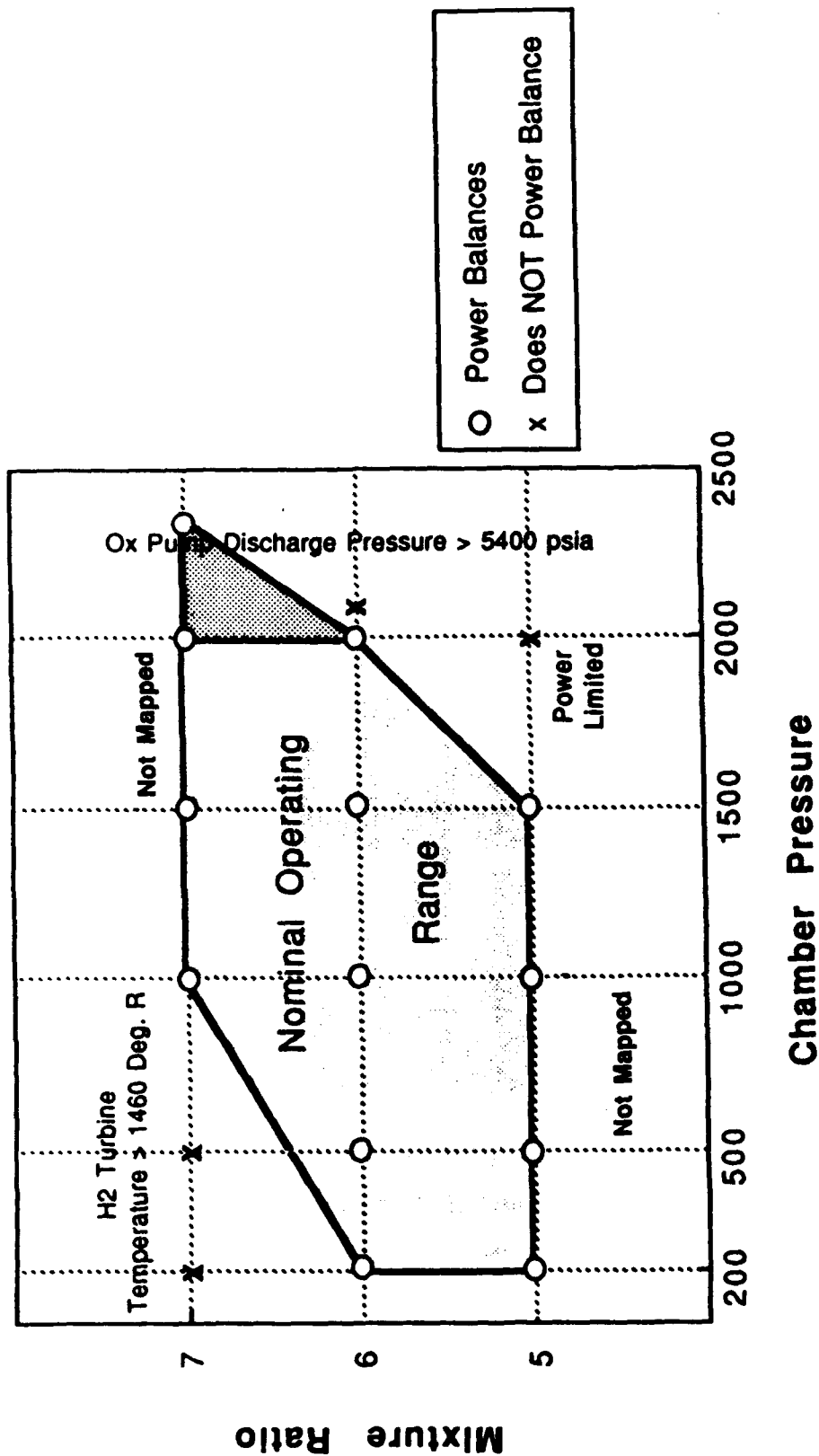


Figure 3.1-10. 7.5K lbf Thrust Preliminary Design Engine Operating Envelope

## MAIN PUMP

Head =  $\Delta H * 778$   
 rpm =  $Q/N$ ,  $H^2//N$  Curves  
 eff = eff Curves  
 HP =  $w * \Delta P / (Rho * eff)$

## TURBINE

$U = Dia * N * CNV$   
 $Co = (2 * g * \Delta H_{ideal})^{.5}$   
 eff =  $f(U, Co) = \Delta H_{ideal} / \Delta H_{actual}$   
 HP =  $w * eff * \Delta H_{ideal}$

## HEAT EXCHANGER

<u>Cool Side</u>	<u>Hot Side</u>
Set Outlet Temperature	$Q_h = -Q_c$
$Q_c = w \Delta H$	
25% Bypass	

## VALVES

Set Flow Area (CdA)  
 Gas or Liquid Orifice  
 Subroutine to calculate  
 Outlet Pressure

Figure 3.1-11. Component Modeling

Table 3.1-5. Advanced Engine Study Turbopump Design Point-Pump Section

Oxygen Pump @MR = 6									
Thrust Level (lbf)	Pin/Pout	DP (psia)	Q/N (gpm/rpm)	Eff	HP (HP)	N (rpm)	W dot (lbm/sec)	Tin (R)	Tout (R)
7500	0.002823	5298	0.001645	0.740	361.3	52833	13.785	162.7	186.2
20000	0.003985	3749	0.005262	0.680	739.7	44773	37.368	162.7	183.1
25000	0.004008	3727	0.007415	0.680	922.1	39853	46.874	162.7	183.0
35000	0.004011	3724	0.011949	0.680	1276.0	34061	64.532	162.9	183.2
50000	0.003947	3785	0.020100	0.680	1848.6	28869	91.989	162.9	183.6
Hydrogen Pump @MR = 6									
Thrust Level (lbf)	Pin/Pout	DP (psia)	Q/N (gpm/rpm)	Eff	HP (HP)	N (rpm)	W dot (lbm/sec)	Tin (R)	Tout (R)
7500	0.004664	4230	0.001845	0.570	975.0	122725	2.188	38.1	116.5
20000	0.005002	3939	0.006717	0.648	2082.3	95934	6.228	38.1	87.1
25000	0.004993	3946	0.009483	0.648	2618.5	85257	7.812	38.1	87.1
35000	0.004840	4073	0.014935	0.648	3712.3	74579	10.755	38.2	88.8
50000	0.004194	4703	0.022816	0.649	6039.2	69658	15.332	38.3	95.9

\*\*\*\*\*

**Table 3.1-6. Advanced Engine Study Turbopump Design Point-Turbine Section**

Thrust Level (lbf)	Oxidizer Turbine GMR = 6						
	Pin/Pout	DP (psia)	U/Co (fps/fps)	Eff	HP (HP)	Wheel Dia (in)	W dot (lbm/sec)
7500	2.044571	2415	0.3100	0.561	359.5	1.82	12.406
20000	1.436482	1023	0.5080	0.820	743.0	2.54	33.538
25000	1.434136	1014	0.5070	0.820	925.7	2.85	41.906
35000	1.433931	1017	0.5090	0.820	1274.9	3.34	57.725
50000	1.441653	1036	0.5080	0.820	1848.2	3.98	82.102
							Tin (R)
							860.0
							855.0
							856.3
							856.2
							860.0
							Tout (R)
							765.6
							786.1
							787.6
							787.5
							790.1

Thrust Level (lbf)	Hydrogen Turbine GMR = 6						
	Pin/Pout	DP (psia)	U/Co (fps/fps)	Eff	HP (HP)	Wheel Dia (in)	W dot (lbm/sec)
7500	1.565509	1237	0.2290	0.595	972.1	2.35	1.908
20000	1.481043	1153	0.3160	0.814	2082.1	3.09	5.402
25000	1.441422	1053	0.3190	0.814	2616.5	3.47	6.920
35000	1.411629	969	0.3200	0.814	3709.8	4.04	9.544
50000	1.480707	1133	0.3190	0.814	6020.2	4.64	13.397
							Tin (R)
							1373.5
							829.9
							875.1
							960.1
							979.9
							Tout (R)
							1280.1
							759.5
							805.7
							888.0
							896.7

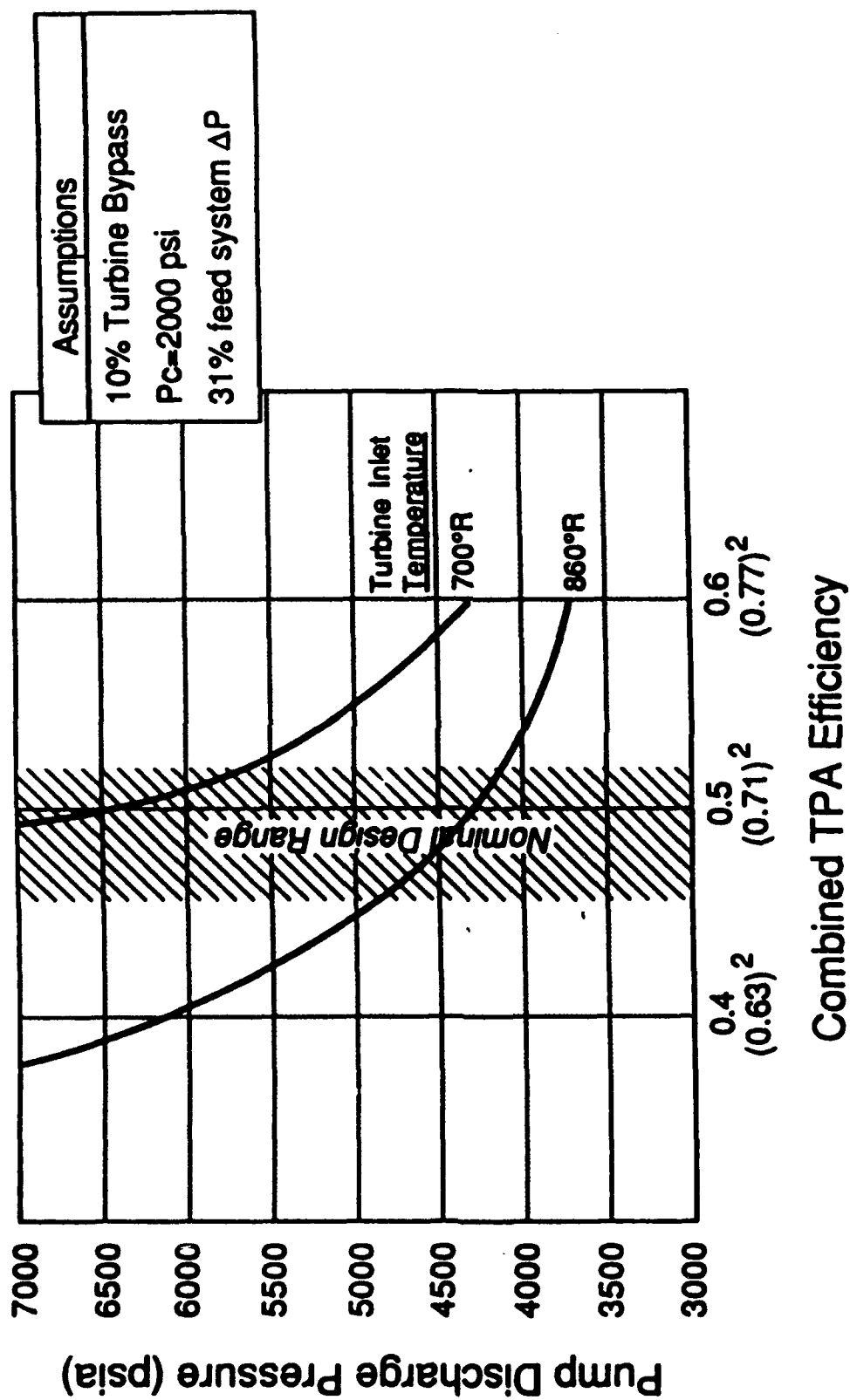


Figure 3.1-12. Oxygen Power Balance - Combined TPA Efficiency

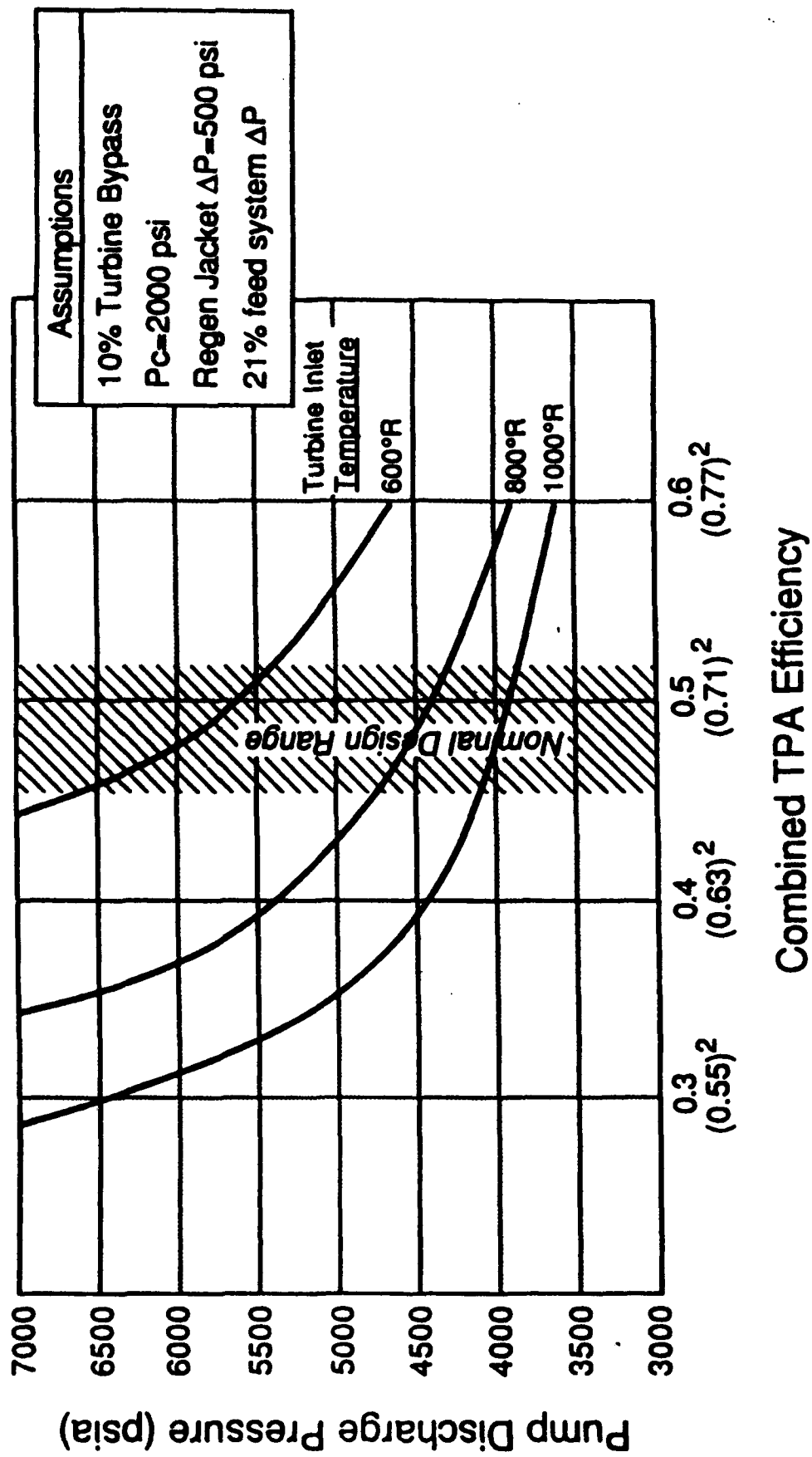


Figure 3.1-13. Hydrogen Power Balance - Combined TPA Efficiency

### 3.1, Design and Parametric Analysis, (cont)

the design maximum at MEOP. The power limiting operating point was expected to be at a chamber pressure of 2300 psia and  $MR = 7$ . Also, the pressure and temperature calculated for this point would be used for stress calculations. This point was not necessarily within the actual operating envelope at all five engine thrust levels. It is a conservative design point. The overthrust capability at 2300 psia chamber pressure is a useful feature of the engine design. With the components modeled, the power balance development followed the logic path as shown in Figure 3.1-14.

The power balance program begins by balancing the oxygen circuit (see Figure 3.1-15). The HEX heat transfer rate is the most significant thermal coupling between the circuits. It is used as an entry to balancing the hydrogen circuit (see Figure 3.1-16). The operator has several inputs that can be adjusted to assist in the balance. It is an interactive program in that the operator can watch the iterations in progress on the computer terminal and make real time adjustments if the iterations show it is not closing. Propellant property data is looked up in NBS or NASA derived tables for accurate calculations at each point in the cycle. This property data lookup capability requires the program be run on the PRIME or the VAX computers. The actual program architecture is based on a commercial spread sheet program.

#### 3.1.2.2 Power Balance Results

The chart in Figure 3.1-17 summarizes the power balance results for the 7.5K lbf thrust engine at rated thrust. One of the features of the program is the ability to iterate the effect of turbine wheel diameter on TPA performance. In this example a 2.35 inch wheel diameter was used. Figure 3.1-18 gives the power balance results for the parallel flow 20K lbf thrust engine. The operating temperature and pressures are much lower for the parallel flow version but the chamber pressure is the same. Tables 3.1-7 through 3.1-12 give the important temperatures and pressures for engines of 20K lbf thrust and 50K lbf thrust at mixture ratios of 5, 6, and 7. A gratifying result of the power balance work was the ability of the cycle to sustain a 2000 psia chamber pressure over the entire thrust range of interest. The engine envelopes were explored to see what the maximum chamber pressure would be, given the baseline component performance. For the 20,000 lbf thrust engine the maximum chamber pressure at  $MR = 7$  was over 2500 psia giving a 25% overthrust capability. For the 50,000 lbf thrust engine the

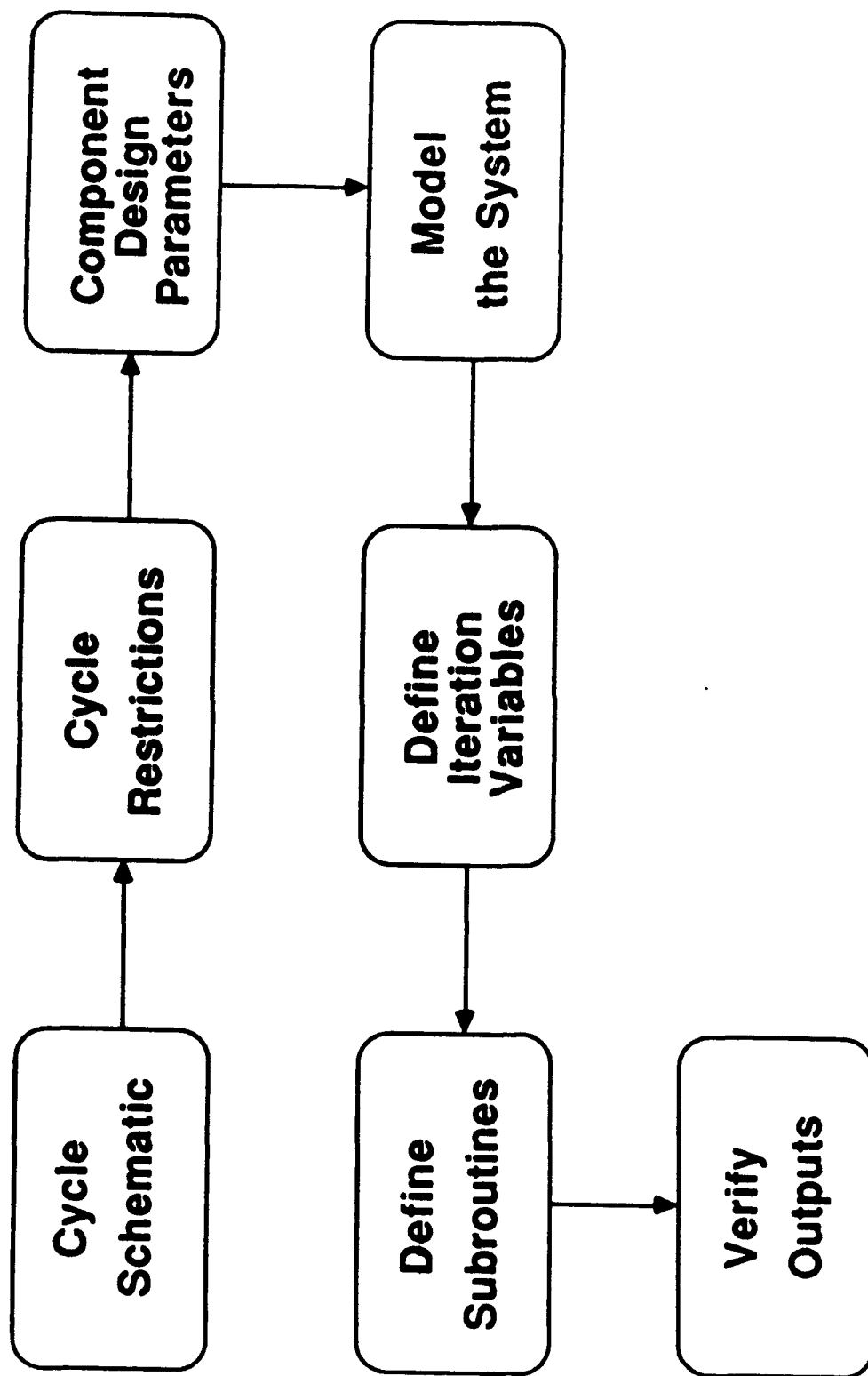


Figure 3.1-14. Logic Path in Computerizing a Power Balance

# OXYGEN CIRCUIT

- Input  $\dot{W}_{pump}$ ,  $P_c$
- Guess  $P_d$ ,  $\dot{W}_{turb}$ ,  $T_{injo}$ ,  $T_{ti}$
- Calculate intermediate  $T$  &  $P$
- Calculate horsepower requirements and horsepower availability

- Iterate until consistent

$$hp \text{ req} / hp \text{ avail} = 1$$

$$T_{injo} / T_{calc} = 1$$

$$\dot{W}_{turb} / \dot{W}_{calc} = 1$$

$$P_d = \text{minimum}$$

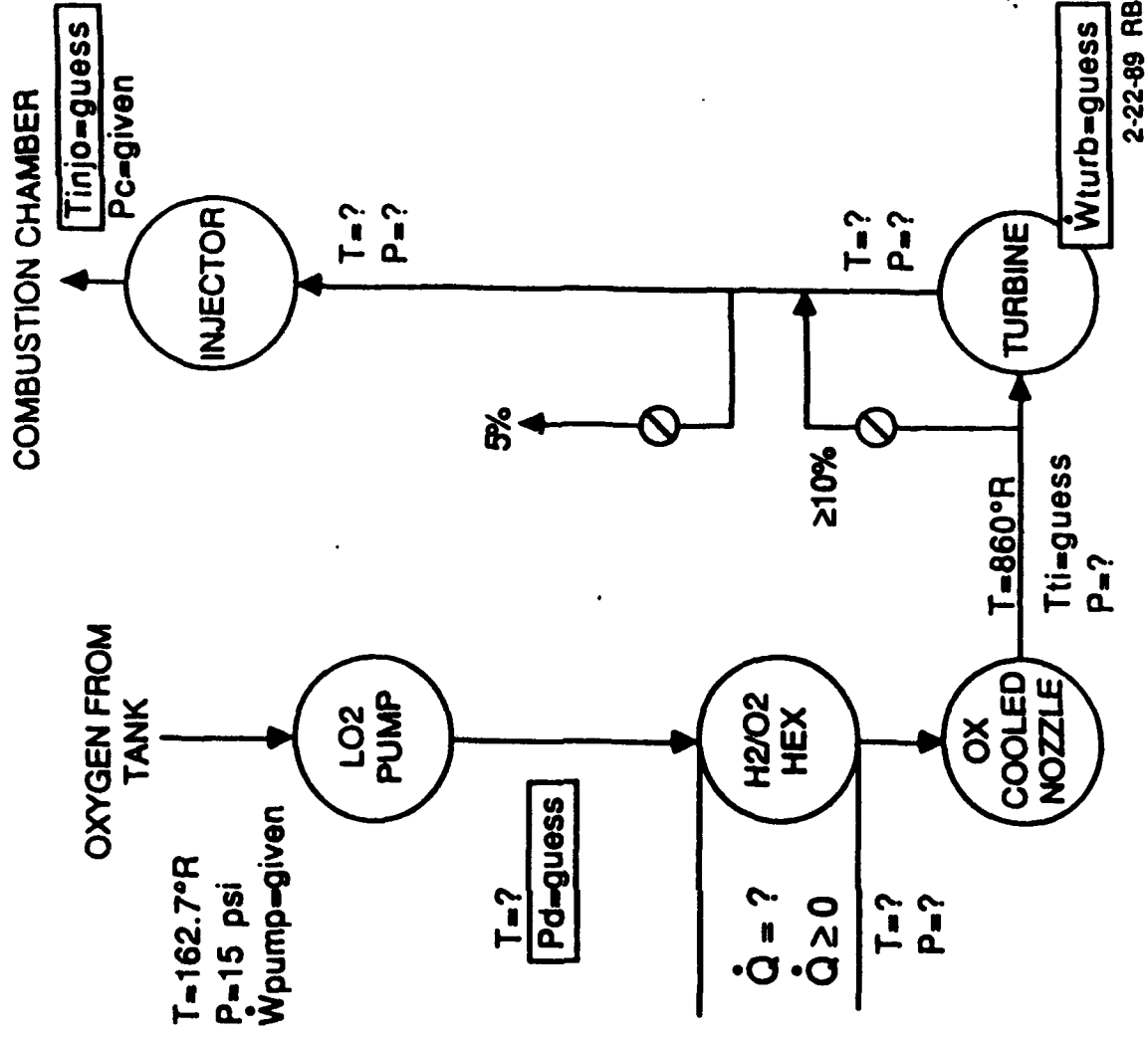
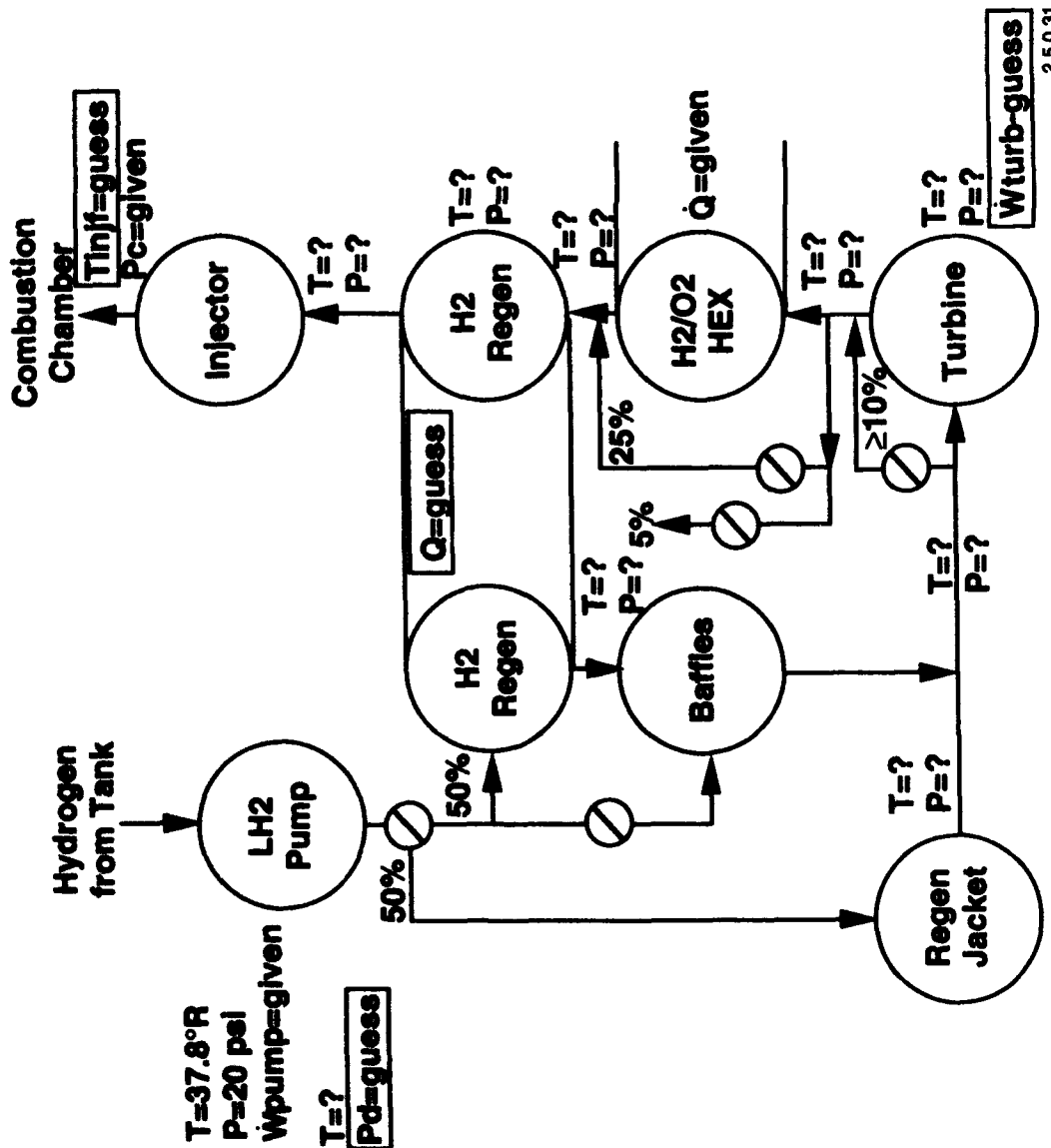


Figure 3.1-15. The Oxidizer Side is Balanced First

# HYDROGEN CIRCUIT



- Input  $\dot{W}_{\text{pump}}$ ,  $P_c$ ,  $Q$
- Guess  $P_d$ ,  $\dot{W}_{\text{turb}}$ ,  $T_{\text{inj}}$ ,  $\Delta T_{\text{regc}}$
- Calculate intermediate  $T$  &  $P$
- Calculate horsepower requirements and horsepower availability
- Iterate until consistent  
 $\text{hp req}/\text{hp avail} = 1$   
 $T_{\text{inj}}/T_{\text{calc}} = 1$   
 $\dot{W}_{\text{turb}}/\dot{W}_{\text{calc}} = 1$   
 $P_d = \text{minimum}$

Figure 3.1-16. The Fuel Side Uses Results from Ox Side Balance

# HYDROGEN CIRCUIT

# OXYGEN CIRCUIT

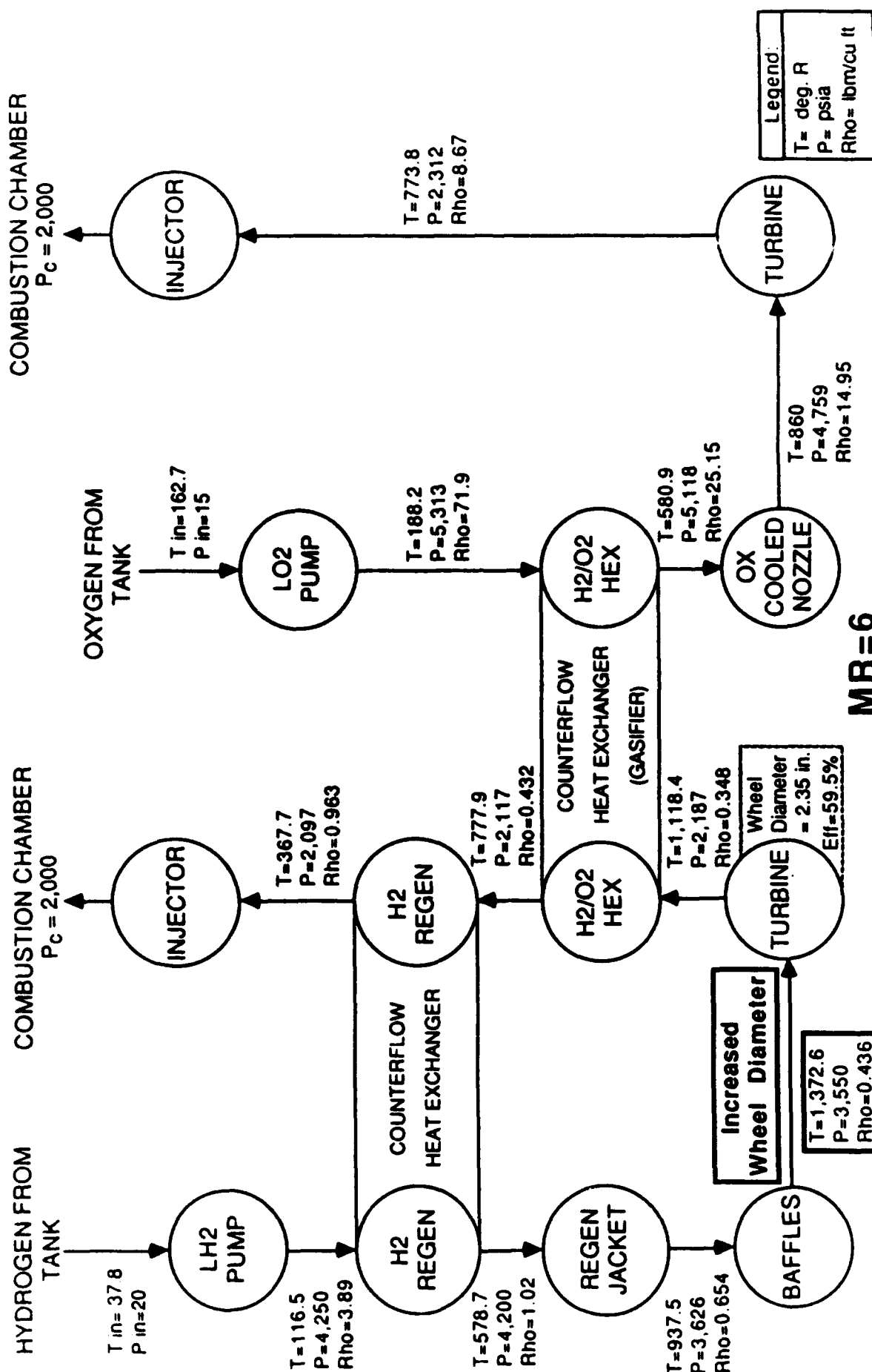


Figure 3.1-17. 7.5K lbf Thrust OTV Engine Preliminary Design Power Balance

## HYDROGEN CIRCUIT

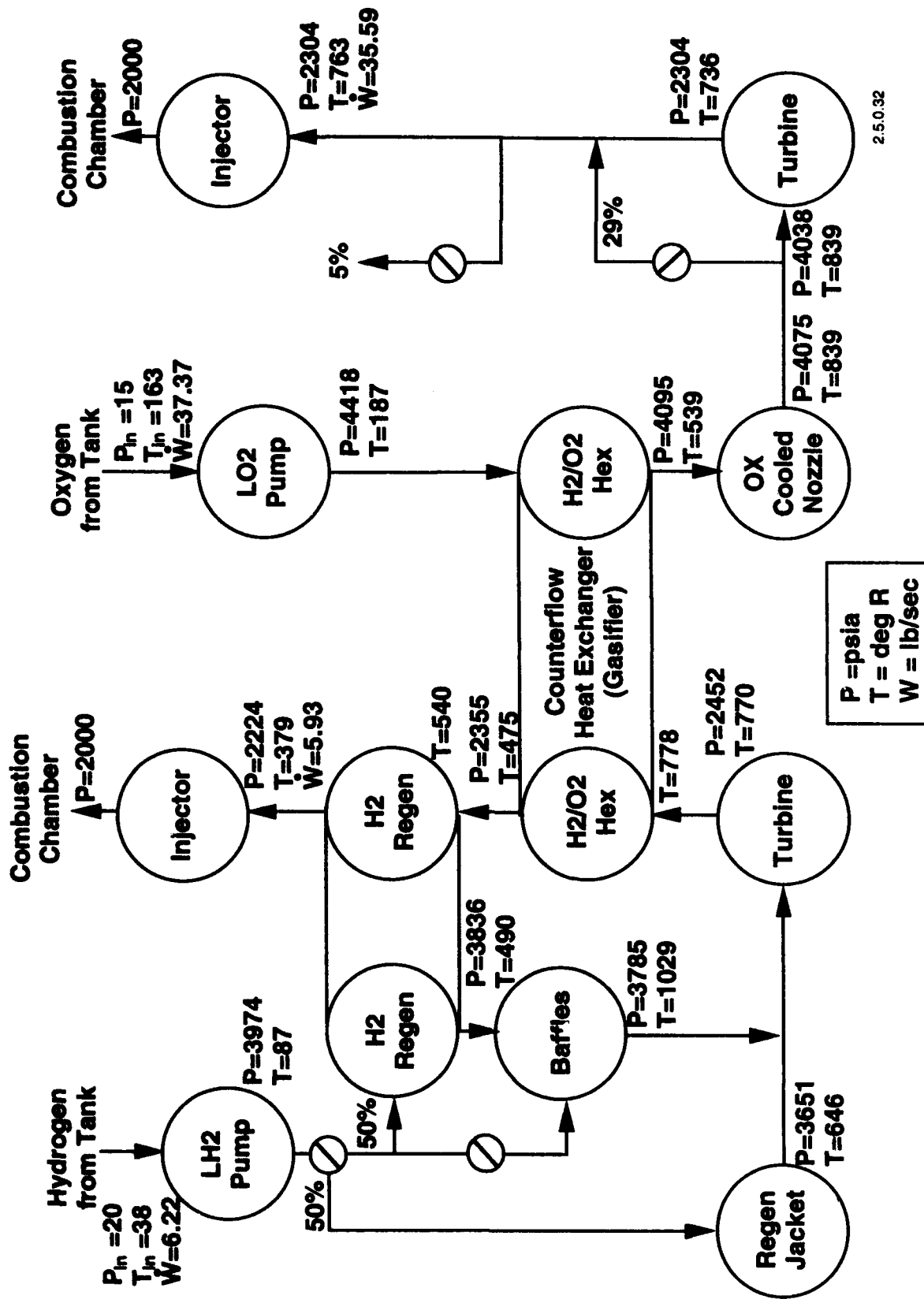


Figure 3.1-18. Power Balance Results for 20K lbf Engine at MR = 6

**TABLE 3.1-7****CTP ENGINE POWER BALANCE  
THRUST = 20K lbf    MR = 5**

	Oxidizer			Fuel	
Tank Conditions	P=	15.0	(psia)	20.0	(psia)
	T=	162.7	(deg R)	37.8	(deg R)
Pump Conditions	P=	3629.8	(psia)	4543.4	(psia)
	T=	182.4	(deg R)	93.5	(deg R)
Ox: Cool Side Heat Exchanger	P=	3319.7	(psia)		
	T=	537.0	(deg R)		
Fuel: Cool Side Regenerator	P=			4363.5	(psia)
	T=			478.4	(deg R)
Regen Jacket	P=			4122.8	(psia)
	T=			601.5	(deg R)
Baffles	P=			4319.1	(psia)
	T=			994.1	(deg R)
Ox Nozzle Cooling	P=	3292.2	(psia)		
	T=	860.0	(deg R)		
Turbine Conditions	P=	2307.6	(psia)	2595.7	(psia)
	T=	794.4	(deg R)	723.2	(deg R)
Hot Side HEX	P=			2409.8	(psia)
	T=			462.0	(deg R)
Gas Side Regenerator	P=			2224.1	(psia)
	T=			373.9	(deg R)
Injector	P=	2009.6	(psia)	2003.3	(psia)
	T=	800.4	(deg R)	373.9	(deg R)
Combustion Chamber, Pc			2000 psia		

**TABLE 3.1-8**

**CTP ENGINE POWER BALANCE**  
**THRUST = 20K lbf      MR = 6**

	Oxidizer			Fuel	
Tank Conditions	P=	15.0	(psia)	20.0	(psia)
	T=	162.7	(deg R)	37.8	(deg R)
Pump Conditions	P=	3764.2	(psia)	3958.7	(psia)
	T=	183.1	(deg R)	87.1	(deg R)
Ox: Cool	P=	3441.0	(psia)		
Side Heat Exchanger	T=	555.0	(deg R)		
Fuel: Cool	P=			3822.5	(psia)
Side Regenerator	T=			466.3	(deg R)
Regen Jacket	P=			3635.0	(psia)
	T=			646.1	(deg R)
Baffles	P=			3782.5	(psia)
	T=			1012.5	(deg R)
Ox Nozzle Cooling	P=	3411.3	(psia)		
	T=	855.0	(deg R)		
Turbine Conditions	P=	2343.3	(psia)	2397.5	(psia)
	T=	786.1	(deg R)	759.5	(deg R)
Hot Side HEX	P=			2300.5	(psia)
	T=			435.6	(deg R)
Gas Side Regenerator	P=			2169.8	(psia)
	T=			365.7	(deg R)
Injector	P=	2015.4	(psia)	2002.9	(psia)
	T=	792.5	(deg R)	365.7	(deg R)
Combustion Chamber, Pc			2000 psia		

TABLE 3.1-9

**CTP ENGINE POWER BALANCE**  
**THRUST = 20K lbf      MR = 7**

	Oxidizer			Fuel	
Tank Conditions	P=	15.0	(psia)	20.0	(psia)
	T=	162.7	(deg R)	37.8	(deg R)
Pump Conditions	P=	3875.3	(psia)	3705.1	(psia)
	T=	183.8	(deg R)	84.9	(deg R)
Ox: Cool Side Heat Exchanger	P=	3547.1	(psia)		
	T=	586.8	(deg R)		
Fuel: Cool Side Regenerator	P=			3600.7	(psia)
	T=			403.7	(deg R)
Regen Jacket	P=			3393.0	(psia)
	T=			675.9	(deg R)
Baffles	P=			3573.1	(psia)
	T=			1009.7	(deg R)
Ox Nozzle Cooling	P=	3512.8	(psia)		
	T=	856.8	(deg R)		
Turbine Conditions	P=	2378.2	(psia)	2305.8	(psia)
	T=	785.2	(deg R)	776.7	(deg R)
Hot Side HEX	P=			2231.8	(psia)
	T=			377.0	(deg R)
Gas Side Regenerator	P=			2133.4	(psia)
	T=			349.4	(deg R)
Injector	P=	2011.6	(psia)	2002.9	(psia)
	T=	792.9	(deg R)	349.4	(deg R)
Combustion Chamber, Pc			2000 psia		

**TABLE 3.1-10**  
**CTP ENGINE POWER BALANCE**  
**THRUST = 50K lbf      MR = 5**

	Oxidizer		Fuel	
Tank Conditions	P=	15.0 (psia)	20.0 (psia)	
	T=	162.7 (deg R)	37.8 (deg R)	
Pump Conditions	P=	3670.7 (psia)	5555.5 (psia)	
	T=	182.9 (deg R)	104.7 (deg R)	
Ox: Cool Side Heat Exchanger	P=	3404.6 (psia)		
	T=	560.0 (deg R)		
Fuel: Cool Side Regenerator	P=		5479.5 (psia)	
	T=		606.9 (deg R)	
Regen Jacket	P=		4044.3 (psia)	
	T=		554.7 (deg R)	
Baffles	P=		5376.1 (psia)	
	T=		1354.0 (deg R)	
Ox Nozzle Cooling	P=	3317.4 (psia)		
	T=	860.0 (deg R)		
Turbine Conditions	P=	2311.9 (psia)	2504.7 (psia)	
	T=	793.2 (deg R)	862.7 (deg R)	
Hot Side HEX	P=		2351.7 (psia)	
	T=		585.6 (deg R)	
Gas Side Regenerator	P=		2224.1 (psia)	
	T=		448.5 (deg R)	
Injector	P=	2006.2 (psia)	2003.6 (psia)	
	T=	799.3 (deg R)	448.5 (deg R)	
Combustion Chamber, Pc				2000 psia

TABLE 3.1-11

**CTP ENGINE POWER BALANCE**  
**THRUST = 50K lbf      MR = 6**

	Oxidizer			Fuel	
Tank Conditions	P=	15.0	(psia)	20.0	(psia)
	T=	162.7	(deg R)	37.8	(deg R)
Pump Conditions	P=	3800.3	(psia)	4722.9	(psia)
	T=	183.6	(deg R)	95.9	(deg R)
Ox: Cool	P=	3523.0	(psia)		
Side Heat Exchanger	T=	582.0	(deg R)		
Fuel: Cool	P=			4665.6	(psia)
Side Regenerator	T=			589.1	(deg R)
Regen Jacket	P=			3588.6	(psia)
	T=			589.6	(deg R)
Baffles	P=			4577.5	(psia)
	T=			1368.6	(deg R)
Ox Nozzle Cooling	P=	3425.8	(psia)		
	T=	860.0	(deg R)		
Turbine Conditions	P=	2346.0	(psia)	2357.1	(psia)
	T=	790.1	(deg R)	896.7	(deg R)
Hot Side HEX	P=			2253.1	(psia)
	T=			550.2	(deg R)
Gas Side Regenerator	P=			2169.7	(psia)
	T=			453.1	(deg R)
Injector	P=	2006.1	(psia)	2004.6	(psia)
	T=	796.9	(deg R)	435.1	(deg R)
Combustion Chamber, Pc			2000 psia		

**TABLE 3.1-12****CTP ENGINE POWER BALANCE  
THRUST =50K lbf      MR =7**

	Oxidizer			Fuel	
Tank Conditions	P=	15.0	(psia)	20.0	(psia)
	T=	162.7	(deg R)	37.8	(deg R)
Pump Conditions	P=	3943.0	(psia)	4193.9	(psia)
	T=	184.4	(deg R)	90.3	(deg R)
Ox: Cool Side Heat Exchanger	P=	3658.1	(psia)		
	T=	607.8	(deg R)		
Fuel: Cool Side Regenerator	P=			4149.4	(psia)
	T=			562.0	(deg R)
Regen Jacket	P=			3315.1	(psia)
	T=			611.3	(deg R)
Baffles	P=			4058.4	(psia)
	T=			1399.9	(deg R)
Ox Nozzle Cooling	P=	3553.1	(psia)		
	T=	857.8	(deg R)		
Turbine Conditions	P=	2387.2	(psia)	2271.3	(psia)
	T=	784.6	(deg R)	929.5	(deg R)
Hot Side HEX	P=			2194.8	(psia)
	T=			506.4	(deg R)
Gas Side Regenerator	P=			2135.1	(psia)
	T=			419.6	(deg R)
Injector	P=	2011.6	(psia)	2004.8	(psia)
	T=	792.2	(deg R)	419.6	(deg R)
Combustion Chamber, Pc			2000 psia		

### 3.1, Design and Parametric Analysis, (cont)

maximum chamber pressure was about 2100 psia at  $MR = 7$ . There is a dropoff with increasing thrust, but it is less than was expected before the study calculations were completed. With these encouraging results the baseline of 2000 psia chamber pressure was kept throughout the study.

Additional power balances are given in Appendix B for the high mixture ratio operation.

#### 3.1.2.3 Modified Liquid Engine Transient Simulation Program (MLETS) Analysis

The power balance program discussed in the previous paragraphs assumes steady state engine operation with no consideration of the time dependency of the engine operation. The MLETS program performs similar mass and energy balances but adds the time dependent features of the components and engine system. The MLETS is the most recent version of the LETS program which has been in development for several years at Aerojet. Its complexity is about an order of magnitude greater than the OTV power balance program. It was also developed for other engine systems and has had to be adapted to the OTV engine. In its present form it still requires some development to make it easily usable with the OTV engine, but the preliminary results presented below show it to be a valuable tool for predicting engine operation and control requirements.

a. Uses of the MLETS Program — The MLETS can provide valuable insight into many design concerns as it includes models for all components and lines. Concerns of current interest are:

- Power balance (backup to the independent power balance program).
- Engine sensitivities to component design changes.
- Control sensitivities to component operation and engine operating scenarios.

### 3.1, Design and Parametric Analysis, (cont)

- Engine stability in operation.
- Engine transient response time and linearity. This includes start, throttling, and shutdown.
- Ready assessment of different engine configurations without extensive code reprogramming due to its modular structure.

The program hours assigned to this task were insufficient to do much more than a preliminary assessment of the engine transient operation. None of the concerns given above were addressed in the depth desired.

b. Preliminary Results of the MLETS Analysis — The simplified engine schematic used for the MLETS analysis is given in Figure 3.1-19. The LI numbers refer to the hydraulic model for that particular line. PU 101 and PU 201 refer to the TPA pump sections while TU 101 and TU 201 refer to the models for the TPA turbines. The HEX is HE 101 and the regenerator is HE 102. It should be evident that the MLETS analysis is limited by the accuracy of the algorithms used to model these and the other components. In particular, the time dependency of component performance is suspect until actual components are built and rates of temperature and pressure change are measured. In practise, the component lags, efficiencies, and other performance parameters were adjusted by the program operator until a relatively stable operating configuration was found. The ability to do this in real time makes the MLETS a valuable design tool. In effect, the component design can be adjusted to match the circuit. When this program shows that a stable design point has been determined this can be fed back to the component design team to be used for details of the actual design.

1. Bootstrap Capability. The oxidizer side of the circuit "bootstrapped" very effectively over the throttle range. This reflects its relative insensitivity to control changes in the hydrogen circuit. The current engine operating scenario calls for thrust to be adjusted by use of the oxygen turbine bypass valve. The MLETS analysis confirmed this as the preferred scenario.



### 3.1, Design and Parametric Analysis, (cont)

The HEX bypass valve placement causes considerable interaction with the hydrogen circuit and hydrogen regenerator bypass valve setting in particular. This interaction can be reduced in a number of ways:

- Allow only a small number of thrust dependent operating points for the HEX bypass valve until it must act as a temperature limiter for the oxygen going into the Ox TPA turbine. This will prevent "hunting" of the regenerator bypass valve.
- Reverse the position of the HEX and the regenerator in the engine circuit. This effectively decouples the hydrogen circuit from the oxygen circuit. There may be a penalty in a larger sized HEX due to the lower delta temperatures. A circuit schematic for this option is given in Figure 3.1-20.

There was a "bootstrapping" problem in the hydrogen circuit. Turbine efficiency was adjusted and turbine bypass decreased until the circuit "bootstrapped," but the required bypass was far lower than energy requirements would indicate. There may be an error in the algorithms that has not been detected. Available energy should be more than adequate over the throttle range for quick response.

There was one mismatch between the MLETS algorithms and the proposed control operations that increased the circuit coupling. An algorithm has not been developed for the HEX bypass valve and the program assumes sufficient energy extraction in the HEX so that oxygen to the turbine is at 400°F. This is a maximum value. As long as the oxygen turbine bypass valve is within the normal control range, the oxygen to the turbine can be less than 400°F. As the oxygen turbine bypass valve approaches 10% bypass, the HEX bypass must reduce the bypass and increase the oxygen temperature until 400°F is reached. That marks the end of the usable range for thrust control on the oxidizer side. With the present engine schematic, movement of the HEX bypass valve should be limited to a few set points to reduce the circuit coupling.



**Figure 3.1-20. Dual Expander Cycle Advanced Engine Study Alternate Schematic**

### 3.1, Design and Parametric Analysis, (cont)

2. Operating Stability. The composite plot in Figure 3.1-21 shows the engine variation with time from the rated thrust operating point with the engine at thermal equilibrium. At  $t = 126$  seconds the engine is allowed to operate without any control changes. By  $t = 148$  seconds the operating variables have shown a very minor drift. The change is so slight and so regular that it could as easily be attributed to minor round off errors in the algorithms as to actual engine instability. The engine is either dynamically stable at the rated thrust point or very close to it. More analysis and experimental testing will be needed to establish the actual condition. What the analysis does, however, is confirm that the engine should be readily controllable. The design baseline is for closed loop control. Relatively slow control rates should be adequate for stability.

3. Engine Throttling. A simulation of engine throttling was attempted using a controller for each circuit. Thrust was controlled by changing the oxygen turbine bypass setting while the hydrogen circuit controller attempted to follow the thrust change by adjusting the hydrogen turbine bypass valve. Proportional plus integral controllers were used for both the thrust and mixture ratio commands. A number of runs were made using different controller gains. In each case the engine eventually went unstable. There was not enough time available to solve this control problem, but a solution should come from reducing the circuit coupling through the HEX and from better modeling of the thermal and flow lags in the system.

The 7.5K lbf thrust engine was modeled using a different dynamic code called TUTSIM. (See Ref. 7). Throttle response for this series flow dual expander cycle is shown in Figures 3.1-22 and 3.1-23. A 10% change in thrust could be completed in about 0.3 seconds. The parallel flow dual expander should have a similar response time. Throttle ratio ( $\Delta$  thrust/unit time) decreases in the low thrust range due to lags in the turbopumps at low speed. The engine should be capable of accelerating from 10% thrust to 100% thrust in 4 to 5 seconds. Throttling down will be somewhat faster. This is an important performance number for the vehicle prime contractors and needs to be better defined early in the engine development.

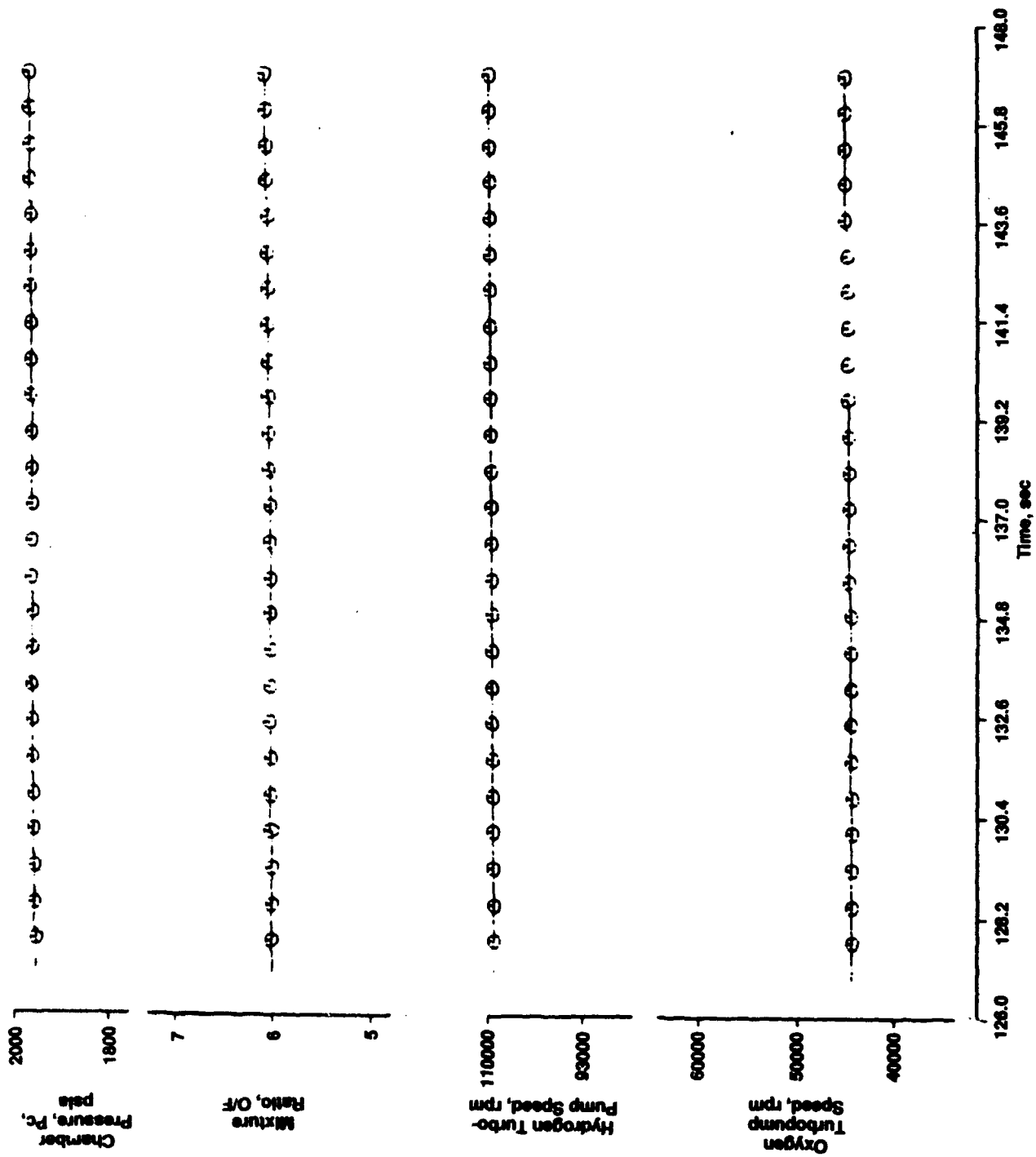


Figure 3.1-21. Advanced Engine Study Stability at Rated Thrust

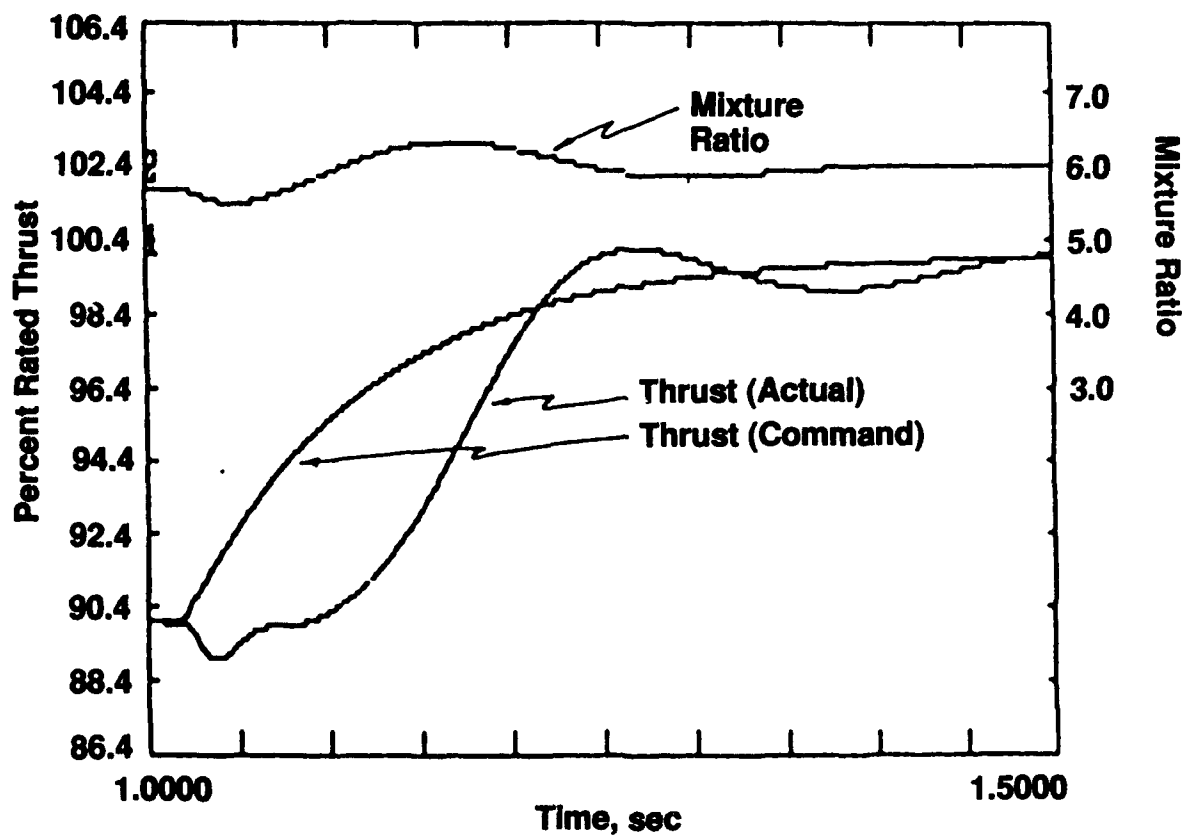


Figure 3.1-22. Predicted Response to 10% Throttle Up Command

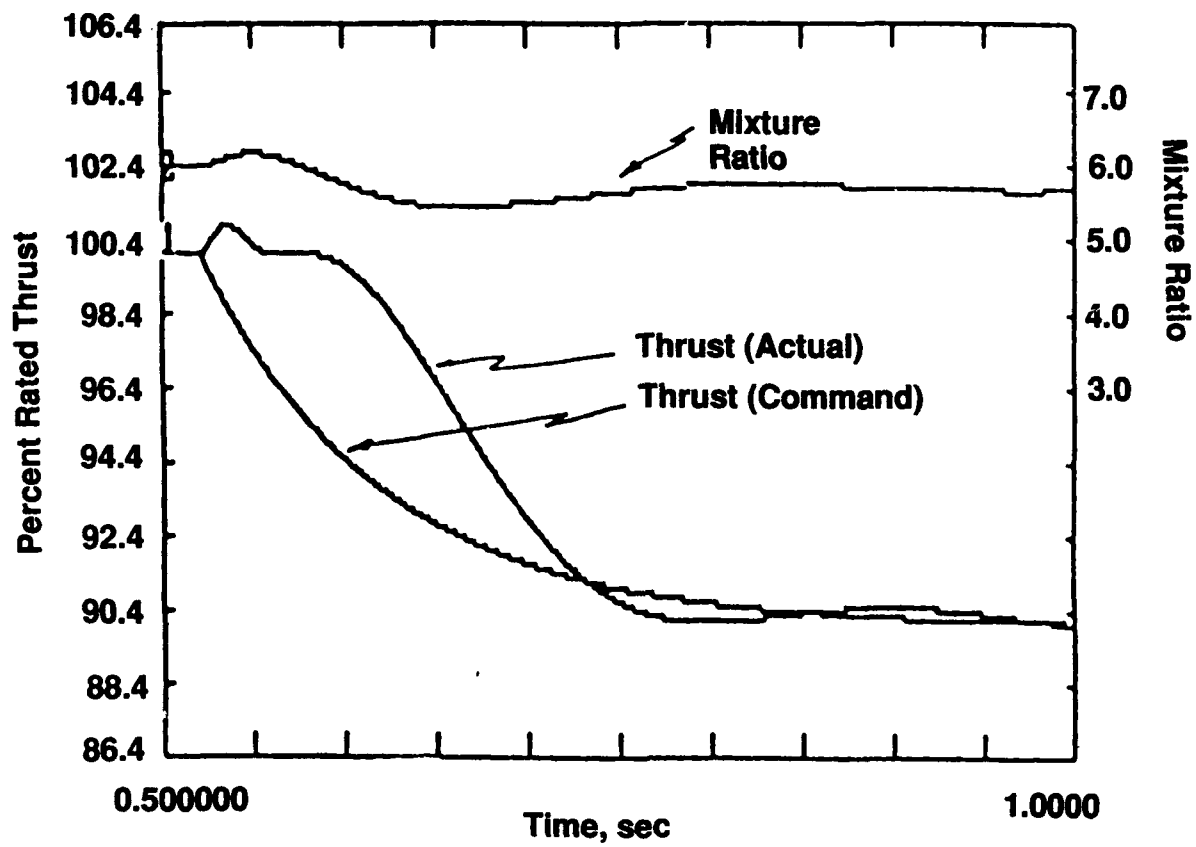


Figure 3.1-23. Predicted Response to 10% Throttle Down Command

### 3.1, Design and Parametric Analysis, (cont)

#### 3.1.3 Performance, Mass and Envelope Parameters

3.1.3.1 Performance — Specific impulse is the best standard for performance measurement with both propellants and area ratio specified. An initial performance comparison over the thrust range used a chamber pressure of 2000 psia and area ratio ( $A_e/A_t$ ) of 1200. Mixture ratio was plotted on the X-axis and thrust variation is shown as the family of 3 curves on Figure 3.1-24. This plot is for delivered specific impulse at steady state engine operation. The theoretical engine performance was first calculated from the One Dimensional Equilibrium model (ODE) and then corrected for kinetic losses using a One Dimensional Kinetic program (ODK) with further corrections for divergence and boundary layer losses. The corrections for divergence and boundary layer losses are calculated using TDK (Two Dimensional Kinetics program) and BLM (Boundary Layer Model). The performance loss accounting is plotted in Figure 3.1-25 for the 7.5K lbf thrust engine. Table 3.1-13 summarizes performance corrections for 7.5K, 20K, and 50K lbf thrust over an MR range of 5 to 13.

Performance changes with thrust are very minor over the range studied. There is no significant advantage in changing engine thrust to improve delivered specific impulse. Thrust selection should be based on other design considerations. Also, the maximum specific impulse is delivered over a mixture ratio range of 5 to 7 with only minor variations from the peak at MR = 6.3. This can be used to the advantage of the vehicle designers by baselining an active propellant management system that can program mixture ratio within this range to use all available propellant in the tanks with no delivered performance penalty. The result is a maximization of the propulsion system average specific impulse. This is usually more important than the nominal engine specific impulse.

The dropoff in specific impulse above MR = 6.3 reflects the changing composition of the exhaust gas species. At higher mixture ratios the average molecular weight increases causing a reduction in the jet velocity,  $V_j$ , according to the equation

$$V_j = \left\{ N_j 2 \frac{\gamma R_u}{\gamma - 1} \frac{T_o}{M} \left[ 1 - \left( \frac{P_j}{P_o} \right)^{\frac{\gamma - 1}{\gamma}} \right] \right\}^{1/2}$$

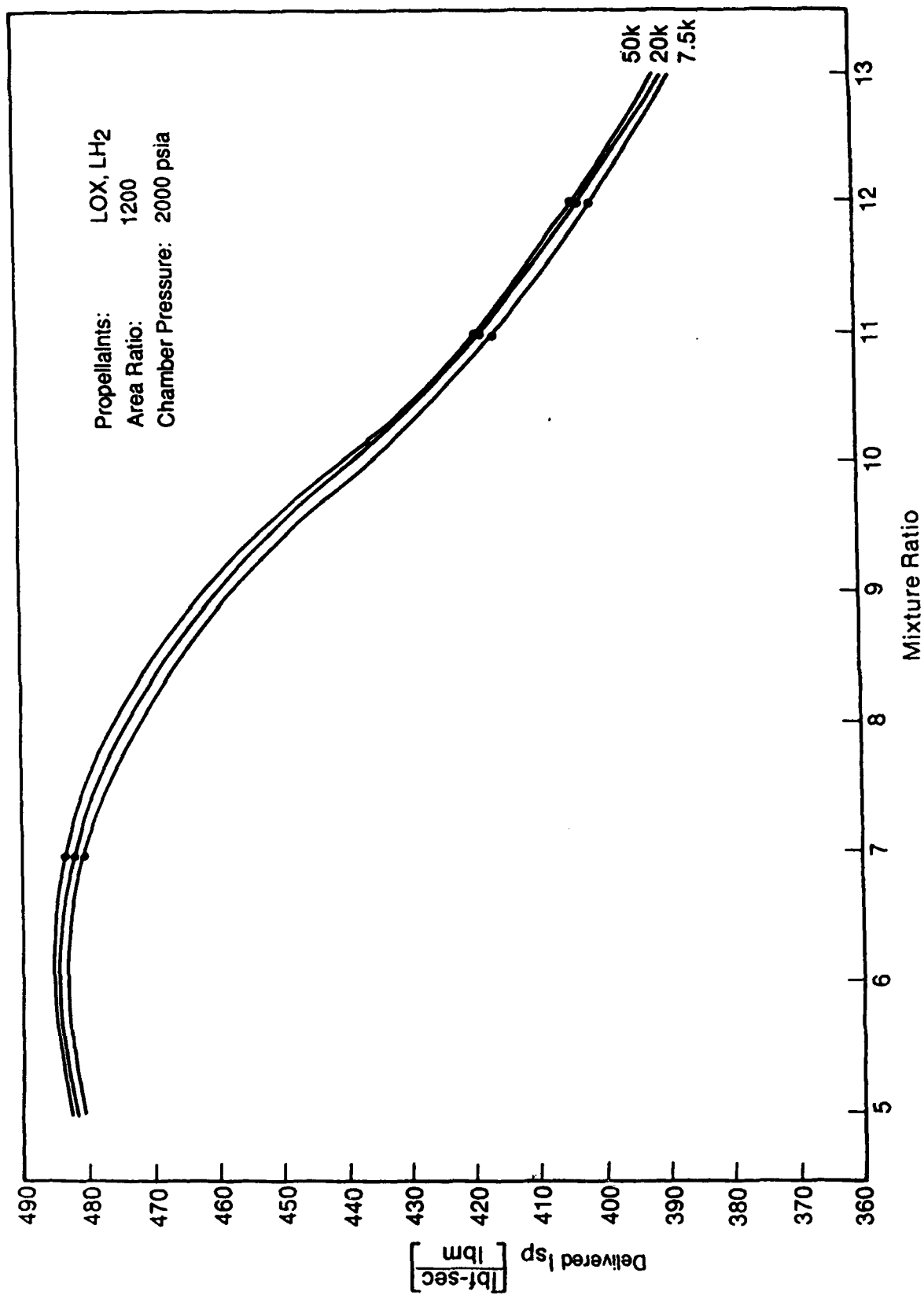


Figure 3.1-24. Advanced Engine Performance

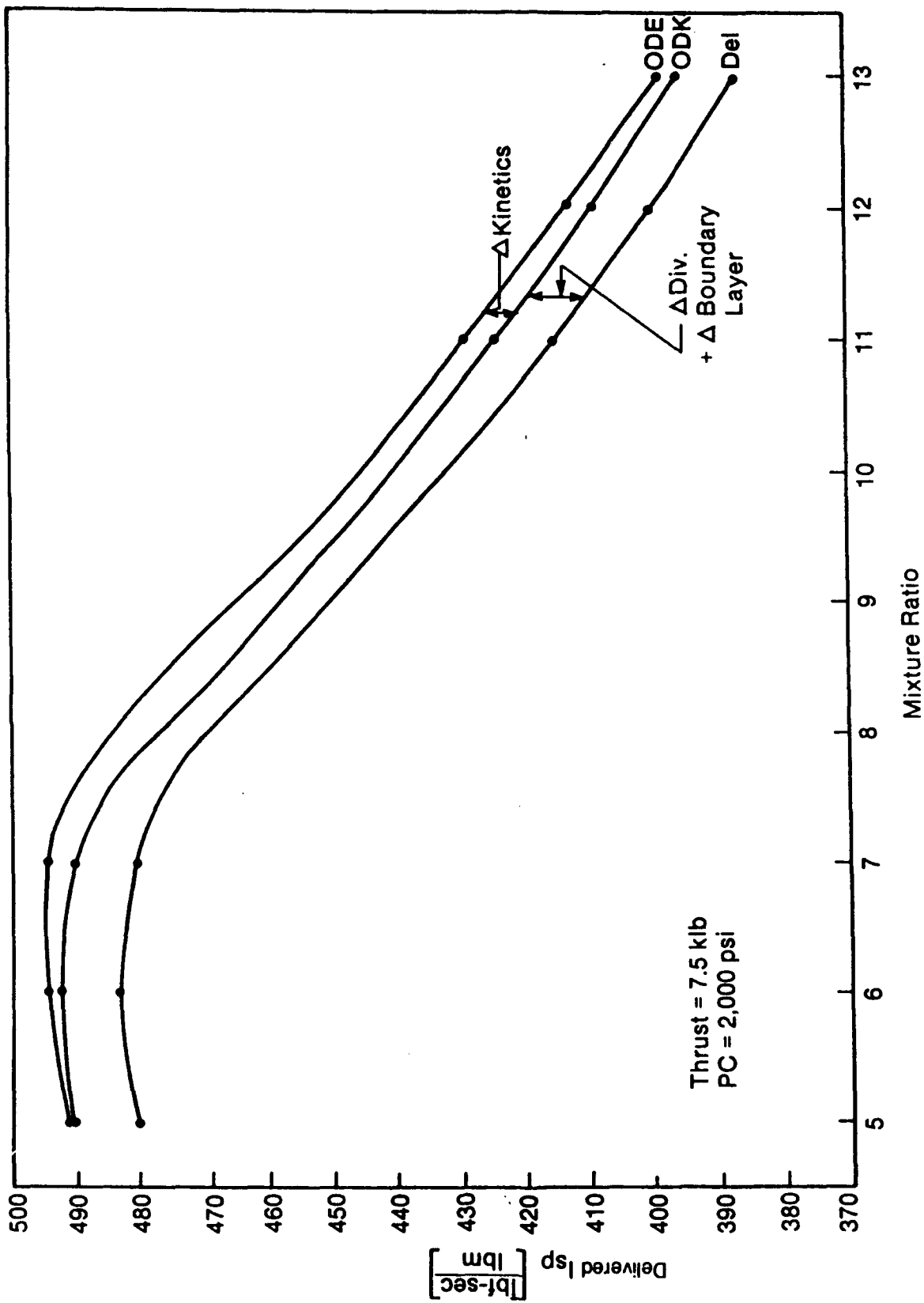


Figure 3.1-25. Performance Loss Accounting

TABLE 3.1-13

PERFORMANCE LOSS ACCOUNTING FOR VARIOUS  
THRUST LEVELS (7.5K, 20K, AND 50K lbf)

## 7.5K lbf Thrust Level

Pc=2000	MR	5	6	7	11	12	13
	ODE	491.1	494.4	494.5	409.7	413.9	399.7
	ODK	490.0	492.5	490.5	424.9	409.8	396.2
	TDK	488.0	490.5	488.5	423.2	408.2	394.6
	$\Delta$ BLM	7.4	7.4	7.4	7.4	7.4	7.4
	P.I. & Del	480.6	483.1	481.1	415.8	400.8	387.2

Throat Radius,  $r_t = 0.765"$ 

## 20K lbf Thrust Level

Pc=2000	MR	5	6	7	11	12	13
	ODE	491.1	494.4	494.6	429.7	413.9	399.7
	ODK	490.3	492.9	491.4	425.7	410.5	396.8
	TDK	488.3	490.9	489.4	424.0	408.9	395.2
	$\Delta$ BLM	6.6	6.6	6.6	6.6	6.6	6.6
	P.I. & Del	481.7	484.3	482.8	417.4	402.2	388.6

Throat Radius,  $r_t = 1.25"$ 

## 50K lbf Thrust Level

Pc=2000	MR	5	6	7	11	12	13
	ODE	491.1	494.4	494.5	429.7	413.9	399.7
	ODK	490.5	493.3	492.1	426.3	411.1	397.3
	TDK	488.5	491.3	490.2	424.6	409.4	395.7
	$\Delta$ BLM	6.1	6.1	6.1	6.1	6.1	6.1
	P.I. & Del	482.4	485.2	484.0	418.5	403.3	389.6

Throat Radius,  $r_t = 1.97"$

### 3.1, Design and Parametric Analysis, (cont)

where

- $M$  = average exhaust gas molecular weight
- $R_u$  = universal gas constant
- $\gamma$  = ratio of gas specific heat at constant pressure and constant volume
- $N_j$  = efficiency factor relating theoretical and delivered jet velocity to the engine losses
- $T_o$  = stagnation chamber temperature
- $P_o$  = stagnation chamber pressure
- $P_j$  = jet pressure at the exit plane

The  $T_o/M$  ratio decreases consistently as mixture ratio increases despite the maxima of  $T_o$  at the stoichiometric point ( $MR = 7.94$ ). At any  $MR$  above stoichiometric the amount of unreacted oxygen steadily increases in the exhaust stream. The operation of this engine at high mixture ratios ( $>7$ ) must be an economic decision; there is no performance justification.

One other engine operating parameter derived from performance is the total propellant flowrate. Figure 3.1-26 graphically presents flowrate for each of the five thrust levels. Table 3.1-14 gives the propellant flowrates in more detail. This is on a per engine basis. For a vehicle with a four engine propulsion set multiply by four. This figure can be readily used to calculate the total propulsion operating time (burn time) at rated thrust for a given propellant load. For instance, for a set of four 20,000 lbf thrust engines, the flowrate is about 174 lbm/sec. A 288,000 lbm propellant load is one of the figures used for the Lunar Transfer Vehicle (LTV). For a total propulsion operating time of:  $288,000 \div 174 = 1655$  seconds. Propellant residuals and a correction for attitude control system propellant use would have to be subtracted from the loaded propellant weight to determine the usable propellant. For a 4 hour total engine operating time without maintenance, this represents about 8 missions.

#### 3.1.3.2 Engine Mass Computations

A detailed weight and center of mass computation for the 7.5K lbf thrust engine was completed during the preliminary design task (Task D.5). The results are presented in Table 3.1-15. The interface for separating engine weight from vehicle

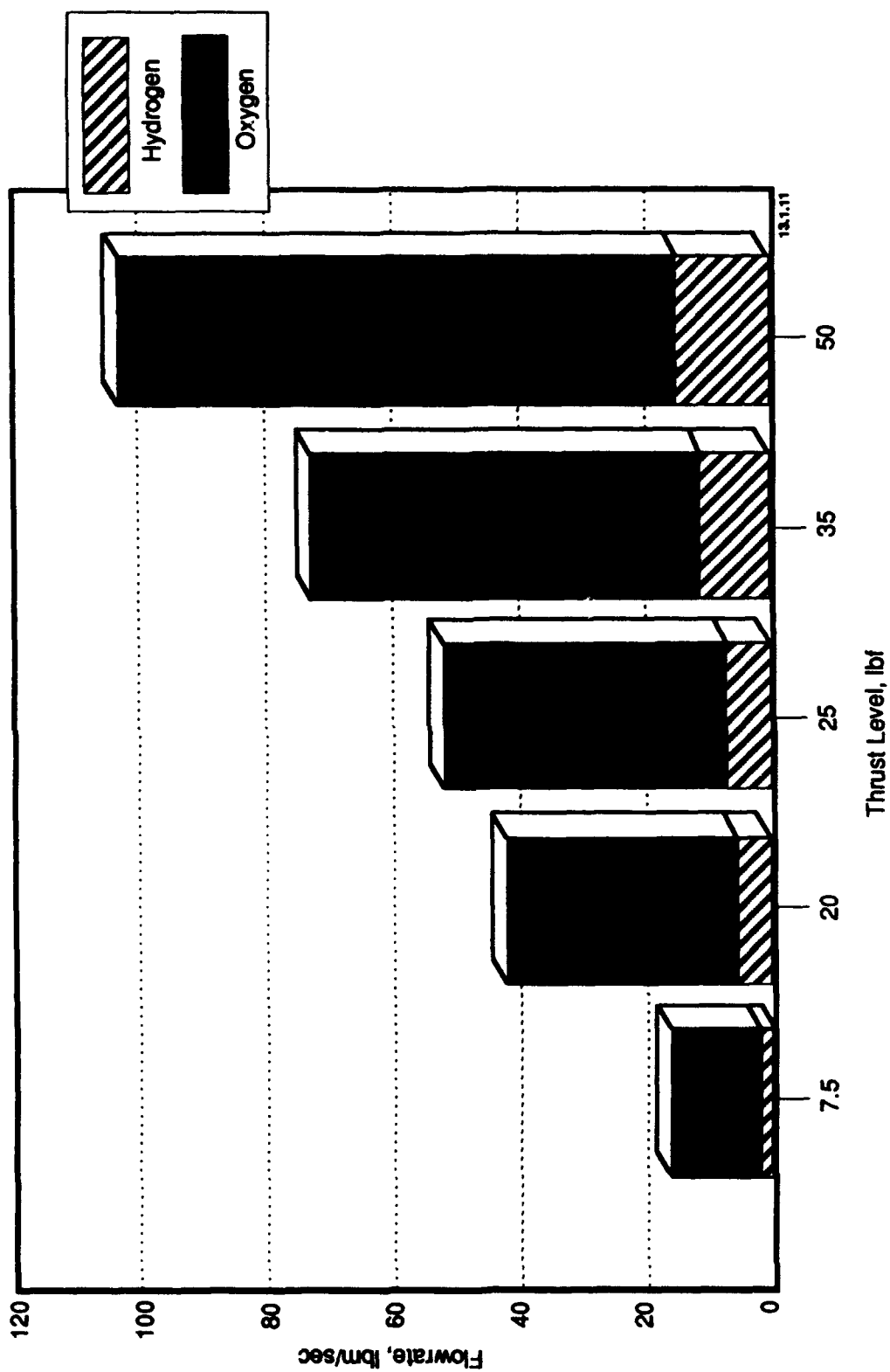


Figure 3.1-26. Space Transfer Vehicle Propellant Flowrate vs Engine Thrust

TABLE 3.1-14

LTV/LEV ENGINE PROPELLANT FLOWRATES

<u>Thrust</u>	<u>7.5K lbf</u>	<u>20K lbf</u>	<u>25K lbf</u>	<u>35K lbf</u>	<u>50K lbf</u>
<u>Propellant Flow Rate to Engine</u>					
• Total (lbm/sec)	16.38	43.49	54.36	75.96	108.29
• Oxygen (lbm/sec)	14.04	37.28	46.60	65.12	92.82
• Hydrogen (lbm/sec)	2.34	6.21	7.77	10.85	15.47
<u>Autogenous Tank Pressurization Flow Engine</u>					
• Total (lbm/sec)	0.82	2.17	2.72	3.79	5.41
• Oxygen (lbm/sec)	0.70	1.86	2.33	3.26	4.64
• Hydrogen (lbm/sec)	0.11	0.31	0.39	0.54	0.77
<u>Propellant Flow for Combustion</u>					
• Total (lbm/sec)	15.56	41.32	51.65	72.17	102.88
• Oxygen (lbm/sec)	13.34	35.42	44.27	61.86	88.18
• Hydrogen (lbm/sec)	2.22	5.90	7.38	10.31	14.70

---

Notes:

1. Autogenous propellant flow assumed to average 5% of flow to engine.
2. Table based on a mixture ratio of 6.
3. Propellant flow at thrusts below nominal are higher than a straight line extrapolation would predict as specific impulse decreases as the engine is throttled down.

**TABLE 3.1-15**  
**7.5K LBF THRUST PRELIMINARY ENGINE WEIGHT ESTIMATE**

	Current Weight		C of M from Datum (inches)		
	(-20%)	Nominal	(+20%)	X	Y Z
Thrust Chamber	(40.0)	50.0	(60.0)	125.5	0.0
Ext. Nozzle	(78.6)	98.3	(118.0)	148.0	0.0
Ox TPA	(7.2)	9.0	(10.8)	112.0	3.3
Fuel TPA	(12.0)	15.0	(18.0)	111.0	-1.5
Ox Boost Pump	(4.8)	6.0	(7.2)	104.0	5.0
Fuel Boost Pump	(4.0)	5.0	(6.0)	104.0	-5.0
H2 Regen	(3.6)	4.5	(5.4)	115.0	-5.0
O2/H2 HEX	(14.4)	18.0	(21.6)	127.0	0.0
Valves					
Ox Turb Bypass	(7.4)	9.2	(11.0)	113.0	9.0
Fuel Turb Bypass	(7.4)	9.2	(11.0)	125.0	0.0
Ox Back Press	(4.0)	5.0	(6.0)	114.0	6.0
Fuel Back Press	(2.4)	3.0	(3.6)	108.0	0.0
Ox Tank Press	(2.1)	2.6	(3.1)	101.0	8.3
Fuel Tank Press	(2.1)	2.6	(3.1)	101.0	-8.3
Fuel Idle	(4.0)	5.0	(6.0)	112.0	-2.0
H2 Regen Bypass	(7.4)	9.2	(11.0)	126.0	-8.0
Ox/H2 HEX Bypass	(5.4)	6.8	(8.2)	130.0	-10.0
Valves Subtotal	(42.1)	52.6	(63.1)	118.4	-0.7
Lines	(16.0)	20.0	(24.0)	117.0	0.0
Misc	(16.0)	20.0	(24.0)	117.0	0.0
TOTAL SYSTEM	274.4	298.1	322.1	128.8	-0.2

### 3.1, Design and Parametric Analysis, (cont)

weight was the mounting plane. The gimbal actuators and ICHM system were considered above this plane and are not included in the weight summary. An equally valid interface would define engine weight as the sum of all items necessary for engine operation exclusive of the thrust takeout structure and propellant lines above the mounting plane. These additions and a total are given in Table 3.1-16. Several other interfaces could be defined with some validity. For example, the engine dry weight as delivered to the vehicle contractor is a reasonable definition of engine weight based on a contract requirement.

Table 3.1-16 includes a figure for engine insulation although this could be applied after engine delivery. It does not include thrust takeout structure as this is commonly a function of the vehicle design. There is no weight for any nozzle snubbing system to secure the nozzle when the extendible nozzle section is retracted. There is no weight for a helium purge system as this engine does not require one. Those engines that do require a helium system often compute engine weight without it on the assumption that it is a vehicle system. Users of engine weight data are cautioned to put each manufacturers weight computations on the same basis before comparisons are made. Note that a helium purge system can add several hundred pounds to the vehicle weight, and would not normally be considered as engine weight, but it is required for the turbopump assembly of a conventional expander cycle engine.

Another source of variability in engine weight estimates is material selections. A lightweight material still in development can be proposed even though it is unlikely to be used. Also, there may be design uncertainties that, when resolved, will favor one material over another. An example is the radiation cooled nozzle material. Table 3.1-17 contrasts the weights of four nozzles, any one of which could be selected for the final design, yet there is a 2:1 weight ratio from lightest to heaviest. Part of the selection criteria will be based on structural requirements, part on operating temperature, and part on a trade-off of weight versus delivered payload. An example of payload sensitivity is given in Figure 3.1-27 for the four nozzles of Table 3.1-17.

The weight computation results for the engines used in the Advanced Engine Study are given in Table 3.1-18. Note that this is the weight for the components as would normally be delivered by the engine contractor to the vehicle

TABLE 3.1-16

7.5K LBF THRUST PRELIMINARY ENGINE WEIGHT ESTIMATE  
COMPLETE ENGINE

<u>Component</u>	<u>Current Weight Estimate</u>
Propellant Flowmeters (4)	3.0 lbm
Hydrogen Main Shutoff Valve	8.5
Oxygen Main Shutoff Valve	8.0
Primary Gimbal Actuators (2)	17.0
Engine Out Gimbal Actuator	14.0
ICHM System Electronics	12.0
Insulation	<u>10.0</u>
Sub-Total	72.5
Nominal Gimballed Component Weight (From Table 3.1-15)	<u>298.1</u>
TOTAL	370.6

TABLE 3.1-17

PRELIMINARY NOZZLE SYSTEM WEIGHT ESTIMATES,  
7.5K LBF ENGINE

	<u>Columbium</u>		<u>Carbon-Carbon</u>	
	<u>0.020-in.</u>	<u>0.030-in.</u>	<u>0.050-in.</u>	<u>0.060-in.</u>
Nozzle Skin	48.3	72.4	20.6	24.7
Nozzle Attach	18.1	18.7	7.0	7.0
Nozzle Stiffener	4.7	4.7	1.5	1.5
Ballscrew (3)	8.4	8.4	8.4	8.4
Gearbox (3)	8.1	8.1	8.1	8.1
Ball Nut (3)	5.4	5.4	5.4	5.4
28VDC Motor (3)	9.0	9.0	9.0	9.0
Flex Cable (6)	4.2	4.2	4.2	4.2
Support Strut (6)	5.0	5.0	5.0	5.0
TOTAL (per TCA)	111.2	135.9	69.2	73.3

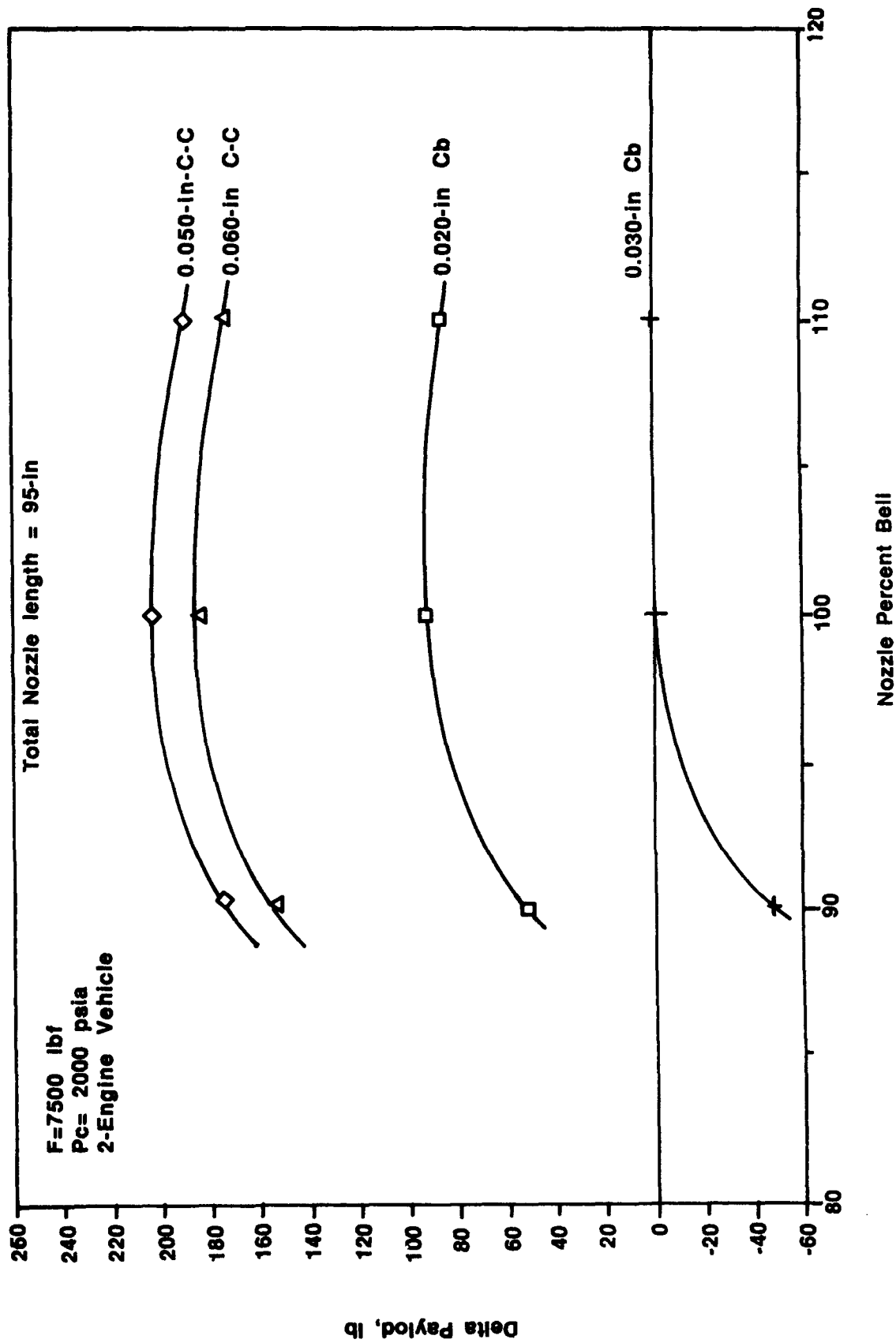


Figure 3.1-27. Delta Payload vs. Nozzle Percent Bell

**TABLE 3.1-18**

**ADVANCED FLIGHT ENGINE WEIGHT ESTIMATES**

Material	Component	Engine Thrust, Pounds Force					7.5K	20K	25K	35K	50K
		7.5K	20K	25K	35K	50K					
		Weight in Pounds					Percent of Total Weight				
GlidCop & NiCo	Thrust Chamber	36.66	64.51	84.95	131.34	197.63	14.79	13.47	13.93	14.66	14.51
Ni Base	Injector	24.08	45.97	56.24	79.07	121.15	9.71	9.60	9.22	8.84	8.89
ZrCu	Baffles	8.50	9.79	14.03	22.08	35.17	3.43	2.04	2.30	2.47	2.58
TCA SubTotal		69.24	120.27	155.22	232.48	353.95	27.93	25.10	25.45	25.98	25.99
Be	Ox Cooled Nozzle	14.20	38.80	49.50	71.80	109.10	5.73	8.10	8.11	8.02	8.01
C-C	Rad. Cooled Nozzle	73.34	143.95	175.11	248.50	378.37	29.58	30.05	28.71	27.77	27.78
	Ox TPA	10.00	16.67	23.33	36.67	56.67	4.03	3.48	3.83	4.10	4.16
	Ox Boost Pump	18.60	31.00	43.40	68.20	105.40	7.50	6.47	7.11	7.62	7.74
	Fuel TPA	10.00	16.67	23.33	36.67	56.67	4.03	3.48	3.83	4.10	4.16
	Fuel Boost Pump	6.40	10.67	14.93	23.47	36.27	2.58	2.23	2.45	2.62	2.66
TPA SubTotal		45.00	75.00	105.00	165.00	255.00	18.15	15.66	17.21	18.44	16.72
Be	H2/H2 Re-generator	0.84	7.12	7.10	7.06	8.58	0.34	1.49	1.16	0.79	0.63
Be	H2/O2 HEX	3.98	14.10	16.40	20.90	30.00	1.61	2.94	2.69	2.34	2.20
HEX & Reg SubTotal		4.82	21.22	23.50	27.96	38.58	1.94	4.43	3.85	3.12	2.83
	Valves, Lines, & Misc.	41.32	79.85	101.67	149.15	227.00	16.67	16.67	16.67	16.67	16.67
SubTotal		206.60	399.23	508.33	745.74	1134.99	83.33	83.33	93.33	83.33	83.33
Total		247.92	479.08	610.00	894.89	1361.99	100.00	100.00	100.00	100.00	100.00
Orig. Total		291.80	486.33	680.87	1069.93	1653.53					

### 3.1, Design and Parametric Analysis, (cont)

prime. A graphical presentation of the engine weights is given in Figure 3.1-28. This is based on materials choices as indicated in Table 3.1-18. A more conservative materials choice could add 10% to the totals as given.

Figure 3.1-29 plots the thrust/weight ratio versus engine thrust over the range of interest. This engine cycle optimizes at about 20K lbf thrust with a ratio of 28 lbf thrust for each pound of engine. Another graphical presentation of the same calculations is given in Figure 3.1-30 where engine weight is plotted directly against thrust. This plot can be used to estimate engine weight at intermediate thrust points.

#### 3.1.3.3 Engine Envelope

The criteria for the nozzle length is an area ratio of 1200:1 with a contour for optimum performance. Aerojet performance programs were used with each engine thrust, and a common 110% RAO nozzle was found to deliver maximum performance for the 2000 psia chamber pressure and the selected area ratio. The result is a very large engine. Engine half sections are shown in Figure 3.1-31. Note that the 50K lbf thrust engine is 25.4 ft long with the nozzle extended and 13.1 ft long with the radiation cooled nozzle retracted. This is the length behind the aerobrake doors. At the 20K lbf thrust it is 106 inches. The impact on the vehicle is serious enough to warrant an investigation of either mounting the engines where they do not interact with the aerobrake design or of using an alternative to a conventional nozzle such as a plug cluster.

The engine configuration and nozzle contour for any thrust can be calculated using the parametric data given in Tables 3.1-19 and 3.1-20. These tables should be used in conjunction with Figures 3.1-32 which defines the symbols and lengths in terms of a rocket engine half section.

A summary of the basic study engine dimensions is given in Table 3.1-21.

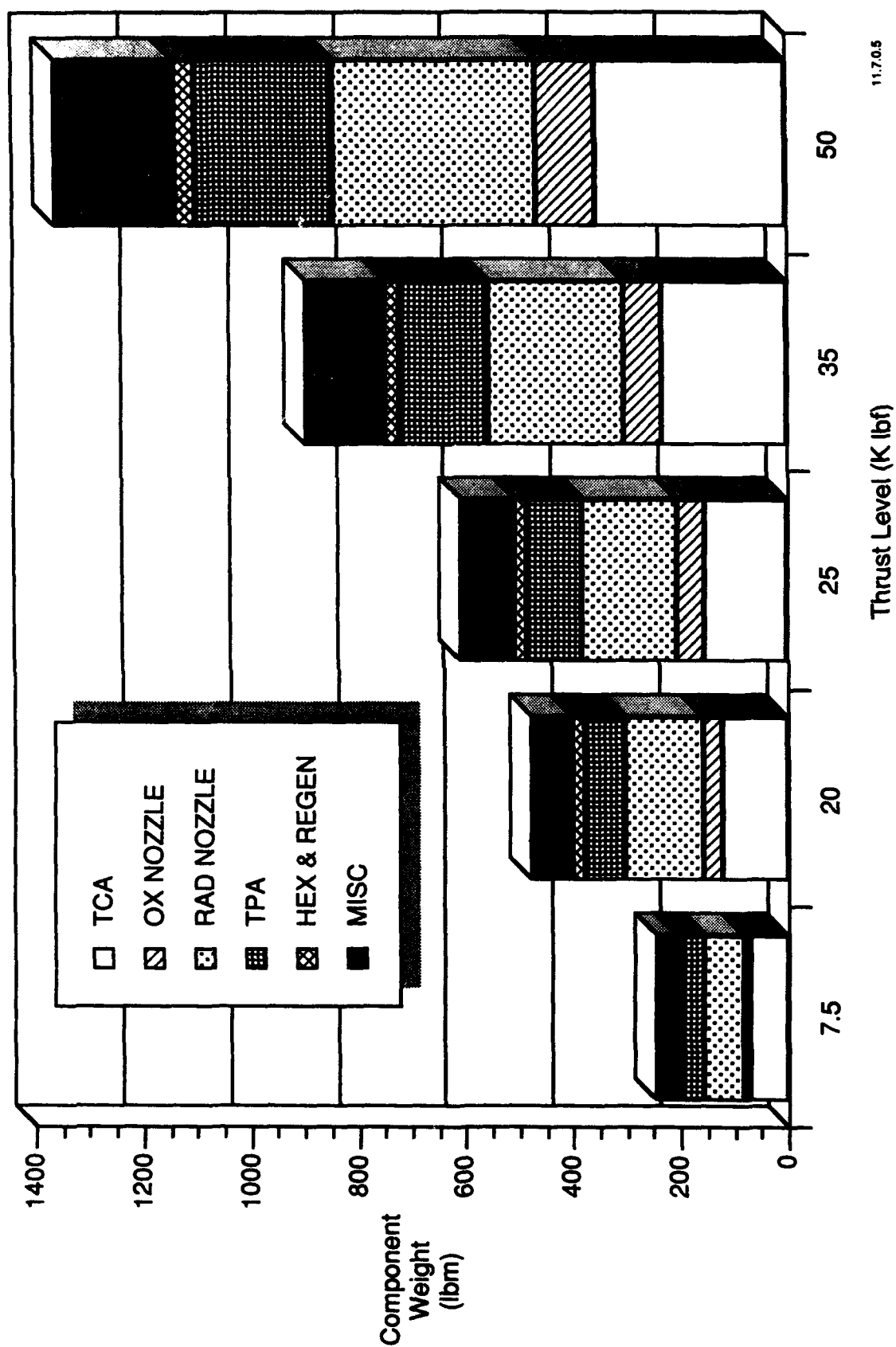


Figure 3.1-28. Advanced Engine Study Parametric Weight Summary

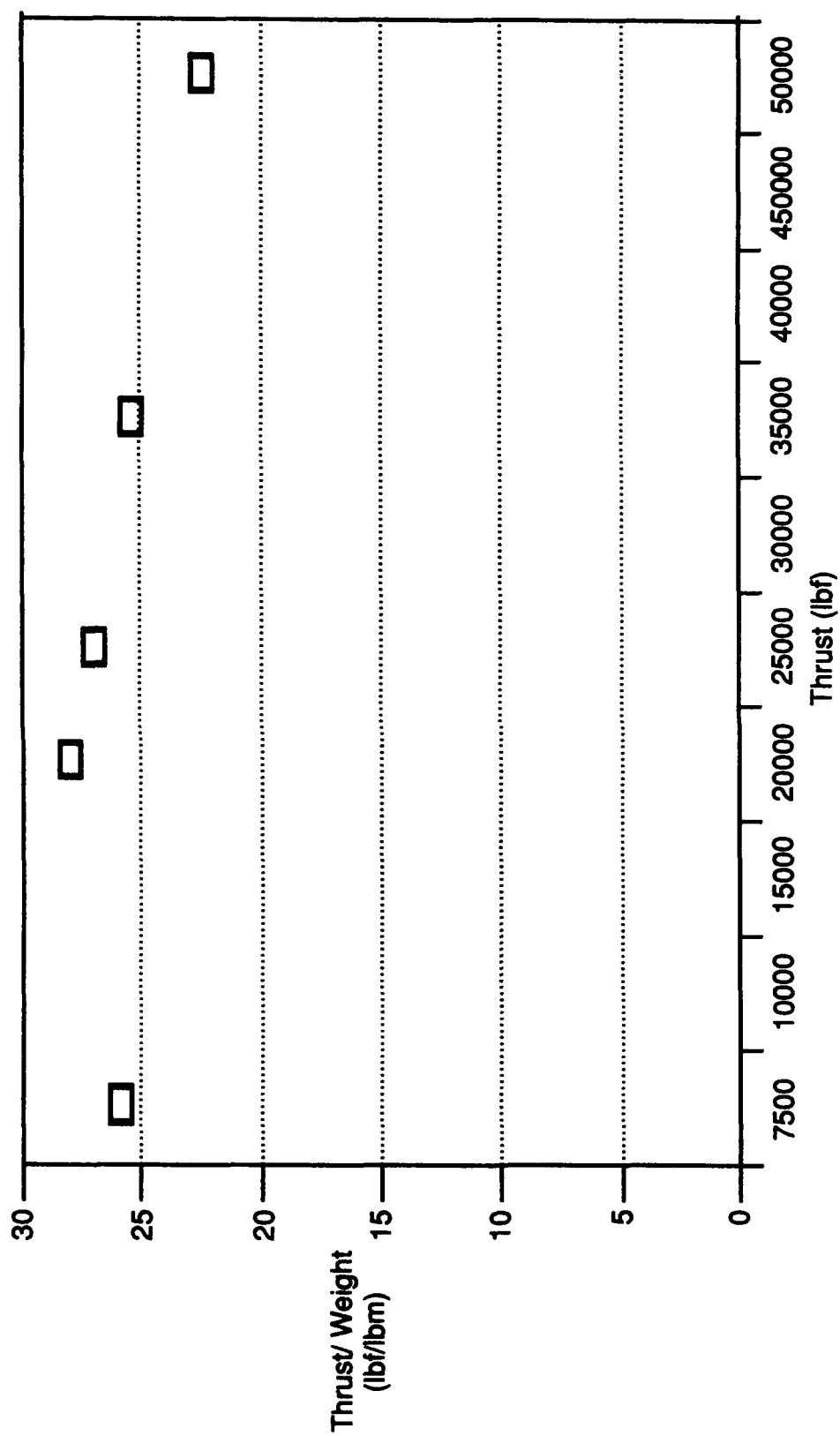


Figure 3.1-29. Engine Thrust/Weight Ratio Versus Thrust

11.7.0.5

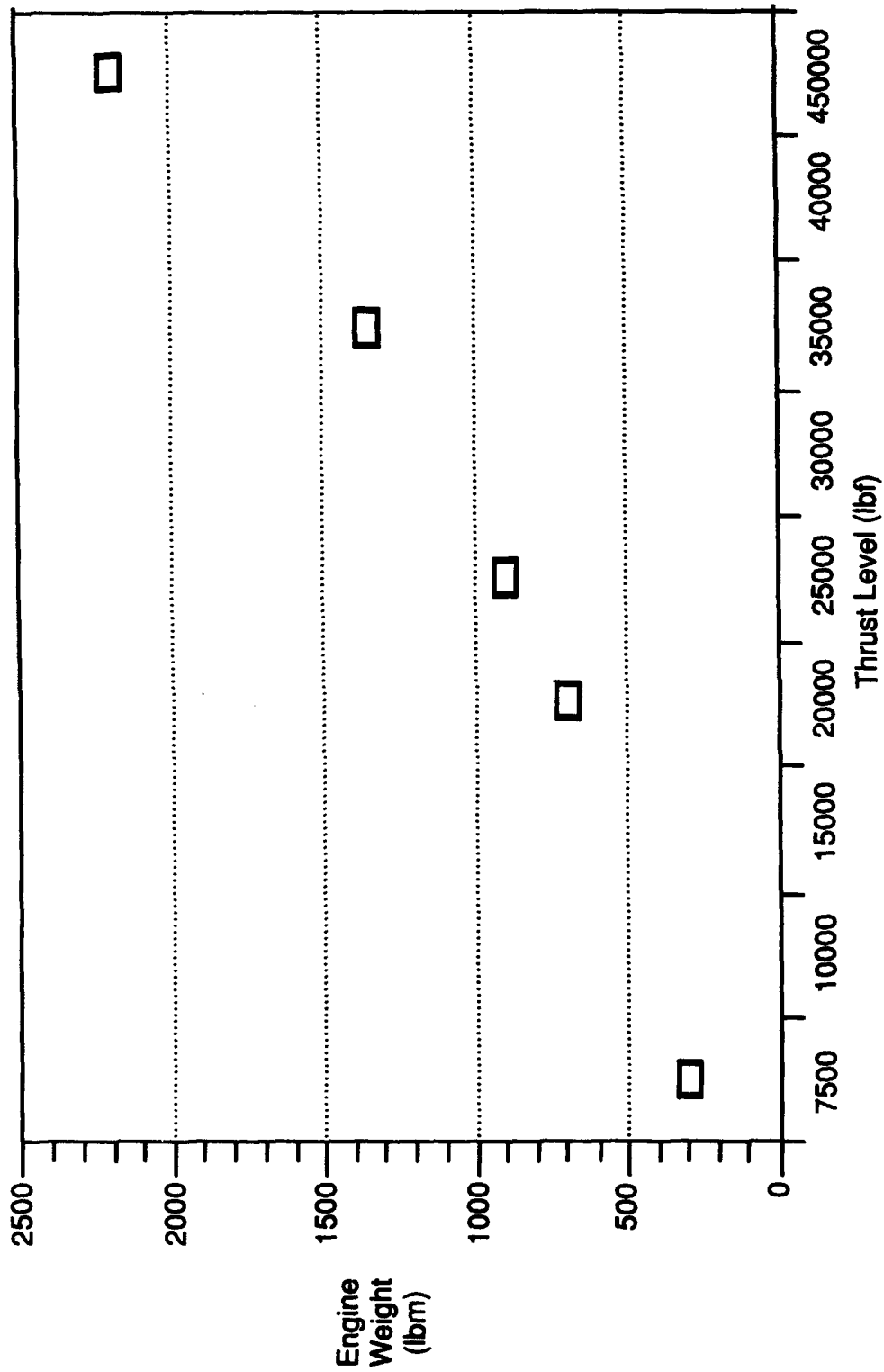
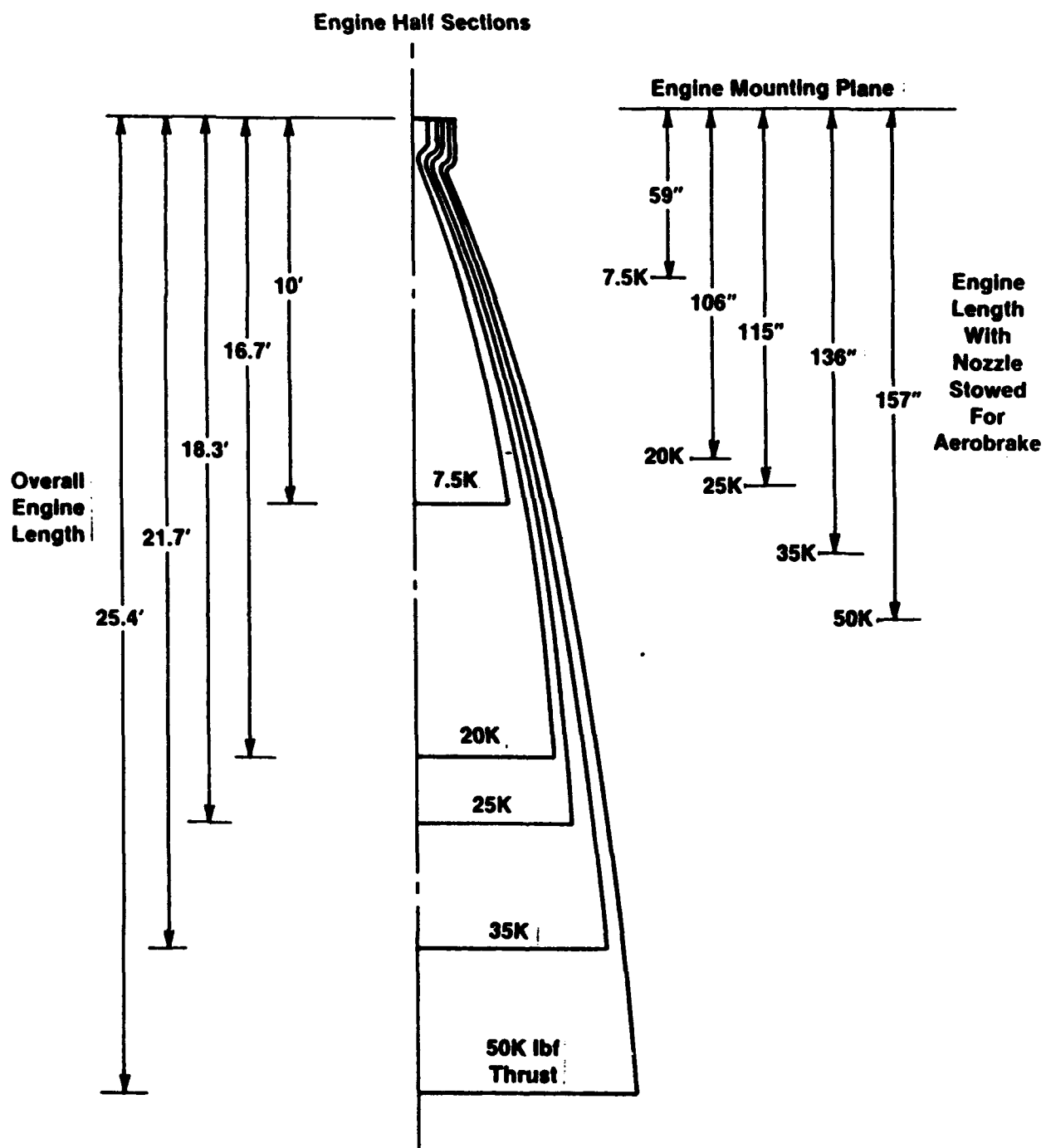


Figure 3.1-30. Advanced Engine Study, Thrust vs. Weight

11.7.0.5



**Figure 3.1-31. Change in Engine Length With Thrust**

TABLE 3.1-19

ADVANCED ENGINE DESIGN STUDY ENGINE CONTOUR  
NORMALIZED BY THE THROAT RADIUS

Engine Thrust, lbs	<u>7.5K</u>	<u>20K</u>	<u>25K</u>	<u>35K</u>	<u>50K</u>
Throat Radius, inches, $r_t$	0.765	1.25	1.395	1.65	1.97
Parameter (non-dimensional)	Normalized Dimensions				
Chamber Length, $L'$	13.73	9.60	9.32	9.09	8.12
Barrel Section Length, $L_c$	6.81	6.58	6.34	6.14	5.30
Chamber Inner Radius at the Injector, $r_c$	6.86	4.80	4.66	4.55	4.06
Radiused Transition, Barrel to Converging, $r_i$	2.0	2.0	2.0	2.0	2.0
Radiused Transition, Converging to Throat, $r_u$	2.0	2.0	2.0	2.0	2.0
Radiused Transition, Throat to Nozzle, $r_d$	2.0	2.0	2.0	2.0	2.0
Nozzle Length, $L_n$	141.318	141.318	141.318	141.318	141.318
Nozzle Exit Radius, $r_e$	34.641	34.641	34.641	34.641	34.641
<u>Angular Relations</u>					
Chamber Barrel to Converging Section, $\theta_i$	30°	30°	30°	30°	30°
Initial Nozzle Divergence Angle, $\theta_n$	30	30°	30°	30°	30°
Nozzle Exit, $\theta_e$	4.9°	4.9°	4.9°	4.9°	4.9°

**TABLE 3.1-20**  
**ADVANCED ENGINE DESIGN STUDY**  
**NORMALIZED NOZZLE CONTOUR\***

Station	Nozzle Length/Throat Radius		Nozzle Radius/Throat Radius	
	L/r <sub>t</sub>		r/r <sub>t</sub>	
1	.75		1.2842	
2	2.50		2.3357	
3	5.00		3.8379	
4	7.50		5.340	
5	8.459		5.916	
6	10.344		7.006	
7	12.100		7.949	
8	15.727		9.727	
9	19.152		11.243	
10	23.758		13.089	
11	30.096		15.349	
12	35.370		17.036	
13	41.893		18.927	
14	56.310		22.513	
15	65.471		24.458	
16	78.448		26.865	
17	103.304		30.589	
18	123.367		32.936	
19	141.318	L=L <sub>n</sub>	34.641	r=r <sub>c</sub>

\* Engines of any thrust in the 7.5K to 50K lbf thrust range have the same nozzle contour.

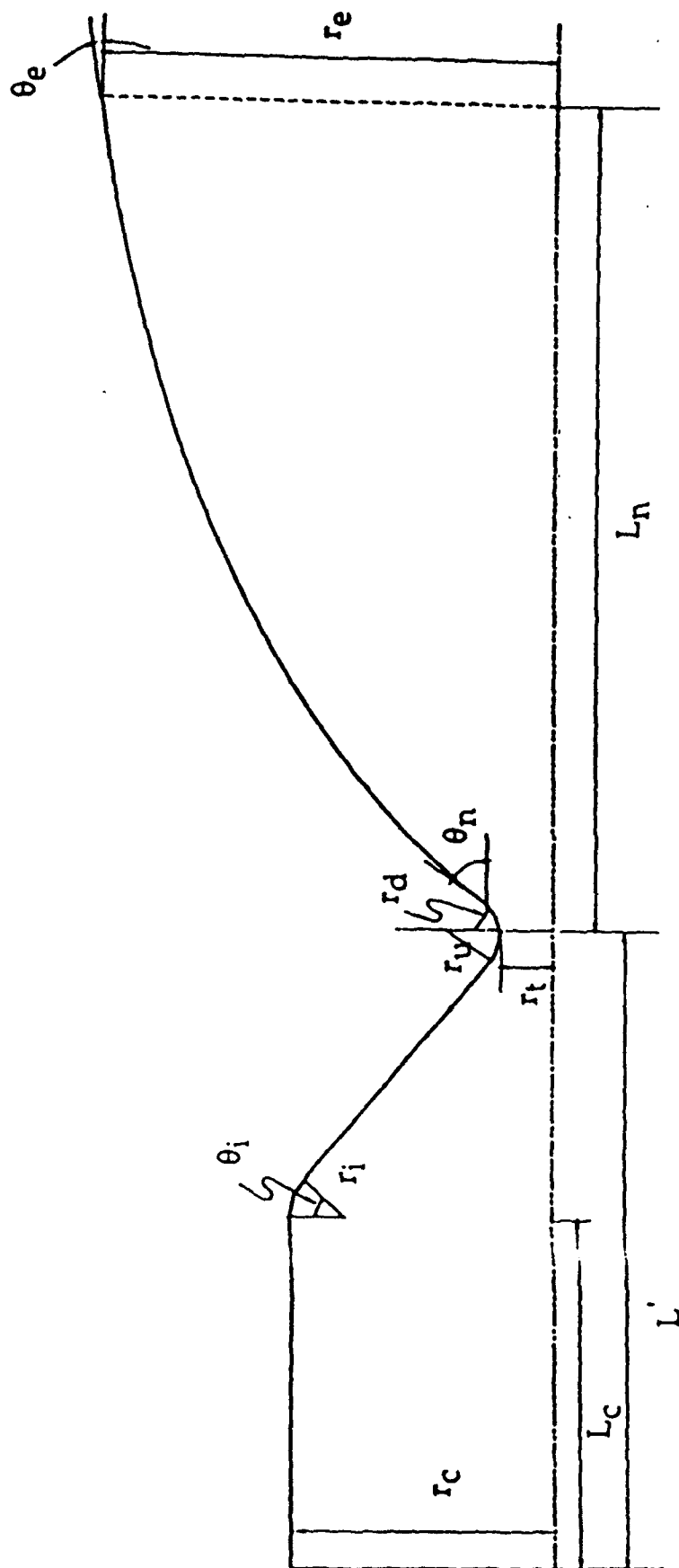


Figure 3.1-32. TCA Half Section

**TABLE 3.1-21****ADVANCED ENGINE DESIGN STUDY  
BASIC ENGINE DIMENSIONS**

<u>Parameter</u>	<u>Thrust, lbf</u>				
	<u>7.5K</u>	<u>20K</u>	<u>25K</u>	<u>35K</u>	<u>50K</u>
Throat Radius, inches, $r_t$	1.53	2.50	2.79	3.30	3.94
Throat Area, inch <sup>2</sup>	1.84	4.89	6.12	8.54	12.18
Chamber Diameter, inches	7.64	9.80	10.92	12.89	15.40
Contraction Ratio Geom.	24.9	15.3	15.3	15.3	15.3
Baffle Cross-Section Area, inch <sup>2</sup>	14	26	32	45	64
Contraction Ratio Less Baffle Area	17.3	10	10	10	10
Chamber Length, L', inches	10.5	12	13	15	16
Nozzle Exit Area, inch <sup>2</sup>	2208	5868	7344	10,248	14,616
Nozzle Exit Diameter, inches	53.	86.44	96.70	114.73	136.42
Nozzle Area Ratio	1395	1200*	1200*	1200*	1200*

---

\*Assumes  $\epsilon = 1200$  is fixed

## 3.2 ENGINE REQUIREMENT VARIATION STUDIES

The first of the two variations from the engine baseline was to look at an extended throttling range. With the new program emphasis on engine capability for missions within Project Pathfinder, there is a requirement for a throttling main engine to land a vehicle on the moon, Phobos, or Mars. The exact throttle engine range needed is a function of the number of engines in the set and the g-load requirements of the vehicle/maneuver. For this subtask the Apollo mission g-load were used and the thrust selected, after considerable coordination, was 20,000 lbf/engine with a four engine set. The throttle range was 20:1 versus 10:1 on the baseline. No throttle rate was given although this is recognized as an important number for mission planning.

The second variation from the baseline engine requirements was an investigation of the effects of high mixture ratio ( $MR > 7$ ) operation on the engine design. The reason for this investigation is the possibility of using oxygen mined from Lunar rocks as a propellant. For this portion of the study, a high MR operating point of  $MR = 12 \pm 1$  was investigated.

A summary of the engine design parameters used for the variation study is given Table 3.2-1. The basic mechanical design of the engine is unchanged but the high mixture ratio study evaluated platinum alloys for the baffle plates as well as the baseline NASA-Z material.

### 3.2.1 Design for 20:1 Throttling

#### 3.2.1.1 Component Design

The turbopump design points for the 10:1 throttling engine were selected using worst case design conditions at a chamber pressure of 2300 psia and mixture ratio 7 (oxygen TPA) or 2000 psia and mixture ratio 5 (hydrogen TPA). Flowrates were calculated based on flow at these conditions plus 5% for autogenous tank pressurization. See Section 3.1.1 for the 10:1 throttling engine baseline. For the 20:1 throttling case a single design point at a nominal thrust of 20,000 lbf was calculated.

A normalized performance chart for this TPA is given as Figure 3.2.1-1. This performance curve is applicable to a single stage for either TPA.

**TABLE 3.2-1****STUDY BASELINE - ENGINE REQUIREMENTS VARIATION**

<u>Parameter, dimension</u>	<u>20:1 Throttling</u>	<u>High Mixture Ratio</u>
Engine Thrust, lbf (Nominal)	20,000	TBD
Specific Impulse, lbf-sec/lbm	484	Varies
Mixture Ratio Range	5 to 7	7 to 13
Chamber Pressure, $P_c$ , psia, (Nominal)	2000	TBD
Maximum Gas Side Wall Temp., Thrust Chamber, °F	1050	1050
Baffle Plate Maximum Wall Temp., °F		
• Copper (NASA-Z Alloy)	1050	1050
• Platinum (pure or 10% Rhodium)	2000	2000
Oxygen TPA Turbine Inlet Temp., °F (Maximum)	400	400
Chamber/Baffle Hydrogen Flow Split, %	30 to 70	30 to 70
Turbine Bypass Minimum Flow, %	10	10
Regenerator Bypass Minimum Flow, %	25	25
LOX/GH <sub>2</sub> HEX Bypass Minimum Flow, %	10	10
Fuel Idle Valve Range, % of H <sub>2</sub> Flow	0 to 10	0 to 10
Regen Cooled Chamber Material (for Property Data)	NASA-Z Copper	NASA-Z Copper, Gold Plated
Oxygen Cooled Nozzle Material (for Property Data)	NASA-Z Copper	NASA-Z Copper, Gold Plated
Regen Chamber Inlet Area Ratio, $\epsilon$	28:1	28:1
Oxygen Cooled Nozzle Inlet Area Ratio, $\epsilon$	35:1	35:1
Oxygen Cooled Nozzle Exit Area Ratio, $\epsilon$	600:1	600:1
Chamber Internal Diameter, inches	9.8	9.8

TABLE 3.2-1

STUDY BASELINE - ENGINE REQUIREMENTS VARIATION  
(CONTINUED)

<u>Parameter, dimension</u>	<u>20:1 Throttling</u>	<u>High Mixture Ratio</u>
Chamber Contraction Ratio, $A_{inj}/A_t$	15.3:1	15.3:1
Radiation Cooled Nozzle Area Ratio, $A_c/A_t$ ( $\epsilon$ )	1200:1	1200:1
Nozzle Contour		
• To $\epsilon = 35$	27° Angle	27° Angle
• To $\epsilon = 1200$	Rao, Optimum Bell	Rao, Optimum Bell
Regen Channel Geometry in Throat	.011" x .083" Depth	.011" x .083" Depth
Channel Land Width in Throat, inches	.010	.010

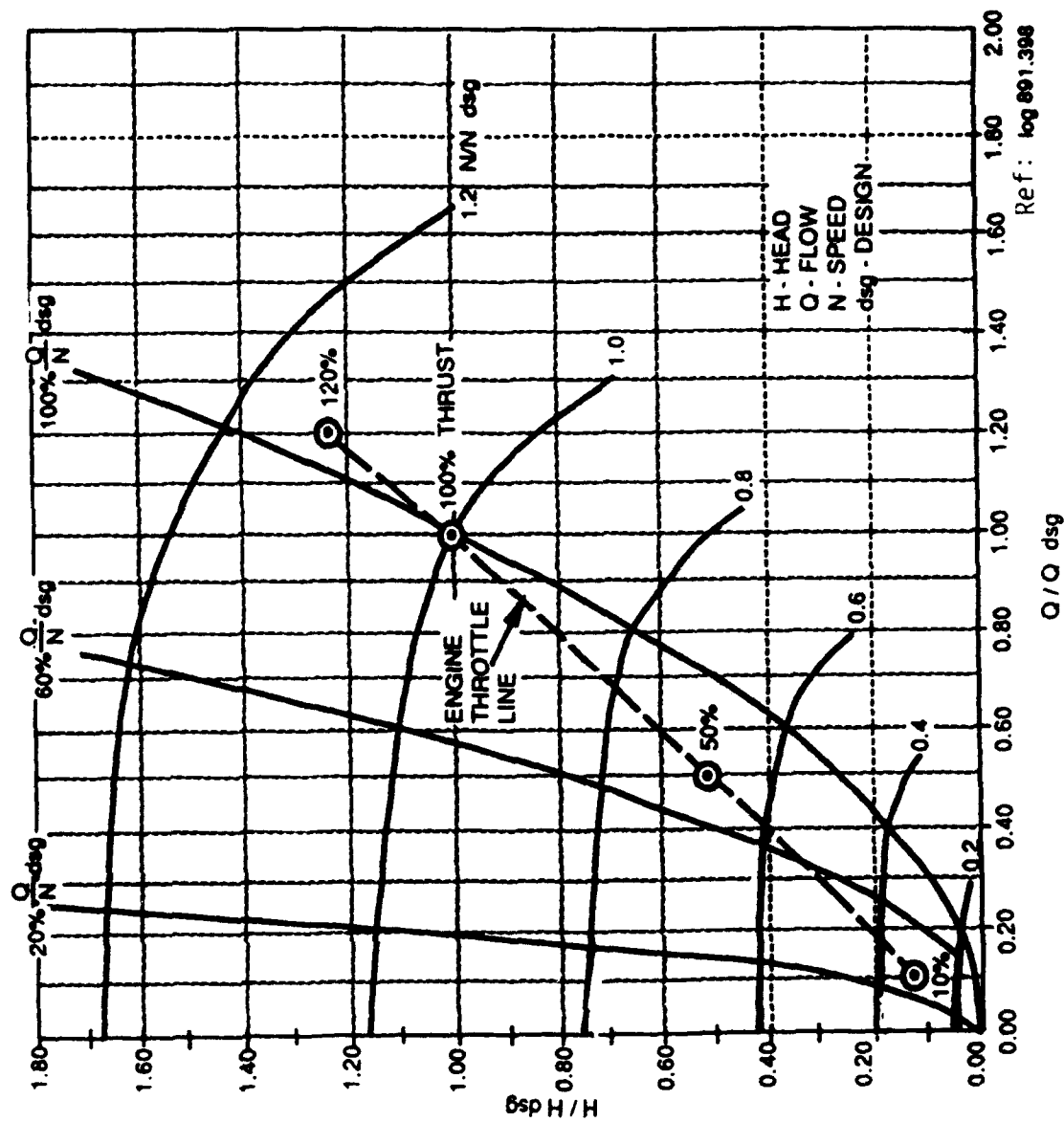


Figure 3.2.1-1. Predicted OTV Off-Design Performance Meets 10:1 Throttling Operating Requirements :

### 3.2, Engine Requirement Variation Studies, (cont)

Note that the speed ratio lines (N/N design) have a negative slope from Q/Q design = 0 throughout the operating range. This characteristic was considered necessary to avoid low speed stall and other instabilities. The predicted engine throttle line is also plotted on this figure for reference. The stall line for this TPA design falls on the Y-Axis. Cavitation performance can be inferred from Figure 3.2.1-2 where head loss is plotted against suction specific speed.

The concern in designing for 20:1 throttling was the TPA performance at low chamber pressures. The design point was selected to assure stable pump performance at the low speeds corresponding to a 100 psia chamber pressure. This changed the top end performance, in particular, the overthrust capability. The selected TPA design points given in Table 3.2.1-1 will only give a 5% overthrust capability at MR = 7. Broad band performance is traded for low speed controllability and stability. The engine operating envelope is depicted in Figure 3.2.1-3.

With a wide throttling range it is important to consider injector low frequency combustion stability or "chug". Tests of the I-Triplet injector have shown stability over a range representative of the 20:1 in this study. Appendix C includes a discussion and test reference for "chug" stability.

Extended operation at the low throttle limit is dependent on the chamber and baffle temperatures at equilibrium. With NASA-Z /Narloy-Z chamber liner and baffles, the maximum operating temperature is 1050°F based on material heat treated at 1700°F for 2 hours with aging at 900°F for 4 hours. A stress versus temperature plot for the Narloy-Z material is given as Figure 3.2.1-4. The design allowable 0.2% yield strength curve was added to the Rockwell chart. There will be a gradual reversion to annealed properties at 1050°F that will set a life limit for the chamber. The desired normal operating temperature limit is 900°F.

The chamber at the 20:1 throttle down point should be designed not to exceed 900°F. With platinum baffle plates this is readily accomplished by biasing the hydrogen flow to the chamber and letting baffle temperatures reach 2000°F. With copper baffles, the recourse is to reduce the chamber length. This shortens the hydrogen flow path and transient time. It also reduces the enthalpy pickup of the hydrogen that is needed at nominal thrust., Figure 3.2.1-5 shows the hydrogen circuit enthalpy pickup required for the nominal thrust condition for each of the three active components:

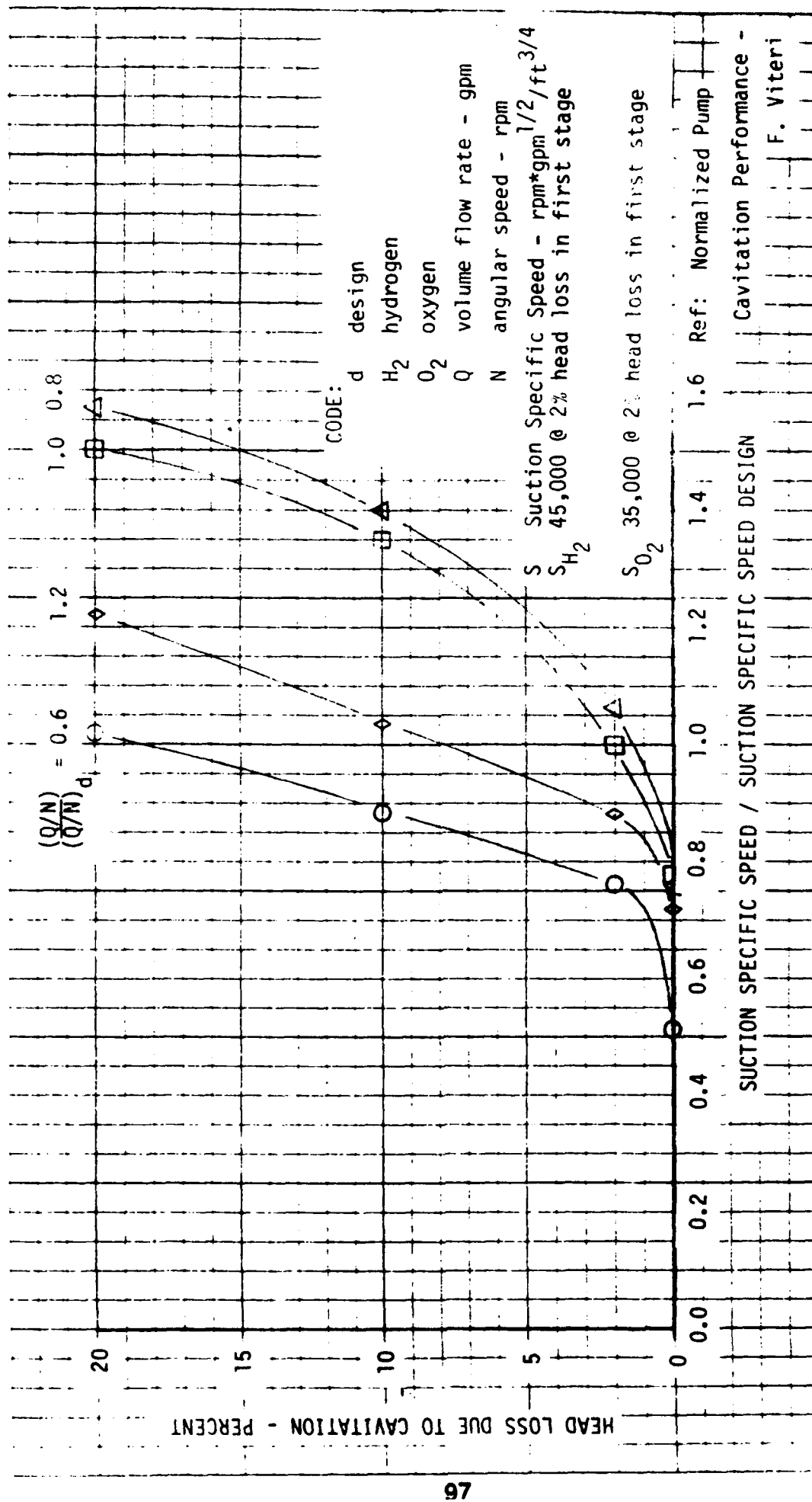


Figure 3.2.1-2. Estimated Head Loss Due to Cavitation

TABLE 3.2.1-1

ADVANCED EXPANDER ENGINE TURBOPUMP DESIGN SPECIFICATION

<u>Engine Conditions</u>	<u>Value</u>	<u>Fuel</u>	<u>Oxidizer</u>
Rated Thrust, F, lbf	20,000		
Throttle Range	20:1		
Chamber Pressure, Pc, psia	2,000		
Overthrust Pc, psia	2,300*		
Propellant		LH <sub>2</sub>	LOX
Propellant Inlet Temp., °R		38	163
Propellant Inlet Pressure, psia			
To Low Speed Boost Pumps**		20	15
To TPA's		50	50
<u>Pump Conditions</u>	<u>Dimensions</u>	<u>Fuel</u>	<u>Oxidizer</u>
Propellant Density	lb/ft <sup>3</sup>	4.42	71.2
Shaft Speed	rpm	150,000	55,230
Total Discharge Pressure	psia	4,650	4,650
Total Suction Pressure	psia	50	50
Total Pressure Rise	psi	4,600	4,600
Total Head Rise (cavitating)	ft	138,231	9,313
Weight Flow	lb/sec	5.903	35.42
Capacity	gpm	599.4	223.3
Specific Speed (Based on Cavitating Head)	$\frac{\text{rpm} \times \text{gpm}^{1/2}}{\text{ft}^{1/2}}$	1,448	1,464
Efficiency	%	65	68
Fluid Horsepower	h.p.	1,483	600
Shaft Horsepower	h.p.	2,279	881
Net Positive Suction Head	ft	1,792	111
Suction Specific Speed	$\frac{\text{rpm} \times \text{gpm}^{1/2}}{\text{ft}^{1/2}}$	13,334	24,133
INLET DIA.	in.	TBA	TBA
DISCHARGE DIA.	in.	2.44	2.44
Q/N		$3.993 \times 10^{-3}$	$4.043 \times 10^{-3}$
$\Delta H/N^2$		$6.144 \times 10^{-6}$	$3.053 \times 10^{-6}$

TABLE 3.2.1-1

ADVANCED EXPANDER ENGINE TURBOPUMP DESIGN SPECIFICATION  
(CONTINUED)

<u>Turbine Conditions</u>	<u>Dimension</u>	<u>Fuel</u>	<u>Oxidizer</u>
Gas		GH <sup>2</sup>	GO <sup>2</sup>
Shaft Power	h.p.	2,349	908
Gas Mass Flow	lbm/sec	5.31	31.9
Gas Inlet Total Temperature	°F	770	400
Pressure Ratio		1.67	2.1
Static Back Pressure	psia	2,460	1,920
Shaft Speed	rpm	150,000	55,230
Efficiency	%	80	80
Gas Inlet Total Pressure	psia	4,109	4,038
Nozzle Area (effective)	in. <sup>2</sup>	0.324	0.414
Specific Heat	BTU/lb°R	(1)	(2)
Specific Heat Ratio		(1)	(2)
Gas Constant	ft/°R	(1)	(2)
Diameter, Mean	in.	2.77	2.42

REFERENCE

- (1) Hydrogen — NBS Technical Note 617 April 1972  
(2) Oxygen — NBS Technical Note 384 July 1971

\* The design point was based on a 15% overthrust rating. The power balance did not confirm this as a viable operating point. The TPAs are slightly overcapacity using this design point.

\*\* Refer to the engine schematic in Figure 3.1-1 for the relationship of the low speed boost pumps to the high speed TPAs.

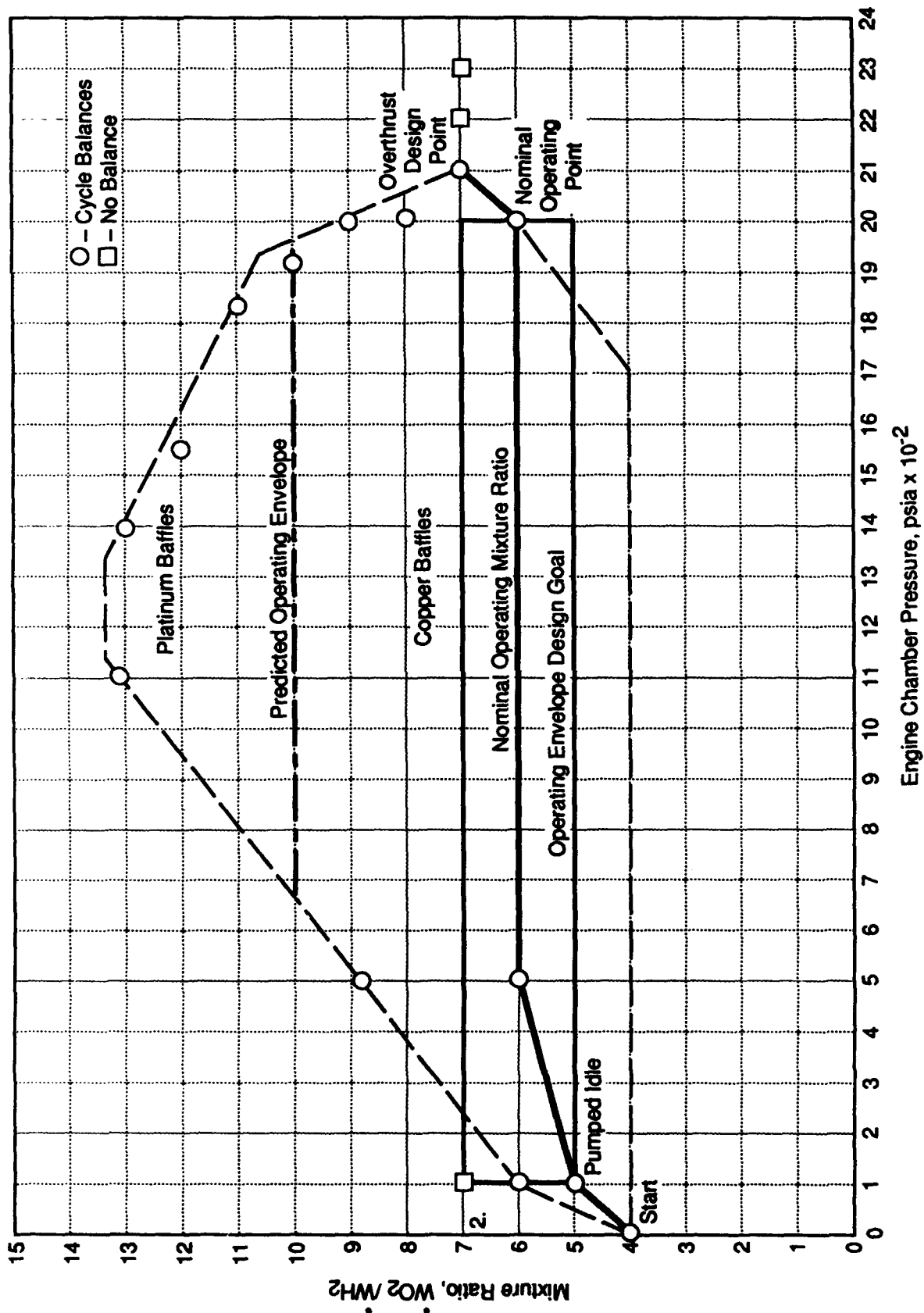


Figure 3.2.1-3. Advanced Engine Study - Engine Operating Range

# NARloy-Z WROUGHT

1700°F-2 h-WQ, 900°F-4 h



## MATERIALS PROPERTIES MANUAL

EXPECTED MINIMUM (90% mean)  
HT 1700F 2 HRS 900F 4 HRS

DATE- 9-1-77

REFERENCE- 7002 -01,02,03,05

2ND EDITION PAGE- 7.3.2.1.2.1A AND .2

7002.26.10.70-01

NARLOY Z	7002
TENSILE STRENGTH	.28
HTOUGHT	.10
STA	.70
PAGE NUMBER	-01

SEC 880170-143

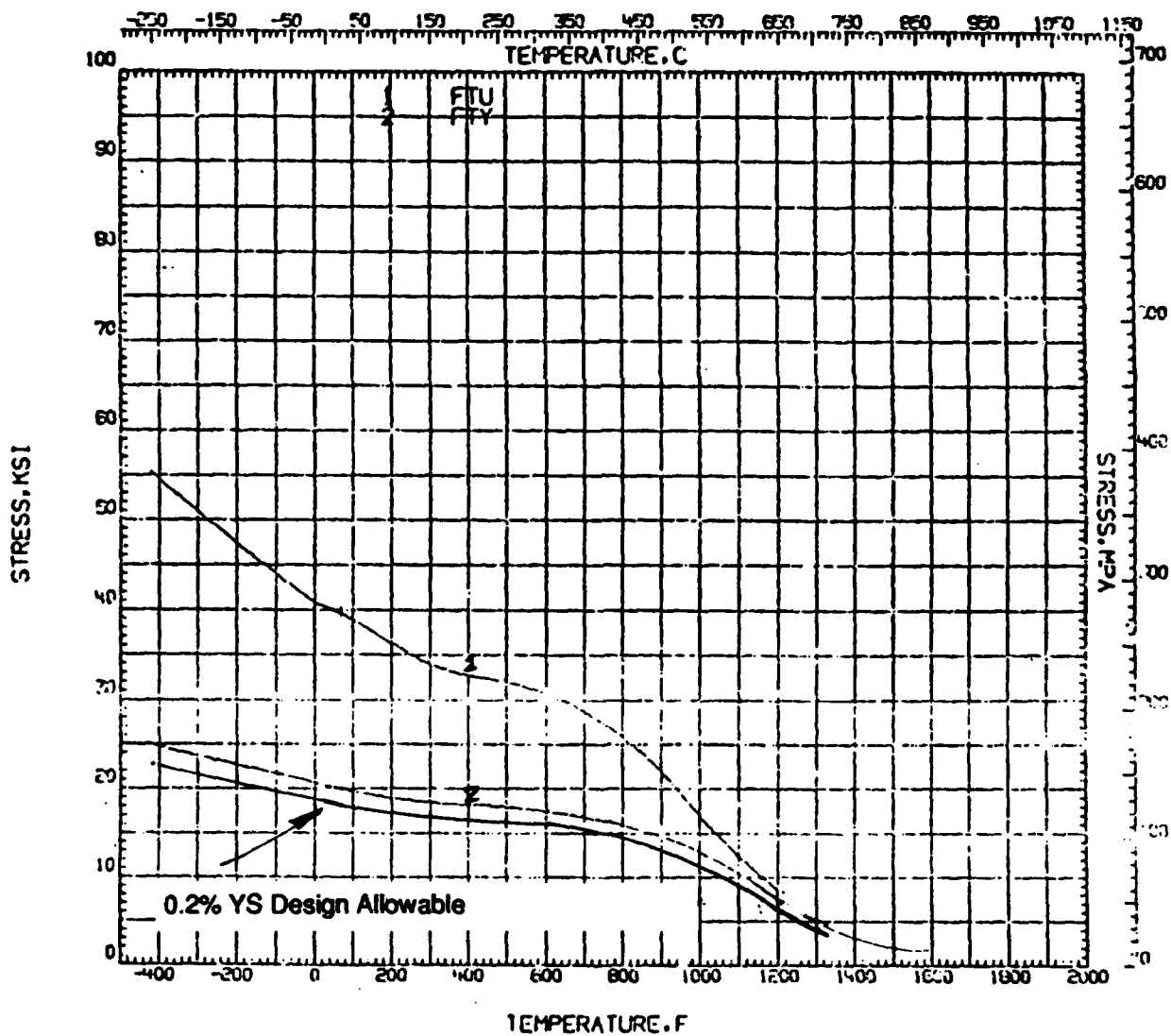
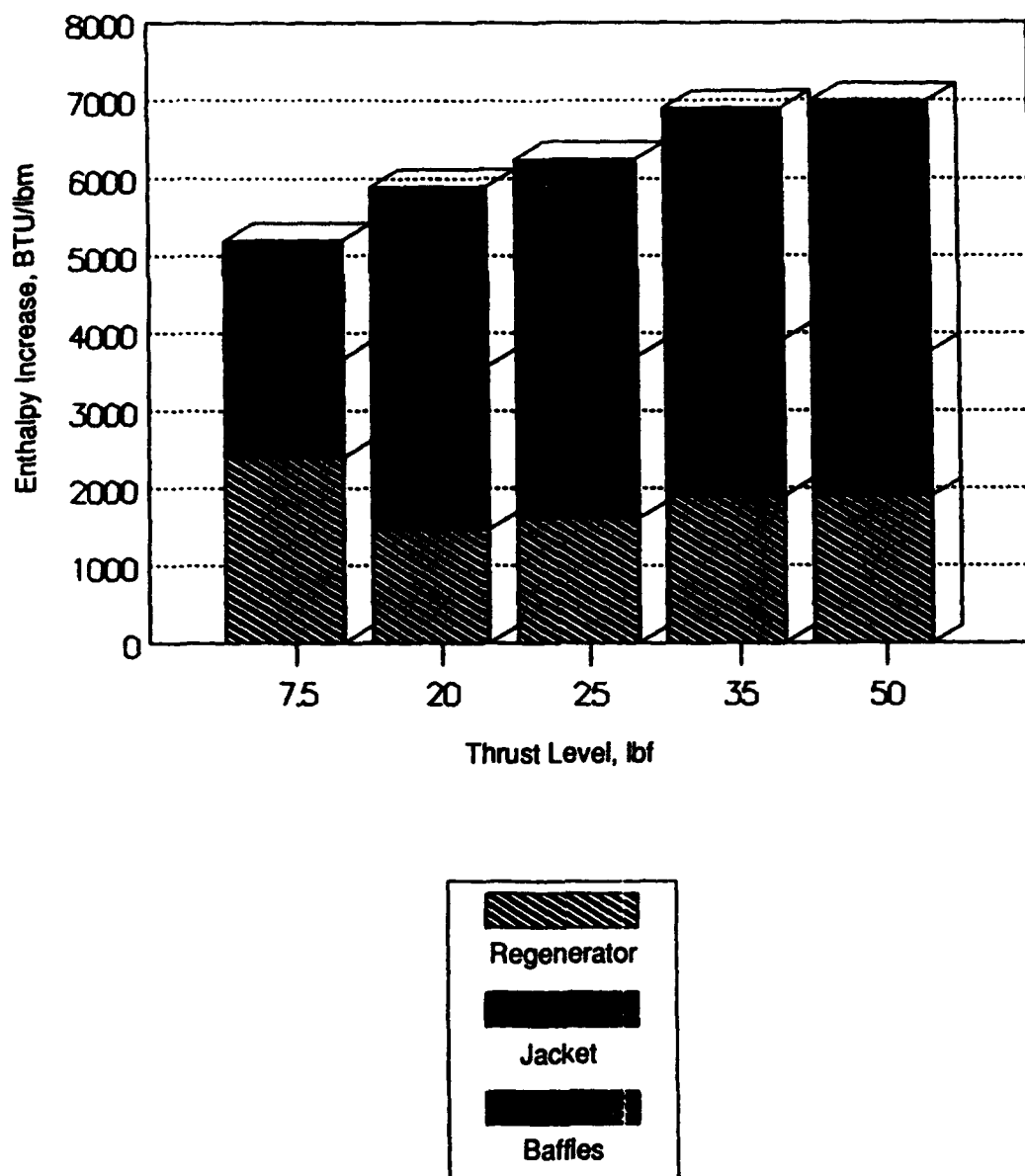


Figure 3.2.1-4.



**Figure 3.2.1-5. Hydrogen Circuit Enthalpy Pickup**

### 3.2, Engine Requirement Variation Studies, (cont)

hydrogen regenerator, regeneratively cooled chamber, and hydrogen cooled baffles. At the 20K lbf thrust level the regen jacket input is very important. Reducing the enthalpy input in the jacket would require more energy extraction at the regenerator with a consequent increase in its size and weight. This can be one of the penalties for a wide throttle range.

For reference, the enthalpy pickup plot for the oxygen circuit is given in Figure 3.2.1-6. The oxygen picks up about 2/3 of its enthalpy increase in the HEX with the balance acquired in the oxygen cooled nozzle. The enthalpy increase per pound is substantially lower than for the hydrogen, but the oxygen flowrate is six pounds per pound of hydrogen at nominal conditions. There is some interplay in HEX and regenerator sizing. The regenerator must increase in size if more energy is extracted from the incoming hydrogen from the turbopump turbine by the HEX. The regenerator has lower delta temperatures for heat transfer. During throttle down operation, all components are effectively "oversized". The regenerator and HEX bypass valves will be bypassing most of the hot hydrogen flow around these components.

#### 3.2.1.2 Power Balance at 20:1 Throttling

A power balance was run at a chamber pressure of 100 psia to evaluate the engine operation when throttled 20:1. Results are given in Table 3.2.2-1. The actual throttle ratio at this point is 20.67:1 and predicted specific impulse is 453.7 lbf sec/lbm. This represents a decline of 30.6 lbf-sec/lbm from the 484.3 lbf-sec/lbm at 20,000 lbf thrust. Losses come from a small decrease in mixing efficiency but mainly from boundary layer losses. The thrust chamber is no longer optimum size at the throttle down conditions.

Temperatures are within the design limits. Note that the hydrogen out of the regen cooled chamber is at 587°F and out of the baffles it is at 653.7°F. Maximum wall temperature with a 50/50 hydrogen split from the proportioner valve (assumed by the power balance) is 1030°F for the regen cooled chamber and 810°F for the baffle. The proportioner valve split should be changed to better optimize these temperatures, but they are still within design limits.

# Oxygen Circuit

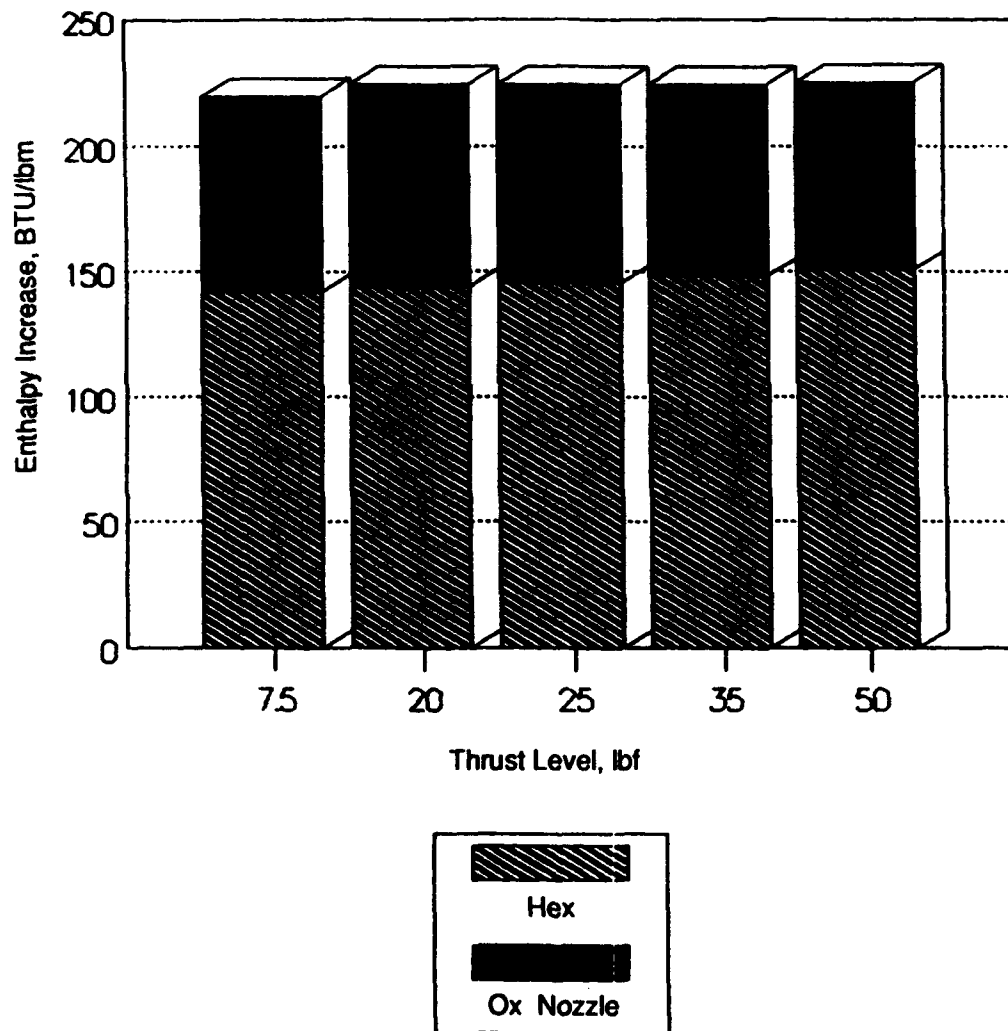


Figure 3.2.1-6. Enthalpy Pickup

**Table 3.2.2-1**  
**Engine Power Balance**  
**At 20:1 Throttle Down Condition**

OTV ENGINE POWER BALANCE				Page 1
Off-Design Run		Oxidizer	Fuel	
	R	= 579.70 (in/deg R)	R	= 9202.00 (in/deg R)
Tank Conditions	Pout	= 15.00 (psia)	Pout	= 20.00 (psia)
	Tout	= 162.70 (deg R)	Tout	= 37.80 (deg R)
	Hout	= -57.17 (BTU/°)	Hout	= -117.35 (BTU/°)
	Rho out	= 71.17 (°/cuft)	Rho out	= 4.34 (°/cuft)
Shut-off Valve	Pin	= 15.00 (psia)	Pin	= 20.00 (psia)
	Pout	= 15.00 (psia)	Pout	= 20.00 (psia)
	Delta P	= 0.00 (psi)	Delta P	= 0.00 (psi)
	T	= 162.70 (deg R)	T	= 37.80 (deg R)
	H	= -57.17 (BTU/°)	H	= -117.35 (BTU/°)
	Rho in	= 71.17 (°/cuft)	Rho in	= 4.34 (°/cuft)
	Rho out	= 71.17 (°/cuft)	Rho out	= 4.34 (°/cuft)
	CdA	= 8.03000 (in <sup>2</sup> )	CdA	= 10.00000 (in <sup>2</sup> )
Pump Conditions	Pin	= 16.00 (psia)	Pin	= 21.00 (psia)
	Pout	= 137.85 (psia)	Pout	= 156.88 (psia)
	Tin	= 162.70 (deg R)	Tin	= 37.83 (deg R)
	Tout	= 164.37 (deg R)	Tout	= 43.44 (deg R)
	Rho in	= 71.1705 (lb/ft <sup>3</sup> )	Rho in	= 4.3349 (lb/ft <sup>3</sup> )
	Rho out	= 70.9994 (lb/ft <sup>3</sup> )	Rho out	= 4.1746 (lb/ft <sup>3</sup> )
	Wdot	= 1.919 (lb/sec)	Wdot	= 0.320 (lb/sec)
	Eff (hyd)	= 0.360	Eff (hyd)	= 0.301
	Eff (mch)	= 1.000	Eff (mch)	= 1.000
	N	= 7361.48 (rpm)	N	= 17529.54 (rpm)
	HP	= 2.34 (HP)	HP	= 6.97 (HP)
	Q/N	= .0016436 (gpm/rpm)	Q/N	= .0016669 (gpm/rpm)
Ox: Cool Side Heat Exchanger	Pin	= 137.85 (psia)	Pin	= 156.88 (psia)
	Pout	= 123.20 (psia)	Pout	= 156.27 (psia)
	Delta P	= 14.45 (psi)	Delta P	= 0.42 (psi)
	Tin	= 164.37 (deg R)	Tin	= 43.44 (deg R)
	Tout	= 164.37 (deg R)	Tout	= 67.30 (deg R)
	Delta T	= 0.00 (deg R)	Delta T	= 23.85 (deg R)
	Hin	= -56.30 (BTU/°)	Hin	= -97.36 (BTU/°)
	Hout	= -56.30 (BTU/°)	Hout	= 122.02 (BTU/°)
	Rho in	= 71.00 (°/cuft)	Rho in	= 4.17 (°/cuft)
	Rho out	= 71.00 (°/cuft)	Rho out	= 0.58 (°/cuft)
	Qdot	= 0.00 (BTU/s)	Qdot	= 26.41 (BTU/s)
Fuel: Cool Side Regenerator	Wdot	= 1.92 (°/sec)	Wdot	= 0.12 (°/sec)
	% bypass		% bypass	= 25.00

**Table 3.2.2-1  
Engine Power Balance  
At 20:1 Throttle Down Condition (Cont.)**

OTV ENGINE POWER BALANCE			Page 2
	Oxidizer	Fuel	
Regen Jacket		P <sub>in</sub>	= 156.68 (psia)
		P <sub>out</sub>	= 143.92 (psia)
		Delta P	= 12.76 (psi)
		T <sub>in</sub>	= 43.44 (deg R)
		T <sub>out</sub>	= 1043.44 (deg R)
		Delta T	= 1000.00 (deg R)
		H <sub>in</sub>	= -97.38 (BTU/#)
		H <sub>out</sub>	= 3562.64 (BTU/#)
		Rho in	= 4.17 (#/cuft)
		Rho out	= 0.03 (#/cuft)
		Wdot	= 0.16 (#/sec)
Baffles		P <sub>in</sub>	= 156.27 (psia)
		P <sub>out</sub>	= 146.74 (psia)
		Delta P	= 9.53 (psi)
		T <sub>in</sub>	= 57.31 (deg R)
		T <sub>out</sub>	= 1113.31 (deg R)
		Delta T	= 1056.00 (deg R)
		H <sub>in</sub>	= 67.74 (BTU/#)
		H <sub>out</sub>	= 3805.68 (BTU/#)
		Rho in	= 0.99 (#/cuft)
		Rho out	= 0.03 (#/cuft)
		Wdot	= 0.16 (#/sec)
Ox Nozzle Cooling	P <sub>in</sub>	= 123.20 (psia)	
	P <sub>out</sub>	= 123.12 (psia)	
	Delta P	= 0.08 (psi)	
	T <sub>in</sub>	= 104.37 (deg R)	
	T <sub>out</sub>	= 540.70 (deg R)	
	Delta T	= 376.33 (deg R)	
	H <sub>in</sub>	= -56.30 (BTU/#)	
	H <sub>out</sub>	= 116.67 (BTU/#)	
	Rho in	= 71.00 (#/cuft)	
	Rho out	= 0.68 (#/cuft)	
	Wdot	= 1.92 (#/sec)	

**Table 3.2.2-1**  
**Engine Power Balance**  
**At 20:1 Throttle Down Condition (Cont.)**

OTV ENGINE POWER BALANCE						Page 3
Oxidizer			Fuel			
Turbine Conditions	Pin	= 125.11 (psia)	Pin	= 143.92 (psia)		
	Pout	= 111.92 (psia)	Pout	= 128.31 (psia)		
	Wdot	= 0.985 (lb/sec)	Wdot	= 0.129 (lb/sec)		
	Tin	= 540.70 (deg R)	Tin	= 1079.38 (deg R)		
	Tout	= 532.99 (deg R)	Tout	= 1064.34 (deg R)		
	Hin	= 116.87 (BTU/#)	Hin	= 3664.19 (BTU/#)		
	Hout	= 115.00 (BTU/#)	Hout	= 3635.02 (BTU/#)		
	Rho in	= 0.68 (#/cuft)	Rho in	= 0.02 (#/cuft)		
	Rho out	= 0.63 (#/cuft)	Rho out	= 0.02 (#/cuft)		
	Eff.	= 0.532	Eff.	= 0.408		
	HP	= 2.33 (HP)	HP	= 8.95 (HP)		
	PR	= 1.100 (Pin/Pout)	PR	= 1.122 (Pin/Pout)		
	U/Co	= 0.206 (fps/fps)	U/Co	= 0.098 (fps/fps)		
Hot Side Heat Exchanger	Wheel dia	= 2.542 (in)	Wheel dia	= 3.090 (in)		
	%bypass	= 48.64	% bypass	= 59.74		
			Pin	= 128.31 (psia)		
			Pout	= 127.31 (psia)		
			Delta P	= 1.00 (psi)		
			Tin	= 1072.79 (deg R)		
			Tout	= 1072.79 (deg R)		
			Delta T	= 0.00 (deg R)		
			Hin	= 3664.45 (BTU/#)		
			Hout	= 3664.45 (BTU/#)		
			Rho in	= 0.02 (#/cuft)		
			Rho out	= 0.02 (#/cuft)		
			Qdot	= 0.00 (BTU/s)		
			Wdot	= 0.23 (#/sec)		
			% bypass	= 25.00		
Gas Side Regenerator			Pin	= 127.31 (psia)		
			Pout	= 125.51 (psia)		
			Delta P	= 1.80 (psi)		
			Tin	= 1072.79 (deg R)		
			Tout	= 1047.66 (deg R)		
			Delta T	= 24.91 (deg R)		
			Hin	= 3664.45 (BTU/#)		
			Hout	= 3576.42 (BTU/#)		
			Rho in	= 0.02 (#/cuft)		
			Rho out	= 0.02 (#/cuft)		
			Qdot	= -26.41 (BTU/s)		
			Wdot	= 0.30 (#/sec)		
Injector	Pin	= 111.92 (psia)	Pin	= 125.51 (psia)		
	Pout	= 100.07 (psia)	Pout	= 99.87 (psia)		
	Tin	= 536.74 (deg R)	Tin	= 1047.66 (deg R)		
	Rho in	= 0.62 (#/cuft)	Rho in	= 0.02 (#/cuft)		
	Rho out	= 0.58 (#/cuft)	Rho out	= 0.02 (#/cuft)		
	Wdot	= 1.827 (lb/sec)	Wdot	= 0.305 (lb/sec)		
	Drop	= 11.85 (psia)	Drop	= 25.64 (psia)		
	CdA	= 1.06919 (in^2)	CdA	= 0.67923 (in^2)		
Combustion Chamber	PC	= 100.00 (psia)	MR	= 6.00 (O/F)		
	DPe	= 0.18 (psia)	Wdot	= 2.13 (lb/sec)		
	ERE	= 1.000	Dthroat	= 2.500 (in)		
	F	= 997.20 (lbf)	isp	= 453.66 (sec)		

## 3.2, Engine Requirement Variation Studies, (cont)

### 3.2.1.3 Conclusions

The baseline engine design readily accommodates 20:1 throttling with only a shift in the turbopump operating points through the control of the hydrogen and oxygen back pressure valves (Figure 3.1-1) to assure stable low speed performance and control. Thermal margins are adequate for unrestricted operation at the throttle down condition. The penalties for 20:1 throttling versus 10:1 throttling come in top end engine overthrust capability as usable overthrust is reduced to 21,000 lbf from 23,000 lbf for the nominal 20,000 lbf thrust engine. There seems to be no significant effect on engine weight or life.

### 3.2.2 High Mixture Ratio Operation

The ground rules for the high mixture ratio subtask were:

- 1) The engine design defined for the 20:1 throttling variation is to be used for the high MR variation without major component changes.
- 2) Throttle ratio at high MR need not be as great as at nominal MR.
- 3) Maximum thrust could be below the nominal for  $MR = 6$ .
- 4) A thrust/MR combination is within the operating envelope if it is capable of continuous operation without violating thermal design limits.
- 5) Oxygen flowrates above the oxygen TPA design point were not considered in the operating envelope (oxygen side limitation).
- 6) Hydrogen flowrates through either the regen cooled chamber or baffle plates that were insufficient to keep the gas side wall temperature below design limits (1050°F wall, 800°F throat) are outside of the operating envelope. (Hydrogen side limitation).
- 7) Any high MR region where control instability is encountered is outside of the operating envelope. (There were insufficient hours available in the program to evaluate high MR control stability).

### 3.2, Engine Requirement Variation Studies, (cont)

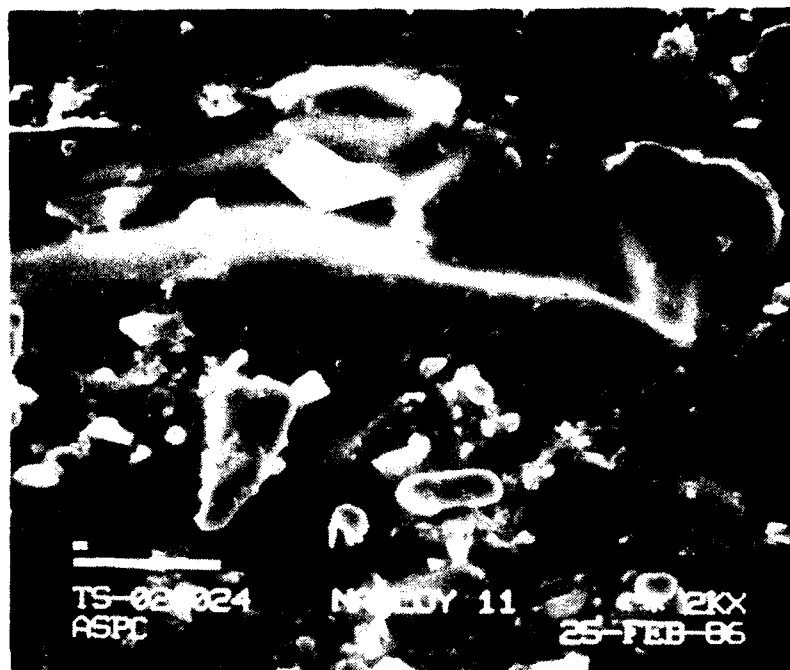
In essence, these groundrules say that the engine used for nominal MR operation must be used for high MR operation without any design change or special modification. One of the gratifying results of this analysis was the confirmation that the engine operating envelope includes operation up to  $MR = 10$  with copper baffle plates, and to  $MR = 13$  with platinum baffle plates. (See Figure 3.2.1-3). The operating envelope is unusually expanded for a rocket engine.

#### 3.2.2.1 Thrust Chamber Life at High Mixture Ratios

A hot copper surface ( $>600^{\circ}\text{F}$ ) will rapidly oxidize in the presence of even small amounts of free oxygen. Chamber life becomes a major issue at any MR approaching stoichiometric ( $MR = 7.94$ ) or higher. For instance, at  $MR = 10$ , atomic oxygen is present in the combustion gases at 1.6 volume percent (chamber pressure = 3000 psia, gases at chemical equilibrium). The small diameter of the oxygen atom allows it to diffuse into the metal lattice where it reacts with a copper atom to form copper oxide. During subsequent operation where the  $MR = 7$  and  $P_c = 3000$  psia, there will be 2.7 volume percent atomic hydrogen that diffuses into the copper surface where it will reduce the copper oxide to elemental copper and form water vapor. Later thermal cycling and water coalescence can generate water bubbles with internal pressures of 200,000 psia. Grain boundaries are enlarged, and cracks and blisters are formed in the surface of the metal. (See References 9 through 11, and Figure 3.2.2-1 for photomicrographs).

#### Chamber Blanching

The progressive oxidation/reduction reaction described above leaves visual effects on a copper chamber wall that have been termed "blanching" due to the whitish, new-copper penny appearance. Blanched surfaces are commonly interconnected by subsurface "wormholing," severe interconnected porosity, and cracks running parallel to the coolant flow passages. Surface roughness of 300 microinch CLA (Center Line Average) is common. Blanched areas have indicated surface temperatures on the order of  $1988^{\circ}\text{F}$  with substrate temperatures greater than  $1700^{\circ}\text{F}$ . Structural properties of all common copper alloys (NASA-Z, OFHC, ZrCu, etc.) are severely degraded at such temperatures. Blanching can progress until the thrust chamber fails due to crack penetration of coolant channels and subsequent chamber burn through. See Figure 3.2.2-2.



Mag 2000X



Mag 2000X

The TGA Specimen Exposed to a Reducing Environment Shows a Reasonably Smooth, Undulating Surface (Top), While an Oxidized Specimen Shows a Granular Surface (Bottom)

Figure 3.2.2-1. NARloy-Z Exposed to Oxidizing/Reducing Environments

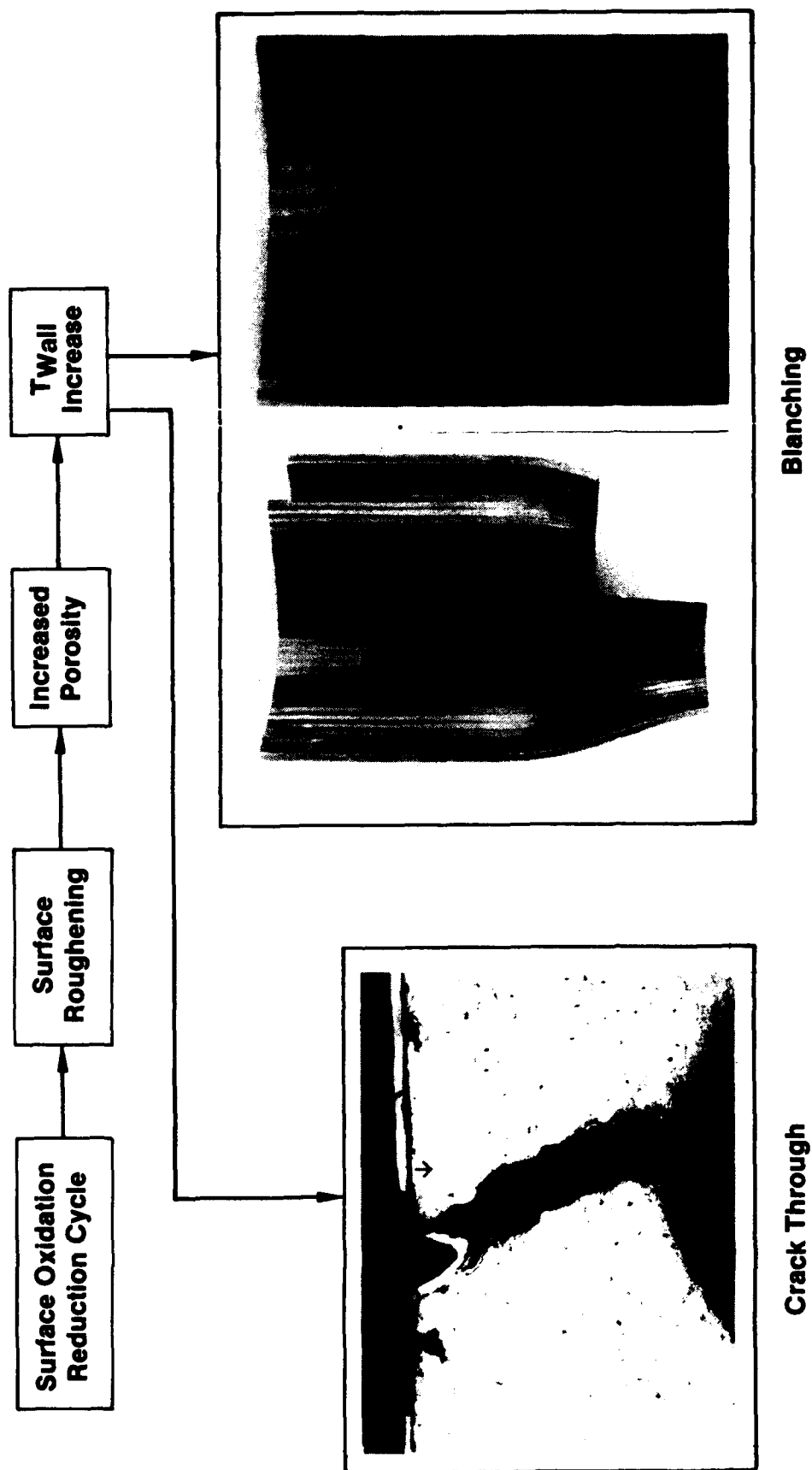


Figure 3.2.2-2. Blanching and Cracking

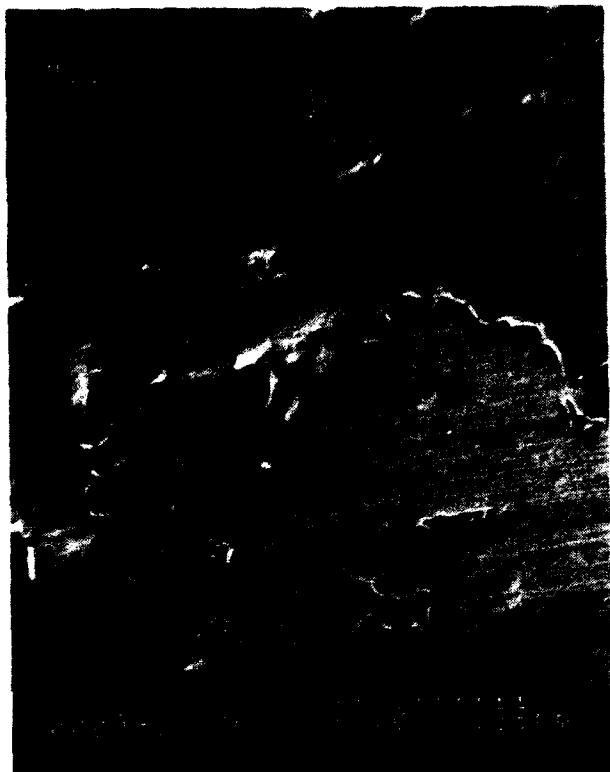
### 3.2, Engine Requirement Variation Studies, (cont)

The high surface temperatures are due to the porosity and increased surface roughness which decreases the material thermal conductivity due to the loss of contact at many points. Photomicrographs of a blanched surface are given in Figures 3.2.2-3 and 3.2.2-4 where the increase in roughness is apparent. The combination of increased wall temperature, reduced structural integrity and degradation of material properties over several cycles leads to cracking. Strain is an effect of blanching, not a cause. Refer to Reference 11 for an in depth discussion of the phenomenon as it relates to rocket engine chambers.

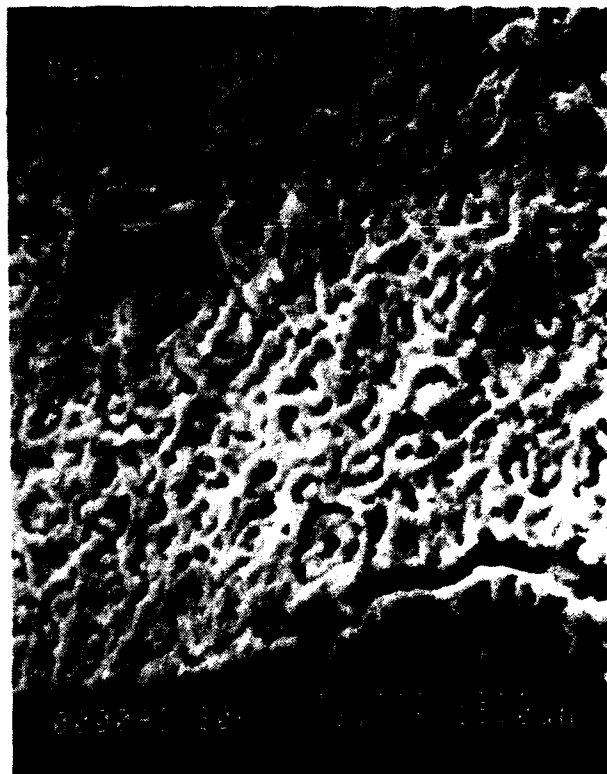
Another chamber concern is the progressive imbalance in the oxygen/hydrogen momentum ratio at the "T"-triplet element as mixture ratios increase. One of the objectives of Contract NAS 3-23772 Task C.4 is to improve the element/chamber wall compatibility by tailoring the momentum ratio and hydrogen impingement pattern. Reduced hydrogen flow restricts the effectiveness of this element tailoring by greatly increasing the momentum ratio. At high MRs the oxygen rich stream will have more wall contact than at lower MRs. In short, element/wall compatibility degrades while the oxidizing potential of the gas stream increases. This is of particular concern in the portion of the chamber within 2 or 3 inches of the injector face. Careful design of the injector hydrogen face bleed openings protect the face of the injector and the first inch or so of the chamber and baffle walls, but element optimization is considered the best means of assuring injector/chamber compatibility. The next best solution is to prevent blanching from occurring despite some element asymmetry.

#### Blanching Prevention

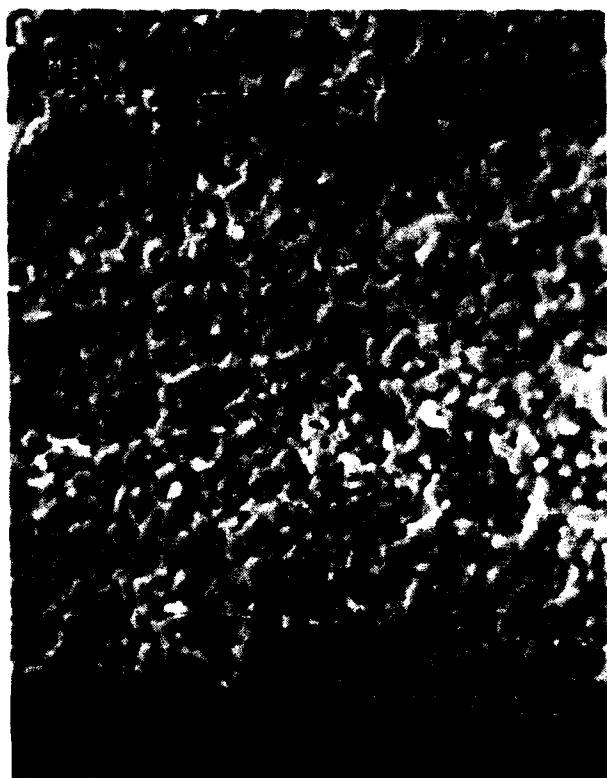
Preventive measures tried to date include 1) surface smoothing, 2) wall temperature reduction, 3) reducing oxygen concentration at the wall, and 4) protective surface coatings. The SSME Narloy Z chamber is refurbished after blanching becomes evident by mechanically smoothing the surface by a combination of peening and grinding. This reduces surface roughness and porosity, but is limited in application as material is removed each time it is done. It also requires engine disassembly and is manhour intensive. The second method, wall temperature reduction, depends on channel cooling that will keep the wall temperature at or below 600°F. This may not be practical, and may be ineffective as coolant channel deposits form or injector element



a



b



c

Tested at 1100°F, MR = 10, 300 psi, O<sub>2</sub>/H<sub>2</sub> Cycle

- a) Cu-Skin
- b) Indication of Blanching on Cu-Skin
- c) Oxide Layer Beneath Cu Skin

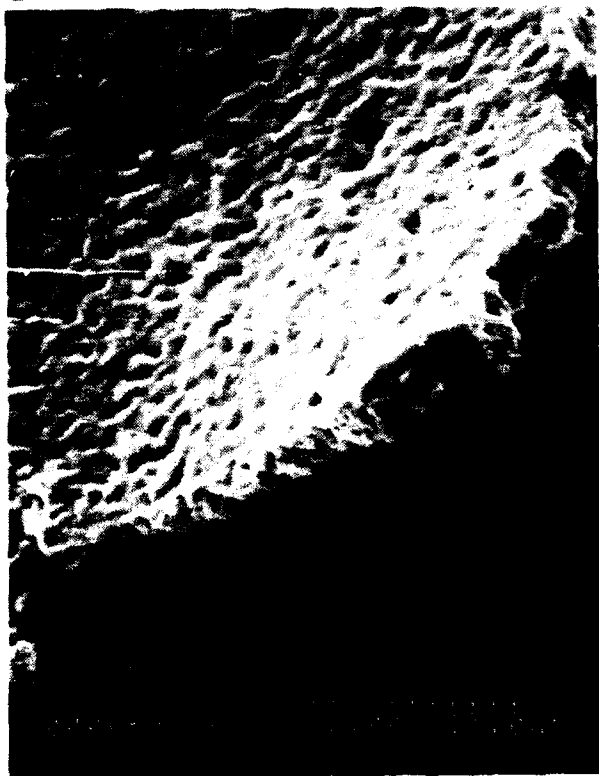
**Figure 3.2.2-3. Uncoated NASA-Z Cylinder After Oxidation and Reduction Test Cycle-26 Slot Area (1.8% Strain)**



a



b



c

Tested at 1100°F, MR = 10, 300 psi, O<sub>2</sub>/H<sub>2</sub> Cycle

- a) Cu Skin
- b) Indication of Blanching on Cu Skin
- c) Cu Skin and Oxide Layer Underneath

**Figure 3.2.2-4. Uncoated NASA-Z Cylinder After Oxidation and Test – Center Area (>2.7% Strain)**

### 3.2, Engine Requirement Variation Studies, (cont)

asymmetries lead to higher wall temperatures. The third method would require hydrogen film cooling for the complete chamber or operation at mixture ratios below 7 for all phases of engine operation (no oxidizer lead or tailoff). This compromises engine operating flexibility. The last option is to apply a thin non-oxidizing coating to the copper surfaces. This was the method selected by Aerojet.

An evaluation of the gas species distribution over the engine mixture ratio range (see Figure 3.2.2-5) shows that atomic and molecular oxygen in a fully mixed combustion gas stream increase rapidly above  $MR = 6$ . At  $MR = 13$  molecular oxygen is second only to water vapor among the species present. An engine expected to operate at high MR must cope with the hot oxygen present. The use of a nonoxidizing coating or a noncopper alloy chamber liner must be considered. The results of the MCA program (Reference 11) show that such coatings are practical.

The MCA investigators tested three coatings: nickel aluminide, nickel, and gold. Two types of nickel aluminide were deposited on copper test articles by a gas diffusion process. The coatings were bomb tested, checked for oxidation resistance at high temperature and oxygen concentration, and then subjected to bend tests. The nickel aluminide protected the copper surface from blanching but suffered some tensile cracking in the bond test. The nickel was brush plated on the copper test articles and tested. There was no cracking or spalling but many pin holes were observed in the material and, on sectioning, many transverse subsurface cracks had formed in some specimens. It was concluded that an effective nickel plating technique would require some development time.

The gold coating was excellent in all respects when gold plating was done on a 30 millionths thick nickel strike. Without the nickel strike there was a void formation, typically called Kirkendall voids, due to the gold propensity to diffuse into the copper surface. After reviewing the discussion in the MCA report (Ref. 11) the Aerojet team has no reservations in recommending the gold plating as the method of choice for preventing blanching of the copper chamber. This is cheap enough protection to baseline it for the engine design even if high MR operation is not an operational requirement.

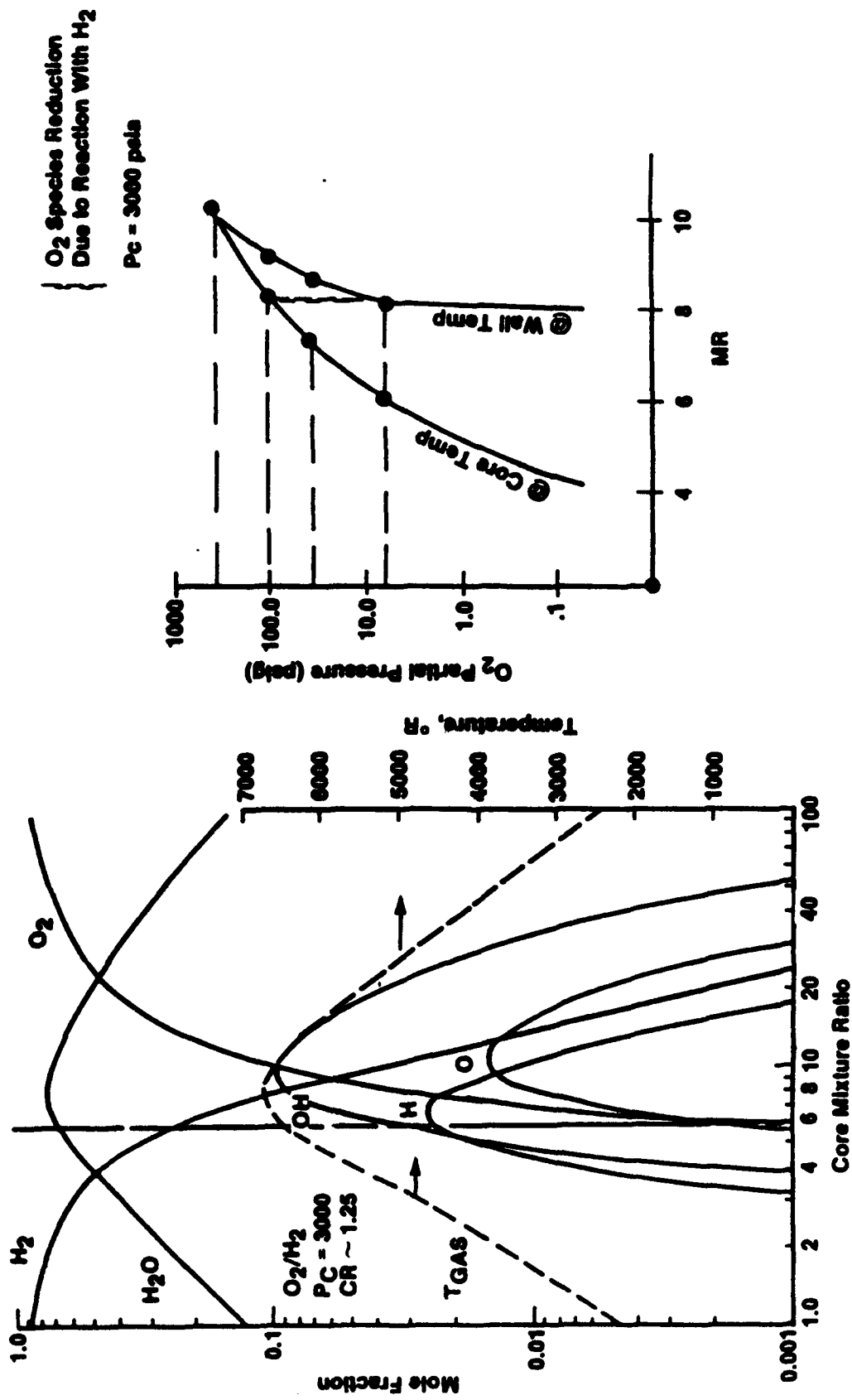


Figure 3.2.2-5 Variation of Combustion Gas Species With MR and Temperature

### 3.2, Engine Requirement Variation Studies, (cont)

#### 3.2.2.2 High Mixture Ratio Performance

For a constant propellant mass flow rate engine thrust will vary with specific impulse:

$$F = I_{sp} \dot{m}$$

Where F = Thrust

$I_{sp}$  = Specific Impulse

and:

M = Propellant Flowrate

$$\frac{F_{12}}{F_6} = \frac{I_{sp @ 12}}{I_{sp @ 6}}$$

Subscripts Refer to Mixture Ratio

but:

T = Absolute Temperature of Combustion

$$\frac{I_{sp @ 12}}{I_{sp @ 6}} \propto \sqrt{\frac{T_{12}/\text{Ag. Gas Mol Wt. @ 12}}{T_6/\text{Ag. Gas Mol Wt @ 6}}} \cong 0.81$$

The baseline OTV Engine operated at MR = 12 and maximum oxygen flowrate should produce about 81% of rated thrust. A more extensive and more rigorous presentation of engine performance change with mixture ratio is given in Figures 3.2.2-6, 3.2.2-7, and 3.2.2-8. Figure 3.2.2-6 is for the 7.5K thrust engine baselined under the current OTV engine contract. All 3 charts have a family of curves for chamber pressures between 100 psia and 2000 psia. This represents a throttling range of 20:1. These are theoretical performance predictions and it should not be assumed that an engine can operate over the entire charted range. Figure 3.2.2-7 is the performance prediction for a 20K lbf thrust engine, and Figure 3.2.2-8 is the chart for a 50K lbf thrust engine. Note that there is a slight performance improvement for the higher thrust cases at any given MR and chamber pressure. At MR = 12 and  $P_c = 2000$  psia the specific impulse is at or slightly above 400 seconds. This is 83% of specific impulse at MR = 6 which confirms the simpler analysis based on combustion temperature and gas molecular weight changes.

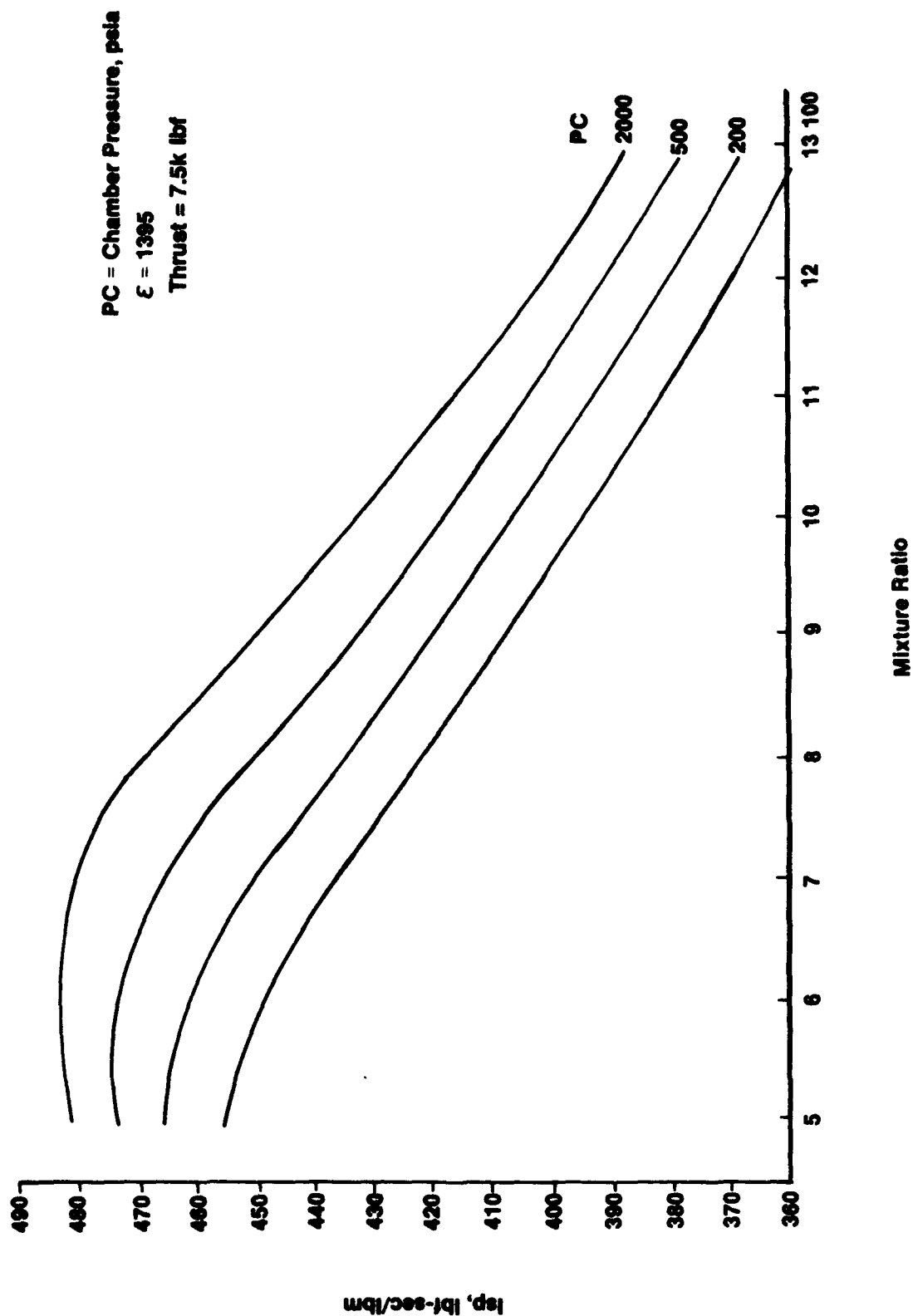


Figure 3.2.2-6 Variation in Specific Impulse With Mixture Ratio for Oxygen/Hydrogen  
 Propellants - 7.5K lbf Thrust Engine

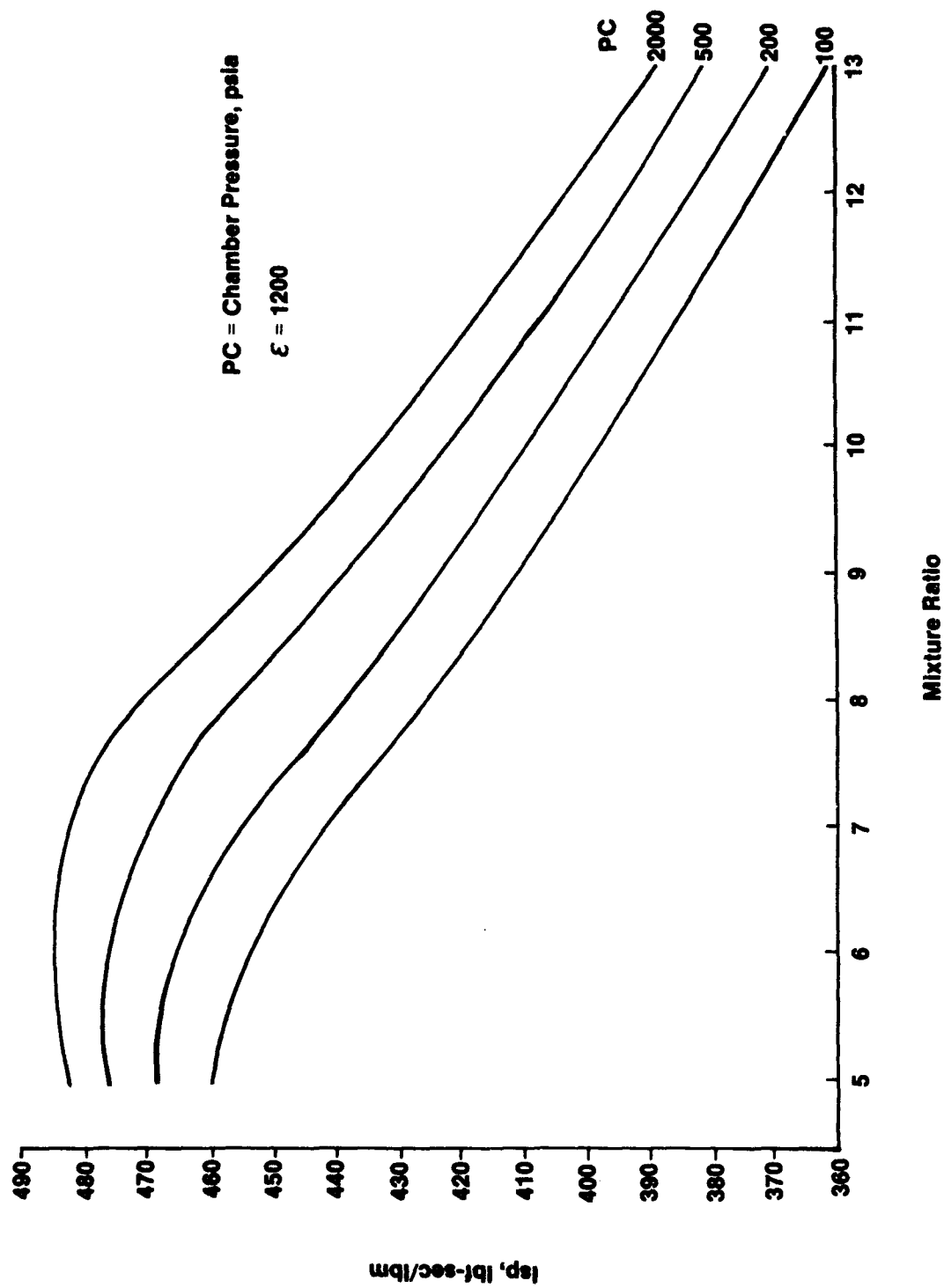
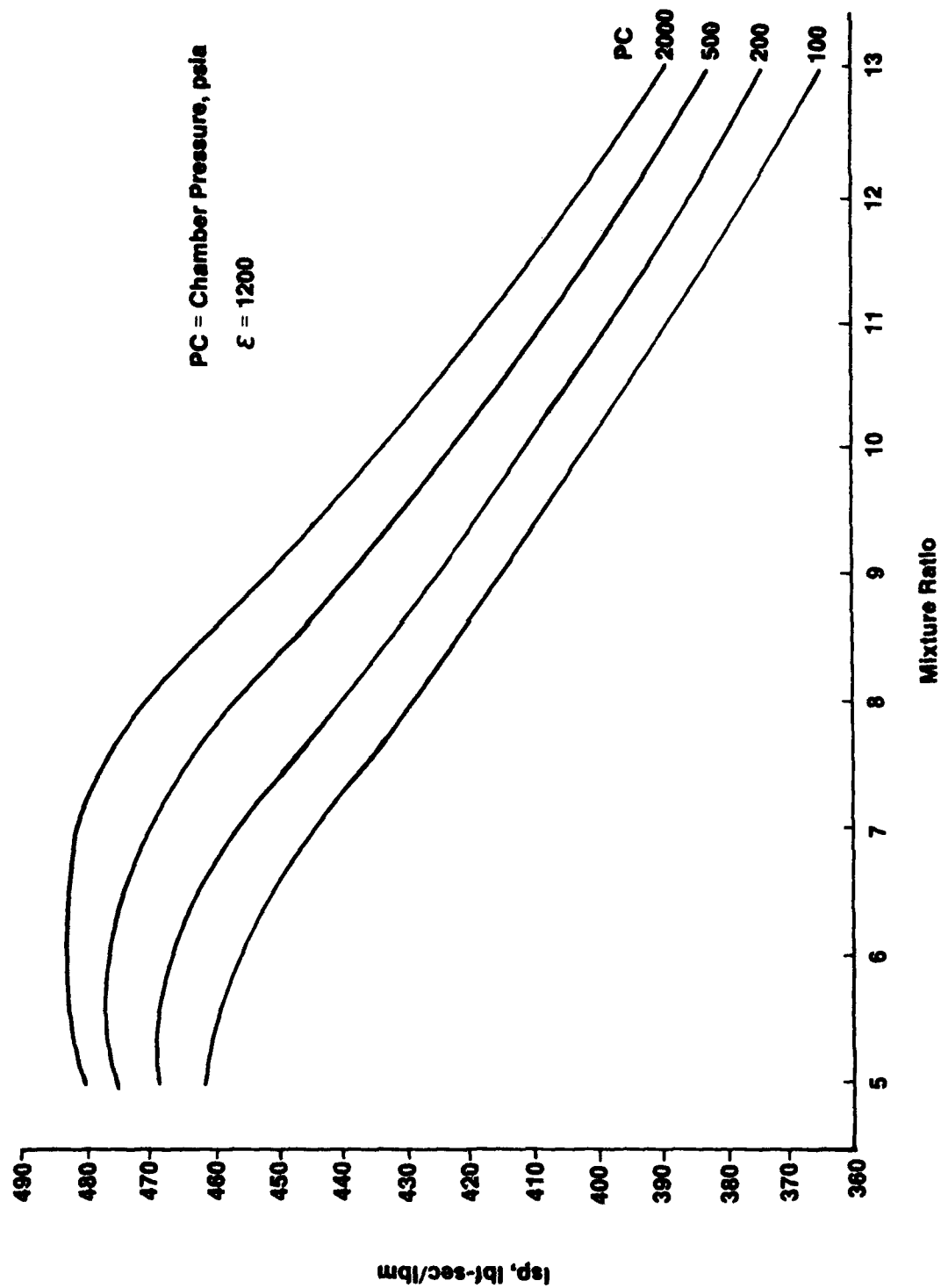


Figure 3.2.2-7 Variation in Specific Impulse With Mixture Ratio for Oxygen/Hydrogen  
 Propellants - 20,000 lbf Thrust Engine



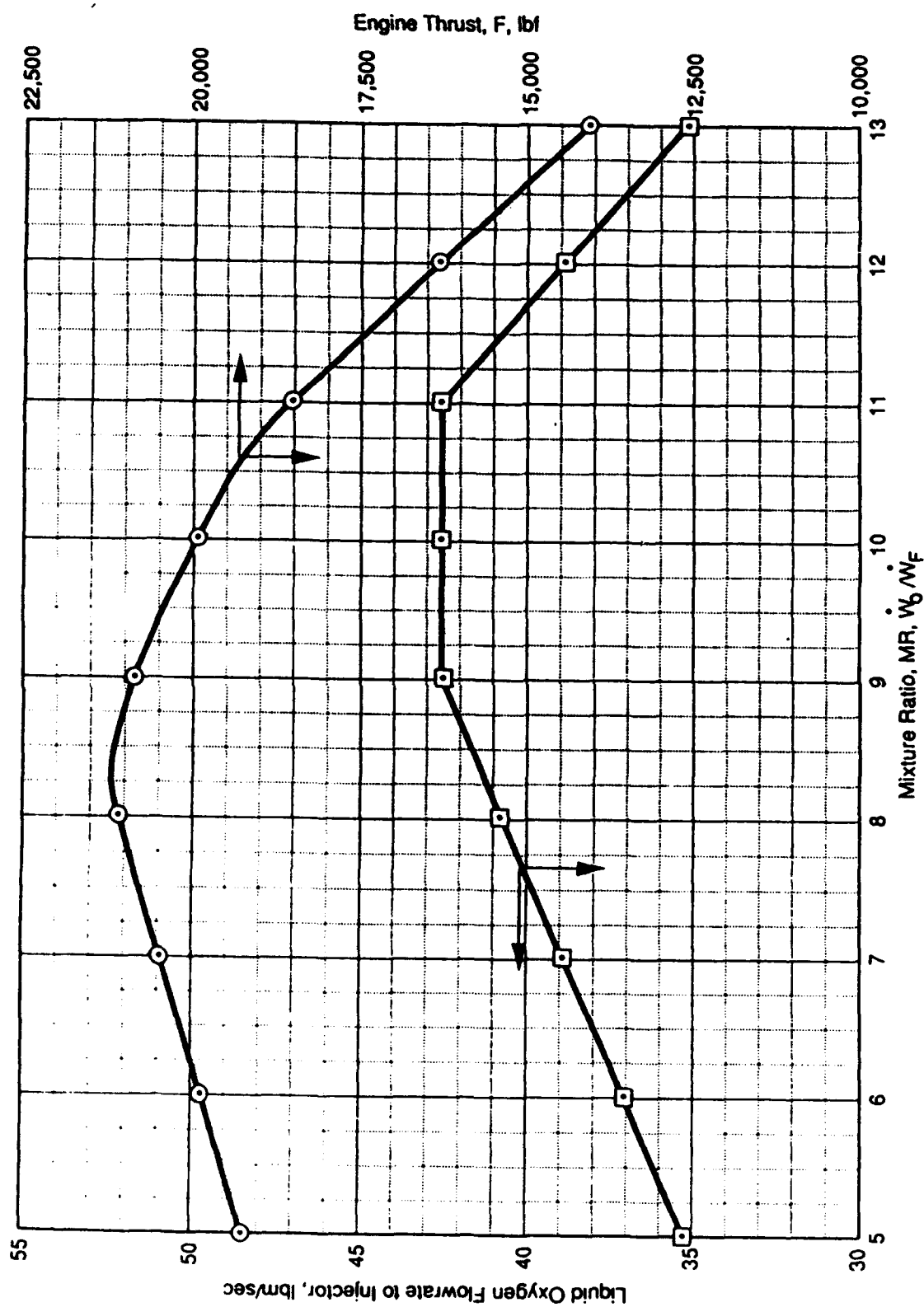
**Figure 3.2.2-8 Variation in Specific Impulse With Mixture Ratio for Oxygen/Hydrogen Propellants - 50,000 lbf Thrust Engine**

### 3.2, Engine Requirement Variation Studies, (cont)

These delivered performance predictions assume a 100% energy release efficiency (ERE) is attained. This is not an unreasonable assumption based on I-triplet element efficiency and the mixing afforded by a chamber length greater than 10 inches. Baseline performance for the 7.5K and 20K, and 50K lbf thrust engines ( $MR = 6$ ,  $P_c = 2000$  psia,  $E = 1200$ ) measured in delivered specific impulse ( $I_{sp}$ ) is expected to be 483:1, 487.3, and 485.2 lbf-sec/lbm, respectively. The  $I_{sp}$  loss in throttling down from 2000 to 100 psia chamber pressure is 30 to 45 lbf-sec/lbm. The loss in  $I_{sp}$  by going to high mixture ratio is much greater, and can only be justified by the economies realized by using oxygen recovered from lunar material.

Under the guidelines for the high MR study, engine thrust could vary from the nominal at  $MR 6 \pm 1$ . Power balance runs over the full MR range used a maximum oxygen turbopump capacity as one of the limiting parameters. The design point for the oxygen turbopump was set at the flow condition for  $MR = 7$ ,  $P_c = 2300$  psia on the assumption that this was a realistic operating point (15% overthrust). This was the design point in the 7.5K lbf engine preliminary design. For a nominal 20,000 lbf thrust engine this is a flow of 43.66 lbm/second of oxygen. The design flowrate includes an additional 5% for autogenous tank pressurization. The lower curve in Figure 3.2.2-9 plots oxygen flow to the injector. This curve flattens at  $MR = 9$  as it reaches LOX TPA rated capacity. The upper curve in Figure 3.2.2-9 plots thrust versus MR and shows an engine thrust peak at slightly above  $MR = 8$  (near stoichiometric). At higher mixture ratios thrust falls off rapidly. The engine cycle does balance at  $MR = 13$ , however. An interesting result of this analysis is that engine thrust loss at high MR does not become a concern until  $MR \geq 10$ . Actual maximum engine thrust is attained at  $MR = 8.3$  where an overthrust of 21,200 lbf is reached.

The baseline regen cooled chamber and baffle plates were evaluated extensively at  $MR = 12$  for their thermal performance. The evaluation was done at two chamber pressures: 2000 psia and 1500 psia. Later power balance work showed that 2000 psia was not attainable for  $MR = 12$  operation while the actual maximum was about 1550 psia. The analysis also evaluated both NASA-Z and platinum baffle plates. Results of the 2000 psia analysis are given in Figures 3.2.2-10 and 3.2.2-11. With the hydrogen regenerator preheating hydrogen to the baffle plates ( $T_{in.} = 499^\circ\text{F}$ ) the NASA-Z or Narloy baffle wall temperature is above the thermal limit for all settings of



MIS-1-10

Figure 3.2.2-9 Advanced Engine Study - Mixture Ratio Versus LOX Flowrate and Thrust

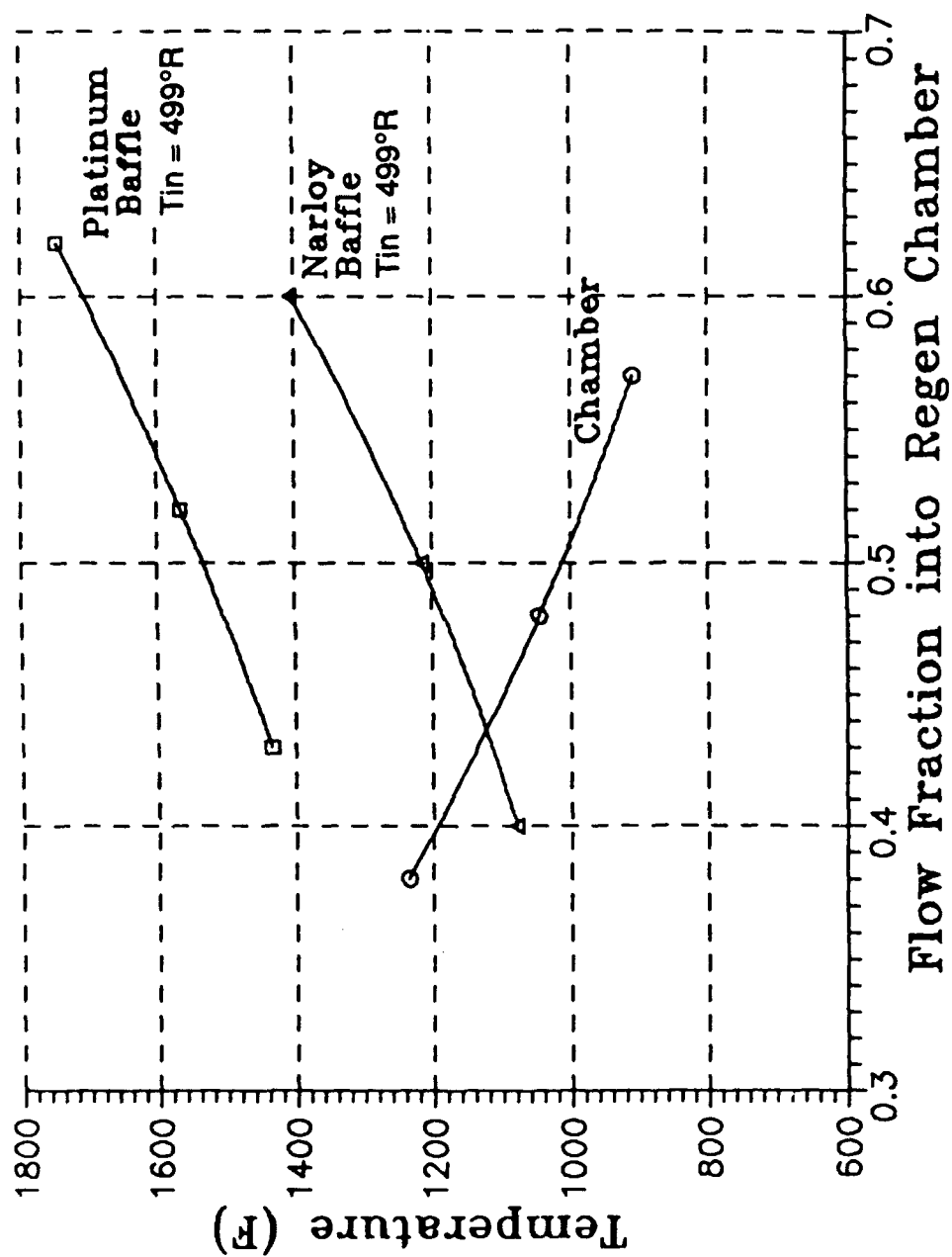


Figure 3.2.2-10. Engine Maximum Wall Temperature for  $P_c = 2000$  psia,  $MR = 12$

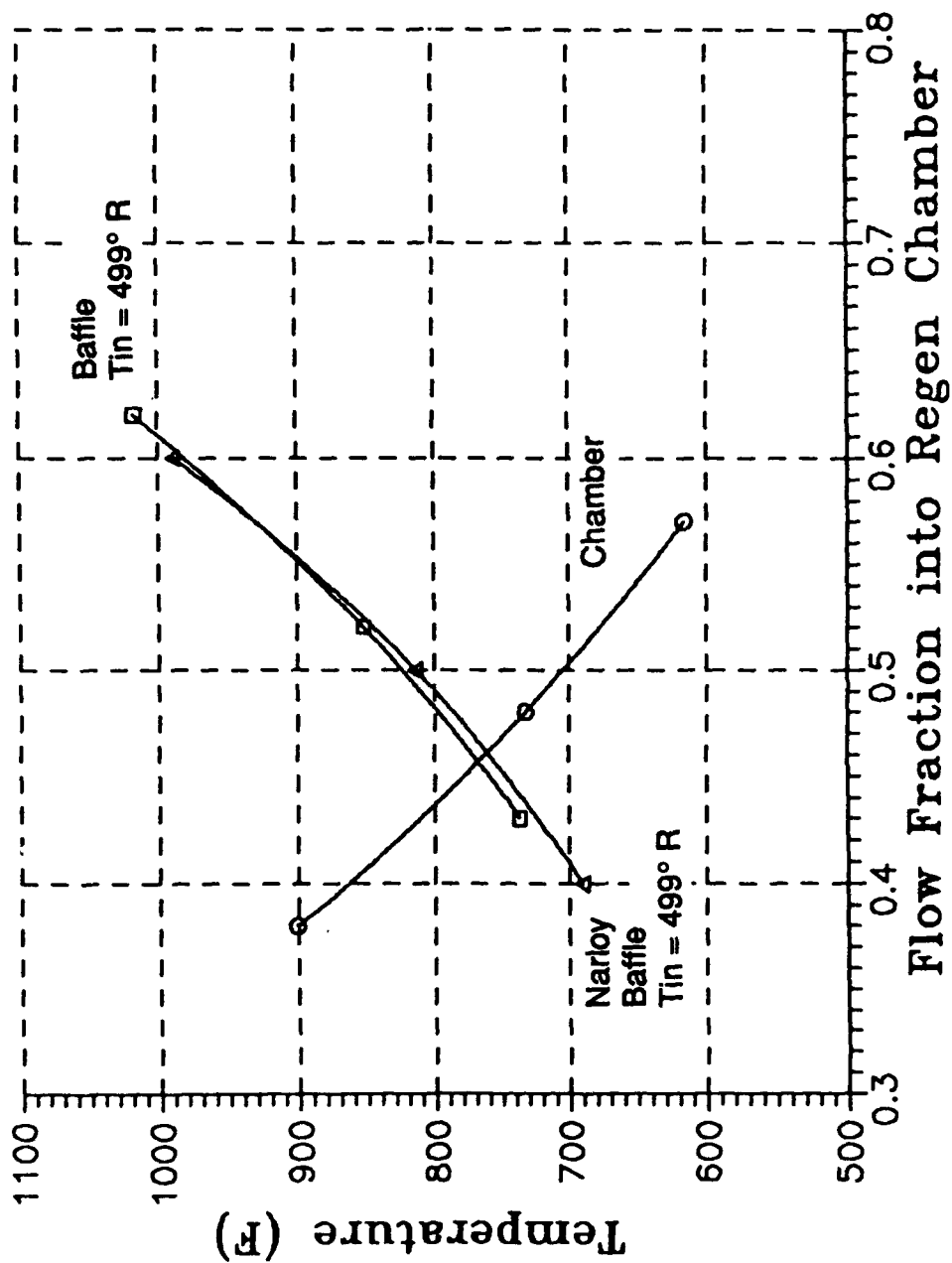


Figure 3.2.2-11. Engine H<sub>2</sub> Bulk Temperature Rises for  $P_c = 2000$  psia,  $MR = 12$

### 3.2, Engine Requirement Variation Studies, (cont)

the flow proportioner valve. A platinum baffle, however, is well within design capability at proportioner valve settings where the chamber is also below thermal design limits. The next chart, Figure 3.2.2-12, assumes the regenerator is not used at all and hydrogen enters both the chamber and baffles at 90°R. For this case, the optimum proportioner valve setting has 54% of the hydrogen flow going to the chamber, and the copper alloy baffle is adequate. A platinum baffle would provide more margin as indicated on the plot. Figure 3.2.2-13 gives the actual bulk temperature rise where Figure 3.2.2-10 gave the actual maximum wall temperature.

Design margins and engine life are set by the hot gas side wall temperatures, but the engine power capability is a function of the bulk temperature rise of the hydrogen in the channels. This is presented in Figures 3.2.2-14 and 3.2.2-15 for various settings of the hydrogen proportioner valve and  $MR = 10$ . A design goal for continued development of this engine would be to optimize the sum of the enthalpy gains by adjusting chamber and baffle geometries as well as the proportioner valve setting.

One issue that has to be addressed in the design is the equalization of pressure drops over the two parallel hydrogen circuits. Figure 3.2.2-16 shows the pressure drops for various settings of the proportioner valve. Two possible solutions are to 1) increase the velocity and pressure drop in the baffle circuit by restricting the channel size, and 2) orificing the baffle outlet circuit before it mixes with the regen chamber outlet to increase pressure drop. The criteria is to equalize the pressure drops downstream of the proportioner valve with circuit elements. Otherwise, they will equalize hydrodynamically and, in effect, change the flow distribution from that desired and commanded at the proportioner valve.

#### 3.2.2.3 Chamber and Baffle Wall Temperature Limits

A high mixture ratio implies a reduced hydrogen flow rate for this design study. This is shown in Figure 3.2.2-13 where hydrogen flowrate to the TPA (which includes 5% autogenous pressurization flow) is plotted against mixture ratio at the condition of maximum engine thrust for that mixture ratio. The maximum thrust condition is determined by an iteration process during the power balance, and has small errors that cause the curve as plotted to have some minor inflections. It should be a smooth curve.

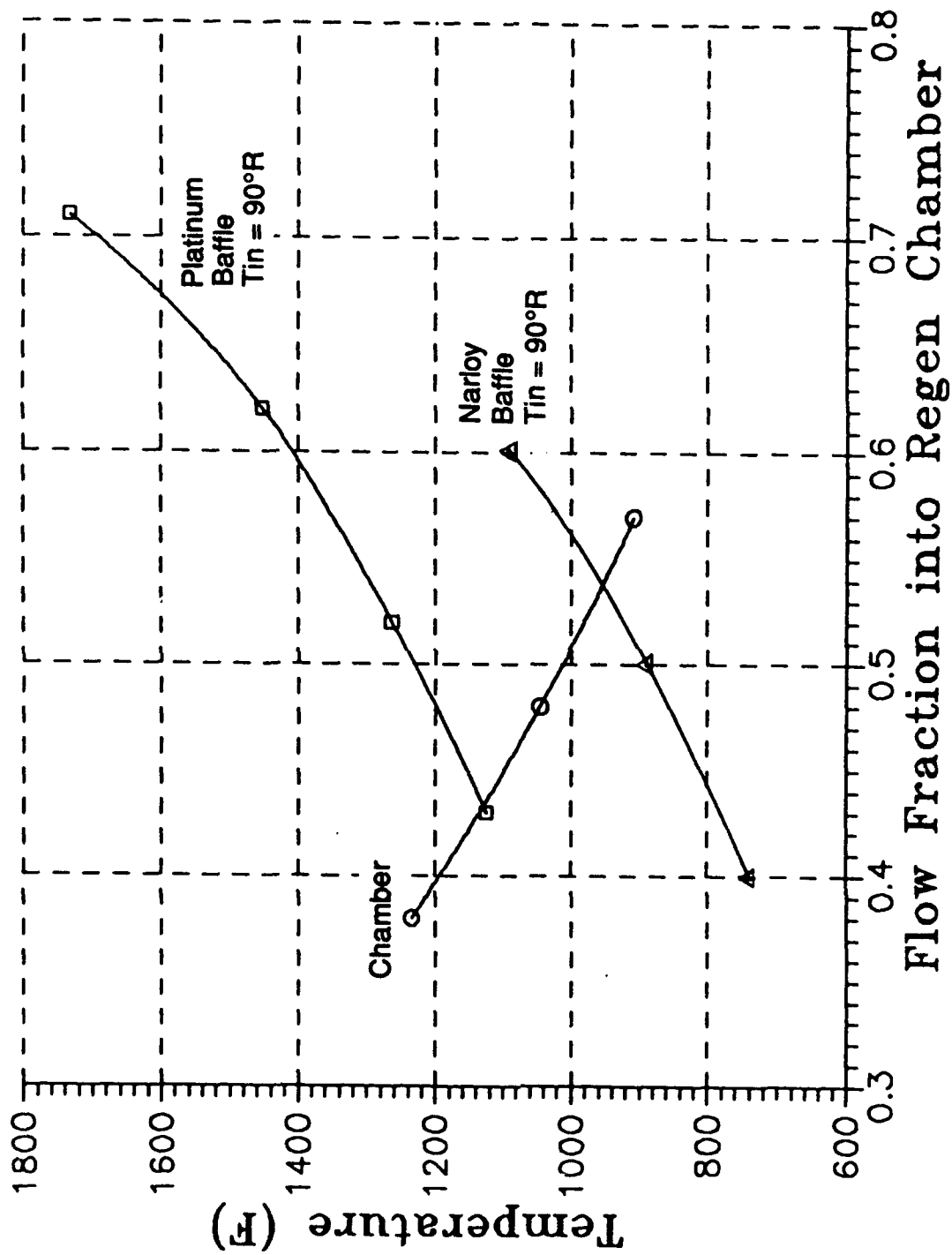
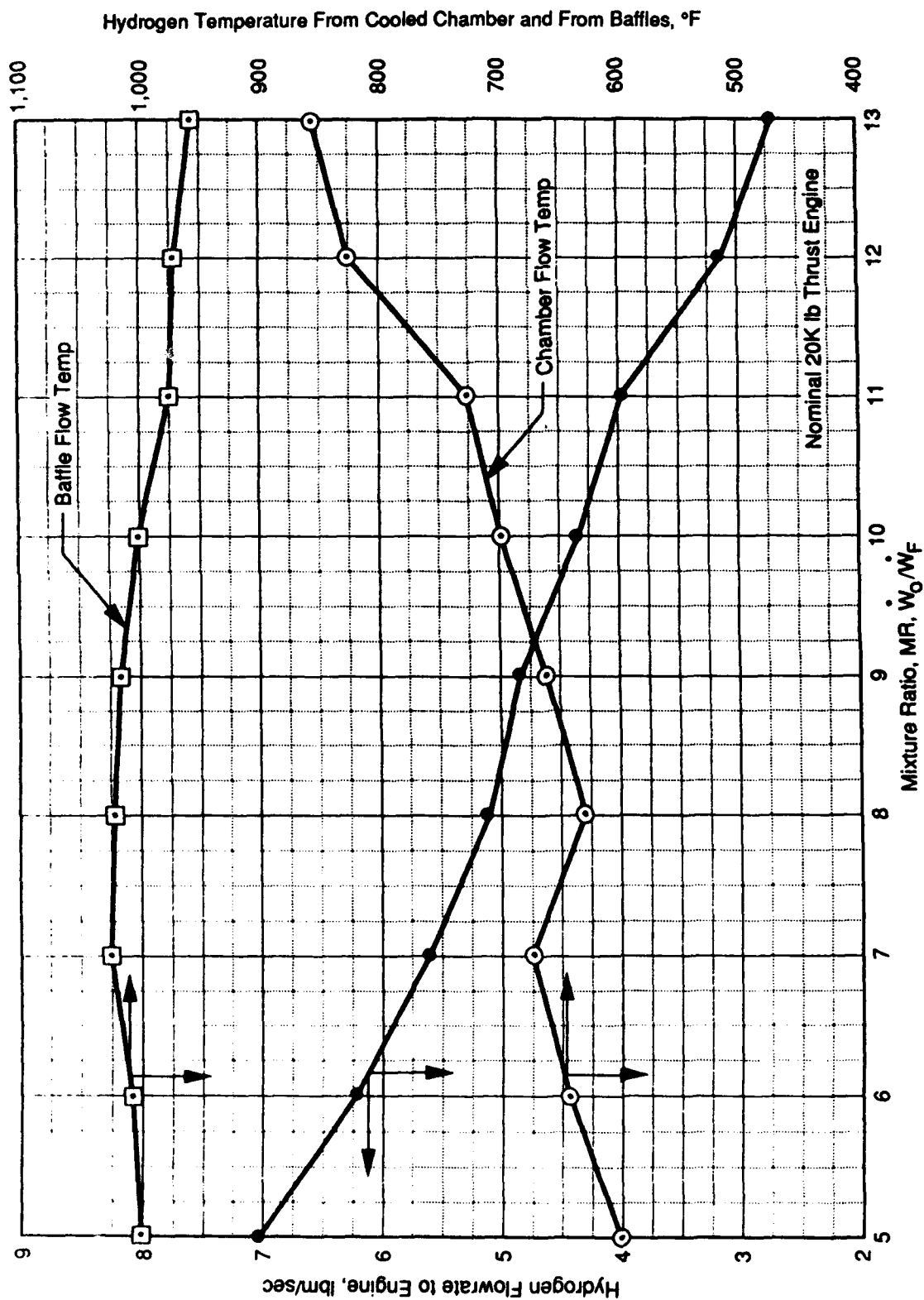


Figure 3.2.2-12. Engine Maximum Wall Temperature for  $P_c = 2000$  psia,  $MR = 12$



MI 5-1-11

Figure 3.2.2-13. Advanced Engine Study - Mixture Ratio Versus Hydrogen Flowrates and Hydrogen Temperature at Maximum Thrust

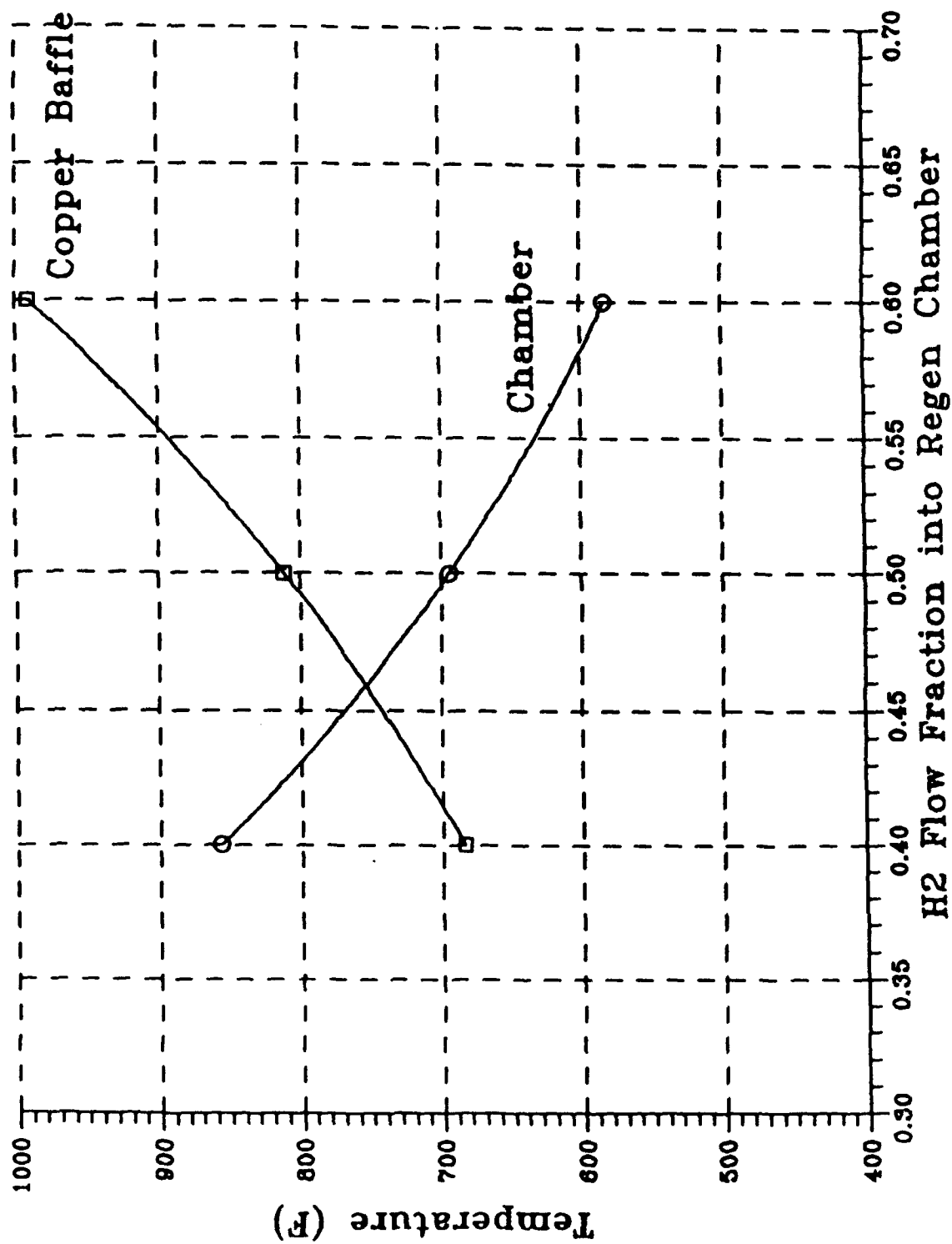


Figure 3.2.2-14. Engine Hydrogen Bulk Temperature Rises -  $P_c = 1917$  psia -  $MR = 10$

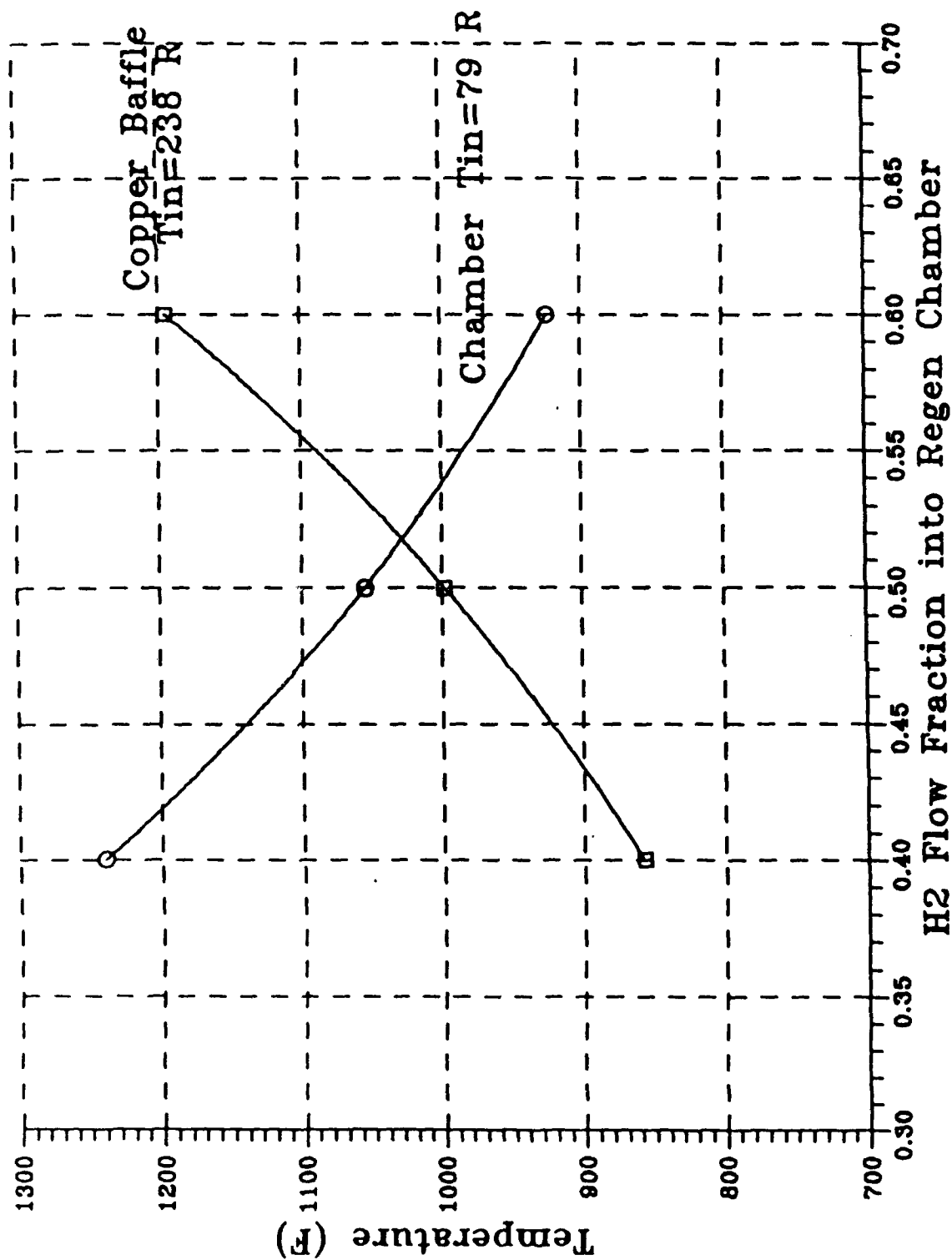


Figure 3.2.2-15. Engine Maximum Wall Temperature -  $P_c = 1917\text{ psia}$  -  $MR = 10$

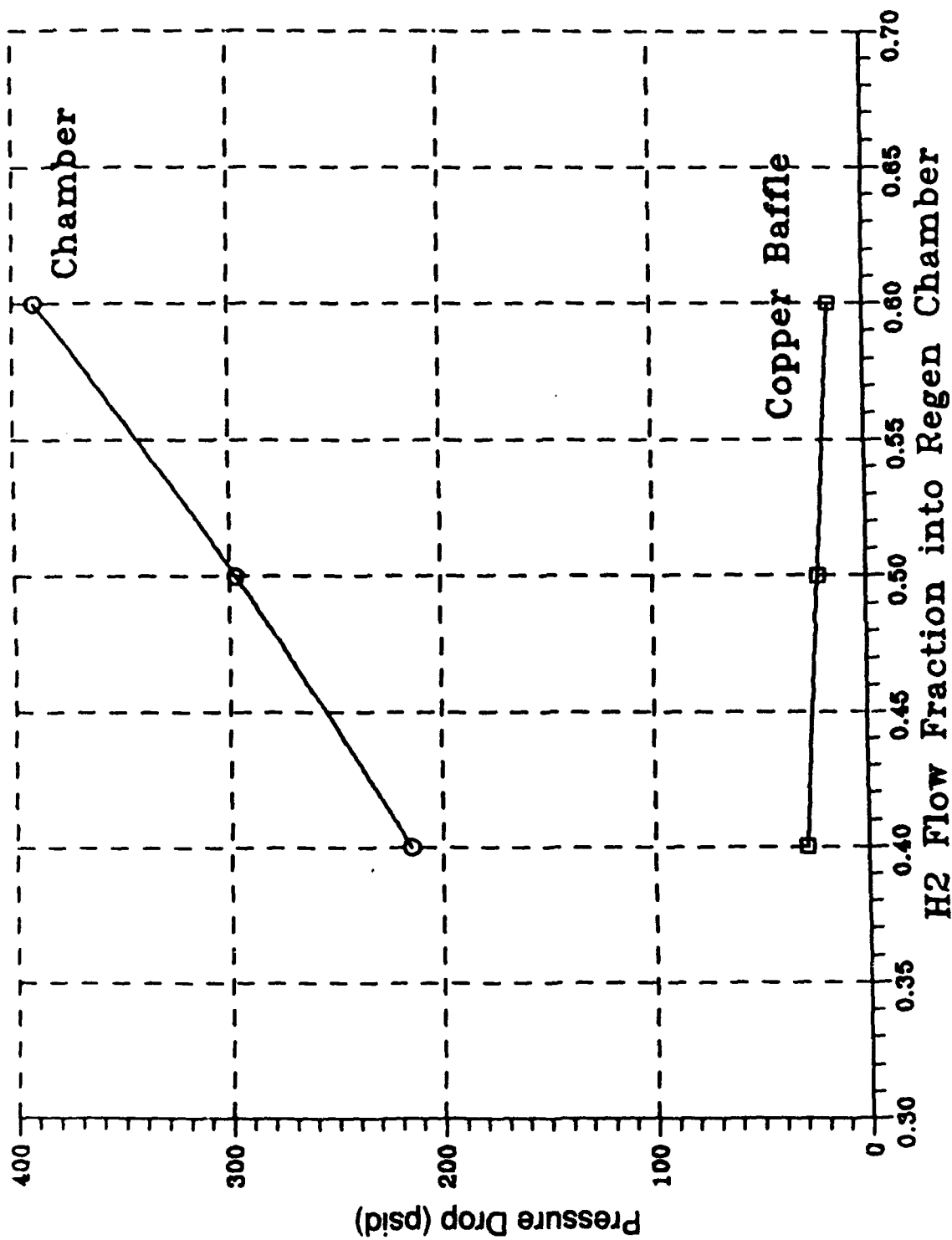


Figure 3.2.2-16. Engine Pressure Drops -  $P_C = 1917$  psia - MR = 10

### 3.2, Engine Requirement Variation Studies, (cont)

As hydrogen flow is progressively reduced, the velocity through the chamber slows and the residence time of the hydrogen in the heated channels increases. The result is a bulk temperature rise at lower flow rates. This is shown in Figure 3.2.2-13. The thermal control limits set in the power balance program correspond to a maximum throat hot gas side wall temperature of 800°F (1259.6°R), a chamber wall temperature near the injector face of 1050°F (1509.6°R), and a baffle gas side wall temperature of 1050°F for copper alloy baffles. A platinum baffle would increase the allowable wall temperature to 2000°F (2459.6°R). The plots as shown in Figure 3.2.2-13 are for copper alloy chamber and baffles, but hydrogen baffle outlet flow temperature would be little changed if platinum were used as the lower thermal conductivity of platinum compensates for the higher hot gas side wall temperature. This indicates that actual enthalpy pickup is relatively independent of the material selected and the use of platinum does not compromise performance capability.

The design concern is the chamber maximum wall temperature. At mixture ratios above 10 the wall temperature begins to exceed the design limit of 1100°F for the NASA-Z material. If the hydrogen proportioner valve is adjusted to route more hydrogen to the chamber circuit, the baffle temperature increases. This relationship is shown in Figure 3.2.2-15. Note that the crossover point is at a proportioner valve setting of 0.52 flow fraction to the regen chamber for the copper chamber and baffle. If platinum baffles are used, the proportioner setting can be increased, reducing chamber wall temperature. This relationship between the two circuits establishes an important design limit. At any mixture ratio up to 10, copper baffles give adequate design margin. At mixture ratios from 10 to 13 a platinum baffle would have to be used to keep the regen chamber temperature within design limits. The platinum baffles would also improve engine life at lower mixture ratios as the operating point could be biased towards lower chamber temperature.

Similar plots are given in Figures 3.2.2-17, 3.2.2-18, and 3.2.2-19 for the 1500 psia chamber pressure condition. Again, the platinum baffle allows for a lower regen chamber maximum that should improve engine life. Note in Figure 3.2.2-18 that there is some separation of the curves for the copper versus the platinum baffles where hydrogen bulk temperature rise is evaluated. This discrepancy can be readily evened

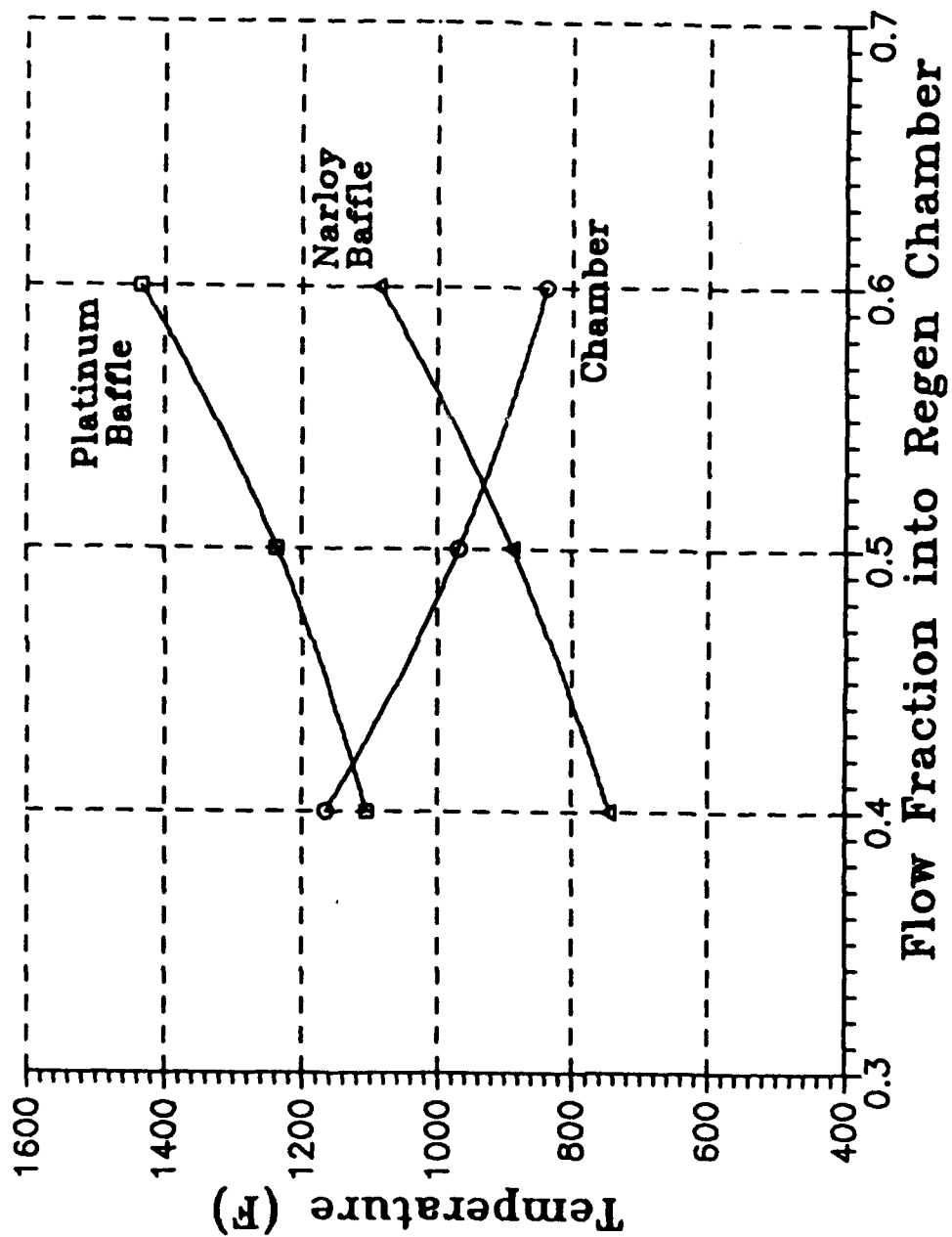


Figure 3.2.2-17. Engine Maximum Wall Temperature for  $P_c = 1500$  psia,  $MR = 12$

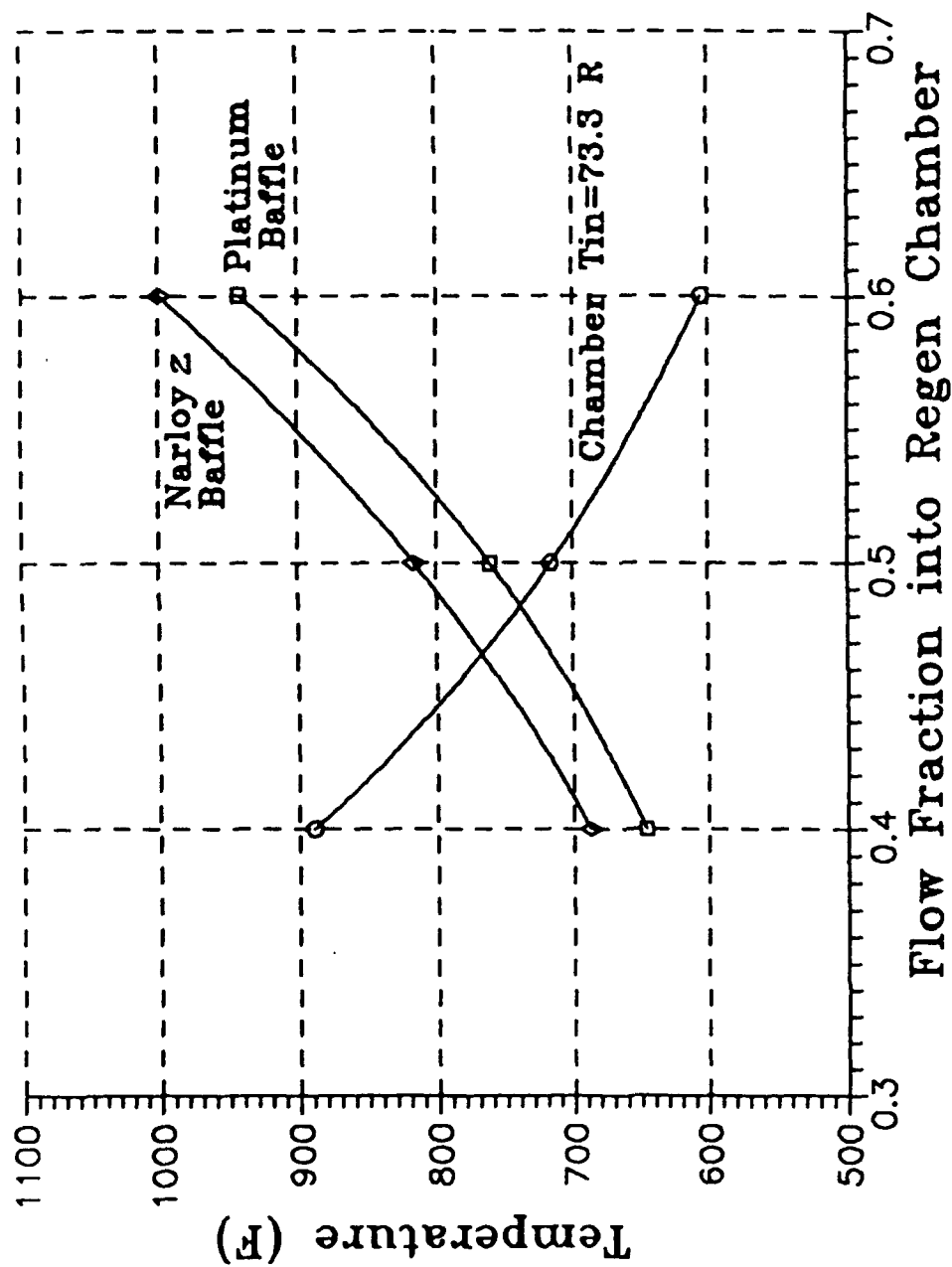


Figure 3.2.2-18. Engine Maximum Hydrogen Temperature for  $P_c = 1500$  psia,  $MR = 12$

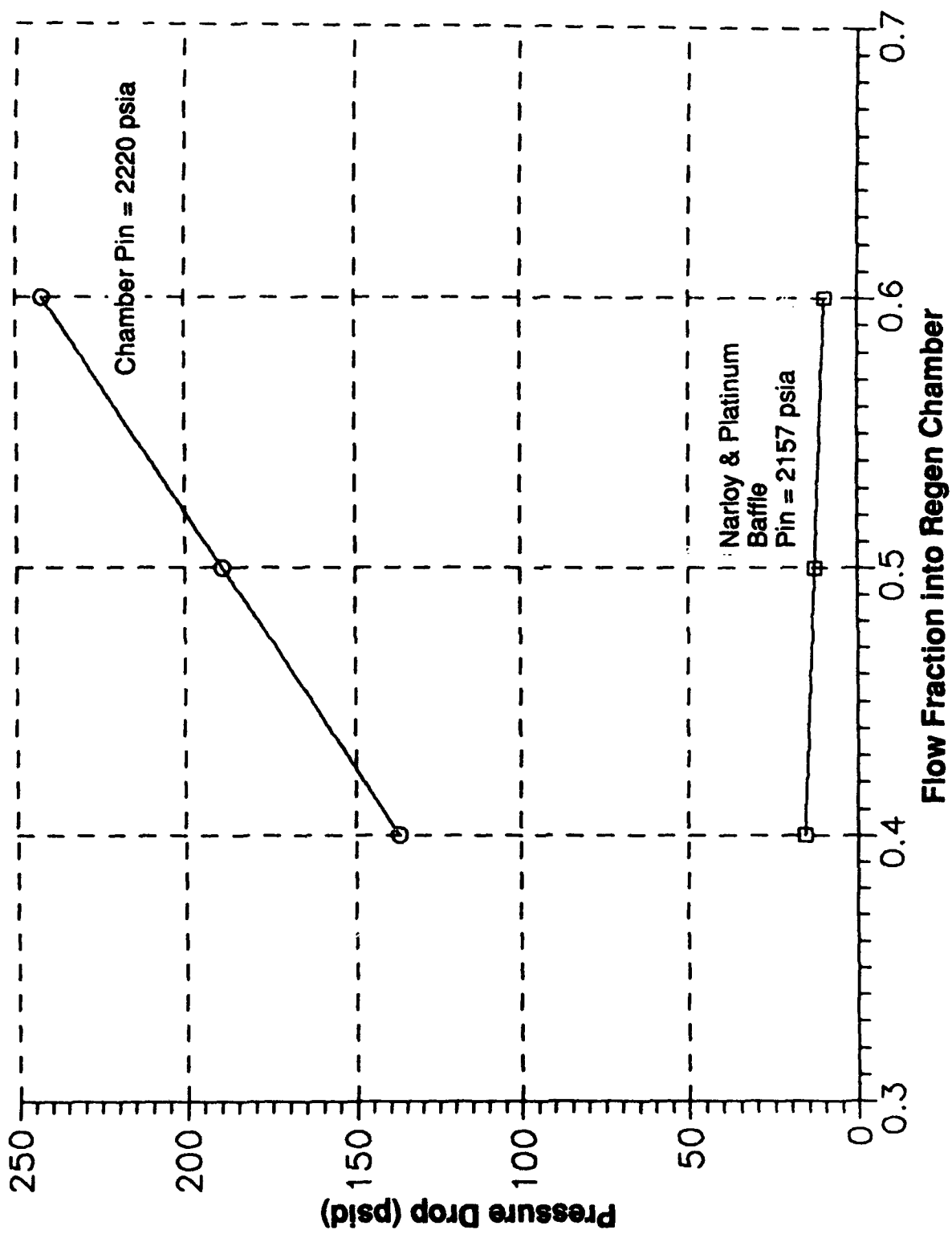


Figure 3.2.2-19. Engine Pressure Drop for  $P_c = 1500$  psia,  $MR = 12$

### 3.2, Engine Requirement Variation Studies, (cont)

out by a slight adjustment of the regenerator bypass valve. Figure 3.2.2-19 gives the chamber and baffle pressure drops at  $MR = 12$  over the range of the hydrogen proportioner valve. The baffle circuit would have to be orificed to equalize the pressure drops prior to stream mixing.

### 3.3 VEHICLE/ENGINE STUDY COORDINATION

One of the study objectives was to coordinate the work of the three contractor engine study teams with the simultaneous work of the Boeing and Martin-Marietta vehicle study teams. Aerojet, Pratt and Whitney, and Rocketdyne are under contract to the NASA Lewis Research Center while the two vehicle primes are under contract to NASA Marshall Space Flight Center. This required coordination between the NASA centers on data requirements, format, distribution, and meeting attendance. An initial problem was the late start of the two primes on the vehicle study contract. The Advanced Engine Study was well underway before vehicle study contracts were let. The coordination effort was also affected by the NASA's need to prepare a response to President Bush's new space initiative. Nearly all of the material in this section was generated to support that effort. The kind of vehicle prime/engine contractor coordination envisioned at the start of the study was never accomplished. In particular, the engine/vehicle interface definition had very little work or discussion. The material that follows is an edited version of the original submission to LeRC and MSFC. In some instances corrections were made where errors were found in the material as submitted. Also, some material is updated based on later work done in the study.

#### 3.3.1 Engine Design, Development, Test and Engineering Cost Estimates

During 1988 and 1989, Aerojet TechSystems made major changes to system cost estimating techniques during contract work on the Advanced Launch System (ALS). The improved cost methodology was used in estimating ALS engine costs, and initial comments from reviewers were highly favorable. Reference 14 has a summary section covering the application of the system to the ALS with a breakout of costs in specific areas such as design, fabrication, and test. The same methodology was used to cost DDT&E for the CTP engines. The methodology was considered appropriate for the following reasons:

### 3.3, Vehicle/Engine Study Coordination, (cont)

- Customer test and acceptance requirements should be very similar as MSFC is the customer for both the ALS engine and the flight version of the CTP engine.
- Both engines use cryogenic propellants.
- Production runs are within the same order of magnitude.
- As both engines would be in development at the same time the technology and industry capabilities are the same.
- Physical size difference of the two engines has only a minor effect on DDT&E cost.

The basic assumptions for the cost study are given in Table 3.3.1-1. The study assumed an on-contract, full funding start on 2 Jan 1991. A breakout by calendar year of design and engineering costs is given in Figure 3.3.1-1. Fabrication would start in 1992 with completion in 1998 as shown in Figure 3.3.1-2. Development testing would also start in 1992 as shown in Figure 3.3.1-3. These three charts are totaled and summarized by cumulative cost in Figure 3.3.1-4. Note that the total cost is about \$950M in 1990 dollars. It should be emphasized that the costs are directly related to the assumptions shown in Table 3.3.1-1. Costs will increase or decrease, for instance, as the number of development and qualification tests are changed from the 960 given in the table. The development schedule is given in Figure 3.3.1-5.

Following submission of the DDT&E costs a clarification of the categories and numbers of tests was requested. The 960 tests assumed a total of 58 equivalent engines for the development program. This includes 15 equivalent engines for component development and a total of 43 engines for development, qualification, reliability demonstration, life testing, flight readiness firing, and cluster testing. The 43 engines have an average life of 30 full duration tests with appropriate refurbishments and major overhauls. The testing program is equivalent to 36 engines x 30 tests/engine = 960 tests.

**Table 3.3.1-1.**  
**LTV/LEV Engine DDT&E Cost**

## **ASSUMPTIONS:**

- 1990 FIXED \$
- COMMON ENGINE FOR LTV/LEV MISSION
- ENGINE THRUST RANGE 20-30K LBF
- FIRST UNIT PRODUCTION COST=\$9-13M
- ENGINE LIFE = 30 MISSIONS
- .85 LEARNING CURVE USED
- NUMBER OF DEVEL/QUAL ENGINES = 32
- TOTAL # OF DEVEL/QUAL TESTS = 960
- SINGLE ENGINE RELIABILITY = 0.990  
@90% CONFIDENCE LEVEL
- CONTROLLER/HEALTH MONITORING  
SYSTEM DERIVATIVE OF ALS STME  
PROGRAM

# DESIGN & ENGINEERING ANNUAL COST

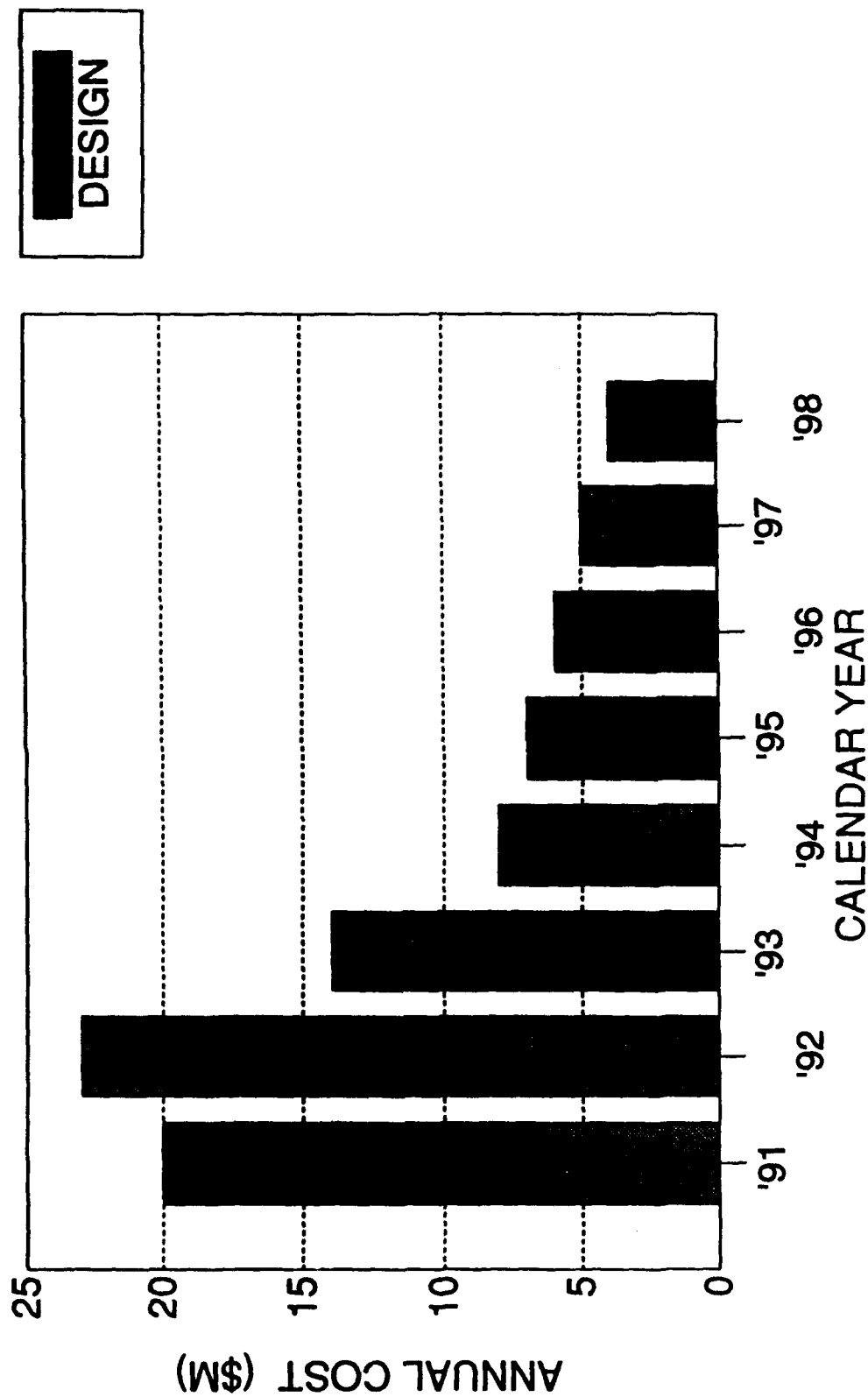


Figure 3.3.1-1. LTV/LEV Engine Development

# DEVELOPMENT AND QUAL ENGINE FABRICATION

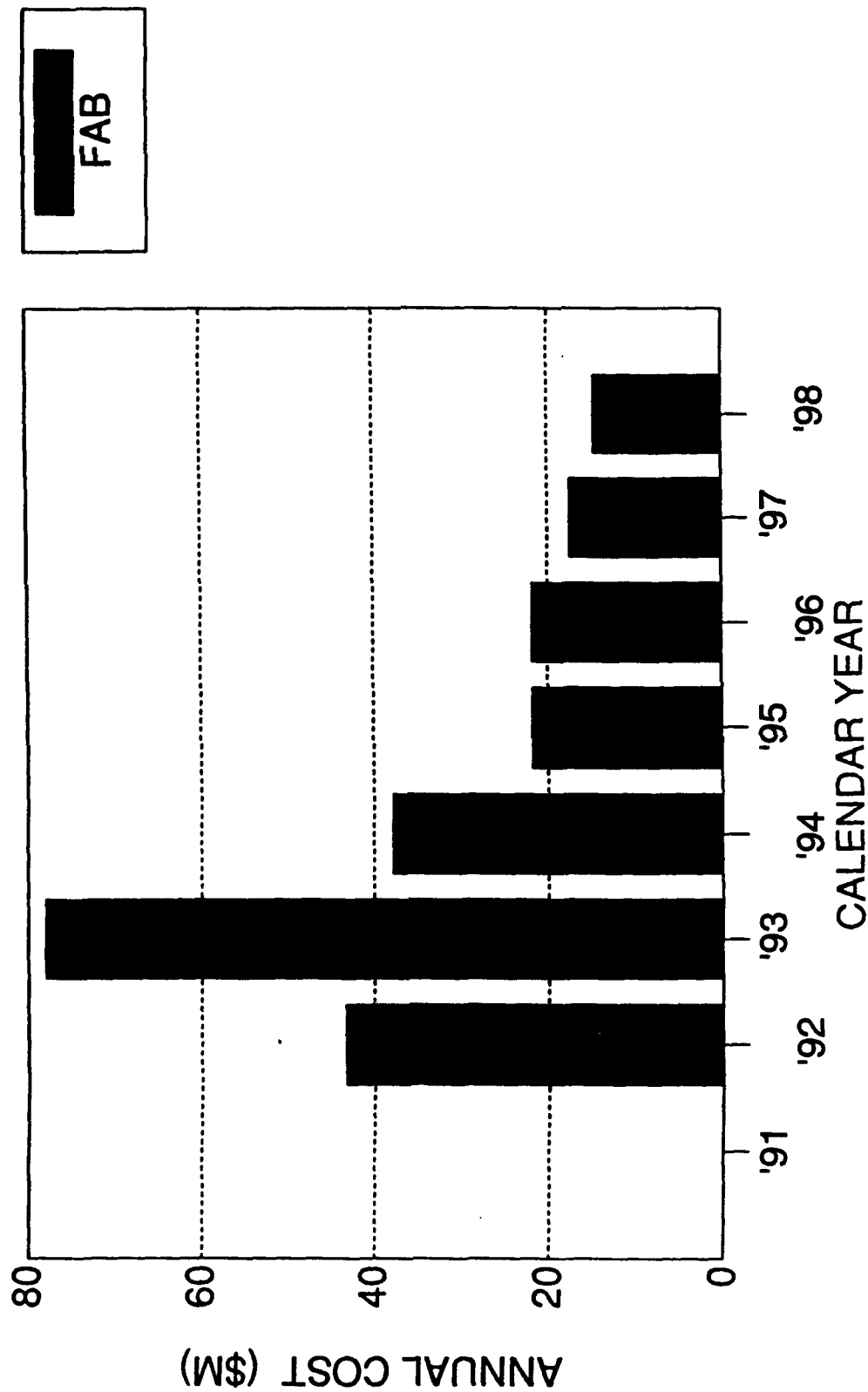


Figure 3.3.1-2. LTV/LEV Engine Development

# DEVELOPMENT AND QUAL TESTING

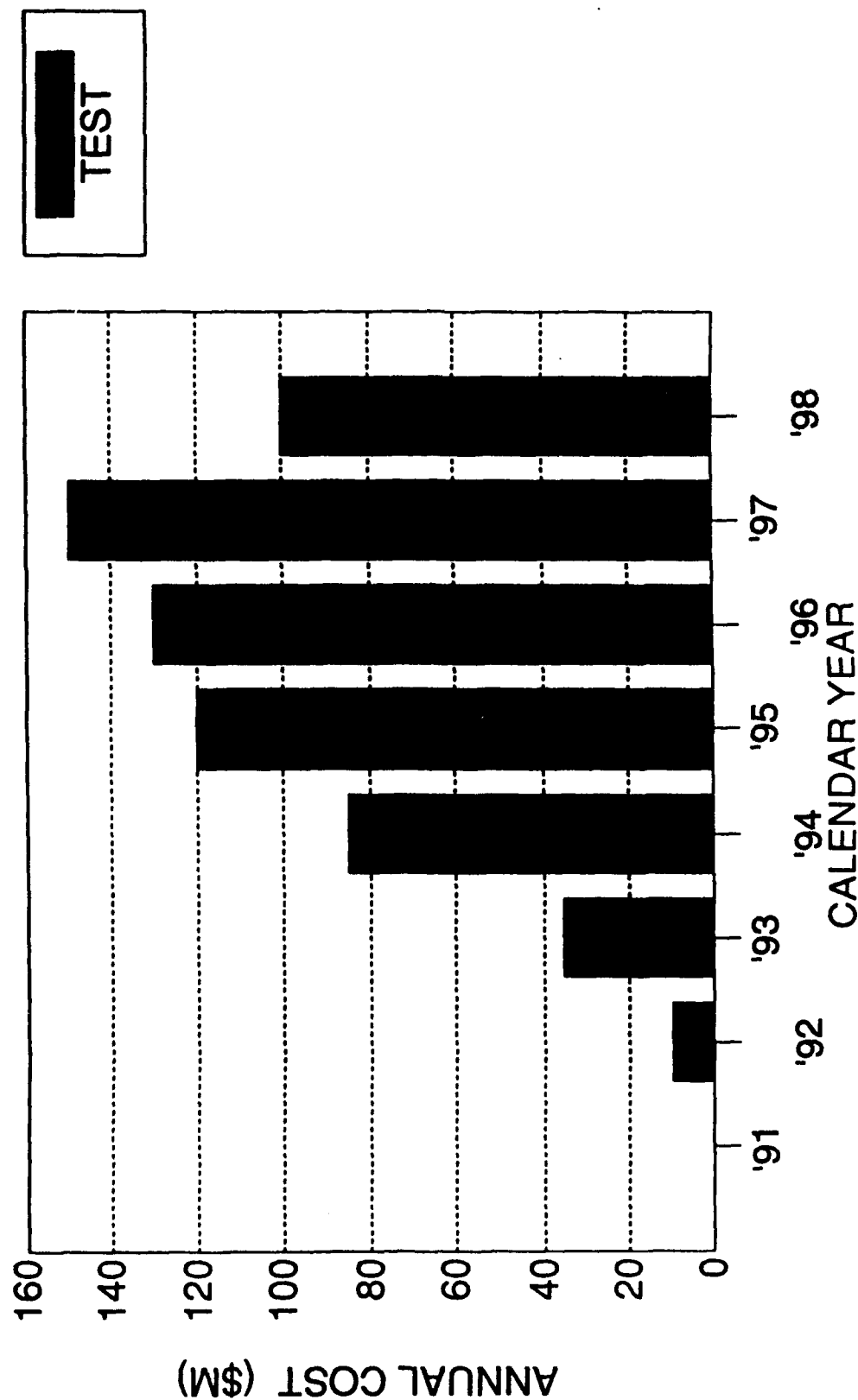


Figure 3.3.1-3. LTV/LEV Engine Development

# TOTAL PROGRAM CUM COSTS

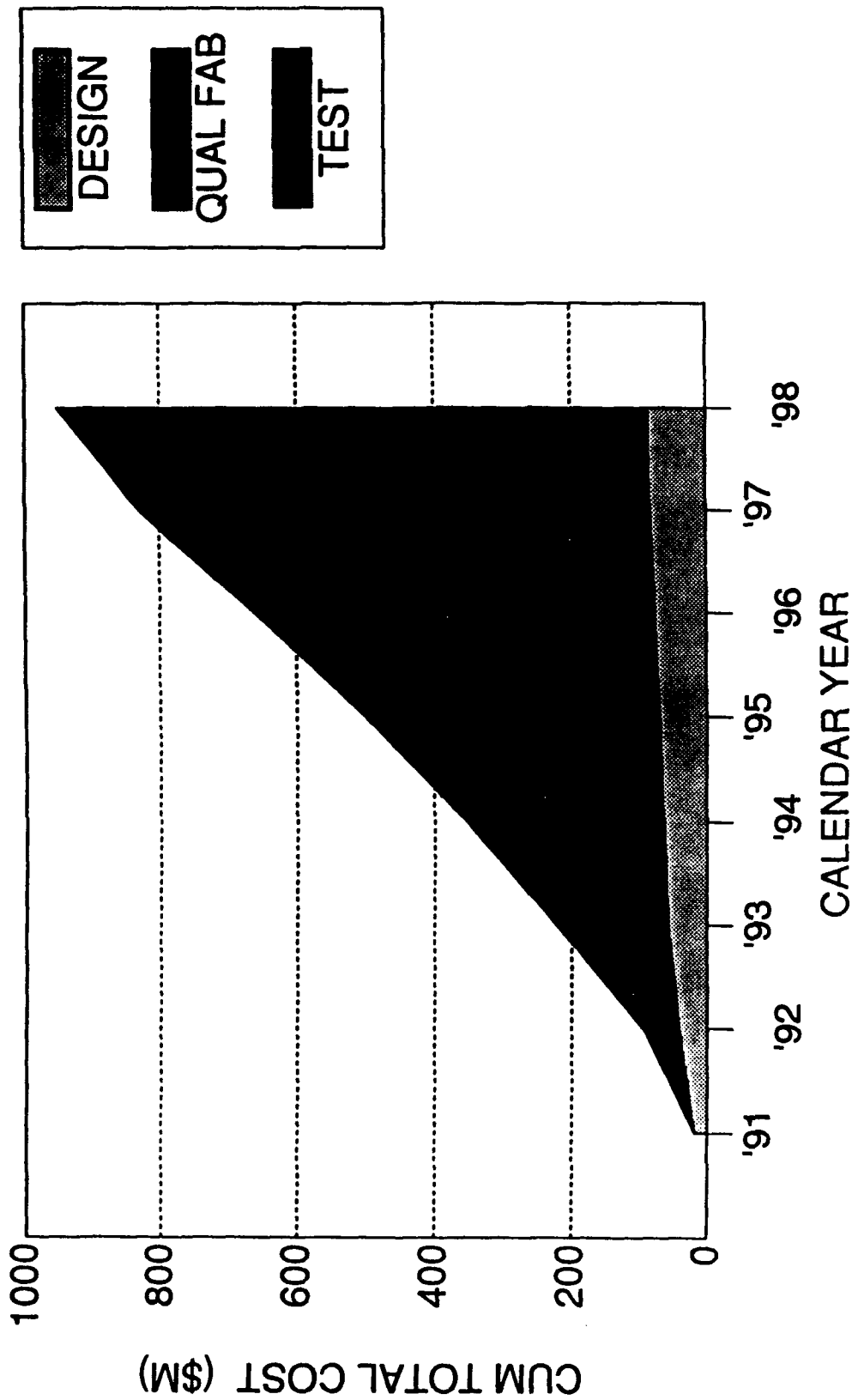


Figure 3.3.1-4. LTV/LEV Engine Development

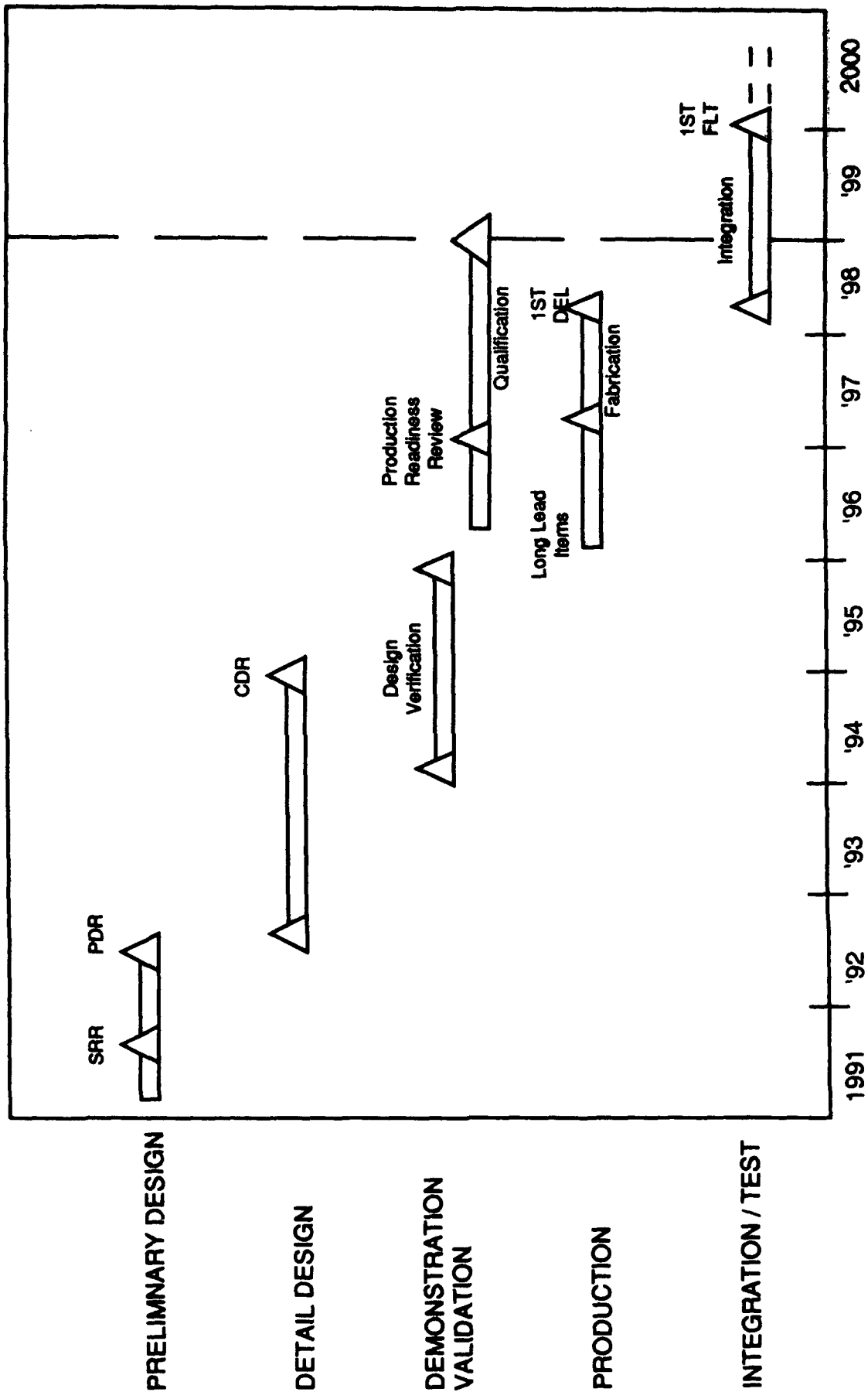


Figure 3.3.1-5. LTV/LEV Propulsion System Program Schedule

### 3.3, Vehicle/Engine Study Coordination, (cont)

Test program, test type, and facilities are planned as follows:

a) Component development database acquisition: 2 stands each for the oxygen and hydrogen turbopumps, and 2 new or existing stands for chamber/injector testing. Tests will be performed at Aerojet using existing facility "J" area zone control room, instrumentation, and tank farm facilities. Oxygen and hydrogen turbopump tests will use new facility gas generators (GG's) and heat exchangers (HX's) to obtain the warm gas oxygen and hydrogen at required inlet temperatures, flowrates and pressures to simulate engine chamber exit conditions. GG's will be a pressure fed O<sub>2</sub>/H<sub>2</sub> design. All thrust chamber/injector tests at the component level will be performed with facility pressure fed propellants. Combustion stability (bomb), mixture ratio, throttling, thermal and performance tests can be performed at this level. These tests may require the use of J area altitude diffuser capabilities due to the cooled thrust chamber/nozzle expansion ratio.

b) Breadboard and prototype engine testing: 2 additional test stands required in "E" area - may require workhorse chamber at sea level expansion ratio to allow system testing without vacuum diffuser. These tests also demonstrate and validate controller and health monitoring systems and instrumentation. Testing uses existing control room capabilities with supplemental provisions for facility controller/engine controller interface and development.

c) Engine level systems testing: will utilize the 2 additional test stands required in the "E" area - also requires supplemental control room and instrumentation capabilities.

d) Reliability demonstration testing: requires 1 additional test stand in J area using existing control room and existing altitude capability. Full up engine testing will be done with the exception of radiation cooled nozzle extension (possible facility limitation for thrust level at very high (>1000) area ratios and long duration burns. Also requires 1 additional identical facility at (TBD), possibly with altitude capabilities.

### 3.3, Vehicle/Engine Study Coordination, (cont)

e) Engine qualification testing: same as reliability testing (d) above.

f) Preliminary Flight Readiness Testing (PFRT): Adaption to test cells at SSC - verifies system level transients and engine interactions, thermal radiation environments. May require a diffuser adapter for unique engine cluster nozzle configuration envelope.

g) Flight Readiness Testing: same as PFRT (f) above.

h) Acceptance testing: each engine will be individually acceptance tested in J area at altitude conditions (same as d).

One question asked by reviewers concerned the number of engine test failures assumed for the test program. The short answer is "none" if the type of failure is catastrophic. This would be of sufficient violence to seriously damage a test stand as well as destroy the test engine. Less serious failures can be expected where a test article is no longer usable. From 6 to 10 of these failures can be expected based on the test history of the RL-10 and SSME engines. One of the goals of the test program is to use the ICHM system to predict and preclude catastrophic failures. The total number of tests per engine, however, will result in some engines exceeding design life, and some failures can be expected.

To summarize:

- 6 test stands required in J area for component development
- 2 test stands and an additional control room required in E area for prototype and engine level testing.
- 1 engine test stand required in J area for reliability/qualification/acceptance testing at altitude conditions.
- 1 test stand required at (TBD) for reliability/qualification/testing at altitude conditions.
- Special diffuser may be required for cluster PFRT and FRT development.

### 3.3, Vehicle/Engine Study Coordination, (cont)

#### 3.3.2 Engine Production Cost

Estimates of engine production cost require 1) a baseline for comparison, 2) the engine thrust, and 3) an expected learning curve. The baseline for comparison is the Pratt and Whitney RL-10 engine. This is a fully mature product now in the portion of the learning curve that is essentially flat. It is also a 15,000 lbf (nominal) thrust engine where the CTP engine is expected to have a thrust in the range of 20K to 30K lbf. The CTP engine, with its increased capability and higher level of technology will be more complex and, therefore, more costly to build. The study used a series of complexity factors from 10% to 50% to gauge the cost impact due to complexity. Learning curves of 80 and 90% were considered likely bounds for this engine with 85% a good median figure. Production cost was then parameterized using thrust, percent learning curve, and production quantity as the entering arguments with a different complexity factor on each chart. The results are given for Figures 3.3.2-1 through 3.3.2-5.

The charts are used by selecting a production quantity, say 48 engines; a thrust, say 20K lbf; a learning curve, say 85%; and then entering the chart with the appropriate complexity factor. For the example given,  $N^{\text{th}}$  unit cost (\$M) is:

Complexity Factor	1.1	1.2	1.3	1.4	1.5
$N^{\text{th}}$ Unit Cost (\$M)	5.5	6.0	6.6	7.2	7.7

These are 1990 dollars. A basic assumption is that DDT&E costs are sunk costs and are not spread over production engine cost. This makes a clean break between development and production costs. One likely area of additional cost is continuing engineering support. This was not estimated but is highly discretionary in any case; the customer can expect to get any level of supporting engineering desired subject to funding constraints.

#### 3.3.3 Mission Related Costs

One of the questions asked after receipt of the Aerojet input on DDT&E costs concerned the impact of having planned engine servicing only versus some unplanned engine servicing.

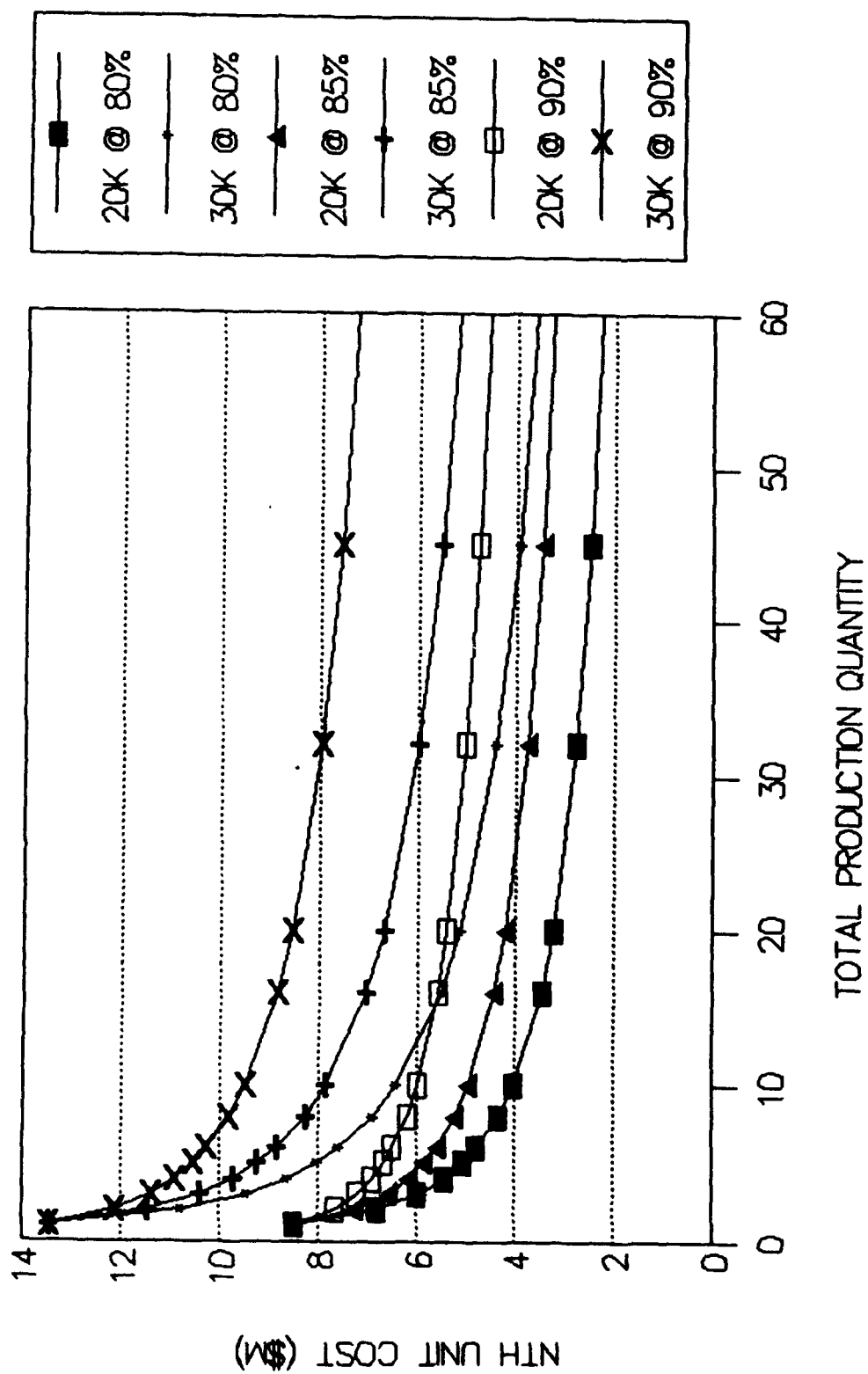


Figure 3.3.2-1. LTV/LEV Engine at Complexity = 1.1 x RL -10 Engine  
Nth Unit Production Cost

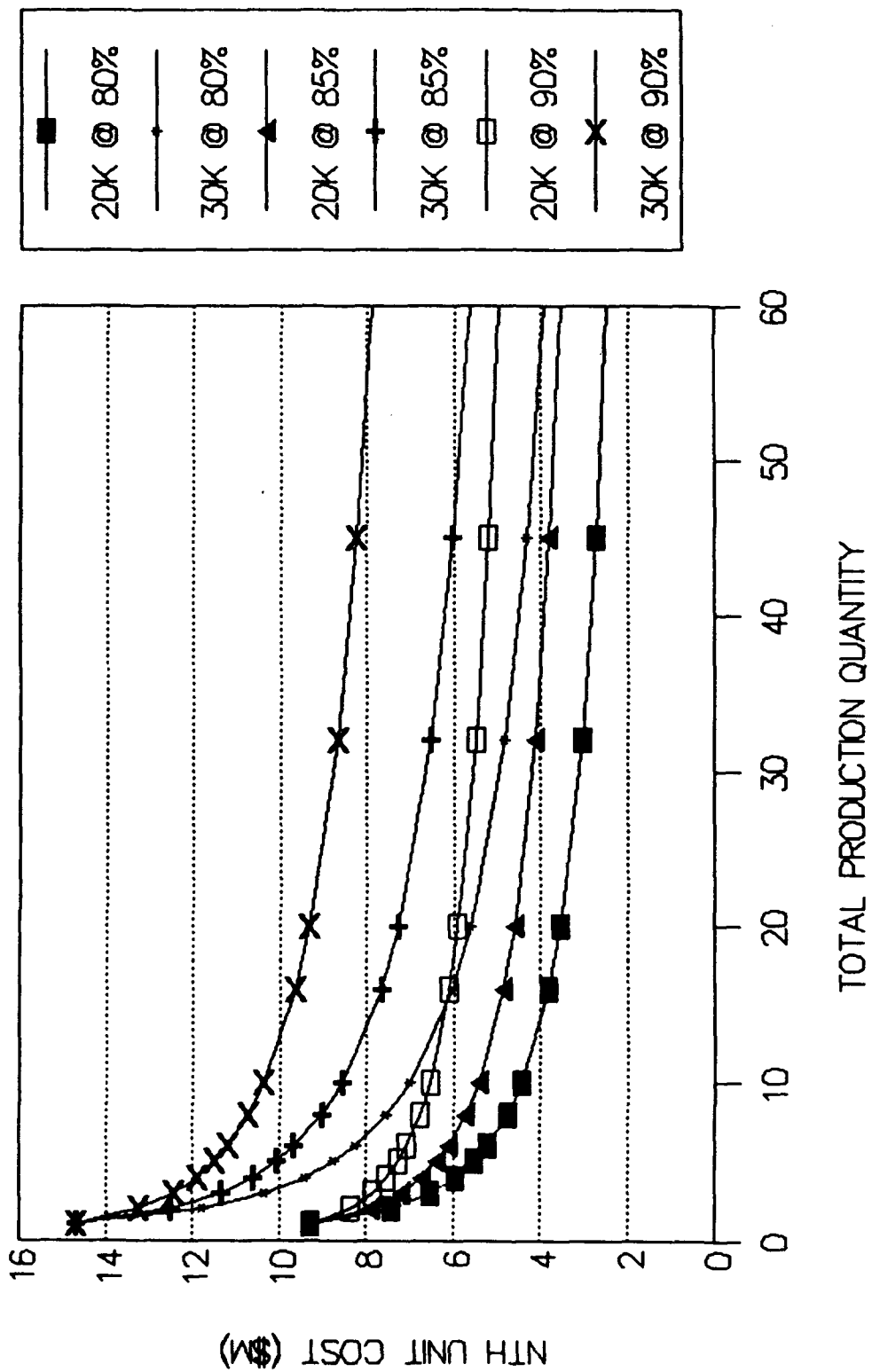


Figure 3.3.2-2. LTV/LEV Engine at Complexity = 1.2 x RL - 10 Engine  
Nth Unit Production Cost

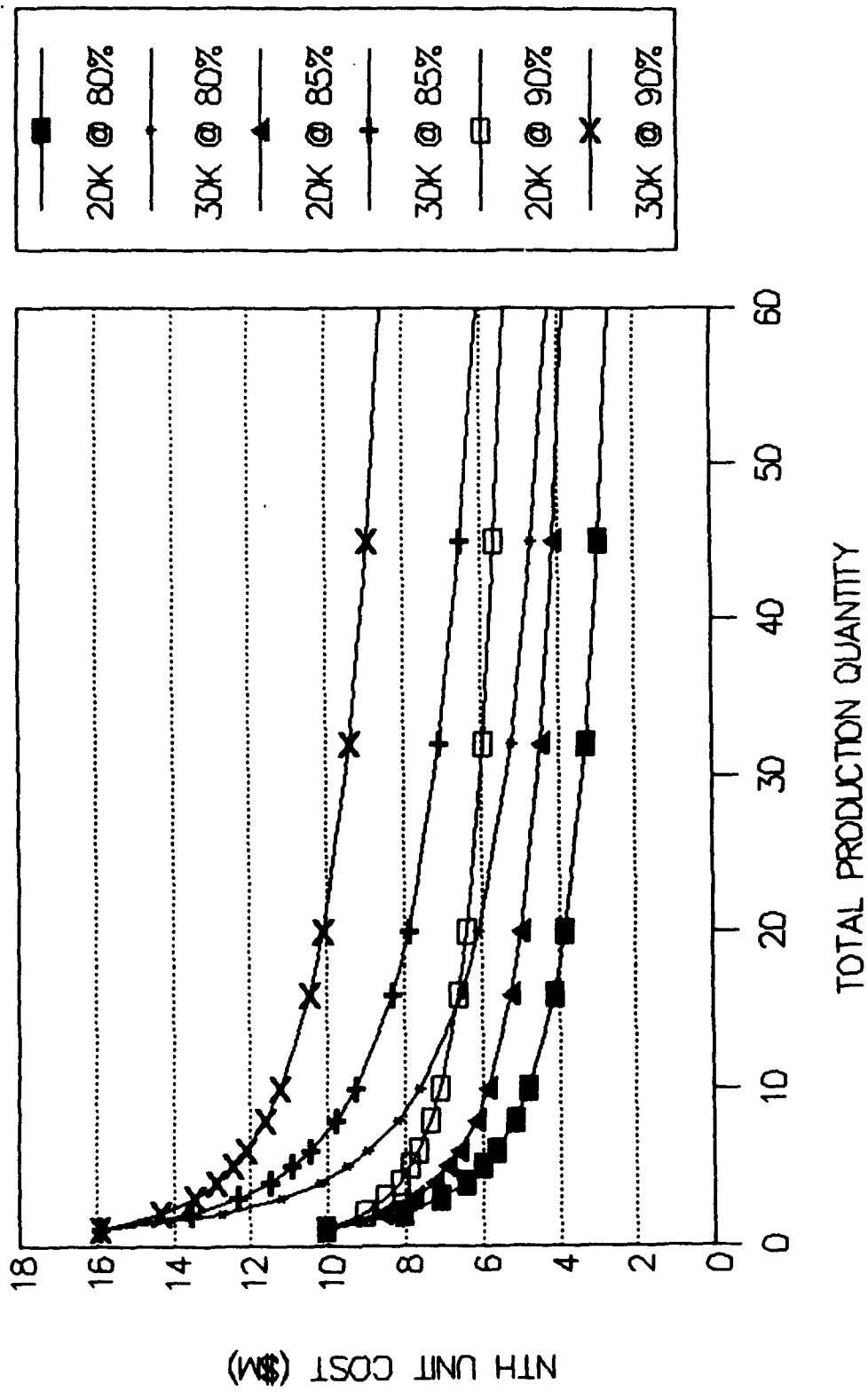


Figure 3.3.2-3. LTV/LEV Engine at Complexity = 1.3 x RL - 10 Engine  
Nth Unit Production Cost

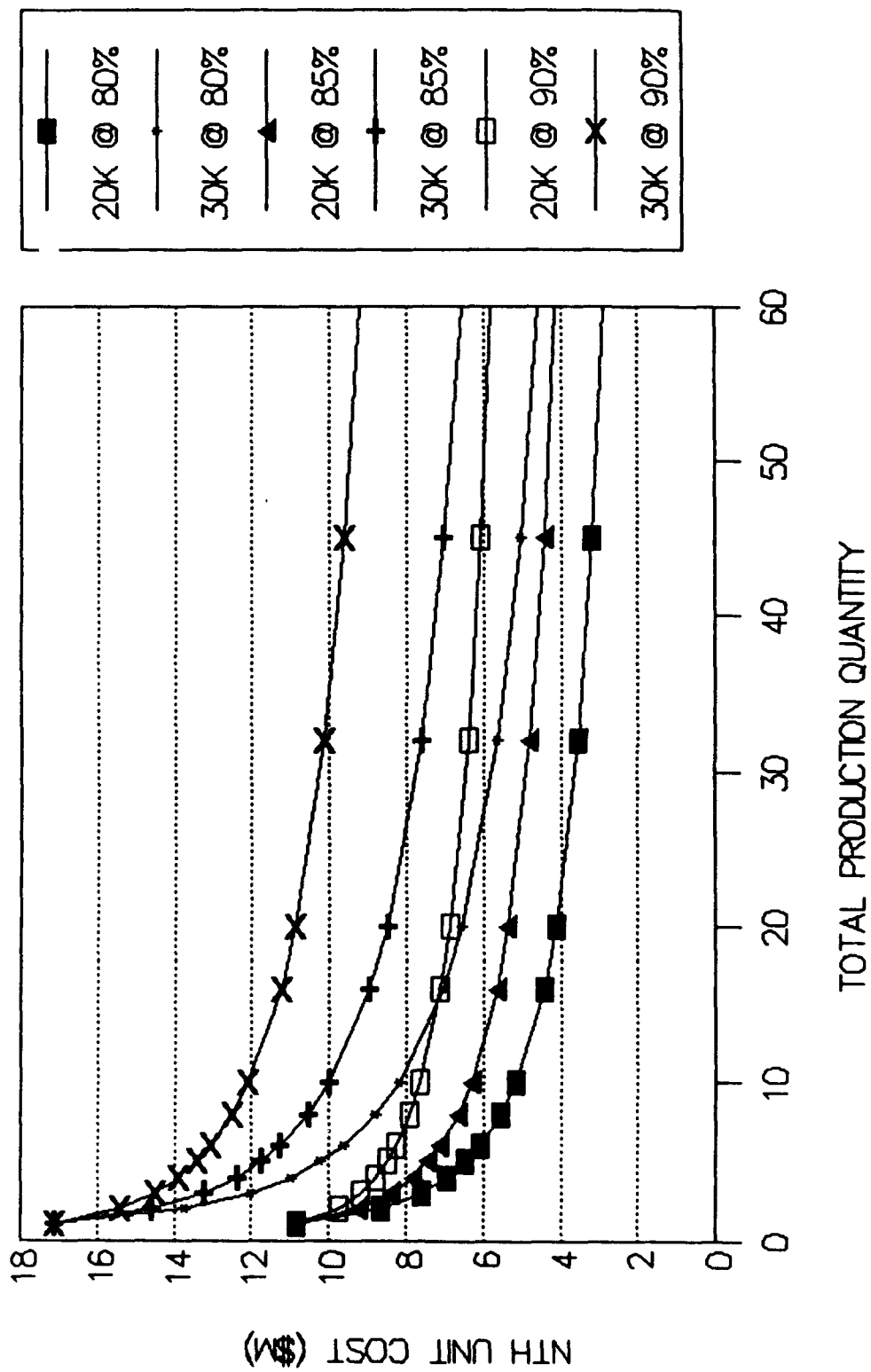


Figure 3.3.2-4. LTV/LEV Engine at Complexity = 1.4 x RL - 10 Engine  
Nth Unit Production Cost

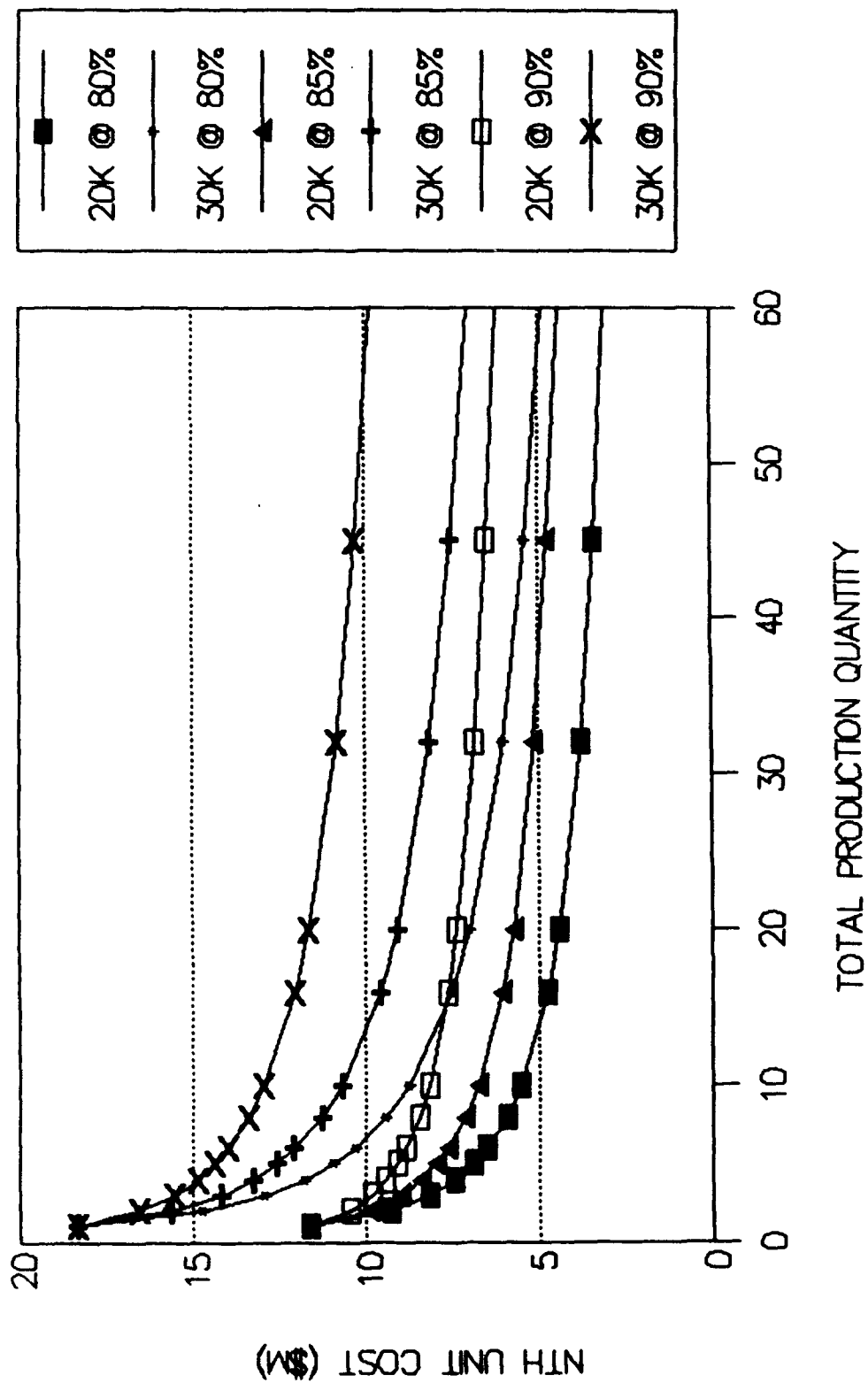


Figure 3.3.2-5. LTV/LEV Engine at Complexity = 1.5 x RL -10 Engine  
Nth Unit Production Cost

### 3.3, Vehicle/Engine Study Coordination, (cont)

The answer is dependent on what the mission architects plan to do, and whether the integrated control and health monitoring system is used for real time maintenance decisions. A maintenance scenario is needed. Some guidelines that may assist the planners are:

- An engine should not be designed for in-space maintenance if the capability is not going to be available during its operational life.  
"Don't pay for something you don't need."
- Series production of an engine can be used to expand the maintenance capability to space-based maintenance as the facility is developed and newer engines are built.
- The basic in-space maintenance capability that must be developed first is engine removal and replacement. Even a block 1 design vehicle should include this capability.
- The vehicle design must provide access to the space maintainable components to a person in a space suit. This is non-trivial, the suits require a lot of maneuvering room.
- A realistic assessment of in-space maintenance costs and timelines is needed to determine the cost effectiveness of component change-out versus engine change-out.
- Maintenance costs include:
  - Training
  - Facility
  - Downtime
  - Spares and Spares Storage
  - Tools/Diagnostic Devices
  - Personnel Costs
  - Inspection/Certification
  - Administration

### 3.3, Vehicle/Engine Study Coordination, (cont)

- In-space maintenance presents problems not encountered in normal shops or flightlines:
  - Vacuum Environment
  - Specialized Tool Kit
  - Lack of Gravity Assistance
  - Limited Effective Working Time
  - Access Problems for Mechanics in Space Suits
- Reliability in reconnecting flow lines after maintenance is a concern.
- Insulation and connections for health management sensors complicate component change out.
- Actual, demonstrated in-space repair operations have been far more time consuming and fatiguing than expected.

The Aerojet 7.5K lbf Thrust Engine Preliminary Design included a careful look at designing for in-space maintenance (see Ref. 2). The first concern was to develop a rapid, uncomplicated engine changeout procedure. All engine removal operations except for the extendible/retractable nozzle are done at the engine/vehicle interface plane. All operations can be done by one person, in a space suit, within normal arm reach once access is gained to the vehicle/engine interface. Table 3.3.3-1 is a list of the required removal steps. Replacement is the reverse of this sequence. A prime mover of some sort is expected to be available for the actual physical handling of the engine.

Engine removal can be done with a tool kit of very few items. Aerojet, for instance, has a design for the engine attachment to the thrust takeout structure that requires only two ball lock devices for keeping the engine in place. Engine removal should not require more than an hour once access is gained to the engine/vehicle interface area.

Some of the questions asked related to the effect on DDT&E cost of various design requirements. In general, there is no impact unless requirements exceed

TABLE 3.3.3-1

CTP ENGINE REMOVAL OPERATIONS

- Engine Centered, Nozzle Extended
- Propellant Isolation Valves Closed
- Electrical Power Removed from the Engine
- Manual Operations:
  - Electrical harness Disconnected, Connectors Capped, Harness Stowed
  - Extendible Nozzle Removed, Screw Assemblies Secured, Regen Cooled Nozzle Edge Protector Installed
  - Main Hydrogen Line Disconnected Below Shutoff Valve, Capped
  - Main Oxygen Line Disconnected Below Shutoff Valve, Capped
  - Hydrogen Tank Autogenous Pressurization Line Disconnected Below Shutoff Valve, Capped
  - Oxygen Tank Autogenous Pressurization Line Disconnected Below Shutoff Valve, Capped
  - Engine Handling Fixture Connected
  - Control Gimbal Actuators Disconnected
  - Flex Lines Restrained, Upper Engine Covered with Protective Material
  - Prime Mover Connected to Engine
  - Engine Thrust Structure Locking Devices Removed
- Engine Moved Out of Engine Compartment

### 3.3, Vehicle/Engine Study Coordination, (cont)

those listed in Table 2.1-1. This is true of such things as throttle range and reliability requirements. Life cycle costs are implied by questions regarding the number of uses between missions and whether the engine is expended after five missions.

The OTV engine design requirement is for five missions prior to engine removal and refurbishment. This would be for a mature system with some operational history. During early operation of the vehicles a removal and inspection may be planned after two or three missions. In all cases anomalous or out of limits operation recorded by the integrated control and health monitoring system (ICHM) would be justification for an engine change. Also, an optical inspection of the engine after each mission (by remote video unit and/or astronaut) could detect a cause for an engine change. There are a number of things that are hard to predict when building a new system. We do not have experience with a complex system routinely maintained in space. (Skylab is a possible exception). The number of uses prior to the end of service life is dependent on the maintenance scenario. Our design requirement has been an operational life equivalent to 40 missions with periodic maintenance following every fifth mission. The engine would be discarded after 40 missions (equivalent of 20 hours operation and 500 starts). The economics of refurbishment in space versus returning the engine to earth for refurbishment are not defined. The present space station design has no provision for a maintenance facility. Our baseline engine design emphasizes a quick engine change-out capability assuming that will be the most important maintainability feature during the early years of operation. If the engine is returned to earth for refurbishment after five missions it could, in terms of a space deployed system, be considered expended even though it was returned to operation at a later date.

The LTV duty cycle (typical) would have a translunar injection burn, a lunar orbit burn, a de-orbit and earth return burn, two midcourse correction burns, a pre-airbrake correction burn, and a post airbraking circularization burn for a total of seven engine starts each mission. Total LTV propellant (288,000 lbm) is sufficient for about 1655 sec operation on 4 engines of 80K lbf total thrust. A fifty mission life would total about 24 hours of engine operation and about 350 starts. This is close to the life goal set for the OTV engine program. With 5 reuses prior to scheduled maintenance each engine would accumulate 35 starts and about 2.4 hours operating time. To put this in perspective, this is about 7 times the operating time accumulated by the space shuttle

### 3.3, Vehicle/Engine Study Coordination, (cont)

main engine (SSME) on an orbiter mission. We are not aware of any SSME that has gone seven missions without extensive maintenance. Some storable propellant engines, such as the OMS engines with a fairly high-margin, conservative design, can meet this maintenance free goal. Meeting it with a high performance cryogenic engine will be a challenge.

One of the capabilities needed at the Lunar base is engine changeout and storage. At some time in its evolution, a greater maintenance capability may be considered necessary if the Lunar Excursion Vehicle (LEV) is based there. The cost of establishing such a capability will be substantial.

#### 3.3.4 In-Space Maintenance and Servicing

The previous section addressed in-space maintenance from the standpoint of factors comprising the life cycle cost. This section addresses design features of the Aerojet version of the engine that will be of concern when assessing the maintainability of the engine. The rapid engine removal/replacement features (see Table 3.3.3-1) received major design emphasis. Component replacement was given less consideration because of the concern for reliability in component changeout with the engine in place.

With a competent in-space maintenance capability the engine components that could (subject to limitations as noted) be replaced is given in Table 3.3.4-1. The list is both engine design and vehicle design sensitive. Without access through the vehicle structure and/or aerobrake some of these components will be inaccessible.

The full range of maintenance and servicing functions involving the engines are given in Tables 3.3.4-2 and 3.3.4-3 respectively. These were adapted from the Phase A vehicle studies. In three of the six servicing operational functions, the engines health monitoring system is used. This system would appear to be very critical to the mission operation and safety. Despite a scheduled maintenance plan, if this system indicates there is an engine problem the decision is likely to be "fix it now, not at the scheduled time." With a sophisticated ICHM system it will be very difficult to adhere to a timephased maintenance plan. Preventive maintenance may very well be engine condition determined, not time determined.

**TABLE 3.3.4-1****CTP ENGINE SPACE MAINTAINABLE COMPONENTS  
7.5K LBF THRUST ENGINE**

<b>Component</b>	<b>Comment</b>
Hydrogen Main Shutoff Valve	Requires Access Near Engine/Vehicle Interface
Oxygen Main Shutoff Valve	Requires Access Near Engine/Vehicle Interface
Hydrogen Boost Pump (Low Press)	Requires Access Near Engine/Vehicle Interface
Oxygen Boost Pump (Low Press)	Requires Access Near Engine/Vehicle Interface
Hydrogen Autogenous Pressurization Valve	Requires Access Near Engine/Vehicle Interface
Oxygen Autogenous Pressurization Valve	Requires Access Near Engine/Vehicle Interface
Hydrogen Regenerator Bypass Valve	Design Dependent; May be a Bolt-On to a Manifold
Oxygen Regenerator Bypass Valve	Design Dependent; May be a Bolt-On to a Manifold
Gimbal Motors	Requires Access Near Engine/Vehicle Interface
Gimbal Actuators	Requires Access Near Engine/Vehicle Interface
Extendible Nozzle	Ready Access
Extendible Nozzle Deployment Motors	Requires Access Near Engine/Vehicle Interface
Extendible Nozzle Dep. Mechanism	Requires Access Near Engine/Vehicle Interface
Fuel Flowmeters	Design Dependent; May be Bolt-On to Low Pressure Boost Pump
Oxygen Flowmeters	Design Dependent; May be Bolt-On to Low Pressure Boost Pump
Controller	One or Two Removable Boxes with Cannon Plugs
Sensor Signal Conditioning Units	Designed to Allow Sensors to Remain in Place, only Electronics Changed (Requires System Recalibration)
Miscellaneous Hardware, Brackets, Wires, External Sensor Elements	Dependent on Access

**TABLE 3.3.4-2**

**SPACE-BASED CTP ENGINE MAINTENANCE FUNCTIONS**

**Perform scheduled maintenance**

- Transfer propellant to and from LTV
- Perform visual inspection (includes engines)
- Determine LTV fault status
- Replace ACS (Altitude Control System) modules (after each mission if packaged storables are used)
- Replace engine module\* (after TBD mission time)
- Perform system operational testing
- Service batteries and fuel cells
- Replenish stored helium (if used)

**Perform unscheduled maintenance**

- Perform damage assessment (beyond scheduled inspection)
- Verify any electrical failure
- Isolate fault to replaceable unit
- Perform damage repair
- Perform required "remove and replace" due to failure

---

\* The vehicle can be developed with replaceable propulsion modules or for individual engine replacement. In-space handling requirements may dictate one or the other design solution. Table 3.3.3-1 lists the steps in removing an engine in Aerojet's design concept.

**TABLE 3.3.4-3**

**CTP ENGINE SERVICING OPERATIONAL FUNCTIONS**

**BERTH LTV**

- Rendezvous LTV with Station
- Capture LTV at Station
- Berth LTV at Station

**TRANSFER PROPELLANT**

- Verify Interface Integrity
- Perform Propellant Leak Check
- Transfer Residual Propellant from LTV To Station Tank Farm

**INSPECT LTV**

- Perform Visual Inspection
- Determine LTV Fault Status\*
- When Fault or Damage Detected\*
  - Perform Damage Assessment (TV/EVA)
  - Initiate Electrical Test Routine to Verify Fault
  - Initiate Fault Isolation Routine
- Formulate Integrated Maintenance Plan\*

**PERFORM LTV MAINTENANCE**

- Perform Scheduled/Unscheduled Maintenance Tasks\*
- Mission Reconfigure
- Perform System Operational Testing\*
- Deactivate and Stow LTV (if not required for mission at that time)

**MATE LTV AND PAYLOAD**

- Transfer Payload to LTV
- Mate Payload to LTV
- Verify LTV/Payload Interface
- Perform LTV/Payload Integration Test

**LAUNCH LTV/PAYLOAD**

- Perform Prelaunch Operations\*
- Transfer Propellant from Station to LTV
- Launch LTV/Payload\*

---

\* Operations where the LTV engine Health Monitor System is used.

### 3.3, Vehicle/Engine Study Coordination, (cont)

#### 3.3.5 Engine Requirements for the Lunar Mission

##### 3.3.5.1 Vehicle Concept

NASA-MSFC provided a vehicle concept for the Lunar Return Mission. With the actual vehicle studies just started the concept may change.

The NASA MSFC concept of the lunar base support proposes two vehicles. One is the lunar transfer vehicle (LTV) which is based at Space Station Freedom. This is a modular vehicle built up from three modules:

- **LTV Core Stage.** This is a single tankset structure with the basic stage propulsion system. Four engines comprise the main propulsion array. An aerobrake is part of the core stage.
- **Separable Tanksets.** The core vehicle has provisions for attaching four tanksets in a cross shaped pattern around the core vehicle. During the trans-lunar injection (TLI) burn two of these tanksets are jettisoned when emptied. The other two are retained for completion of the TLI burn and to transfer propellant to the lunar excursion vehicle (LEV). They are then released for impact on the moon or, possibly, soft landed at the lunar base. The LTV returns to earth on the propellant in the core tankset.
- **Crew Module/Cargo Module.** A payload of 27 metric tons is proposed. This can consist of a 4.8 metric ton crew module plus cargo or can be all cargo for an unmanned logistics support mission. The crew module can be transferred to the LEV in lunar orbit along with the cargo module.

The second vehicle is the lunar excursion vehicle (LEV) which has a set of landing legs for actual operation to and from the lunar surface. As noted above, it is serviced with propellant from the LTV and is actually based at the lunar station. The four engines on the LEV are identical to those on the LTV except the extendible/retractable nozzle extension used on LTV engines has been removed. This reduces the length required for the landing legs. During operation, only two engines

### 3.3, Vehicle/Engine Study Coordination, (cont)

are operated above pumped idle thrust as the thrust requirements for the LEV are lower than those for the LTV. The vehicle is capable of hovering over the touchdown point and of a controlled landing at a fraction of a "g". Conceptual sketches of both vehicles with dimensions and weights are given in Figure 3.3.5-1.

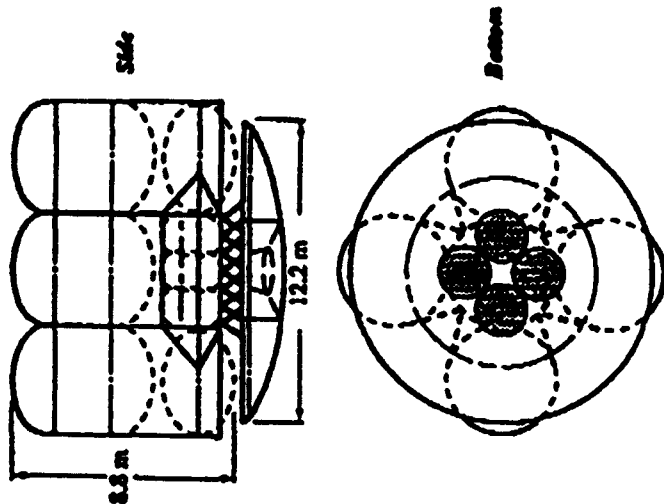
This vehicle concept was evaluated using an engine set of four 20,000 lbf thrust engines. One of the study items was to determine the sensitivity of the LTV weight in low earth orbit at the start of the mission to the engine specific impulse for the baseline 27 metric ton payload. The results of this trade are presented in Figure 3.3.5-2. The importance of a high specific impulse engine is evident. The curve as plotted has inflections that were a result of the assumptions built into the program used to generate the vehicle weights based on the MSFC concept. What is not clearly shown is why, at a 440 seconds specific impulse, the initial weight goes towards infinity. A companion curve could be prepared that would have maximum payload versus specific impulse for a direct evaluation of the effect of specific impulse on payload. As it stands, however, this curve shows why the OTV engine program emphasis on high performance is necessary. The proposed lunar mission profile is given in Figure 3.3.5-3.

#### 3.3.6 Issues in Engine Throttling

The issues in throttling, over any range, are:

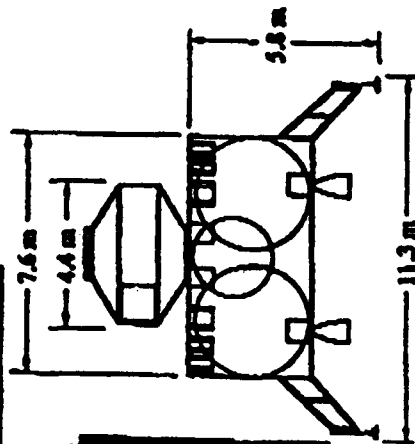
- Control system stability and change rate.
- Hot section temperature rise on throttling down.
- Oxygen circuit liquid-to-gas phase change at low system pressures.
- Combustion stability over the throttling range.

# 1 1/2 Stage LTV



- Payload (Cargo/SS.) 27 t
- Dry Mass 14.0 t\*\*
- Propellant Capacity 129.2 t\*
- Crew Module Mass - Crew 0.8 t
- Dry Mass 5.8 t

# 1 Stage LRV



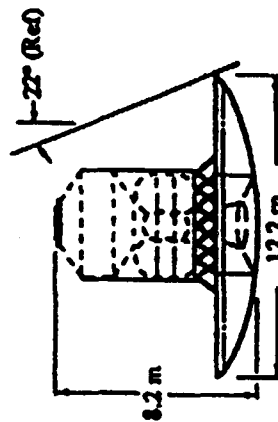
- Payload (Cargo/SS.) 27 t
- Dry Mass 5.4 t
- Propellant Load 24.2 t
- Crew Module Mass - Crew 0.8 t
- Dry Mass 3.6 t

\*Will Have Either Payload (LTE) or the Crew Module, Not Both

# LTV and LRV Scales are Different

• Capacity includes LRV and LTV Core Propellant.

\*\* Dry Mass includes LTV Core Stage and Tanksets.



LTV Core Stage  
(Earth Return)

Figure 3.3.5-1. LTV/LEV Reference Concepts

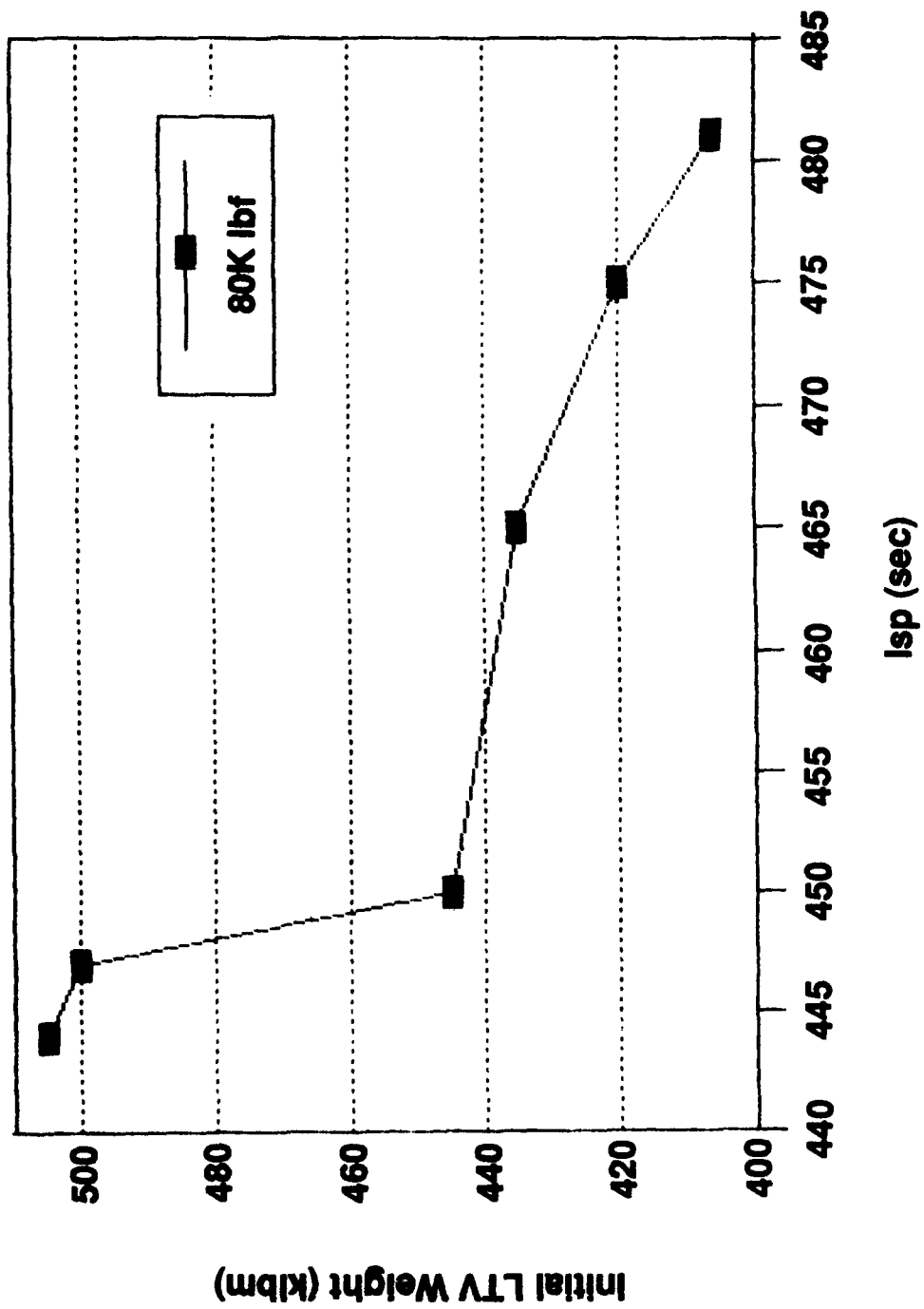
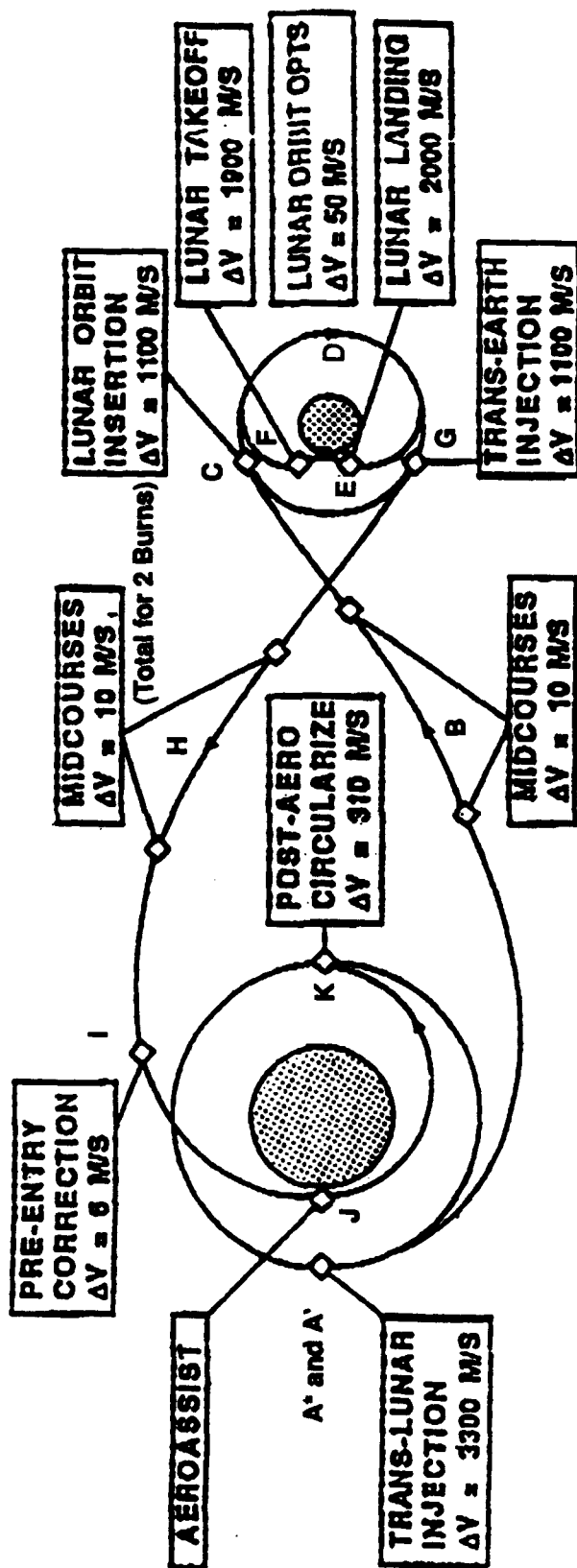


Figure 3.3.5-2. LTV Initial Weight in LEO (1 Burn) vs Isp at Fixed P/L (26.2 MT)

# LUNAR ORBIT MISSION PROFILE



\*Letters are Keyed to "Point" on Each Mission Performance

Figure 3.3.5-3. Lunar Mission Profile

### 3.3, Vehicle/Engine Study Coordination, (cont)

- Turbopump operating range.
- Engine operating envelope restrictions.
- Specific impulse degradation as thrust decreases.

As the throttle range increases beyond 10:1, there is increased concern with hot section (primarily thrust chamber) gas side wall temperature increases due to the lower mass flow and velocity of the hydrogen coolant. A maximum throttle range may be set by the thrust level where the wall temperature reads 1050°F or lower (copper alloy chamber). This is also the range where turbopump operating curves may show dis-proportionate speed changes for the output pressure change. This can lead to some control system instability or a lower response rate.

A special problem is the oxygen phase change. At high system pressures the oxygen makes the transition to gas uneventfully with predictable properties at all times. At lower pressures where the oxygen enters the 2-phase "dome" of the T-S diagram the thermodynamic properties are unpredictable and mass flow rates are erratic due to film boiling and 2-phase flow. A gas-liquid combustion element could show erratic mixture ratio and energy release changes. Aerojet uses a gas-gas element with the oxygen phase change performed in a LOX/GH<sub>2</sub> heat exchanger (HEX) upstream of the injector. This removes the problem from the combustor to a less critical component.

The hot section temperature rise establishes the regeneratively cooled chamber channel length and geometry. For wide variations in throttle ratio the resulting chamber is too short to transfer the thermal energy needed to run the cycle at full thrust. A solution is to use a hydrogen circuit regenerator where the excess energy in the hydrogen gas exiting the hydrogen TPA turbine section is counterflowed with the cold hydrogen entering from the pump section. The resulting heat transfer can increase the engine thrust by 40%. Figure 3.3.6-1 shows the effectiveness of the hydrogen regenerator for CTP engines of various thrusts. Note that the regenerator is a significant contributor to the thermal energy for the cycle at all thrusts above 7.5K lbf.

Refer to Section 3.2 for additional discussion of engine throttling.

### Hydrogen Circuit Enthalpy Change

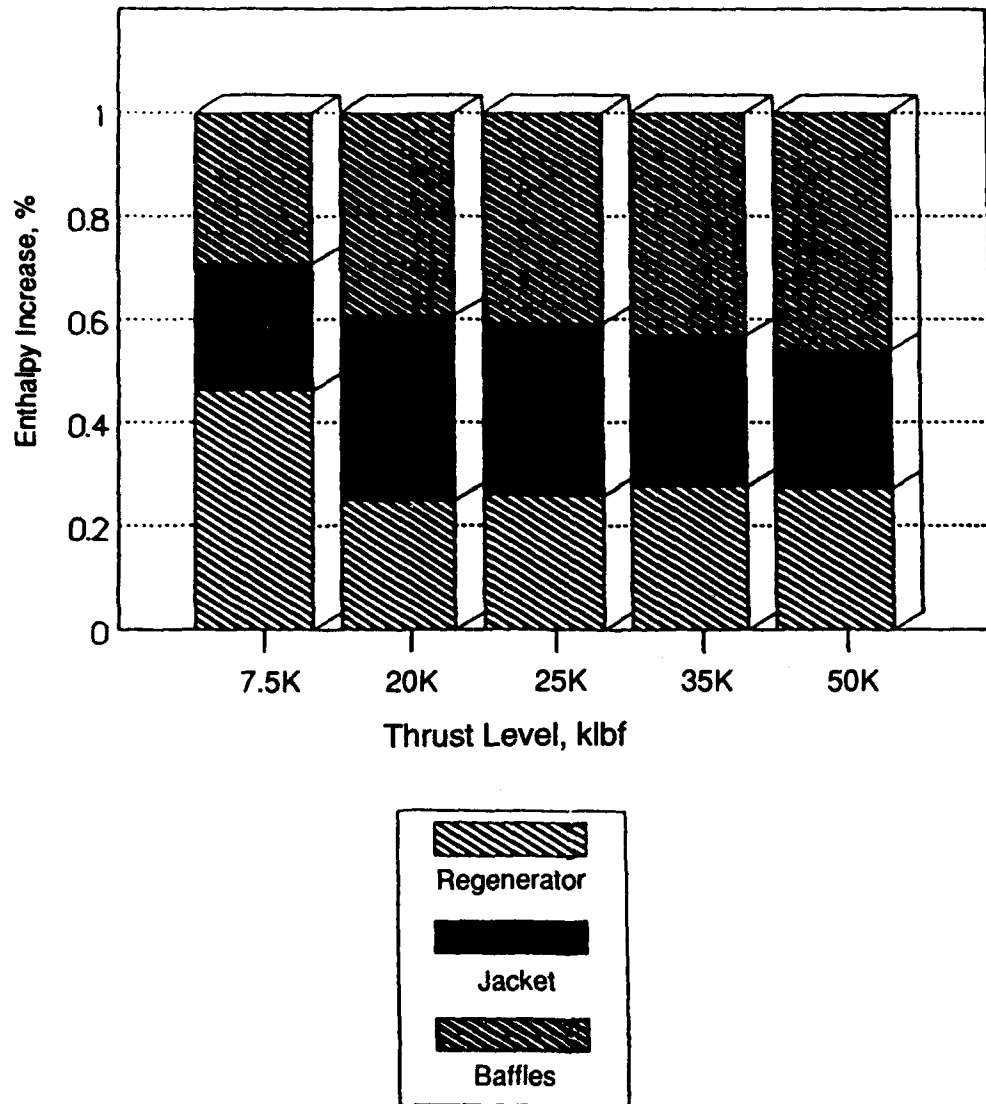


Figure 3.3.6-1. CTP Engine Dual Propellant Expander Cycle

### 3.3, Vehicle/Engine Study Coordination, (cont)

#### 3.3.7 Weight Penalties for Space Basing

Space basing may actually save some engine weight as an inert gas purge system is not needed for the AT version of the CTP engine. The cryogenic propellants are self-purging under vacuum conditions and the hot oxygen driven LOX turbopump baselined for the engine does not require an interpropellant seal purge gas.

Valve actuators, control electronics, gimbal actuators and sensor signal conditioning units will need to be insulated and thermally conditioned with thermostatically controlled heater circuits. This will add a few pounds weight to the assembly.

The most significant weight penalty will be in engine spares and maintenance equipment/facility. This does not add directly to LTV or LEV weight but must still be carried into orbit for a space-based maintenance capability.

#### 3.3.8 Parametric Data Requests

Aerojet responses to request for various types of parametric data are included, for the most part, in the information in Section 3.1. Some requests could not be answered as generation of the information was outside of the contract scope for this study. Now that specific areas of interest are known a follow-on to this study should generate that information. A few items not covered in Section 3.1 are given below.

##### Electrical Power Requirements

Electrical power requirements were determined for the 7.5K lbf thrust engine preliminary design task (see Ref 2). Table 3.3.8-1 gives the power required (worst case) in watts for 13 different engine operation state points. The state points are:

- 00 Nozzle extension/retraction
- 0 Engine Out Gimbal (2 engine vehicle configuration)
- 1 Configure engine for chilldown prior to start
- 2 Chilldown O<sub>2</sub> TPA
- 3 Chilldown H<sub>2</sub> TPA
- 4 Engine Start (tank head)
- 5 Tank head idle

Table 3.3.8-1. Representative Engine Power Requirements, Watts

Component/Operation	00	0	1	2	3	4	5	6	7	8	9	10	11
Ox Turbine Bypass			60					60	60	60	60		
Hydrogen Turbine Bypass			60					60	60	60	60		
Regenerator Bypass			60					60	60	60	60		
HEX Bypass			60					60	60	60	60		
Fuel Idle Valve			50				50				50		
Hydrogen Proportioner							50	50	50	50			
Oxygen Main Valve				97		97	10	10	10	10	97		
Hydrogen Main Valve					97	97	10	10	10	10	97		
Oxygen Igniter Valve						24							
Hydrogen Igniter Valve						24							
Engine Out Gimbal		385											
Normal Gimbal							360	360	360	360	360	360	
Nozzle Extension	100												100
Sensors and Heaters	156	156	156	156	156	156	156	156	156	156	156		156
Controller	70	70	70	70	70	70	70	70	70	70	70		25
Totals*	326	611	516	323	323	468	706	896	896	896	1070	360	281

\*Possible peak wattage required during the operation. Average power will be less.

### 3.3, Vehicle/Engine Study Coordination, (cont)

- 6 Pumped Idle Mode
- 7 Normal Operating range
- 8 Overthrust
- 9 Normal Shutdown
- 10 Normal Gimbal
- 11 Operational Storage

#### External Radiation Environment (Buried Engine)

The engine thrust chamber would be cold to the touch even at full thrust operation from the hydrogen inlet manifold (area ratio 28) to some point above the throat. With the chamber inside a can structure (see Figure 3.1-5) and the lines to and from the injector/baffle circuits insulated, external radiation will be negligible for the upper portion of the engine. The maximum external temperature of the oxygen cooled nozzle would be 400°F near the exit manifold (area ratio 600). The extendible/retractable nozzle will, unless insulated, have much higher outside temperatures. Figure 3.3.8-1 gives the temperature versus area ratio for a columbium nozzle. The two curves are needed to account for the effect of heating by an adjacent engine (near side curve) or exposure to space for direct radiation cooling (far side curve). Figure 3.3.8-2 gives the same variables but for a carbon-carbon nozzle extension.

#### Cluster Constraints

All Aerojet design work to date has assumed a 12 inch clearance between engines at the nozzle exit plane. The adequacy of this clearance is dependent on side loads, mechanical constraints on engine movement, engine nozzle length and flexibility, and gimbal system tolerance. This is one of the items that requires some discussion with the vehicle primes to determine.

#### Attach Points and Gimbal Method

The engine is actually attached to the thrust takeout structure by one pair of the two sets of gimbal brackets. Aerojet has a design where this attachment is made with two ball lock devices that can be connected by a person in a space suit; no nuts, bolts, or other fastening devices. The pitch and yaw axis gimbals are attached to a

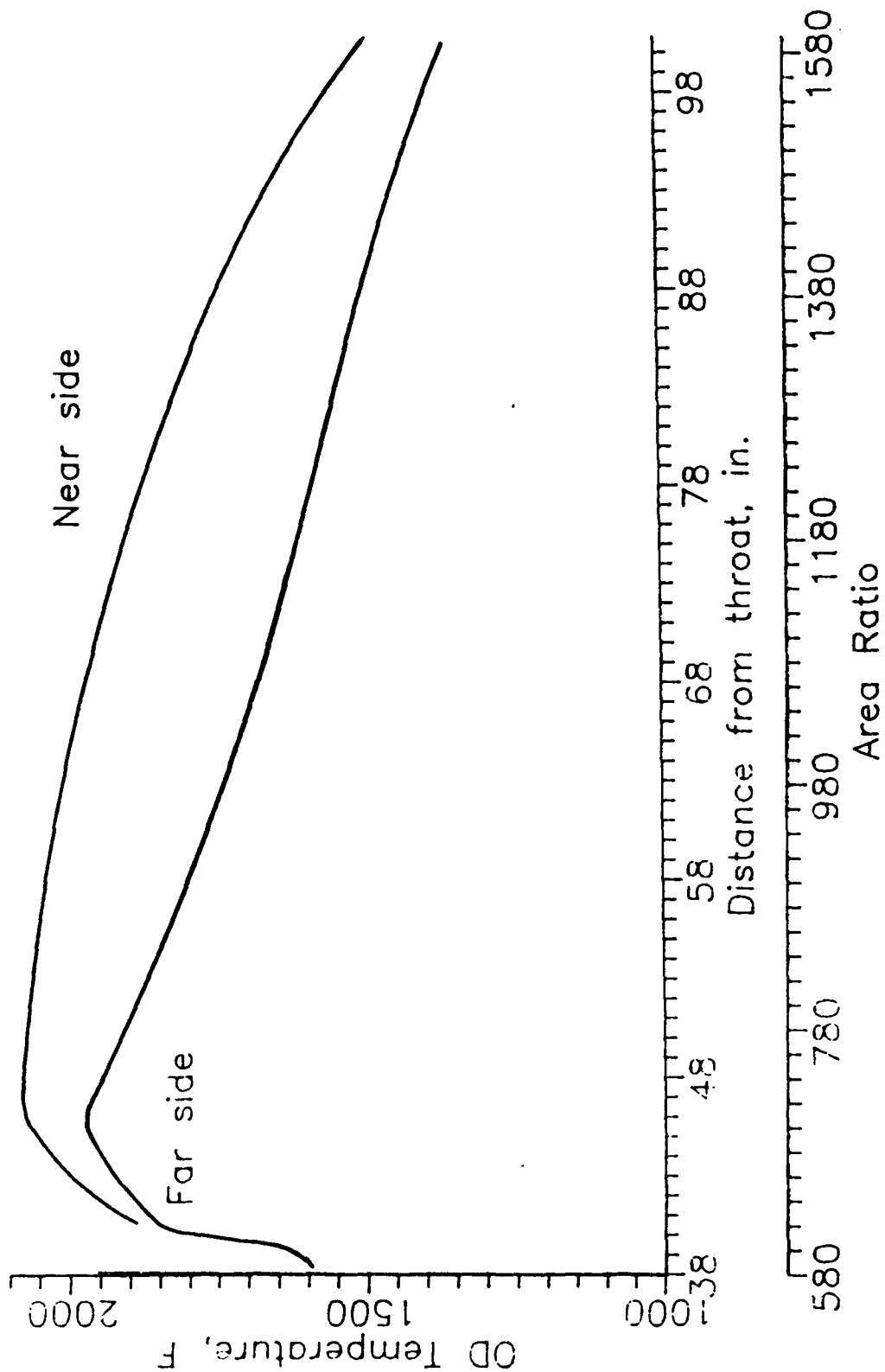


Figure 3.3.8-1. 0.030-in. Columbiu Nozzle Wall Temperature vs. Position

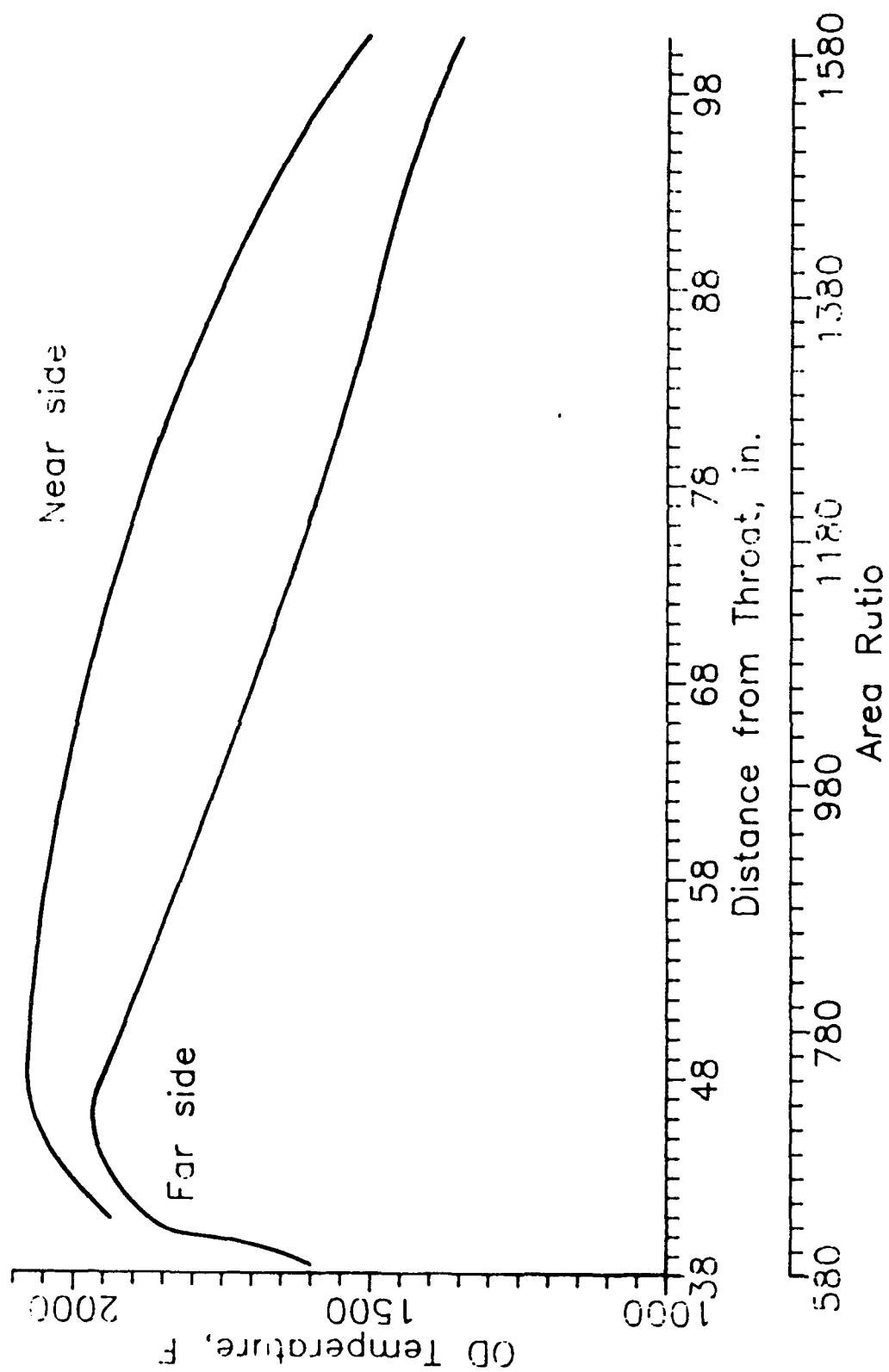


Figure 3.3.8-2. 0.050-In. Carbon-Carbon Nozzle Wall Temperature vs. Position

### 3.3, Vehicle/Engine Study Coordination, (cont)

structure at the top of the engine injector. Actual placement of the gimbal point would be for a true throat gimbal. The gimbal actuator arm connection to the engine could be done by slip-on clamps with securing by thumbscrews so that no tools were required for assembly or disassembly. It is possible that all engine-to-vehicle connections can be made or broken without tools. This would greatly simplify the task of an astronaut making an engine changeout in space.

## 3.4 ENGINE BASELINE DESIGN UPDATE

### 3.4.1 Dual Propellant Expander Cycle

The parallel flow version of this cycle should be an excellent performer. The engine schematic given in Figure 2.1-1 was developed at the beginning of the study based on the thermal design results for the parallel flow dual propellant expander cycle when compared to the series flow cycle developed in the 7.5K lbf thrust engine preliminary design task. It is the current engine design baseline although the version in Figure 3.1-20 should be evaluated. The latter version has the hydrogen regenerator upstream of the HEX for better isolation of the hydrogen circuit from the oxygen circuit. It may be penalized by an increase in HEX weight due to increased surface area needed for the lower delta temperatures. Either version would give the same engine performance. The choice would be made based on engine control capability and weight minimization. The resulting engine promises to be highly flexible with excellent thermal margins for very long life. It represents the current expander cycle state-of-the-art.

### 3.4.2 Engine Control Baseline

This engine will require a closed loop control system, a dozen control valves, and an array of sensors for input to the integrated control and health monitoring system (ICHM). The basic engine valves and sensors are listed in Table 3.4-1. The basic engine operation sequence is outlined in Table 3.4-2. A discussion of valve function is given in Section 3.1.1.10. The corresponding component states are given in Table 3.4-3. The Modified Liquid Engine Transient Simulation Analysis (MLETS) preliminary results indicate that the engine is controllable and is dynamically stable once it is at thermal equilibrium.

**Table 3.4-1**  
**CTP Engine Valves and Sensors for Engine Control**

<u>Valve Name</u>	<u>Abbreviation</u>	<u>Control Function</u>	<u>Primary Sensor Data Source</u>
Hydrogen Turbine Bypass	HTBV	Mixture Ratio	Hydrogen & Oxygen Flowmeters, TPA Speeds, Chamber Pressure, OTBV Position
Oxygen Turbine Bypass	OTBV	Thrust	Oxygen & Hydrogen Flowmeters, TPA Speeds, Chamber Pressure
Heat Exchange Bypass	HEBV	Oxygen Max. Temp.	Oxygen Turbine Inlet Temperature
Hydrogen Regenerator Bypass	HRBV	Hydrogen Max. Temp., Thrust Supplement	Baffle Outlet Temperature, Chamber Pressure
Hydrogen Idle	HIV	Idle Mode Start	Flowmeter Data, Chamber Pressure
Hydrogen Proportioner	HPV	Hydrogen Split (Regen/Baffle)	Baffle & Chamber Outlet Temperatures
Hydrogen Main Shutoff	HMSV	Propellant Isolation	Commanded by OTV Pilot (Engine Start, Stop) or Engine ICHM System
Oxygen Main Shutoff	OMSV	Propellant Isolation	Commanded by OTV Pilot (EngineStart, Stop), or Engine ICHM System
Hydrogen Igniter Control	HICV	Engine Start	Chamber Pressure
Oxygen Igniter Control	OICV	Engine Start	Chamber Pressure
Oxygen Tank Pressurization	OTPV	Tank Pressurization	Tank Pressure, TPA Speed
Hydrogen Tank Pressurization	HTPV	Tank Pressurization	Tank Pressure, TPA Speed

**Table 3.4-2  
Engine Operation Sequence**

<u>Table Entry Number</u>	<u>Operation</u>	<u>Actions/State</u>
00	Nozzle Extension Retraction	28V DC Motor Driven Ball Screws Terminated by Limit Switches/Torque
0	Engine Gimbal	28V DC Driven Actuators (2)
1	Configure Engine for Chillumdown	Close Fuel and Ox Turbine Bypass, Open Fuel Regen Bypass Valve, Close Fuel Idle Valve, Open Hex Bypass Valve, Open Ox Igniter Valve (Ignition Off)
2	Chillumdown O <sub>2</sub> TPA	Open Ox Main Valve (Gaseous O <sub>2</sub> Flows Through the TPA Pump, Hex, Ox Cooled Nozzle, TPA Turbine, Injector, and Out the Engine Nozzle). Close Ox Main Valve on TPA Reaching Operating Temperature, Close Ox Igniter Valve
3	Chillumdown H <sub>2</sub> TPA	Open H <sub>2</sub> Igniter Valve, Open Fuel Main Valve (Gaseous Hydrogen Flows Through the LH <sub>2</sub> Pump, Chamber and Baffle Circuits, H <sub>2</sub> TPA Turbine, Regenerator, Injector, and Out the Engine Nozzle). Close Fuel Main Valve on Reaching the TPA Operating Temperature, Close H <sub>2</sub> Igniter Valve.
4	Lightoff	Open Ox Main Valve, Open Fuel Main Valve, Open Igniter Valves, Actuate Igniters
5	Tank Head Idle	Modulate Fuel Idle Valve for Mixture Ratio Control, Hydrogen Proportioner Valve for Chamber/Baffle Temperature Control, Engine Temperatures Stabilized, Combustion Smooth, Igniters Off
6	Pumped Idle Mode	Modulate Turbine Bypass Valves Towards Closed, Close Fuel Idle Valve, Close Regen Bypass Valve, Close Hex Bypass Valve until Ox Turbine is 400°F. Accelerate TPA's to Pumped Idle Speed, Hold by Modulating Turbine Bypass Valve, Stabilize Engine Temperature. Evaluate Health Monitor System Readings. Begin Main Tank Autogenous Pressurization.

**Table 3.4-2 (cont.)**

<u>Table Entry Number</u>	<u>Operation</u>	<u>Actions/State</u>
7	Normal Operating Range	Command Engine Thrust. Ox Turbine Bypass Valve Moves to Thrust Schedule Setting With Fuel Turbine Bypass Valve Following. Regen Bypass Valve Moves Towards Closed Position to Meet Thrust Requirement Hex Bypass Valve Modulates to Keep Ox Turbine Inlet Temp at 400°F. Hydrogen Proportioner Valve Adjusts to Keep Throat Temperature Within Limits. Mixture Ratio Trimmed by H <sub>2</sub> Turbine Bypass Valve.
8	Overthrust	Command Engine Thrust With Override on Turbine Bypass Control Lower Range. Increase Mixture Ratio to 7. Ox Turbine Bypass Moves to Thrust Schedule Setting With Other Valves Following as in Normal Operation. Health Monitor System Will Reduce Thrust on a Trend Towards Unsafe Temperature. Thrust May Fluctuate as Controller Maintains Mixture Ratio With a Turbine Bypass Valve at Zero Bypass.
9	Normal Shutdown	Shutdown Command Initiates Throttle Down to Pumped Idle Range. At Idle TPA Speeds the Fuel and Oxygen Main Valves are Closed, Turbine Bypass Valves Commanded Full Bypass, Regen Bypass and Hex Bypass Valves to Full Bypass. Idle Valve Full Open. Igniter Valves Open, Ignition On. Residual Propellant is Vented to Space Through the Nozzle. Engine Centered.
10	Normal Gimbal	28 V DC Gimbal Actuators are Activated Per Controller Instructions at Any Time During Engine Operation.
11	Operational Storage	Thermostatically Controlled Heater Power for Valves and Sensor Electronics and DC Motors, Thermal Control Power to ICHM System, Engine Centered, Nozzle Extension Retracted.

**Table 3.4-3  
Component State During Engine Operation**

COMPONENT	PRE START	H <sub>2</sub> PUMP CHILLDOWN	O <sub>2</sub> PUMP CHILLDOWN	TANK HEAD START	TANK HEAD IDLE	PUMPED IDLE	THROTTLE RANGE	RATED THRUST	SHUTDOWN
HYDROGEN MAIN SHUTOFF	CLOSED	OPEN	CLOSED	OPEN	OPEN	OPEN	OPEN	OPEN	CLOSED
OXYGEN MAIN SHUTOFF	CLOSED	CLOSED	OPEN	OPEN	OPEN	OPEN	OPEN	OPEN	CLOSED
O <sub>2</sub> TURBINE BYPASS	0% BP	0% BP	0% BP	100% BP	100% BP	MODULATES	MODULATES	10% BP	100% BP
HYDROGEN TURBINE BYPASS	0% BP	0% BP	0% BP	100% BP	100% BP	MODULATES	MODULATES	10% BP	100% BP
HEAT EXCHANGER BYPASS	100% BP	100% BP	100% BP	25% BP	MODULATES	MODULATES	MODULATES	MODULATES	100% BP
REGENERATOR BYPASS	100% BP	100% BP	100% BP	25% BP	MODULATES	MODULATES	MODULATES	10% BP	100% BP
HYDROGEN IDLE	OPEN	OPEN	OPEN	OPEN	MODULATES	CLOSED	CLOSED	CLOSED	OPEN
HYDROGEN IGNITER	CLOSED	OPEN	CLOSED	OPEN	OPEN	CLOSED	CLOSED	CLOSED	OPEN
OXYGEN IGNITER	CLOSED	CLOSED	OPEN	OPEN	OPEN	CLOSED	CLOSED	CLOSED	OPEN
HYDROGEN PROPOR- TIONER VALVE	NEUTRAL	NEUTRAL	NEUTRAL	NEUTRAL	MODULATES	MODULATES	MODULATES	MODULATES	NEUTRAL
HYDROGEN TANK PRESS.	CLOSED	CLOSED	CLOSED	CLOSED	CLOSED	CYCLES	CYCLE	CYCLES	CLOSED
OXYGEN TANK PRESS.	CLOSED	CLOSED	CLOSED	CLOSED	CLOSED	CYCLES	CYCLES	CYCLES	CLOSED
IGNITERS	OFF	ON	OFF	ON	ON*	OFF	OFF	OFF	ON*
HYDROGEN TPA	STOPPED	WINDMILL	STOPPED	WINDMILL	WINDMILL	PUMP	OUTPUT	RATED OUTPUT	GOES TO STOP
OXYGEN TPA	STOPPED	STOPPED	WINDMILL	WINDMILL	WINDMILL	PUMP	OUTPUT	RATED OUTPUT	GOES TO STOP

\*TO PREVENT POPPING OR UNCONTROLLED IGNITION

### 3.4, Engine Baseline Design Update, (cont)

Basic engine control is accomplished with the two turbine bypass valves. The oxygen turbine bypass valve sets the engine thrust with the hydrogen bypass valve following and then modulating to hold mixture ratio. The HEX bypass valve is primarily a control to regulate oxygen temperature to the OX TPA turbine section. The regenerator bypass valve is used to supplement available energy in the hydrogen stream at higher thrust levels. The hydrogen split between the cooled chamber and the baffle circuit is controlled by the proportioner valve. Other valves are for start and for shutdown or tank pressurization. There is no helium purge system or required helium lines and valves. Once operating, engine control is done through just five valves.

The power balance program was used for an initial assessment of the control curves for both turbine bypass valves. Figure 3.4.2-1 shows turbine bypass flow plotted against engine chamber pressure. Discrete settings of the HEX bypass and regenerator bypass valves were used to reduce the control interaction. These settings are indicated on the plot as well. The linearity is very good considering that the power balance will have a few percent error in the valve settings. These are very acceptable curves for controls modeling. There will be an upward inflection at low chamber pressure points on the curve ( $P_c \leq 100$  psia) as the engine transitions from pumped idle to tank head idle. At 2000 psia the curves crossed because the power balance program was set to adjust the other variables to give a 10% bypass at this point. Note also that power margin condition, at which there is positive bypass flow available to increase power available to the turbine, is not critical until 2000 psia is reached. With some adjustment in the TPA design points even more margin is available for additional chamber pressure (and thrust) at the top end.

#### 3.4.3 Engine Components

The engine component discussion in Section 3.1.1 represents the latest design thinking for the engine baseline. During the study, each component was subjected to a complete reevaluation. To remain in the design it had to survive such questions as:

- Can the engine operate if it is removed?
- Can its function be assigned to another component at a savings in weight and complexity?

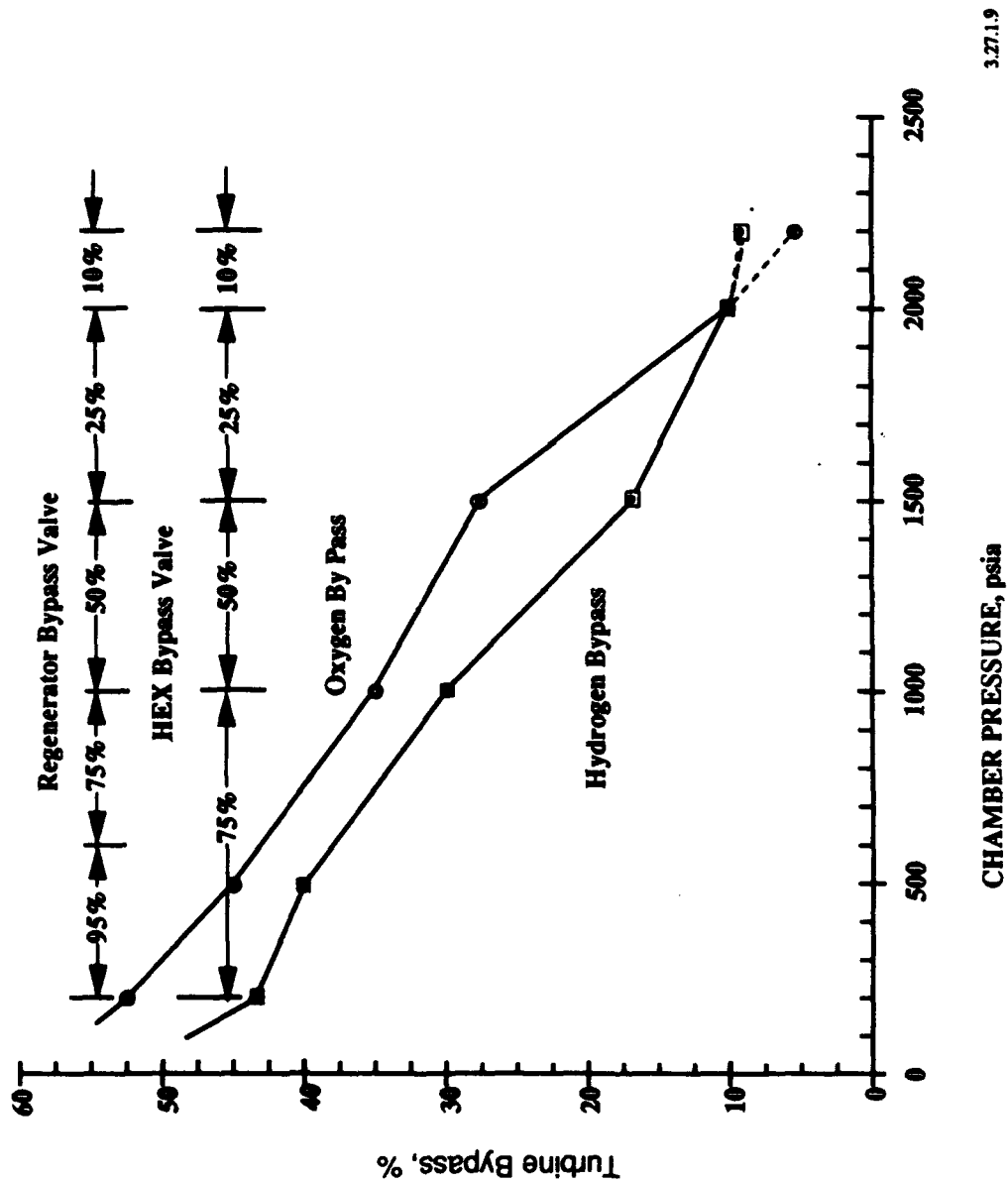


Figure 3.4.2-1. Control Effectiveness – Parallel Flow Dual Expander Cycle Engine

### 3.4, Engine Baseline Design Update, (cont)

- Can the design be changed to save weight?
- Is it producible?
- Does it have safety implications? If so, what are the failure modes and effects?
- Is it an engine life limiter? If so, what changes are needed to improve its life?

Some of the potential design changes that came out of the re-evaluation included:

- 1) Combine the regenerator and HEX into one unit. This was questioned on grounds that packaging may be difficult with one, massive unit.
- 2) Eliminate the regenerator. This was rejected as it was incompatible with either a 10:1 or 20:1 throttling engine.
- 3) Use a stepped valve with only 3 or 4 positions for both the hydrogen regenerator and the HEX bypass valves. This may have merit but requires consultation with the valve designers to be sure that there will be any improvement in reliability or cost over a continuously variable valve.
- 4) Provide a recirculation loop for chilldown of the turbopumps. This would use the propellant dumped in chilldown but would add a line and an additional valve to each circuit. The valve would also have to be positioned where its failure would preclude engine start. A preferred option is engine operation at tank head idle in the latter stages of chilldown if that can be done without severe popping or pressure fluctuations.
- 5) Add line quick connects/disconnects for each major component. This was considered premature until the NASA decides on a specific engine maintenance scenario. The design baseline calls for simplified engine removal. Four propellant lines, several electrical cable connectors, two gimbal actuators, and locking

### 3.4, Engine Baseline Design Update, (cont)

devices at two points on the thrust takeout structure would be in one plane processed through an opening large enough to accommodate an astronaut in a space suit.

6) Add redundant valves for critical applications. This was rejected as adding complexity without necessarily improving reliability. All valves have dual actuating coils powered by physically separate electrical circuits. Each circuit will open on a ground fault within the system. The main propellant shut-off valves are powered open against a spring force and latched in place by a solenoid that releases if power is lost to effect an engine shutdown. It is also possible to build these valves so they can be manually closed or opened from the crew station. The engine valving is either fail operational or fail safe depending on the failure mode.

### 3.5 IDENTIFICATION OF CRITICAL TECHNOLOGIES

A major goal of the OTV engine technology program is to identify the critical LOX/LH<sub>2</sub> engine technology issues and develop design, materials, and systems approaches to put them to practice. Aerojet program personnel believe a great deal of progress has been made over the life of the contract to fulfill this goal. The following discussion should be considered a status report as well as a call to pursue additional technology efforts.

#### 3.5.1 Thrust Chamber Technology

3.5.1.1 Performance Improvement — Performance for a LOX/LH<sub>2</sub> rocket engine is usually stated as the figure for delivered specific impulse (Isp). The Aerojet version of this engine using Aerojet's performance computation methodology will, theoretically, deliver 484 lbf-sec/lbm (at a chamber pressure of 2000 psia, area ratio of 1200:1, and a mixture ratio of 6). In general, Aerojet has a good record of test stand verification of Isp using our methodology. With injector energy release efficiencies (ERE) greater than 95% using well established element designs such as the coaxial and swirl coaxial, a reasonable combustion chamber length will yield very nearly 100% ERE. Although it will be difficult to pick up additional engine Isp in the future, real gains in vehicle performance may come from:

### 3.5, Identification of Critical Technologies, (cont)

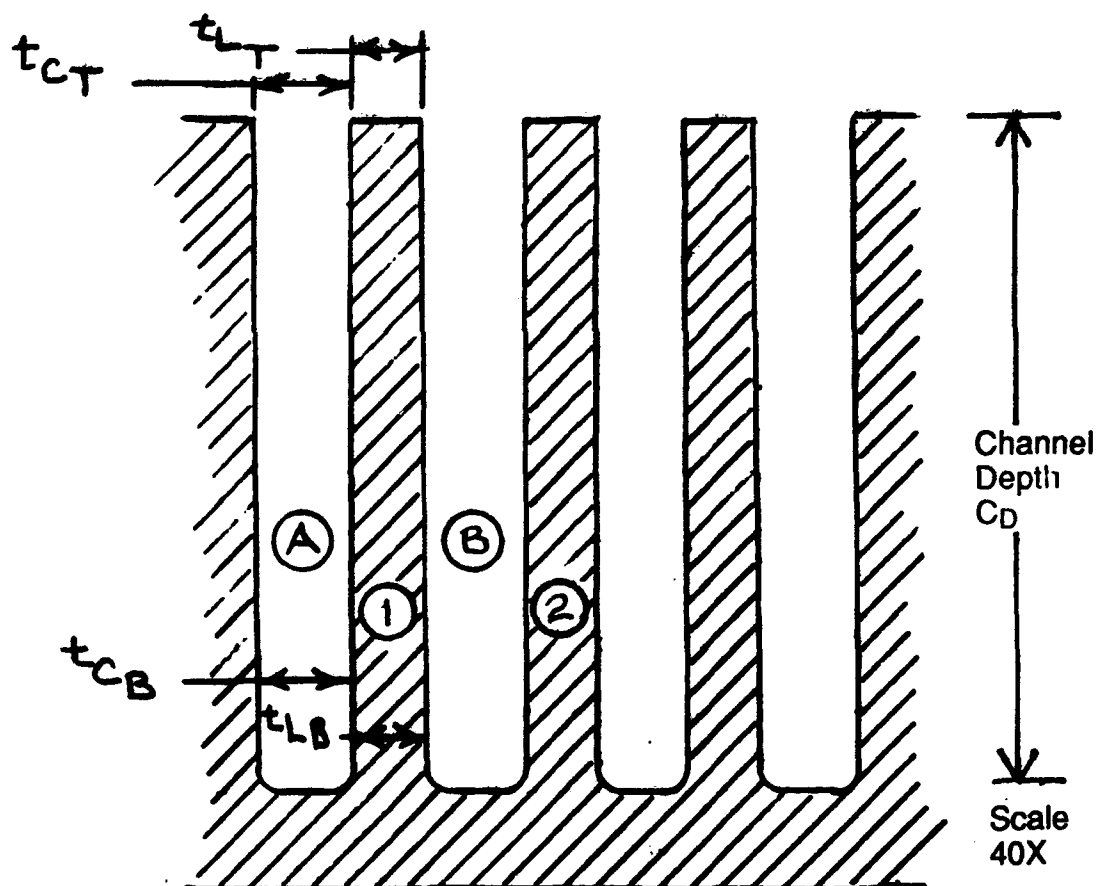
- Reduction of initial chilldown propellant dumping prior to engine start.
- Maintenance of injector energy release efficiency over the entire throttle range (there is a drop off at the lower range with most injector elements).
- Active Propellant Management (APM) systems to minimize tank residuals on each mission.
- Reduction in hydrogen boiloff and consequent reduction in vehicle specific impulse during periods when the engines are shutdown. One approach would utilize the engine as a black body radiator to deep space with the liquid hydrogen circulating through the regen cooled chamber and back to the tanks.
- Improving the efficiency of a LOX/LH<sub>2</sub> attitude control system by using a high pressure gas supply pumped up by the main engines during their operation.
- Reduction in engine physical size and weight. The engine operating envelope includes a high mixture ratio ( $MR \geq 7$ ) overthrust capability (5 to 25% increase in thrust over nominal) that can be used to keep engine size down. Weight is a function of the number of components, materials selection, thrust, and chamber pressure. There is a continuing premium in developing and using strong, lightweight materials with a high (2000 psia or greater) chamber pressure engine.
- Long engine service life. Every item carried into space has a large transportation cost that usually exceeds that of the item. In space maintenance, using people in space suits has been estimated to cost \$100,000 per hour. These formidable costs mandate a long life for a space based engine. Long service life can be the equivalent of higher specific impulse as it reduces the amount of propellant expended to support the actual mission.

### 3.5, Identification of Critical Technologies, (cont)

Engine throttling has two performance aspects. One is the range: 10:1, 20:1, or whatever the mission requires. A high throttle range requires (for the Aerojet design) an added control valve and a regenerator. There is a small engine weight reduction as throttle range is decreased from 20:1. The other performance consideration is throttle rate ( $\Delta$  thrust per unit time). As noted in Section 3.1.1, a preliminary transient analysis indicates a 10% thrust change in 0.3 seconds is possible without violating engine operating parameters. This should be adequate for present state-of-the-art engine controllers, but must be verified by the vehicle prime contractors for mission suitability.

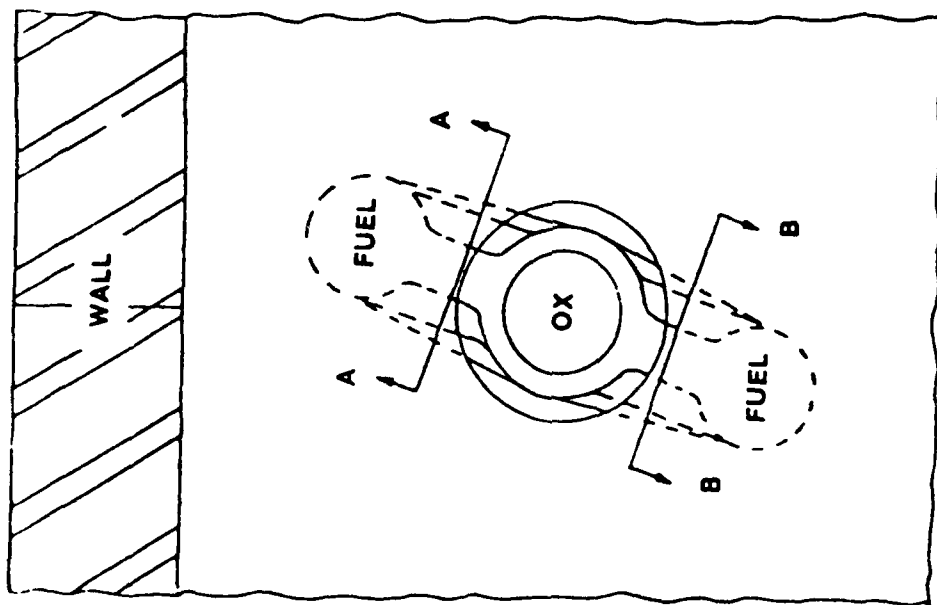
**3.5.1.2 Thrust Chamber Design** — The Aerojet TCA design is defined in some detail in Section 3.1.1. It embodies several state-of-the-art features:

- Microchannel design in the throat for reduced thermal strain and better heat transfer. See Appendix A for dimensions and Figure 3.5.1 for a machined test specimen.
- Codeposited bimetal electroformed closeout. Three combinations (NiMn, NiCo, and NiCr) are recommended to increase strength by a factor of three over a conventional nickel electroform closeout. The NiCo has been demonstrated in the OTV technology program.
- Optimized I-triplet injector elements. Aerojet has selected the I-triplet element (see Figure 3.5-2 for construction) as having the best performance potential of all LOX/LH<sub>2</sub> injector elements. It can attain ~100% ERE within 4 to 8 inches of the injector face. This allows baselining a short chamber, as a long chamber is not needed to get high ERE. The high energy release prompted a modification of the element under Task C.4 to assure better wall compatibility. The resulting patterns are shown in Figure 3.5-3 based on adjustments to the momentum ratio between the oxygen and hydrogen streams. The various patterns were verified by water flow and the mass distributions plotted (See Figure 3.5-4). The success of the element modification program will be measured by an increase in chamber life.

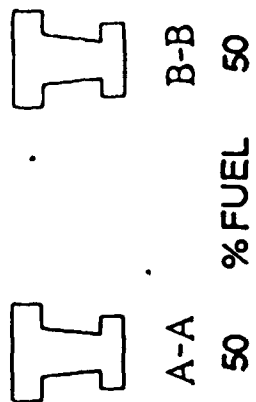


LAND			CHANNEL		
	$t_{LT}$	$t_{LB}$		$t_{CT}$	$t_{CB}$
①	0.01094	0.00875	Ⓐ	0.01109	0.01156
②	0.01125	0.01125	Ⓑ	0.0109	0.01078
NOMINAL	0.011 ± .002		NOMINAL	0.010 ± .002	

Figure 3.5-1. Microchannel Test Specimen Based on 7.5K Thrust Level Design



CURRENT DESIGN



PROPOSED MODIFICATION

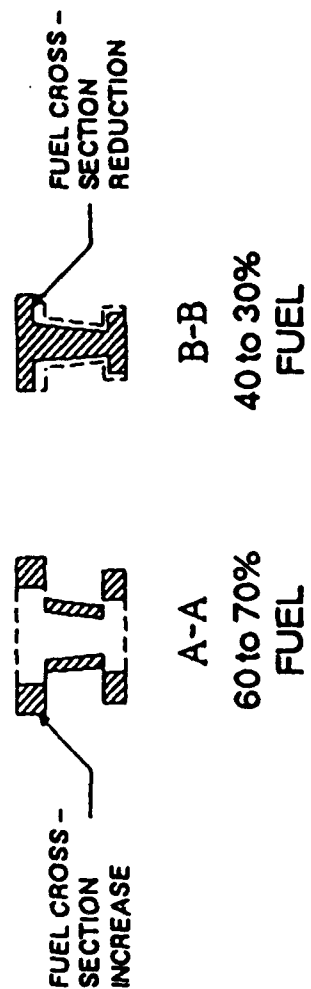
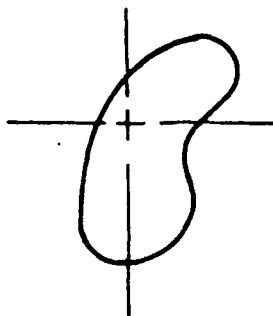


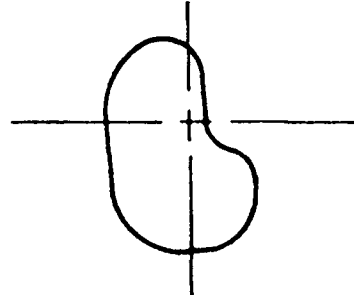
Figure 3.5-2. Modified I-Triplet Injector Elements

**Predicted Mass Flow Patterns for Fuel and Oxidizer Elements**

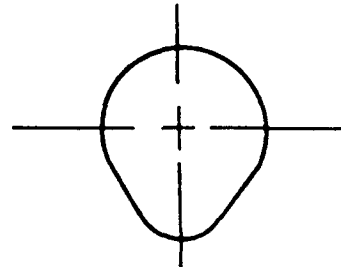
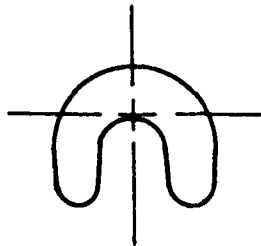
**Left Baffle  
Element**



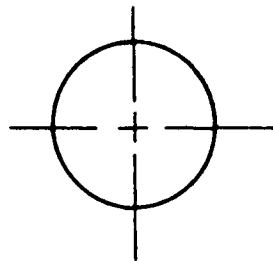
**Right Baffle  
Element**



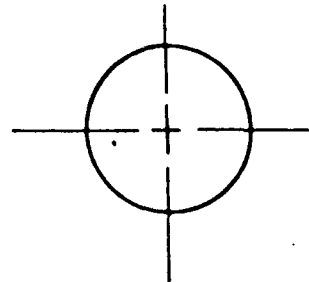
**Center Element  
Wall Element**



**3K Element**



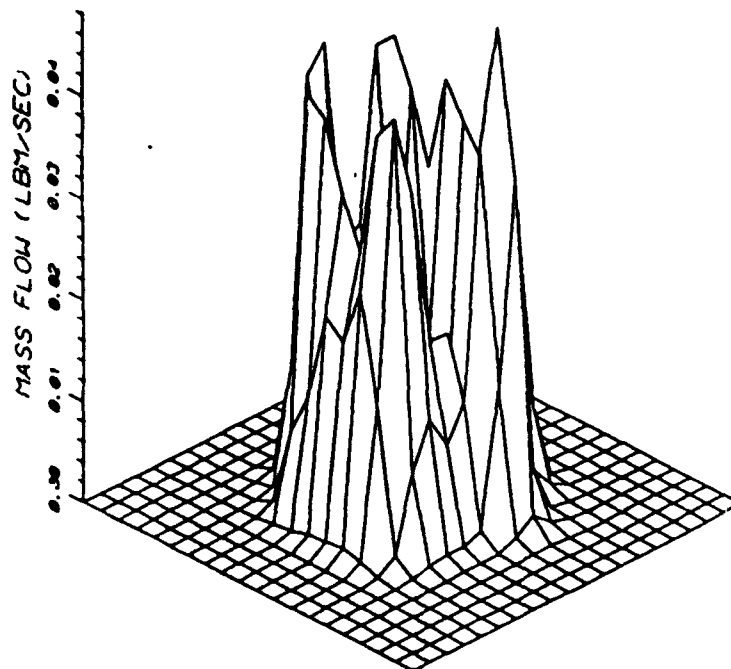
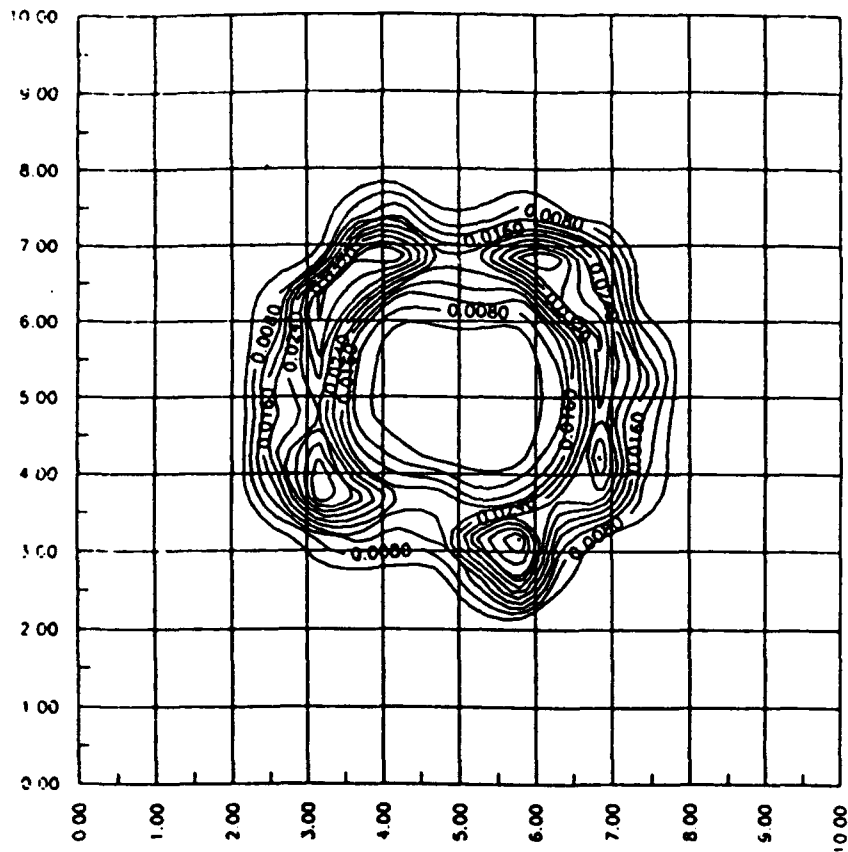
**OX**



**Fuel**

**Figure 3.5-3. Modified Injector Element Patterns**

# SCMML1 OX DISTRIBUTION



# SCMML1 OX MASS DISTRIBUTION

**Figure 3.5-4. Water Flow Patterns For I-Triplet Element**

### 3.5, Identification of Critical Technologies, (cont)

- **Hydrogen cooled baffles.** By dividing the hydrogen flow between the regen cooled chamber and baffle plates the heated metal surface area is increased by 80%. The practical result is an abundance of energy that can be turned into chamber pressure. Chamber pressure is effectively limited only by hot section life capabilities. A further extension of capability to 3000 psia may be possible with consequent reduction in engine size and an increase in throttle range.

The major area for improvements in TCA technology will come in the use of improved materials. Aerojet has begun an investigation of a new family of copper alloys from the SCM company using copper, dispersion hardened by the inclusion of finely dispersed aluminum oxide particles. These GLIDCOP alloys have excellent machining characteristics, very little loss in thermal conductivity compared to pure copper, and excellent mechanical properties at elevated temperatures (See Figure 3.5-5 for a comparison). Work is also being done in copper metal matrix composites that show some promise. Aerojet has also been very successful in adapting platinum and other noble metals to thrust chamber applications. Platinum may well be the material of choice for the baffle plates despite the raw material cost. The emphasis in future work should be on increasing engine life while reducing engine weight.

#### 3.5.2 Turbopump Technology

Aerojet has tested an oxygen turbopump with 50°F oxygen turbine drive gas (See Reference 5 and 6) and a hydrostatic bearing system. A continuation of the oxygen turbopump work including operation with 400°F oxygen turbine drive gas should concentrate on reducing seal leakage and improving overall efficiency. Minor work on low friction surface treatment to minimize wear during the rubbing starts required in a hydrostatic bearing system would be worthwhile.

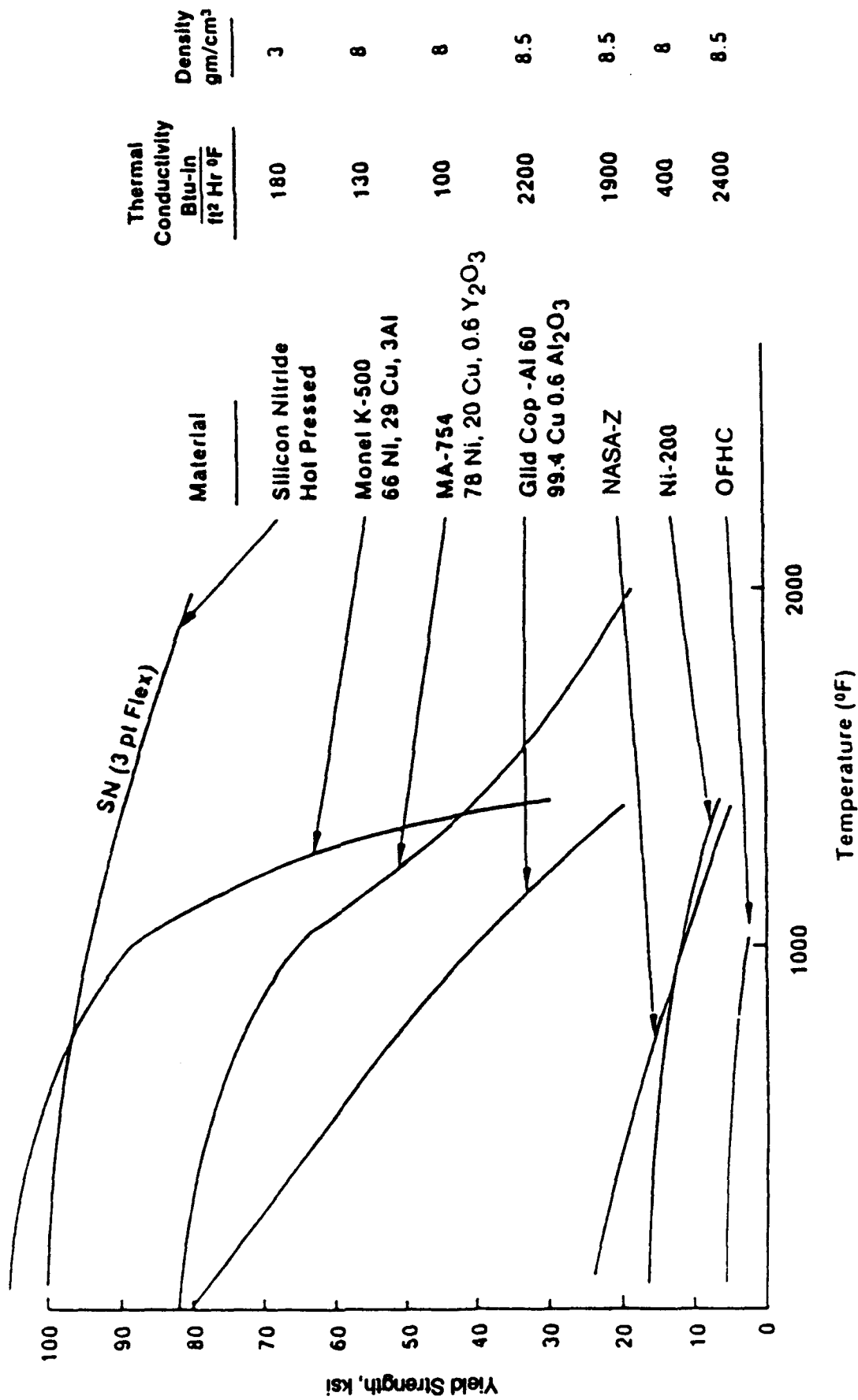


Figure 3.5-5 Structural Property Variation With Temperature

### 3.5, Identification of Critical Technologies, (cont)

The hydrogen turbopump technology currently considered state-of-the-art uses hydrostatic bearing systems with a dual spool configuration (see Figure 3.5-6 for a representative design) for subcritical speed operation. A dual spool six stage hydrogen pump was tested for the Air Force XLR-134 engine program in late 1989 and early 1990. The dual spool concept was proven practical, but the XLR-134 TPA uses a conventional ball bearing system. A demonstration of this critical technology with a hydrostatic bearing system is needed.

Such a hydrogen pump should also be designed to verify design capability at turbine tip speeds greater than 2000 ft/sec, rotating assembly speeds of 200,000 rpm, and pump pressure rise of 7500 to 8000 psid. Various static seal systems could be designed for test using TPA hardware so that seal capability could be assessed with the same basic TPA. This demonstration hydrogen TPA could identify the design problems at the operating limits for any expander cycle turbopump needed by the chemical transfer propulsion program for engines in the 7.5K to 50K lbf thrust range. The current critical technology could be demonstrated for any projected engine for the CTP program and also for NASP.

#### 3.5.3 Heat Exchanger Technology

The Aerojet platelet heat exchanger technology using copper alloys has now reached the flight qualification stage with current testing of a platelet heat exchanger on the Space Shuttle Main Engine. Section 3.1.1 has a discussion of the advanced engine LOX/GH<sub>2</sub> heat exchanger (HEX) and the hydrogen regenerator used with the dual propellant expander cycle engine. The value of these components is twofold: 1) chamber size can be reduced and throttle range greatly increased by using a regenerator, and 2) the HEX provides about 65% of the energy needed to operate the oxygen turbopump with excess heat from the stream leaving the hydrogen turbopump. A bonus is the ability to trim the engine operation with bypass around these components. Nearly any variant of a hydrogen expander cycle engine can benefit from one

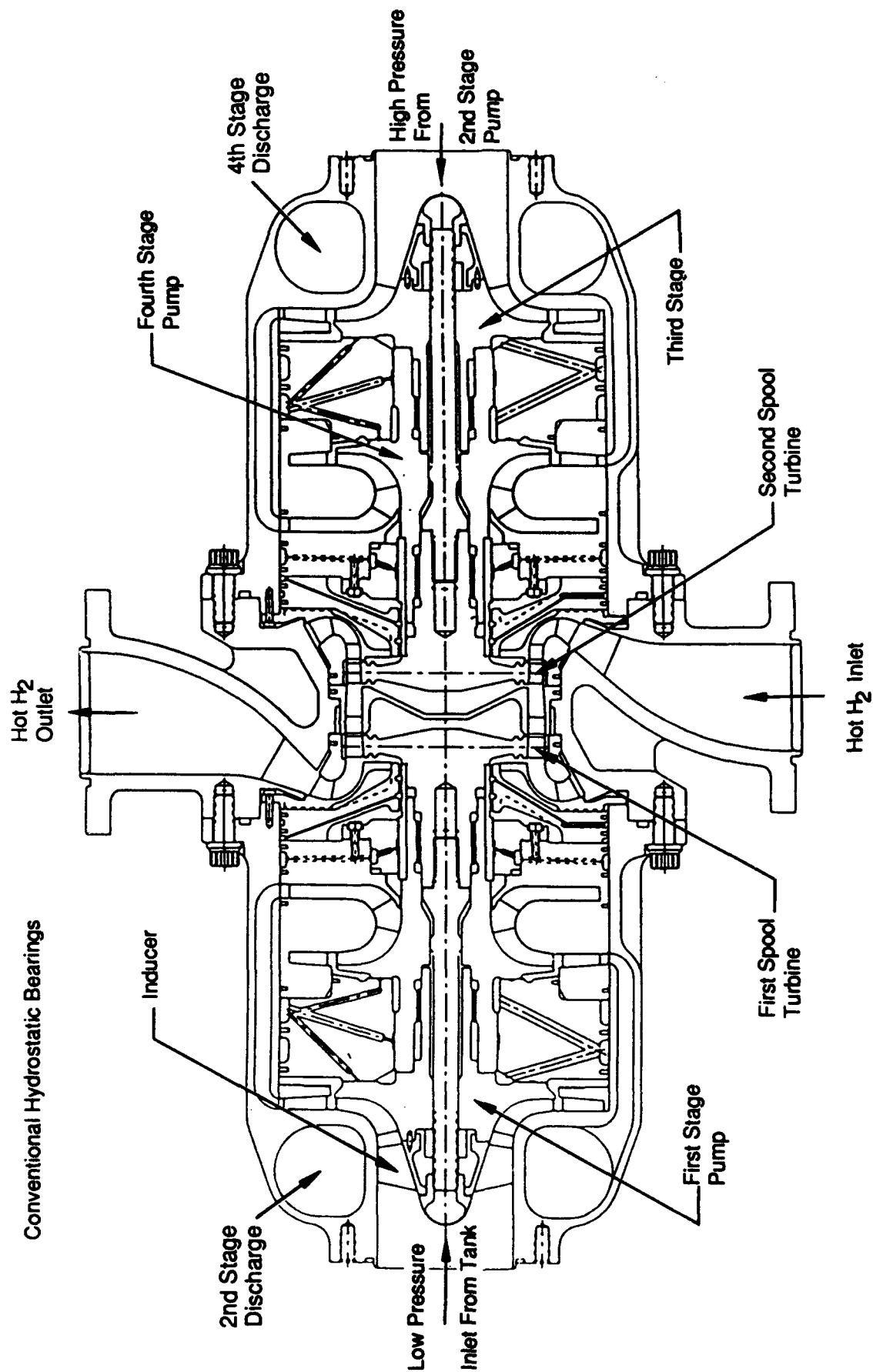


Figure 3.5-6. Dual Spool Hydrogen Turbopump

### 3.5, Identification of Critical Technologies, (cont)

of these heat exchangers. The price is some added complexity and weight. A critical technology for the platelet heat exchanger would be a demonstration of their fabrication in beryllium. This material substitution could reduce the component weight over 70% from the weight in copper alloy. There are also serious questions concerning beryllium compatibility with oxygen that need to be resolved.

A design issue for the HEX is the selection of a channel geometry for the oxygen side that will assure turbulent mixing of liquid oxygen as it reverts to the gas phase under conditions of high velocity and high heat transfer rates. Without mechanical mixing from designed-in channel turbulence generators the oxygen would exit as a two phase stream, and the overall heat transfer coefficient for the HEX would be greatly reduced.

#### 3.5.4 Proportioner Valve Technology

Engine control and thermal balance is dependent on several proportioner valves (see Figure 2-1.1 and Section 3.1.1.10). None of the proposed valves has a production history in the desired configuration. The main development issues are precision metering and reliability. The valve preliminary design task for the 7.5K lbf thrust engine design (see Reference 2) confirmed that 28 volt dc motors would be adequate for these valves. Aerojet proposes that each valve have dual actuating coils with separate power supplies for the redundancy needed for a man-rated system. A loss-of-power type failure would leave the valves in the last position commanded by the controller. A critical technology demonstration would have an oxygen system turbine bypass valve fabricated and tested with 400°F oxygen at pressures expected in normal engine operation. Control response would be verified based on current engine control models.

#### 3.5.5 Oxygen Cooled Nozzle

The dual propellant expander cycle extracts about 35% of the thermal energy needed to operate the oxygen turbopump from the oxygen cooled nozzle extension. The use of oxygen as a coolant has been demonstrated in chamber tests at NASA-LeRC (Ref: Cooling of High Pressure Rocket Thrust Chambers With Liquid Oxygen, NASA-TM-81503). This is a critical technology that should be reduced to practise by designing, fabricating, and testing an oxygen cooled nozzle on a test bed engine.

### 3.5, Identification of Critical Technologies, (cont)

#### 3.5.6 Extendible/Retractable Nozzle

The NASA-MSFC is expected to fund a program to demonstrate the materials and joint for an OTV engine extendible/retractable nozzle. As of this writing the contract had not been awarded. Assuming it is funded and the development successful, a follow-on program should be considered to assess the deployment/retraction mechanism(s) for reliability. This should include an assessment of the seal for leak free operation after numerous cycles. This is a critical technology so long as the CTP engine nozzle is required to operate through an aerobrake with alternate extension and retraction required.

#### 3.5.7 Integrated Control and Health Monitoring System (ICHM)

This has been recognized by NASA LeRC as a critical technology with continued task work under the OTV engine technology program. The most recent task (Task E.7 to Contract NAS 3-23772) addresses in depth the requirements for the CTP engine. Additional development is likely based on recommendations coming from the E.7 task work.

#### 3.5.8 Engine/Vehicle Synergisms

The list of areas for vehicle performance improvement given in Section 3.5.1 requires the collaboration of vehicle and propulsion system designers for several of the items. The collaboration of engine/vehicle designers should also be extended to include gimbal design, thrust take-out structure design, aerobrake door design, optimization of propellant tank pressurization, integration of the attitude control system with the main engine system, and flight station control and display information. The proposed vehicle prime/engine contractor interfacing has not been carried out to the extent intended at the start of the study. Aerojet believes that a number of critical technology items will be identified when such a collaboration takes place. Also, the efficiency of both vehicle and engine design (synergy) will be improved.

## 4.0 CONCLUSIONS AND RECOMMENDATIONS

### 4.1. CONCLUSIONS

Three conclusions stand out due to their importance in meeting the ultimate goal of producing a new high performance LOX/LH<sub>2</sub> rocket engine for space transfer applications:

- 1) The NASA LeRC-sponsored work has materially advanced the state-of-the-art in LOX/LH<sub>2</sub> rocket engine technology to the point where an engine development program can be started at any time with relatively low technical and schedule risks.
- 2) The Aerojet-developed parallel flow version of the dual propellant expander cycle engine is a major advance over the 1960 technology represented by the RL-10 engine in terms of delivered specific impulse, operational envelope, thermal margins, and modern control and health monitoring capability.
- 3) The collaborative efforts in response to President Bush's space initiative helped define vital engine design parameters such as thrust, and showed that vehicle prime contractor/engine contractor interchanges are needed on a regular basis. This engine development is rapidly moving towards a real vehicle application; vehicle primes are working on study contracts; and there is national interest in specific missions where this engine is needed. The program needs to focus on the real near-term application.

Conclusions specific to engine technology and study results include:

- 4) The development of the parallel flow version of the original Aerojet expander cycle improved thermal margins, reduced pump output pressure requirements, and expanded the operating envelope. This may well be the cycle of choice where long engine life and operating flexibility are emphasized.
- 5) A major benefit of the Aerojet cycle is the elimination of any helium purge system. This is a major benefit in the context of the overall vehicle design requirements.
- 6) A throttle range of 20:1 is well within the operating capability of the baseline design with only minor adjustment to the turbopump design points.

#### 4.1, Conclusions, (cont)

7) High mixture ratio ( $MR \geq 7$ ) operation is readily accommodated by the baseline engine cycle and components. Protection of the copper chamber will require a gold plating of 1 1/2 mils. Above  $MR = 10$ , the baffle plates should be constructed of platinum alloy for better thermal margins.

8) Engine delivered specific impulse is very close to realistic upper limits. New work should emphasize improvements to propulsion system specific impulse.

9) A maintenance scenario needs to be developed to assess the need for individual component changeout versus complete engine removal. Access and engine packaging constraints will limit component changeout despite any quick connect/ disconnect features.

10) Materials technology remains a major area for continued research and development. In particular the GLIDCOP copper alloys and platinum alloys for thrust chamber use, and beryllium for heat exchange versus lightweight composite materials can be used in a number of places to replace metals.

11) The question of turbopump life as a limiter to engine service life may be answered by using TPAs with hydrostatic bearing systems.

12) Integrated control and health monitoring system development will remain a fruitful area for continued work for the foreseeable future. The rocket propulsion industry is at least a decade behind other industries in adapting new electronic and sensor technology to rocket engines.

13) Work with the MLETS code showed that analytical tools of this sophistication hold great promise in reducing development risk, but they are time intensive.

#### 4.2 RECOMMENDATIONS

The study work was left incomplete in those areas where a cooperative effort was needed between engine and vehicle contractors. The first three recommendations address this need:

#### **4.2, Recommendations, (cont)**

- 1) The study should be continued with more specific tasks requiring coordination among vehicle contractors and the engine contractors. Such topics as tank head start, gimbaling requirements, and thrust takeout structure design should be included for resolution.**
- 2) A maintenance scenario for these engines needs to be developed as soon as possible as it has engine design implications. This should be included as one of the cooperative tasks for the vehicle contractors working with engine contractors.**
- 3) A focused task to improve propulsion system specific impulse should be included in any follow-up study. Again, this requires vehicle and engine contractor collaboration.**
- 4) Continued work under the OTV engine technology program should include a number of materials development tasks.**
- 5) A demonstration program for a hydrogen TPA using hydrostatic bearings, subcritical rotor design, and a variety of seal designs would resolve concerns on this key component.**
- 6) Development of an engine steady state analysis code adaptable for use throughout the industry should be funded. (This may be a product of the Advanced Expander Test Bed Engine program).**
- 7) ICHM capability should be improved by continued research and development. In particular, some techniques of artificial intelligence decision making should be adapted to handle this propulsion system.**

## 5.0 REFERENCES

1. Sutton, George P., Rocket Propulsion Elements, fifth edition, ISBN 0-471-80027-9, Wiley Interscience, U.S.A., 1986.
2. Hayden, Warren R., and Sabiers, Ralph, "OTV Engine Preliminary Design Final Report", ATC Report 2459-34-1, NASA CR XXXXX, Contract NAS 3-23772, NASA Lewis Research Center, Cleveland, Ohio, October 1988.
3. Schneider, Judy, "Baffled Injector Design, Fabrication, and Verification", Aerojet TechSystems, NASA Contract NAS 3-23772, Task C.4, CR 4387, NASA Lewis Research Center, Cleveland, Ohio, January 1990.
4. Franklin, Jerrold, E., "Combustion Chamber Gas-Side Oxidation/Reduction/Corrosion", IR&D Report ATC 87-12-NLRFC1, Aerojet TechSystems, Sacramento, California, August 1987.
5. Buckmann, P.S., et al, "Orbital Transfer Vehicle Engine Oxygen Turbopump Technology, Final Report, Vol I: Design, Fabrication, and Hydrostatic Bearing Testing", Aerojet TechSystems, NASA Contract NAS 3-23772, Task B.4 and B.6, CR 185175, NASA Lewis Research Center, Cleveland, Ohio, August 1989.
6. Brannam, R.J., et al, "Orbital Transfer Vehicle Engine Oxygen Turbopump Technology Final Report, Vol. II: Nitrogen and Ambient Oxygen Testing", Aerojet TechSystems, NASA Contract NAS 3-23772, Task B.7, CR 185262 NASA Lewis Research Center, Cleveland, Ohio, October 1989.
7. Holtzman, W.A., and W.R. Hayden, "Integrated Control and Health Management, Phase II Task Final Report", Orbit Transfer Rocket Engine Technology Program, NAS 3-23772, Task E.3, CR 182122, Aerojet TechSystems for NASA Lewis Research Center, Cleveland, Ohio, October 1988.
8. Schneider, J. and Hayden, W., "Orbital Transfer Vehicle 3000 lbf Thrust Chamber Assembly Hot Fire Test Program", Interim Report, CR-182145, NASA Contract NAS 3-23772-C.2, Aerojet TechSystems for NASA Lewis Research Center, Cleveland, Ohio, September 1988.

## **5.0, References, (cont)**

9. Anderson, R.E.; M. Murphy; D.C. Rousar; J.A. van Kleeck, "Effects of Oxygen/Hydrogen Combustion Chamber Environment on Copper Alloys", Aerojet TechSystems, Technical paper for the Advanced Earth-to-Orbit Propulsion Technology Conference, Marshal Space Flight Center, Alabama, May 1986.
10. Price, H.G., "Cooling of High Pressure Rocket Thrust Chambers With Liquid Oxygen," NASA-TM-81503, NASA-LeRC, June 1980.
11. Kobayashi, A.C. and Morgan, D.B., "Main Chamber Combustion and Cooling Technology Study", Aerojet TechSystems, NASA Contract NAS 8-36167, Report No. 1370-F-1, NASA MSFC, Alabama, August 1989.
12. Klueh, R.L., "Bubbles in Solids", Science and Technology, pp. 5-13, 1969.
13. Klueh, R.L. and Mullins, W.W., "Some Observations on Hydrogen Embrittlement of Silver", Transactions of the Metallurgical Society of AIME, Vol. 242, pp. 237-243, February 1968.
14. Brandt, W., "Channeling in Crystals", Scientific American, Vol. 218, No. 3, pp. 90-98, March 1968.
15. Bair, E.V., and Schindler, C.M., "Space Transportation Main and Booster Engine Configuration Studies", Final Study Report, Executive Summary, Vol. I, Contract NAS 8-36876 and NAS 8-36855, Aerojet TechSystems for NASA Marshall Spaceflight Center, Alabama, August 1989.
16. Ostrander, N., "Chug Stability of 20K CPT Engine," Engineering - EAR 9984:0055G, 5 March 1990.

# APPENDIX A

## DETAILED ENGINE THERMAL ANALYSIS

### CONTENTS

- A.1 Introduction
- A.2 Design Methodology
  - A. Regeneratively Cooled Chamber and Baffles
  - B. LOX/LH<sub>2</sub> HEX and Hydrogen Regenerator
  - C. Oxygen Cooled Nozzle
- A.3 Boundary Conditions
- A.4 Discussion
  - A. Geometry Allowables - All Components
  - B. Regeneratively Cooled Chamber
  - C. Baffles
  - D. Heat Exchanger and Regenerator
  - E. Oxygen Cooled Nozzle
- A.5 Conclusions
- A.6 References
- A.7 Nomenclature

## A.1 INTRODUCTION

The material contained in this appendix was derived from Aerojet TechSystems Engineering Analysis Report: "OTV High Thrust Feasibility Study", 9985:0234, 10 May 1989. It documents the first in-depth thermal analysis of the parallel flow version of the dual propellant expander cycle engine. K. Dommer, the report's author, was also the lead analyst for the 7.5K lbf thrust OTV engine TCA thermal design.

The thermal analysis evaluated designs for 20K, 35K, and 50K lbf thrust. The 25K lbf thrust engine was assumed to be very similar to the 20K design point.

## A.2 DESIGN METHODOLOGY

A preliminary analysis indicated that the five major components (thrust chamber, oxygen cooled nozzle, H<sub>2</sub> regenerator, HEX, and baffles) could not be analyzed as separate and independent entities, but rather that the analysis had to consider their thermal and hydraulic interdependence. This led to an iterative analytical approach. Estimates of the assumed oxygen and hydrogen pump discharge conditions for each thrust were obtained from the AT Systems Engineering Group and were considered constant over the entire mixture ratio and thrust range. Because the hydrogen inlet condition to the regeneratively cooled chamber is not dependent on the other components, the characterization of the chamber was conducted first. Next, an inlet temperature and pressure to the baffle was assumed and its thermal and hydraulic predictions were made. The mixed mean temperature of the baffle and the regenerative cooled chamber was then determined. This defines the hydrogen temperature at the turbine inlet. The pressure drop through the chamber defines the hydrogen inlet pressure to the turbine. The temperature and pressure drop across the turbine defines the H<sub>2</sub> inlet condition to the heat exchanger. The total energy required to operate the oxygen turbine minus the amount of energy available in the nozzle defines the amount of energy transfer in the heat exchanger. This defines the hot hydrogen HEX exit/regenerator inlet condition. The hot hydrogen inlet temperature to the regenerator then defines the maximum possible temperature the cold H<sub>2</sub> entering the regenerator can attain. If the resulting temperature of the hot hydrogen entering the regenerator is greater than the assumed baffle inlet temperature, the regenerator is evaluated. Finally, the solution is considered converged when the regenerator is sized to give an outlet temperature on the cold hydrogen side which equals the assumed baffle inlet temperature.

## **A.2, Design Methodology, (cont)**

Table A-I gives the analytical assumptions for the start of the analysis. Table A-II gives chamber design parameters. Tables A-III, A-IV, and A-V summarize the inlet conditions for all the components.

### **A. REGENERATIVELY COOLED CHAMBER AND BAFFLES**

The regeneratively cooled chamber and baffles are modeled using the SCALE computer code to predict their hydrogen pressure drop and bulk temperature rise characteristics. The parameters defined in Table A-I are held constant throughout the analysis. Table A-II defines the parameters and their values which are varied for each thrust level.

A preliminary power balance provided estimates of hydrogen inlet temperature and pressure for the regeneratively cooled chamber. The pressure drop through the regenerator is typically small; therefore, the H<sub>2</sub> pump discharge pressure is assumed to represent the H<sub>2</sub> inlet pressure to the baffle as well. The baffle analysis preceded the O<sub>2</sub>/H<sub>2</sub> heat exchanger and hydrogen regenerator work, but the operation of these components is interrelated. An estimate of the H<sub>2</sub> inlet temperature to the baffle has to be estimated initially. As a result, the initial thermal and hydraulic characterization of the baffle was evaluated as a function of H<sub>2</sub> inlet temperature. The trends are shown in Figure A-1 through A-6.

At each thrust level evaluated, an optimum channel geometry profile through the regeneratively cooled chamber is determined for the MR = 6 operating condition. This channel geometry profile is then held constant and the thermal and hydraulic characteristics of the chamber cooling channel design is determined at mixture ratios equal to 5 and 7. The thermal and hydraulic predictions of the chamber are shown in Figures A-7 and A-8.

The baffle channel configuration (channel and land widths, channel depth, gas-side wall thickness, channel back-side wall thickness) of the 7.5K lbf design (Ref. 1) is maintained for this study. The baffle cross-sectional area and number of channels is assumed to increase proportionally with thrust, however. The baffle characteristics are evaluated at the three mixture ratios and thrust levels. The predictions are shown in Figures A-9 and A-10.

# TABLE A-I

## OTV ANALYTICAL ASSUMPTIONS RELATED TO REGENERATIVELY COOLED CHAMBER AND BAFFLES

### I. Operating Conditions and Flow Splits: -----

Chamber Pressure (psia)	2000
Chamber / Baffle Flow Split	50/50
Mixture Ratio	5, 6, 7

### II. Regeneratively Cooled Chamber: -----

Actual Contraction Ratio	10
Geometric Contraction Ratio	15.3
Inlet Area Ratio	28
Gas-Side Wall and Land Material	Narloy Z
Close-Out Material	Ni-Co
Maximum Aspect Ratio	10
Radius of Curvature upstream of convergent section / throat radius	2.0
Radius of Curvature upstream of throat / throat radius	2.0
Radius of Curvature downstream of throat / throat radius	2.0
Convergence angle (degree)	40.0
H2 inlet pressure (psia)	5500
Maximum channel width in nozzle (in)	0.030
Channel width in throat (in)	0.011
Land width in throat (in)	0.010
Land width in Barrel (in)	0.025
Gas-Side Wall Thickness at Throat (in)	0.020
Gas-Side Wall Thickness in Nozzle (in)	0.060
Gas-Side Wall Thickness in Barrel (in)	0.060
Back-Side Wall Thickness (in)	0.020
Channel roughness (in)	60.E-06

### III. Regeneratively Cooled Baffles: -----

Gas-Side Wall and Land Material	Pt-ZGS
Close-Out Material	Pt-ZGS
Channel width (inch)	0.020
Channel land width (inch)	0.020
Channel wall thickness (inch)	0.025
Channel backside thickness (inch)	0.020
Channel depth (inch)	0.100
Channel roughness (in)	60.E-06

**TABLE A-II**

**REGENERATIVELY COOLED CHAMBER AND BAFFLE  
GEOMETRY AND PROPELLANT FLOW RATE  
ASSUMPTIONS VERSUS THRUST**

	THRUST (lbf)		
	20K	35K	50K
Throat area (in**2)	4.89	8.54	12.18
Barrel Diameter (in)	9.76	12.89	15.40
Barrel Length (inch)	6.31	7.49	7.01
L' (inch)	12	15	16
Baffle Length (inch)	4.88	6.45	7.01
Baffle Cross-Sectional Area (in**2)	26	45	64
Total Propellant Flow Rate (lb/s)	41.32	72.17	102.88

TABLE A-III

**REGENERATIVELY COOLED CHAMBER, BAFFLE, AND NOZZLE  
COOLANT INLET CONDITIONS**

THRUST (lbf)			
	20 K	35 K	50 K
<b>A. CHAMBER - coolant = H2</b>			
-----			
Inlet Pressure (psia)			
MR = 5,6,7	5500	5500	5500
Inlet Temperature (°R)			
MR = 5,6,7	90	90	90
Coolant Flow Rate (lb/s)			
MR = 5	3.44	6.01	8.57
MR = 6	2.95	5.16	7.35
MR = 7	2.58	4.51	6.43
<b>B. BAFFLE - coolant = H2</b>			
-----			
Inlet Pressure (psia)			
MR = 5,6,7	5500	5500	5500
Inlet Temperature (°R)			
MR = 5	503	459	430
MR = 6	499	459	430
MR = 7	497	459	430
Coolant Flow Rate (lb/s)			
MR = 5	3.44	6.01	8.57
MR = 6	2.95	5.16	7.35
MR = 7	2.58	4.51	6.43
<b>C. NOZZLE - coolant = O2</b>			
-----			
Inlet Pressure (psia)			
MR = 5	4862	4908	4906
MR = 6	4849	4897	4895
MR = 7	4844	4888	4887
Inlet Temperature (°R)			
MR = 5,6,7	610	610	610
Coolant Flow Rate (lb/s)			
MR = 5	34.43	60.14	85.73
MR = 6	35.42	61.86	88.18
MR = 7	36.16	63.15	90.02

**TABLE A-IV**

**HEX INLET CONDITIONS**

		THRUST		
		20K	35K	50K
<b>O2</b>	<b>INLET TEMPERATURE (°R)</b>			
	MR=5, 6, & 7	188.	188.	188.
<b>O2</b>	<b>INLET PRESSURE (PSIA)</b>			
	MR=5, 6, & 7	5168.	5168.	5168.
<b>H2 GAS INLET TEMPERATURE (°R)</b>				
	MR=5	805.	869.	868.
	MR=6	841.	905.	903.
	MR=7	874.	940.	940.
<b>H2 GAS INLET PRESSURE (PSIA)</b>				
	MR=5	3229.	2971.	2601.
	MR=6	3287.	3096.	2829.
	MR=7	3295.	3180.	2980.
<b>TOTAL FLOW RATE (LBS/SEC)</b>		41.32	72.17	102.9
<b>H2 FLOW RATE WITH 25% BYPASS (LBS/SEC)</b>				
	MR=5	5.17	9.02	12.86
	MR=6	4.43	7.73	11.02
	MR=7	3.87	6.77	9.65
<b>O2 FLOW RATE (LBS/SEC)</b> <b>(105% OF FLOW RATE)</b>				
	MR=5	36.15	63.15	90.02
	MR=6	37.19	64.95	92.59
	MR=7	37.96	66.31	94.52

TABLE A-V

## REGENERATOR INLET CONDITIONS

	THRUST		
	20K	35K	50K
=====			
H2 HOT INLET TEMPERATURE (°R)			
MR=5	579.	642.	641.
MR=6	572.	633.	631.
MR=7	564.	624.	624.
H2 HOT INLET PRESSURE (PSIA)			
MR=5	3096.	2838.	2448.
MR=6	3190.	3001.	2725.
MR=7	3221.	3109.	2904.
H2 COOL INLET TEMPERATURE (°R)			
MR=5,6,7	90.	90.	90.
H2 COOL INLET PRESSURE (PSIA)			
MR=5,6,7	5500.	5500.	5500.
H2 HOT FLOW RATE (LBS/SEC)			
MR=5	6.89	12.03	17.15
MR=6	5.90	10.31	14.70
MR=7	5.17	9.02	12.86
H2 COOL FLOW RATE (LBS/SEC) (50% OF FLOW RATE)			
MR=5	3.58	6.32	9.00
MR=6	3.10	5.41	7.72
MR=7	2.69	4.74	6.75
=====			

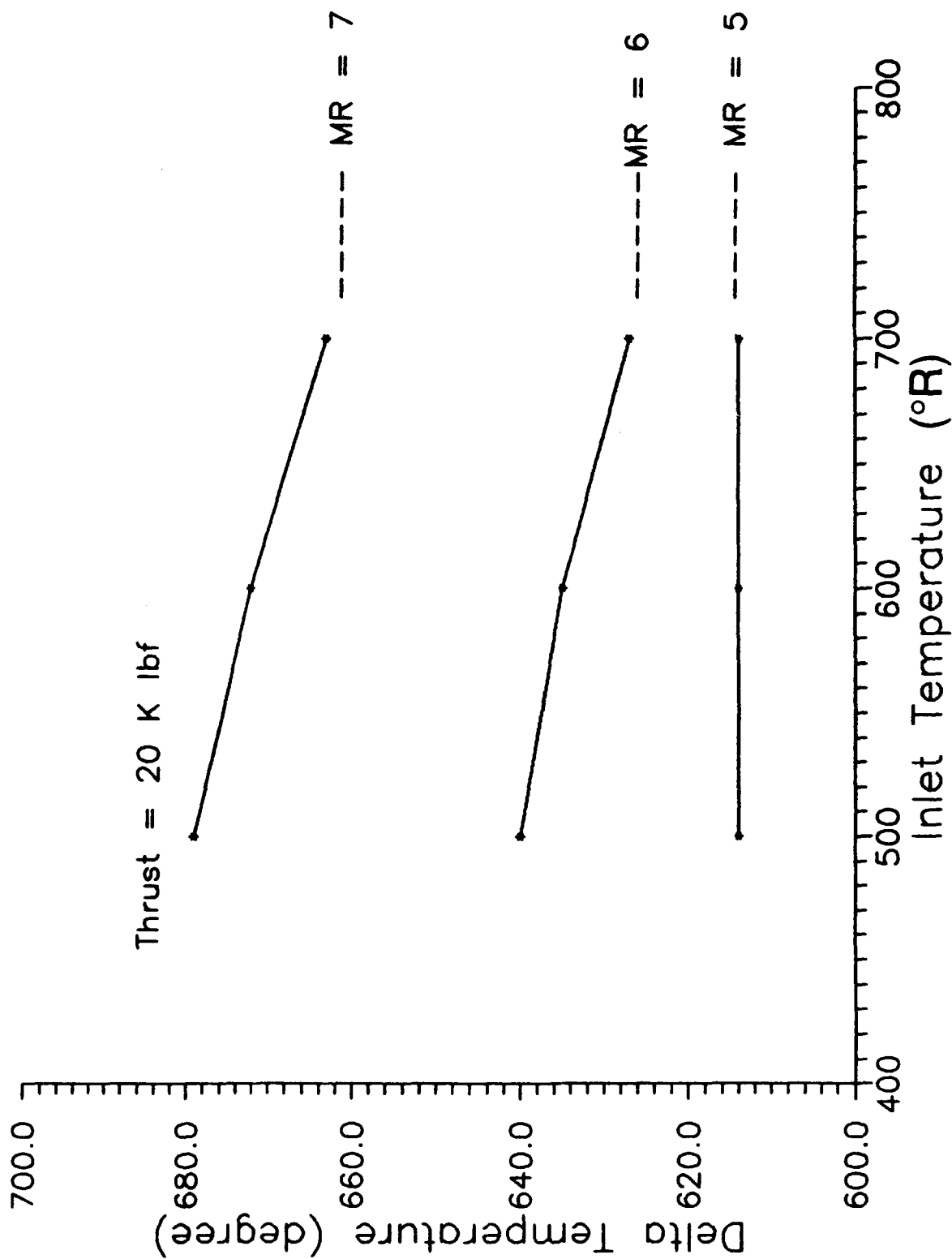


Figure A-1. Baffle H2 Delta Temperature vs H2 Inlet Temperature

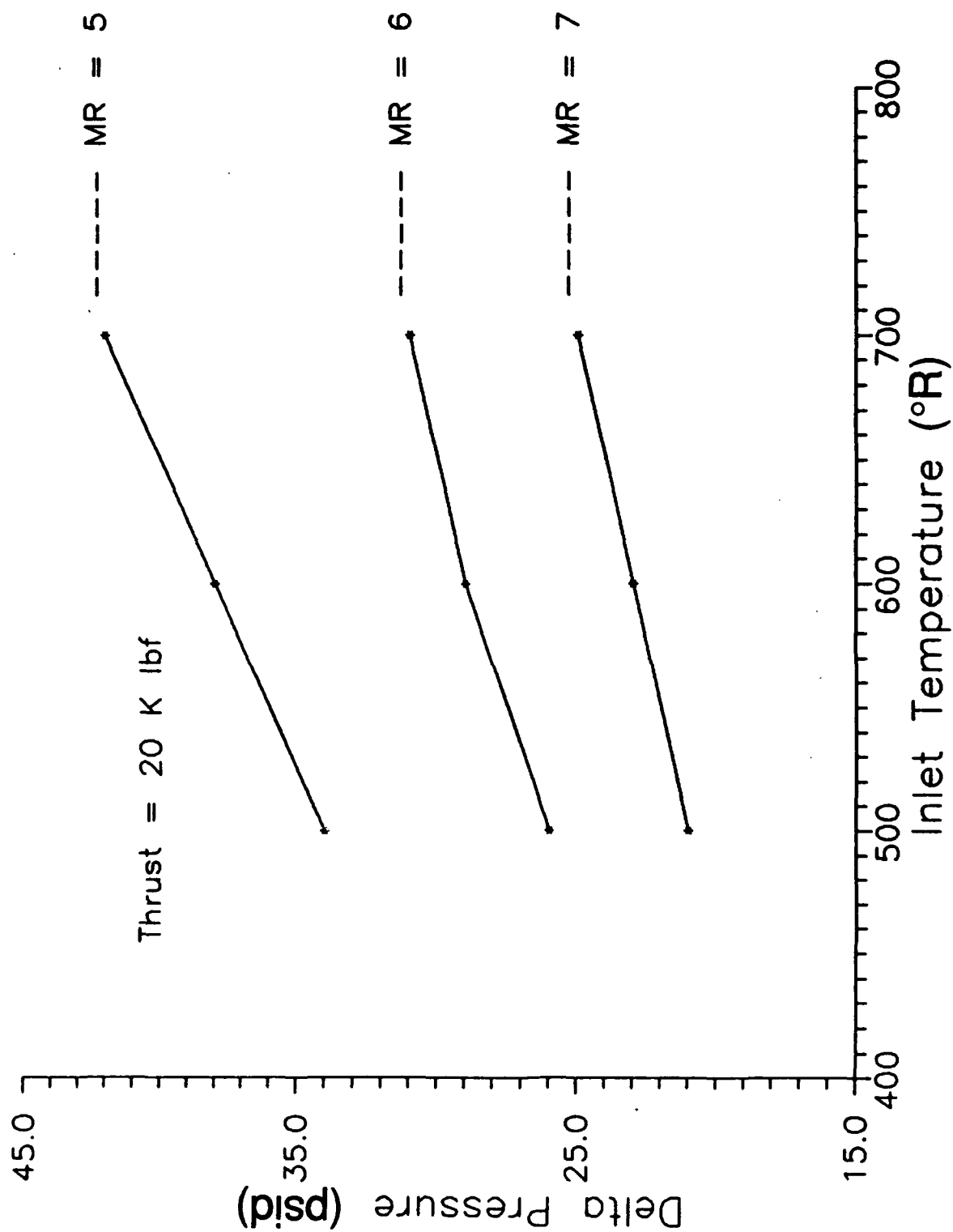


Figure A-2. Baffle H2 Pressure Loss vs H2 Inlet Temperature

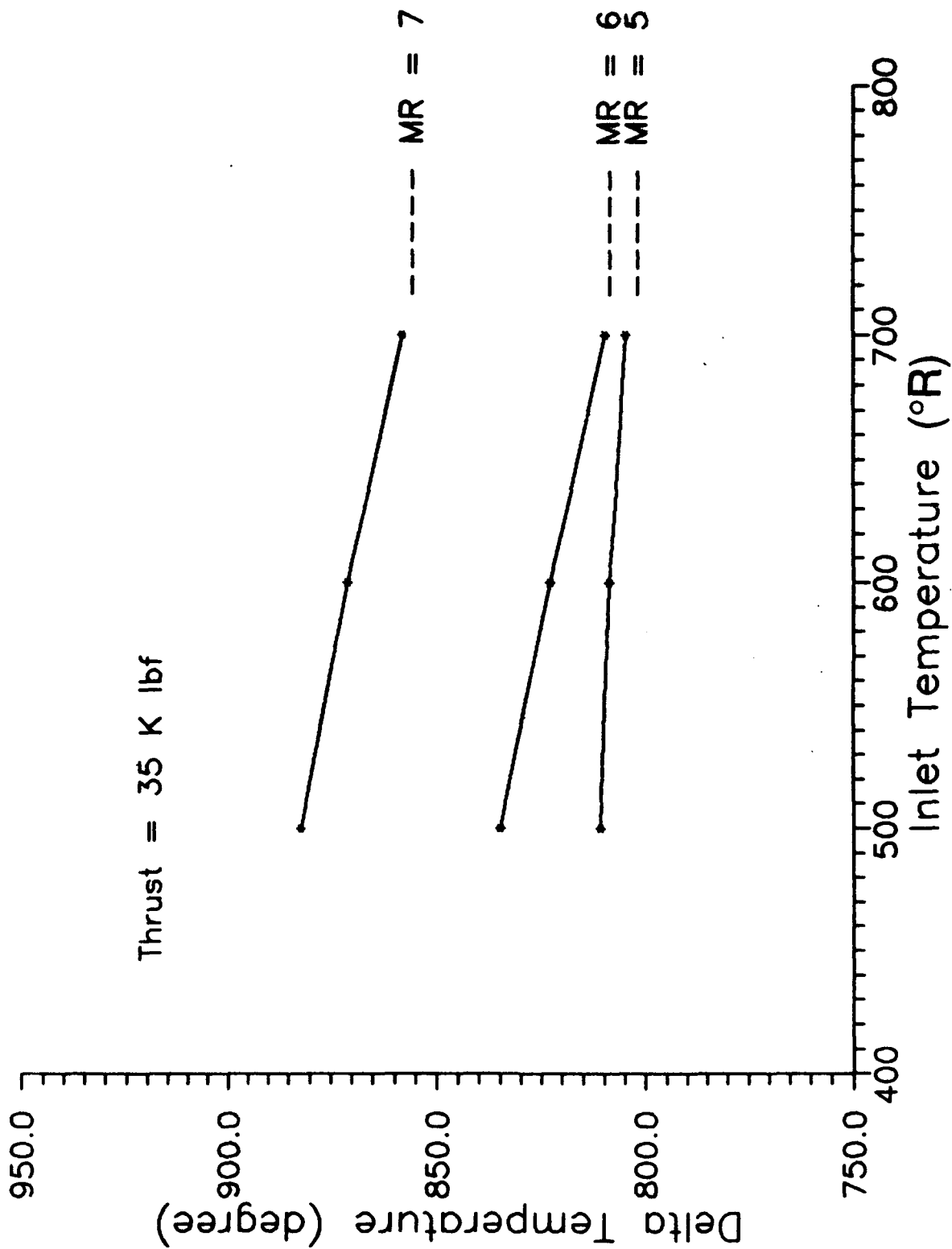


Figure A-3. Baffle H2 Delta Temperature vs H2 Inlet Temperature

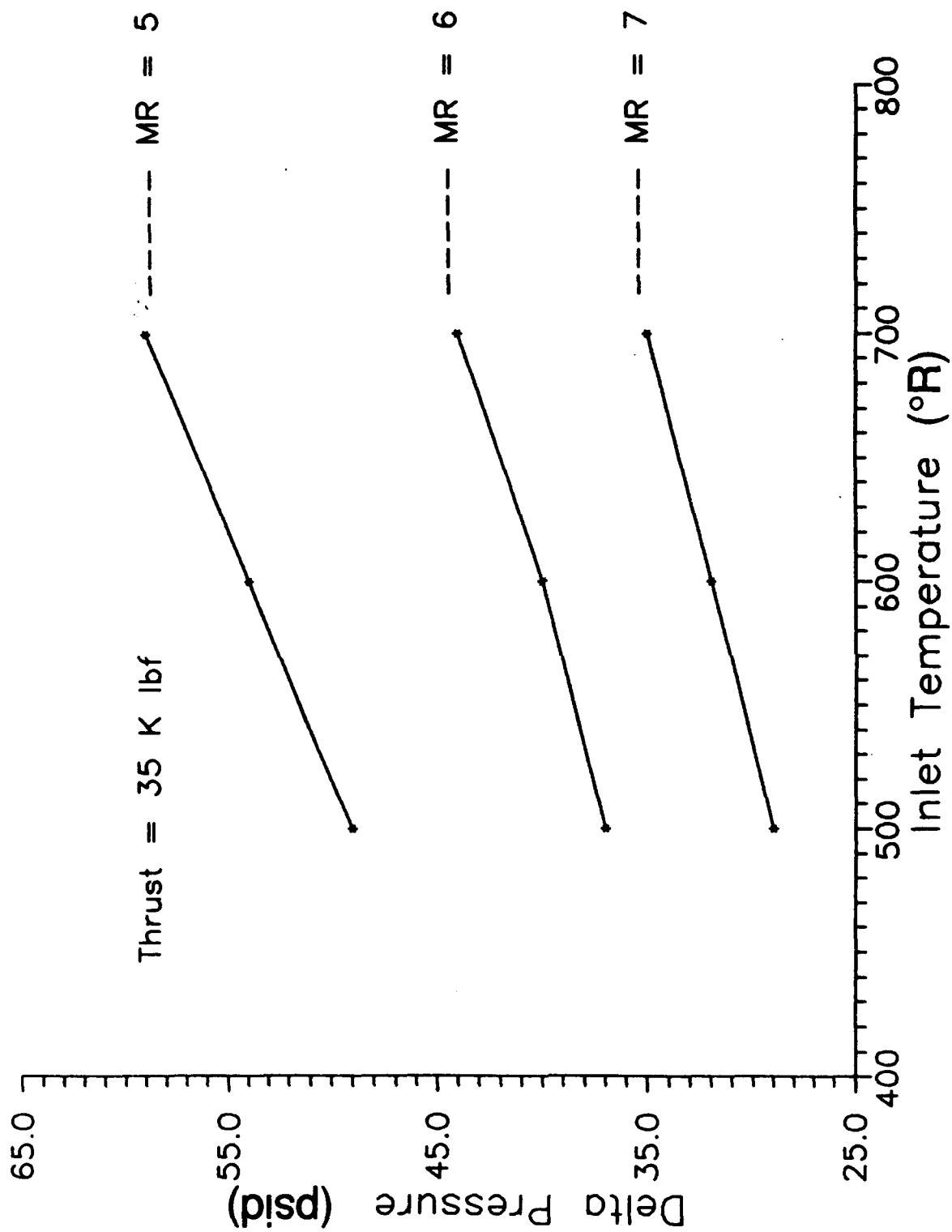


Figure A-4. Baffle H2 Pressure Loss vs H2 Inlet Temperature

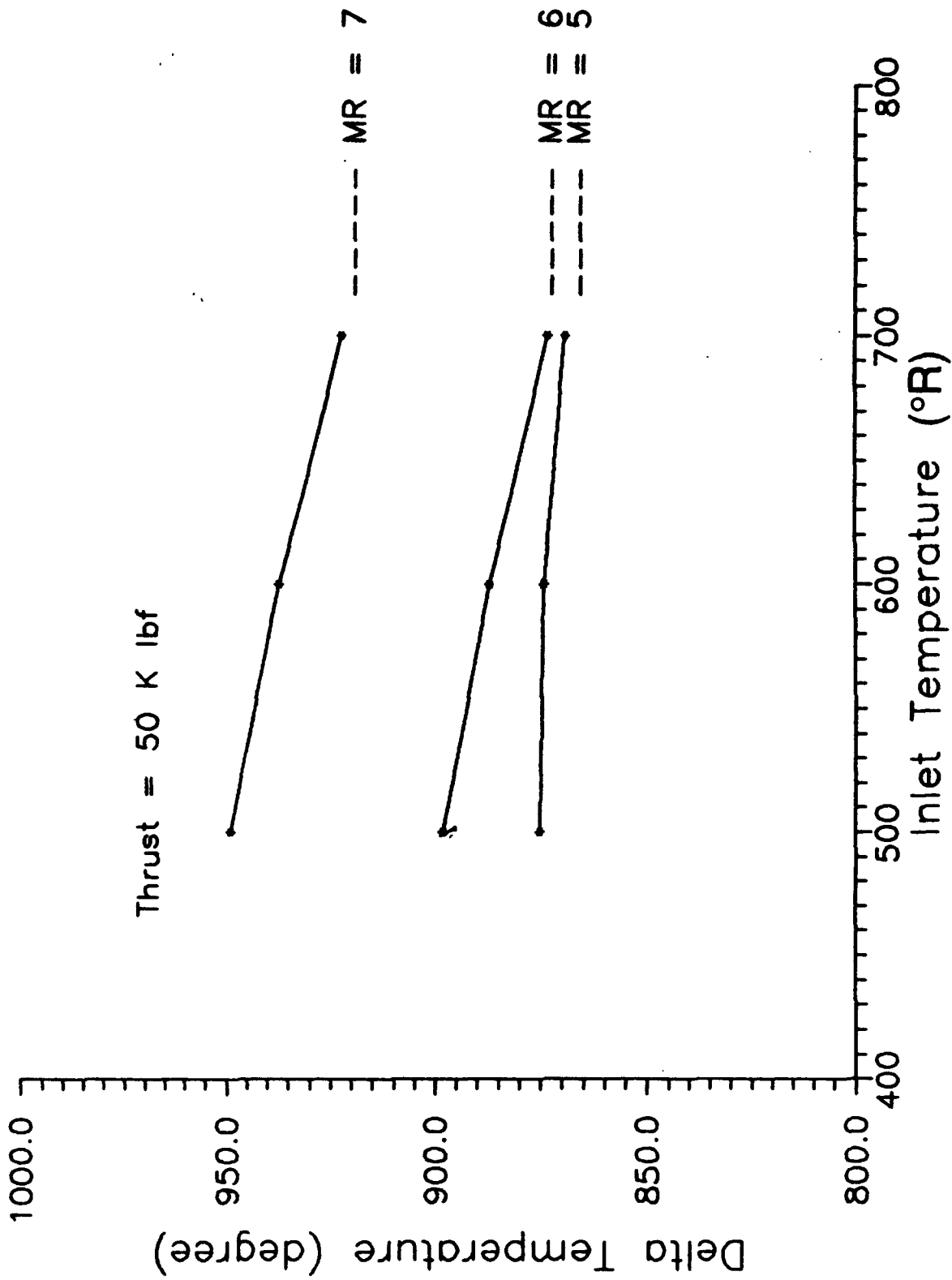


Figure A-5. Baffle H2 Delta Temperature vs H2 Inlet Temperature

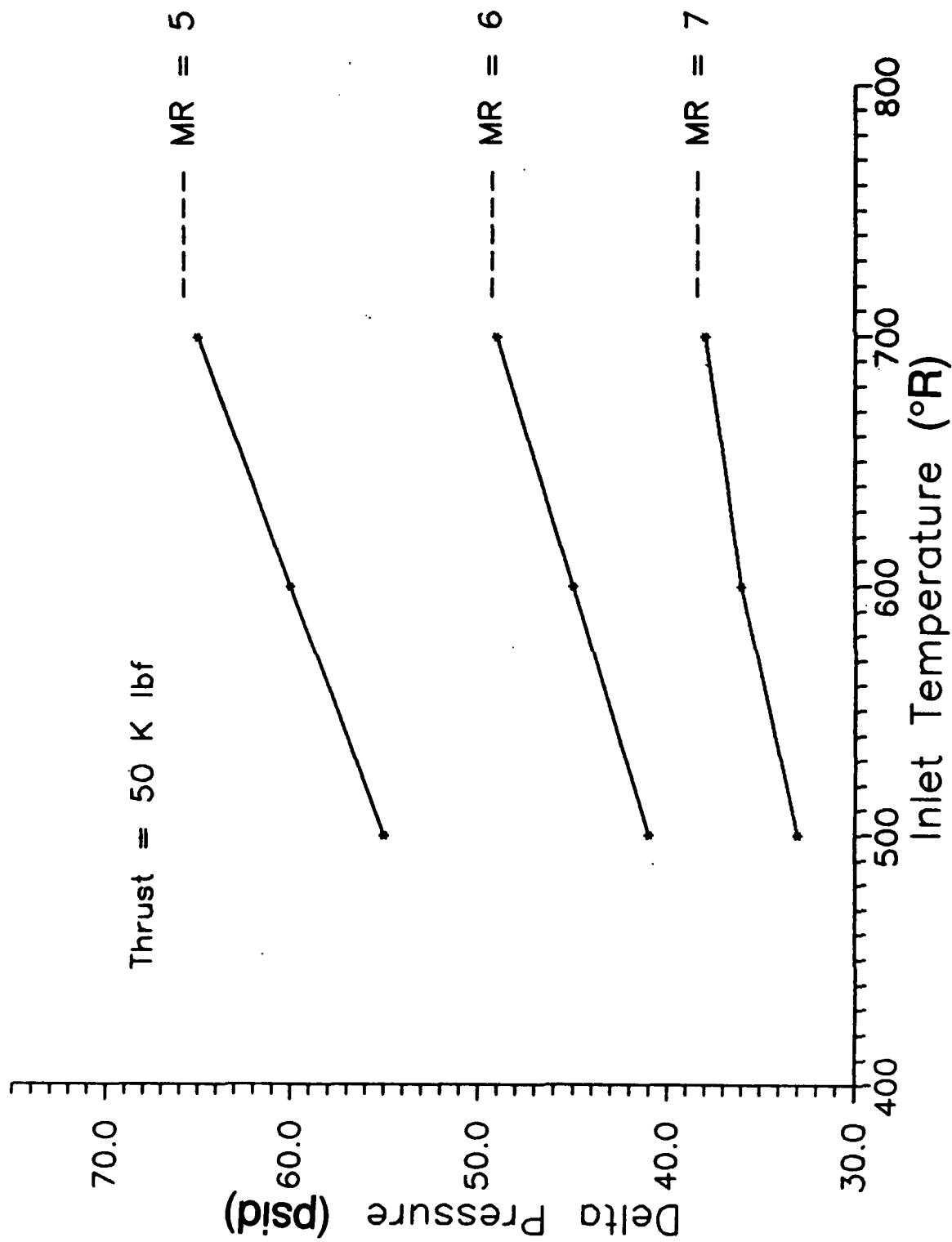


Figure A-6. Baffle H2 Pressure Loss vs H2 Inlet Temperature

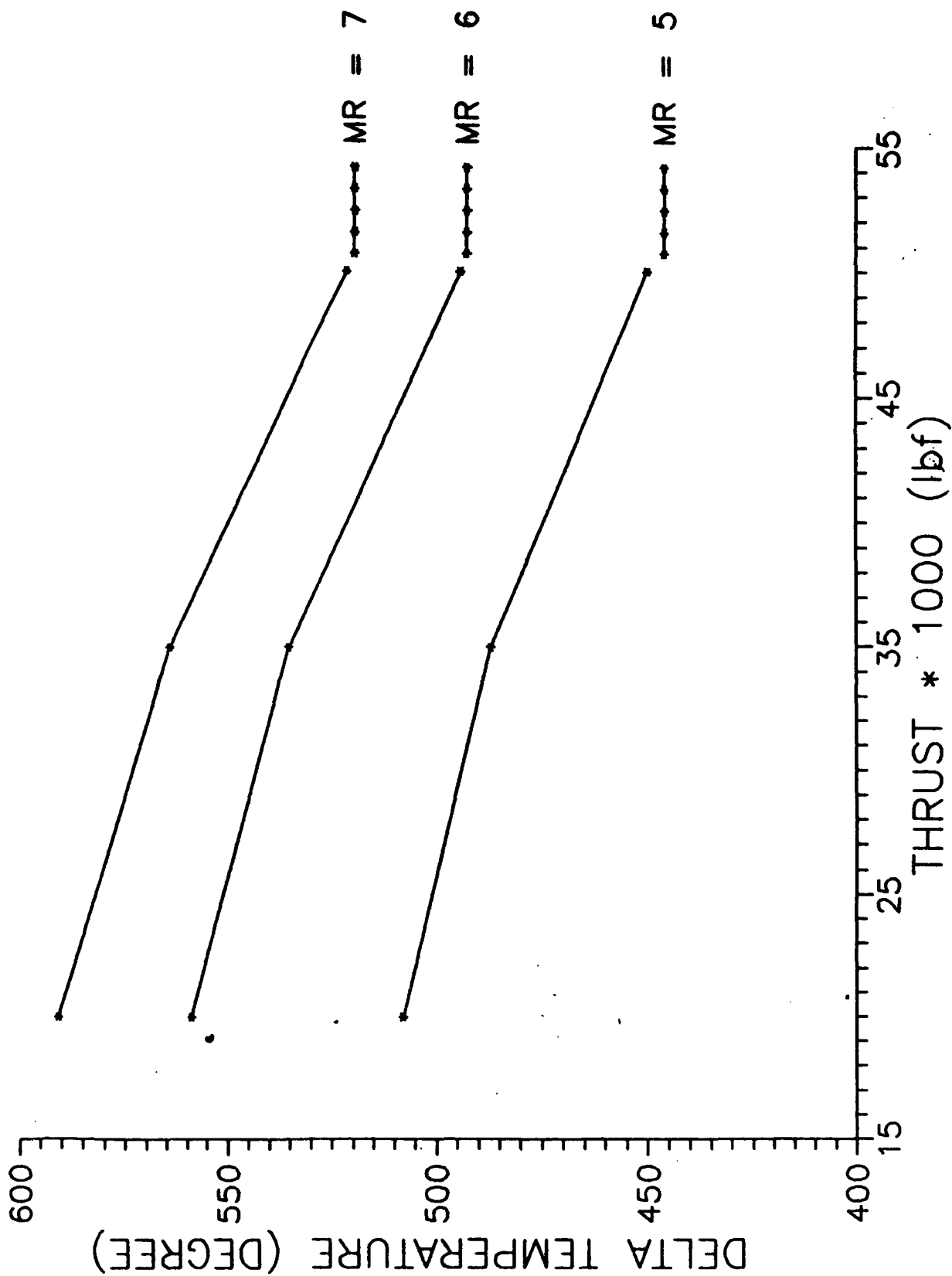


Figure A-7. OTV Regeneratively Cooled Jacket H2  
Temperature Rise vs Thrust

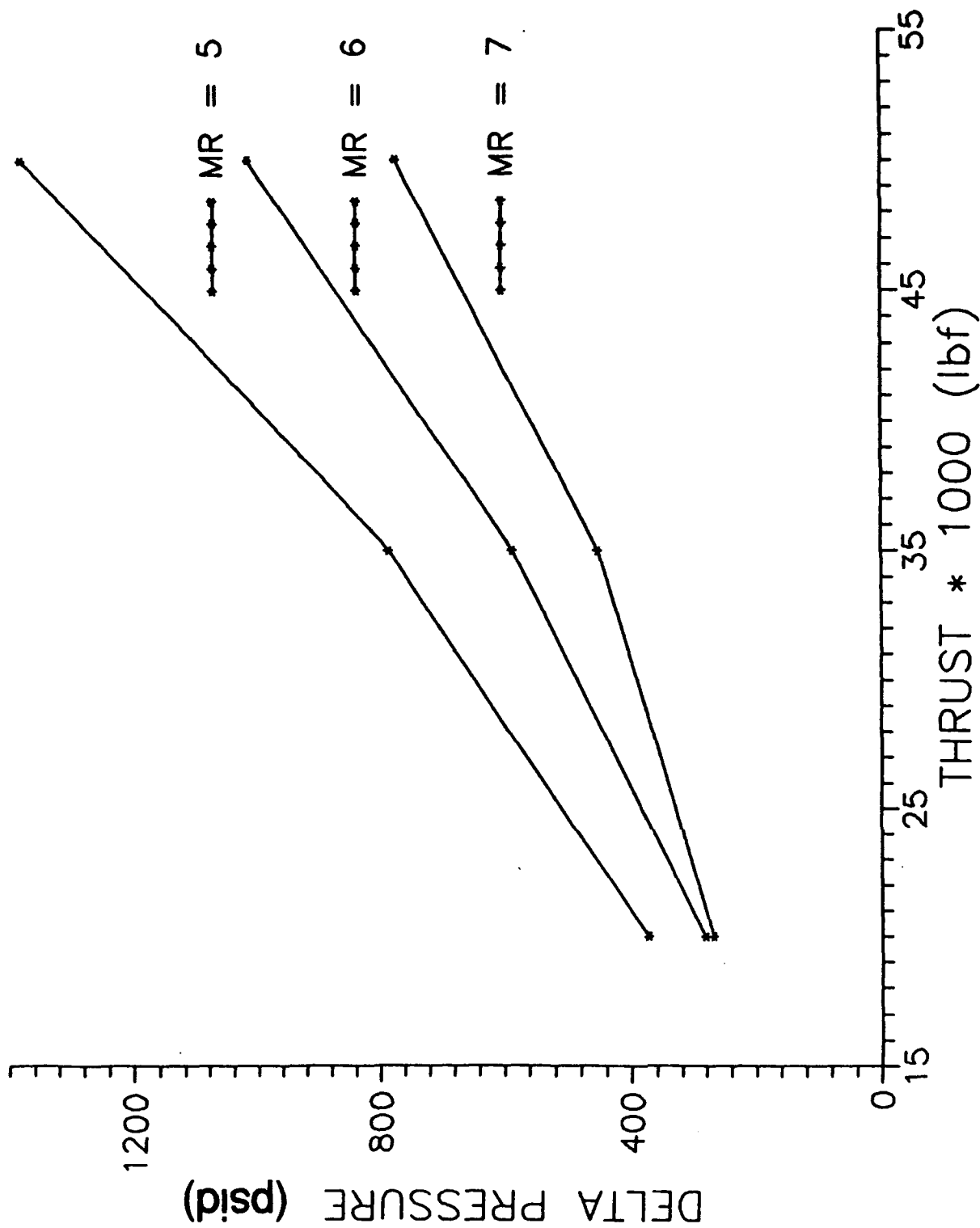


Figure A-8. OTV Regeneratively Cooled Jacket H2  
Pressure Drop vs Thrust

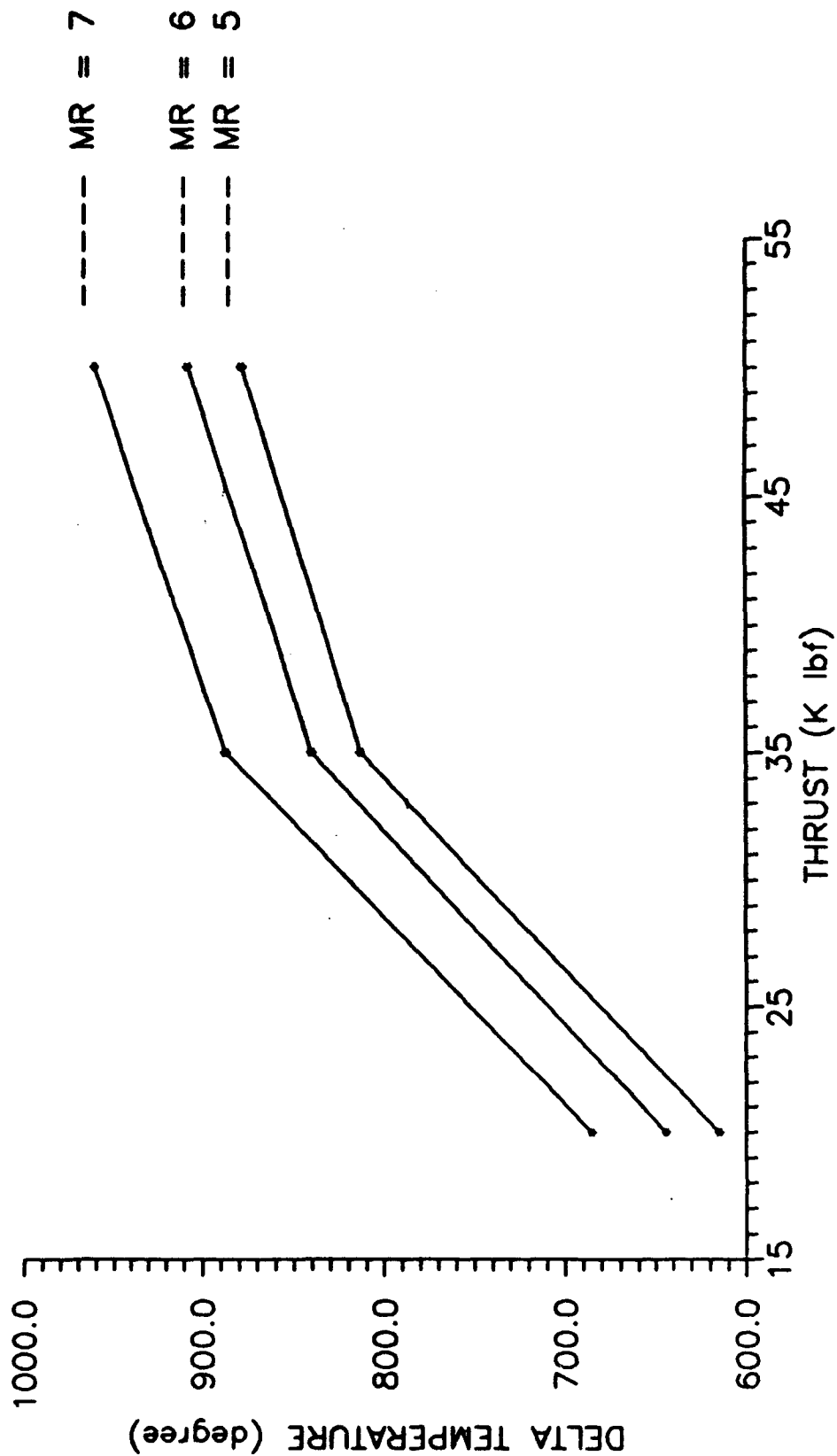


Figure A-9. OTV Regeneratively Cooled Baffle H2  
Delta Temperature vs Thrust

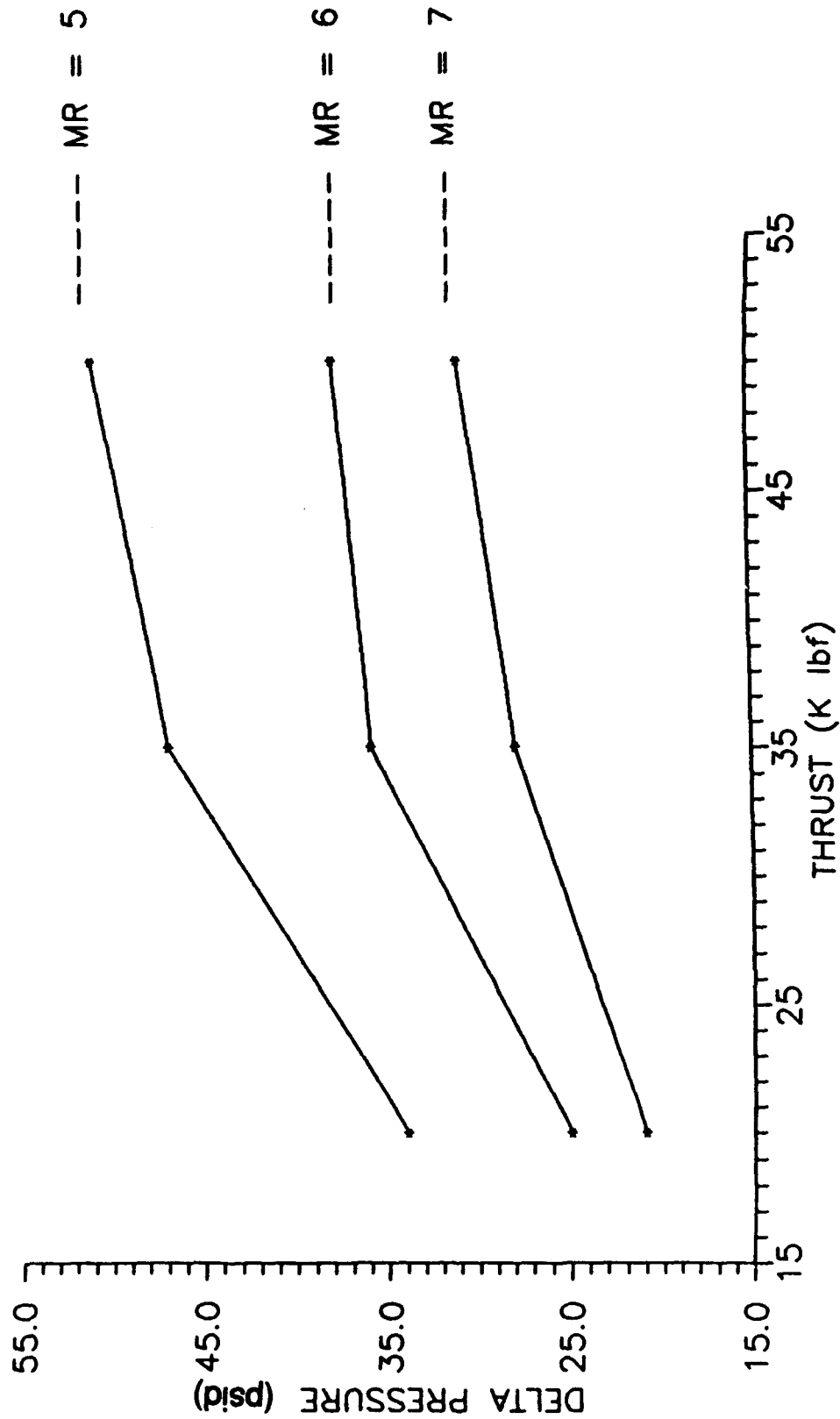


Figure A-10. OTV Regeneratively Cooled Baffle H2  
Pressure Drop vs Thrust

## A.2, Design Methodology, (cont)

### B. OXYGEN/HYDROGEN HEAT EXCHANGER AND HYDROGEN/HYDROGEN REGENERATOR

The steady state counterflow heat exchanger model, HEXSS, is used to determine the pressure drops and the energy exchange between the working fluids in the  $H_2/O_2$  heat exchanger (HEX) and the  $H_2/H_2$  hydrogen regenerator. The HEXSS code uses an iterative technique to solve the steady state energy and momentum equations for the cooled and heated fluid streams. The channel geometry, the core length, and fluid inlet conditions and the desired fluid outlet conditions are provided to run the program. Design parameters for the HEX and hydrogen regenerator are given in Table A-VI.

The heat exchanger and the regenerator channel geometry are assumed to be the same as those of the 7.5K lbf/thrust engine design (Ref. 2). The cross-sectional area of the two components are assumed to increase with thrust, however, to maintain a similar mass flux per channel as that of their corresponding 7.5K lbf engine component. The total number of channels and the core length needed to obtain the required fluid outlet temperature are determined at the MR = 6 operating condition for each thrust level. The thermal and hydraulic characteristics for the complete MR range at each thrust level are then determined using that baseline geometry. The predictions for the HEX are shown in Figures A-11 through A-14. The regenerator predictions are shown in Figures A-15 through A-18.

The  $O_2$  liquid inlet temperature and pressure to the HEX were determined in a preliminary power balance. The  $O_2$  outlet temperature from the HEX is based on an estimate of the total energy required to run the oxygen turbine and the energy available in the oxygen cooled nozzle. The  $H_2$  inlet pressure to the HEX is based on the pressure drop through the regeneratively cooled chamber and a 37% loss across the turbine. This pressure loss percentage is based on the turbine loss used in the preliminary power balance using turbopump design points provided by the turbomachinery group.

Because the initial value of the baffle inlet temperature is unknown and effects the performance of the downstream components, the baffle inlet temperature is iterated until the corresponding inlet temperature to the hot side of the hydrogen regenerator is greater than the assumed baffle inlet temperature. This assures that there is

**TABLE A-VI**

**DESIGN PARAMETERS AND ASSUMPTIONS  
FOR THE H<sub>2</sub>/O<sub>2</sub> HEX AND H<sub>2</sub>/H<sub>2</sub> REGENERATOR**

<b>HEX WALL MATERIAL</b>	<b>ZrCu</b>
<b>CHANNEL DEPTH O<sub>2</sub></b>	<b>.03 IN.</b>
<b>CHANNEL DEPTH H<sub>2</sub></b>	<b>.04 IN.</b>
<b>CHANNEL WIDTH</b>	<b>.06 IN.</b>
<b>WALL THICKNESS BETWEEN LIKE CHANNELS</b>	<b>.043 IN.</b>
<b>WALL THICKNESS BETWEEN HOT AND COLD CHANNELS</b>	<b>.036 IN.</b>
<b>OXYGEN CRITICAL PRESSURE</b>	<b>730. PSIA</b>
<b>REGENERATOR WALL MATERIAL</b>	<b>ZrCu</b>
<b>CHANNEL DEPTH H<sub>2</sub> COOL</b>	<b>.02 IN.</b>
<b>CHANNEL DEPTH H<sub>2</sub> HOT</b>	<b>.04 IN.</b>
<b>CHANNEL WIDTH</b>	<b>.056 IN.</b>
<b>WALL THICKNESS BETWEEN LIKE CHANNELS</b>	<b>.043 IN.</b>
<b>WALL THICKNESS BETWEEN HOT AND COLD CHANNELS</b>	<b>.034 IN.</b>
<b>HYDOGEN CRITICAL PRESSURE</b>	<b>188. PSIA</b>
<b>ASSUME INCOMPRESSIBLE FLOW</b>	

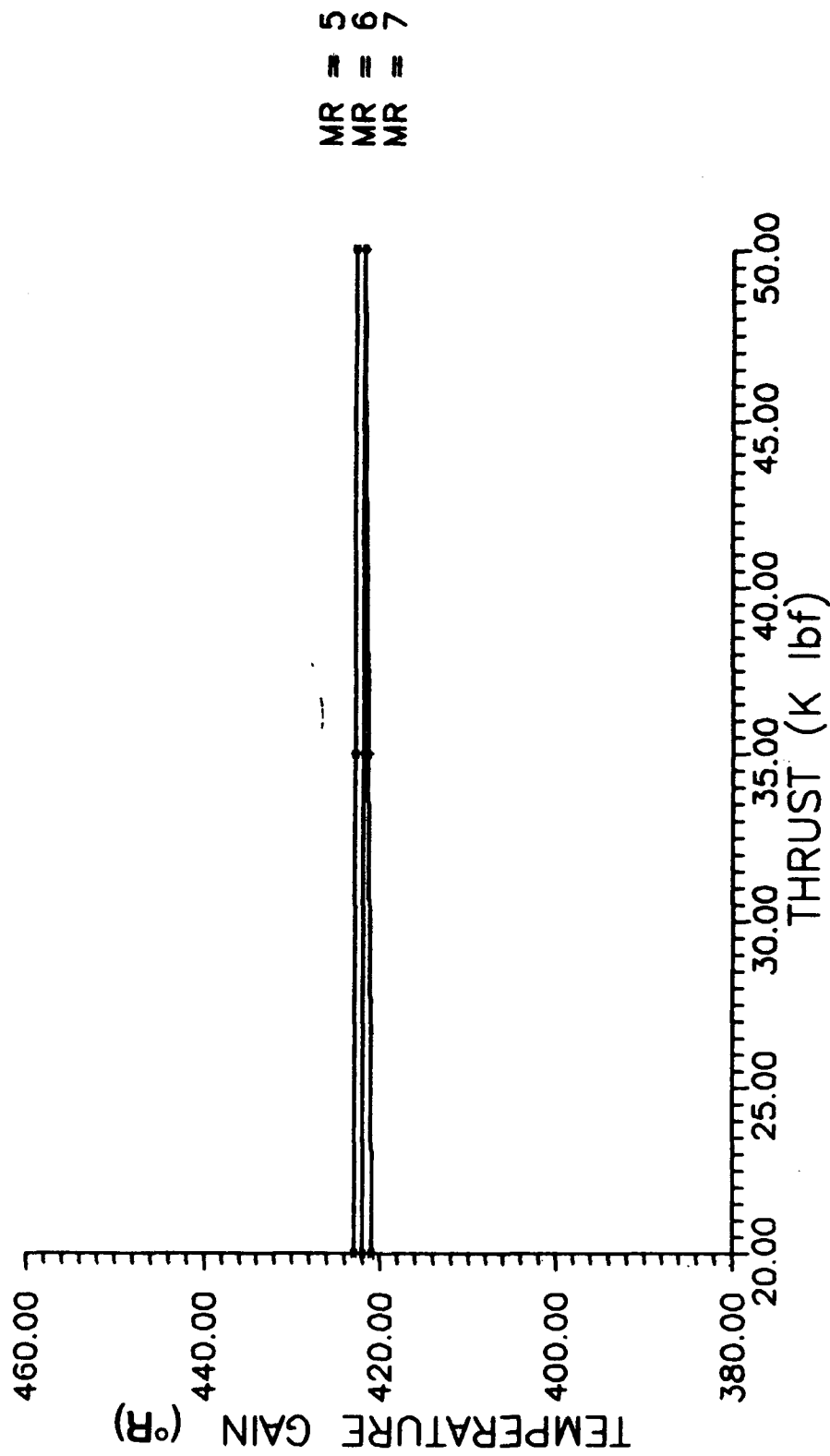


Figure A-11. Temperature Gain 02 Hex vs Thrust

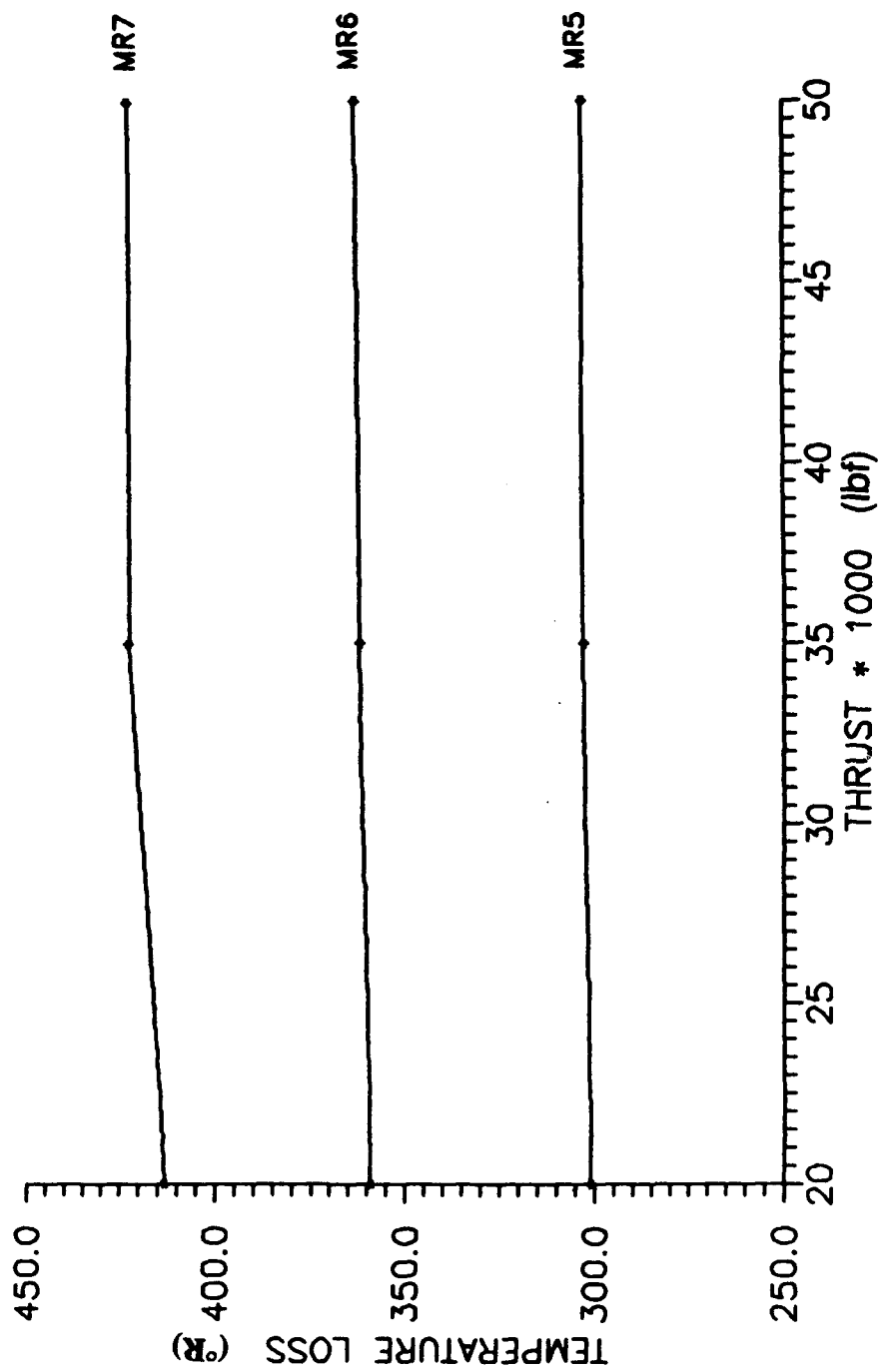


Figure A-12. Temperature Loss H2 Side Hex vs Thrust

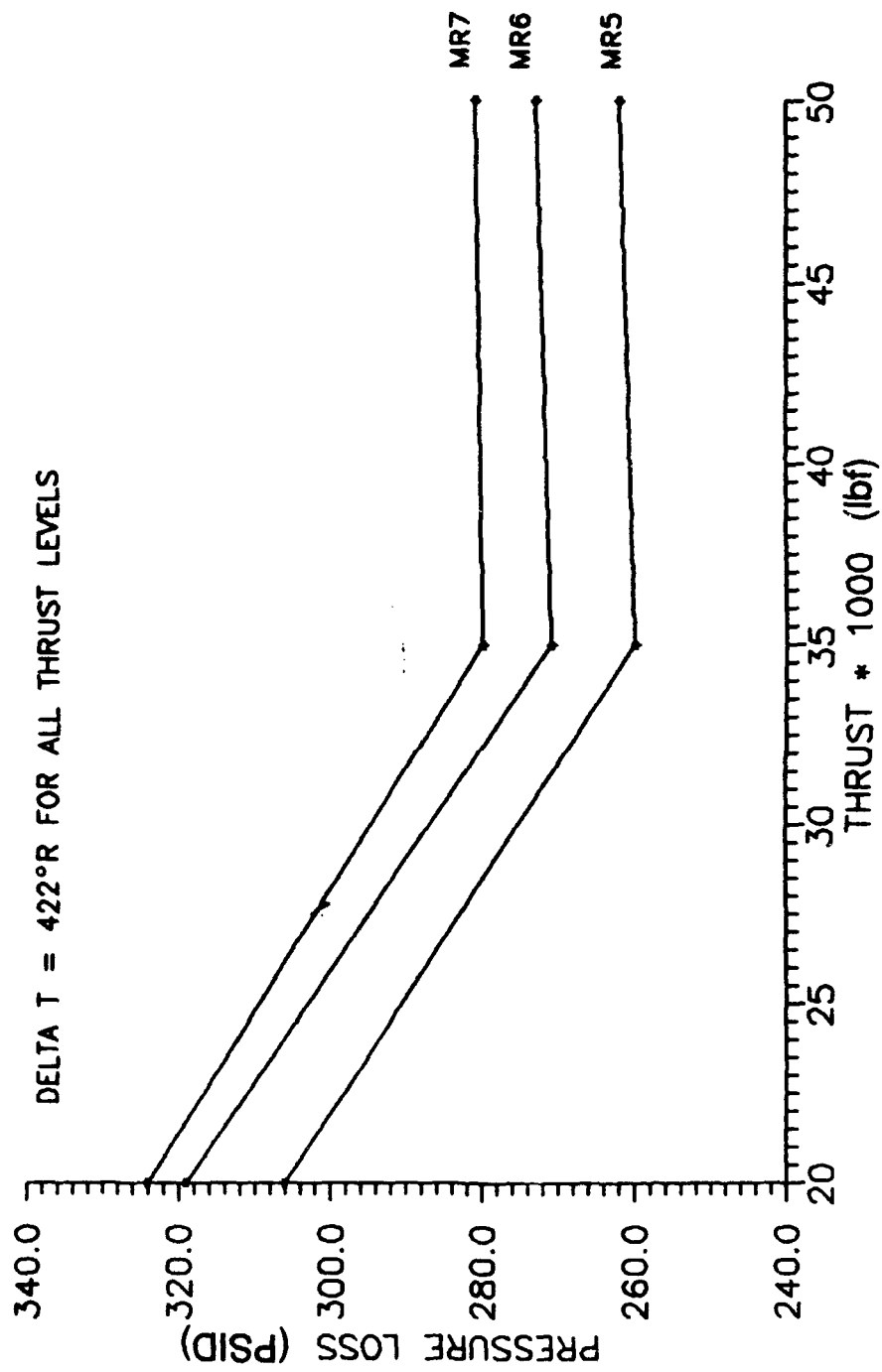


Figure A-13. Pressure Loss 02 Side Hex vs Thrust

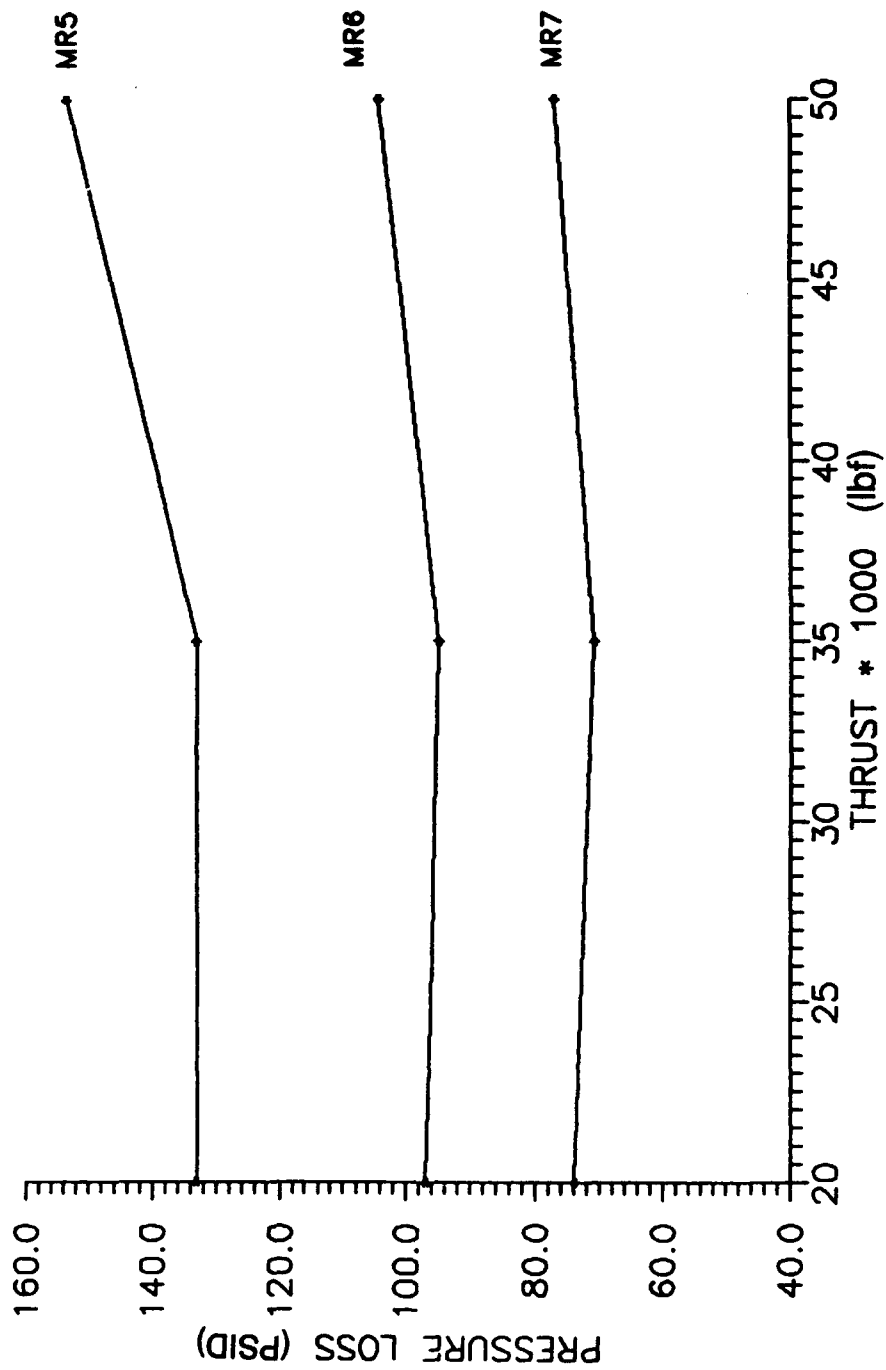


Figure A-14. Pressure Loss H2 Side Hex vs Thrust

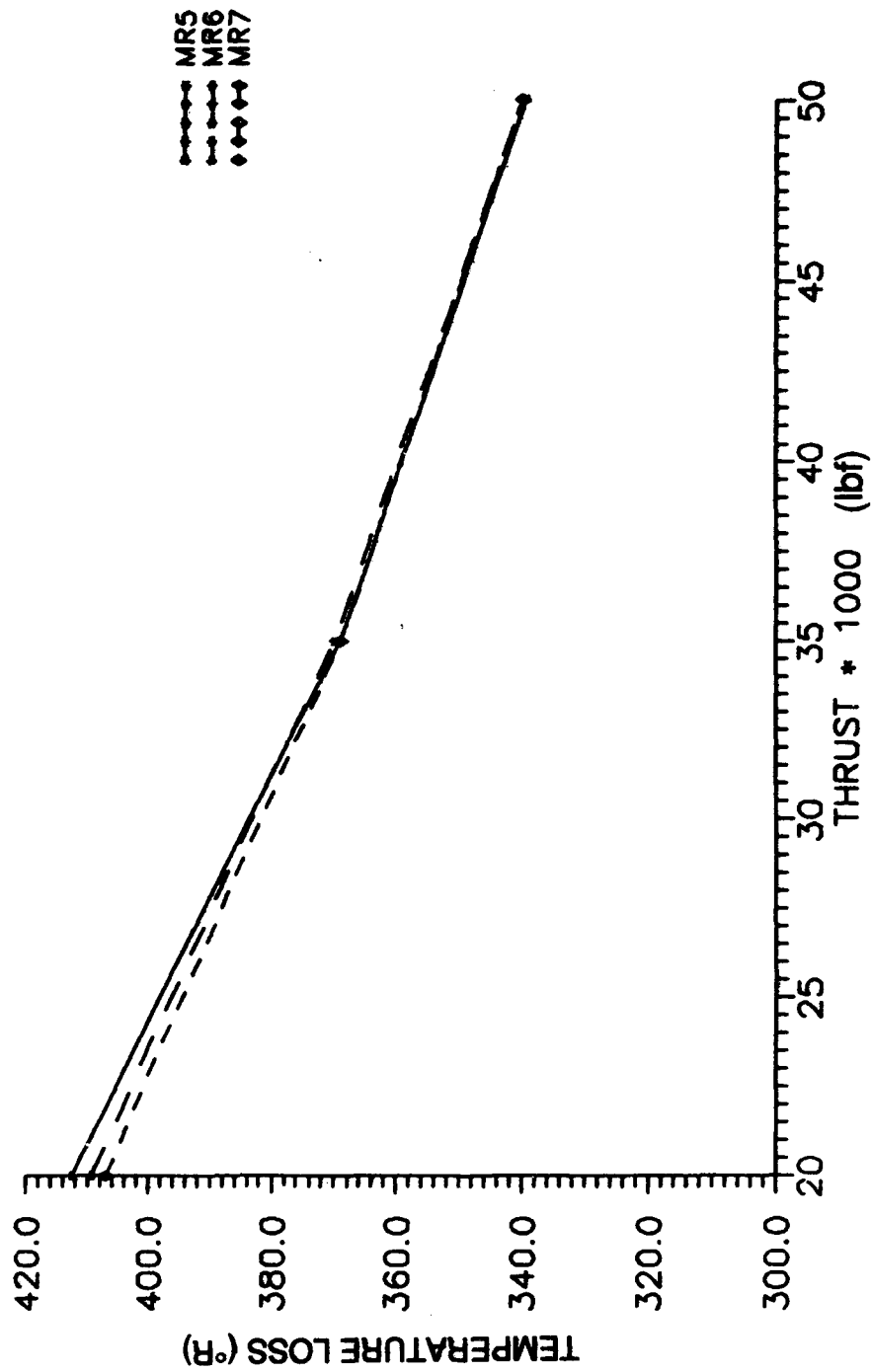


Figure A-15. Temperature Loss Hot Side Regenerator vs Thrust

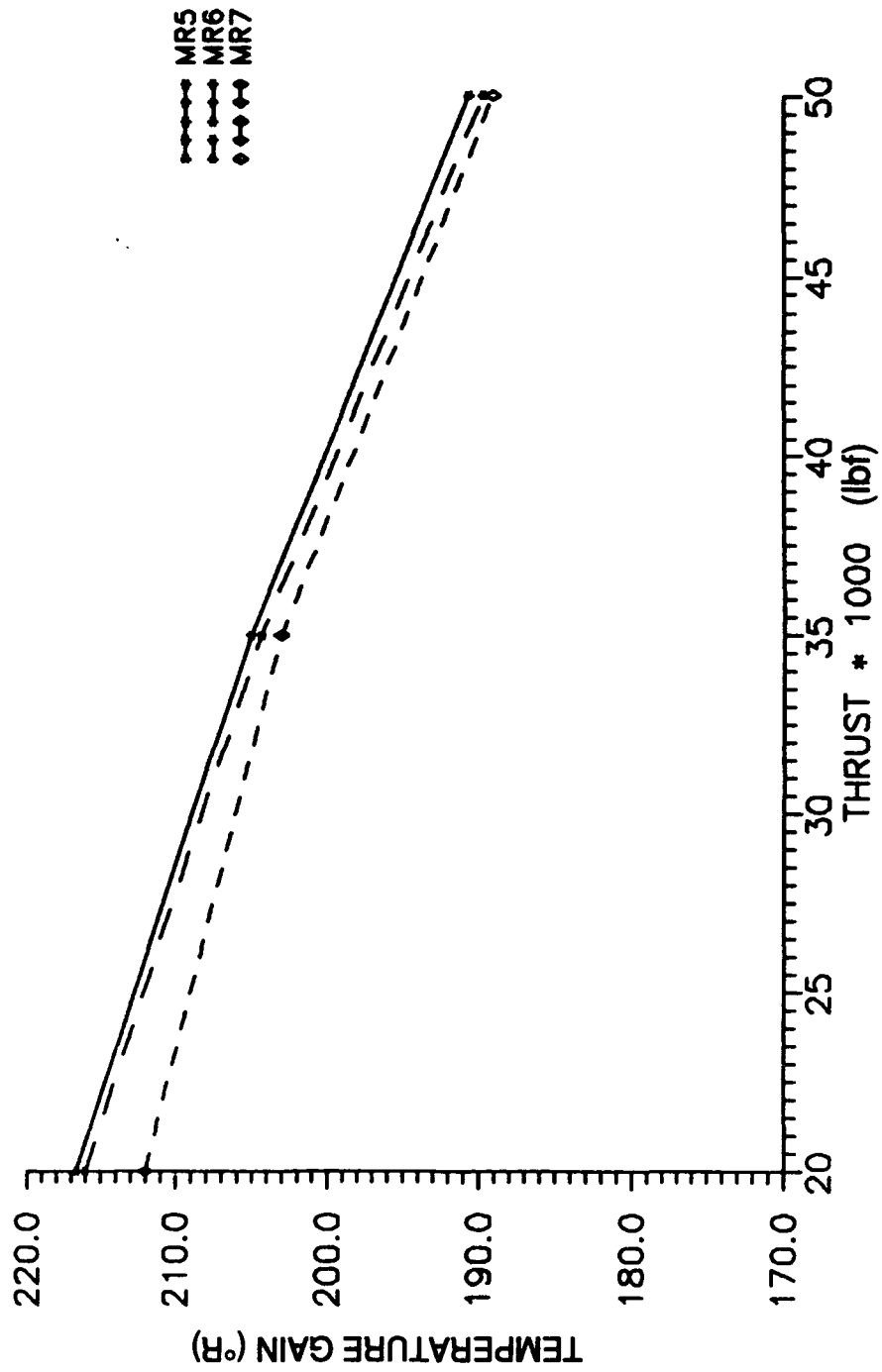


Figure A-16. Temperature Gain Cool Side Regenerator vs Thrust

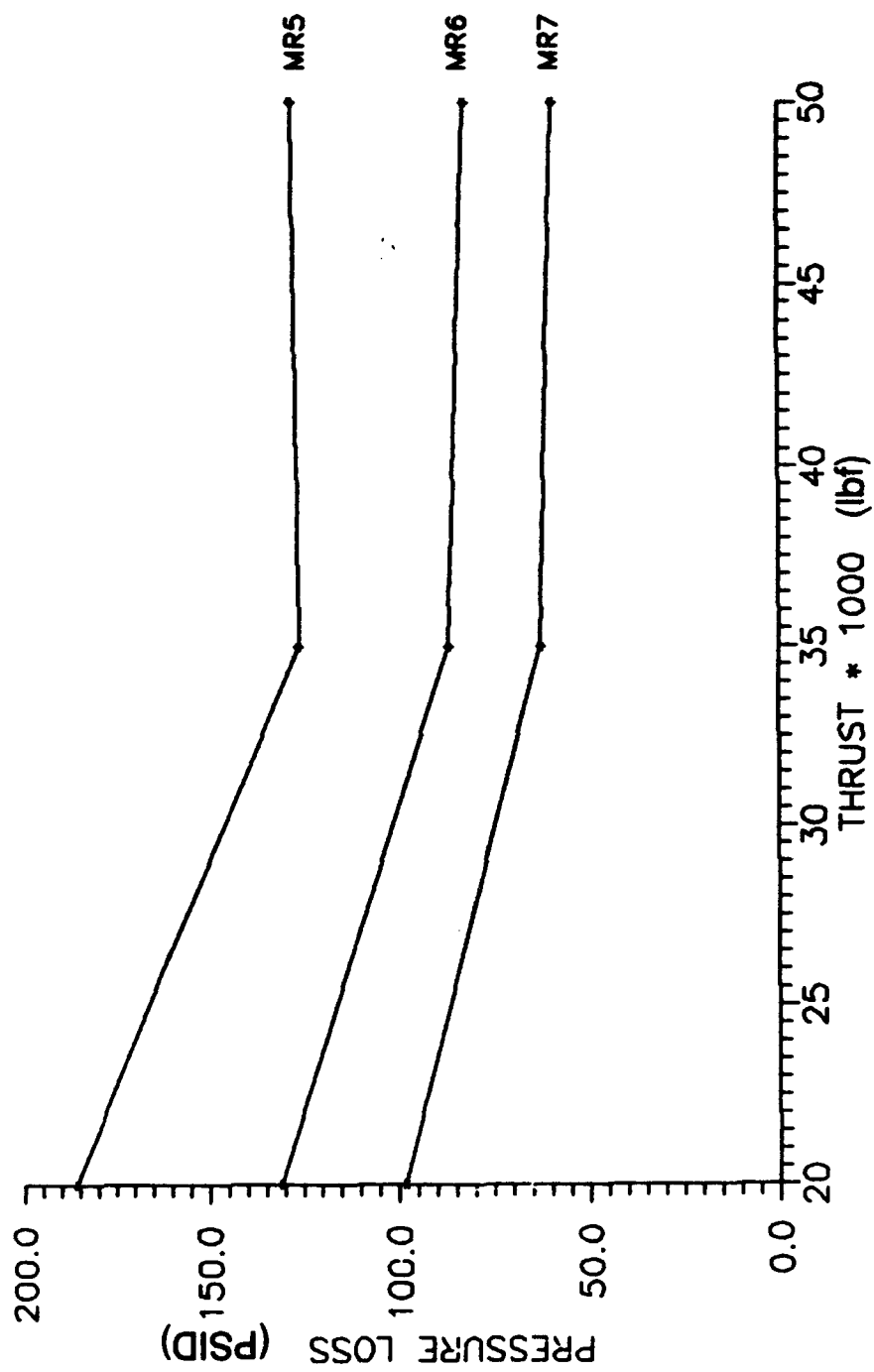


Figure A-17. Pressure Loss Hot Side Regenerator vs Thrust

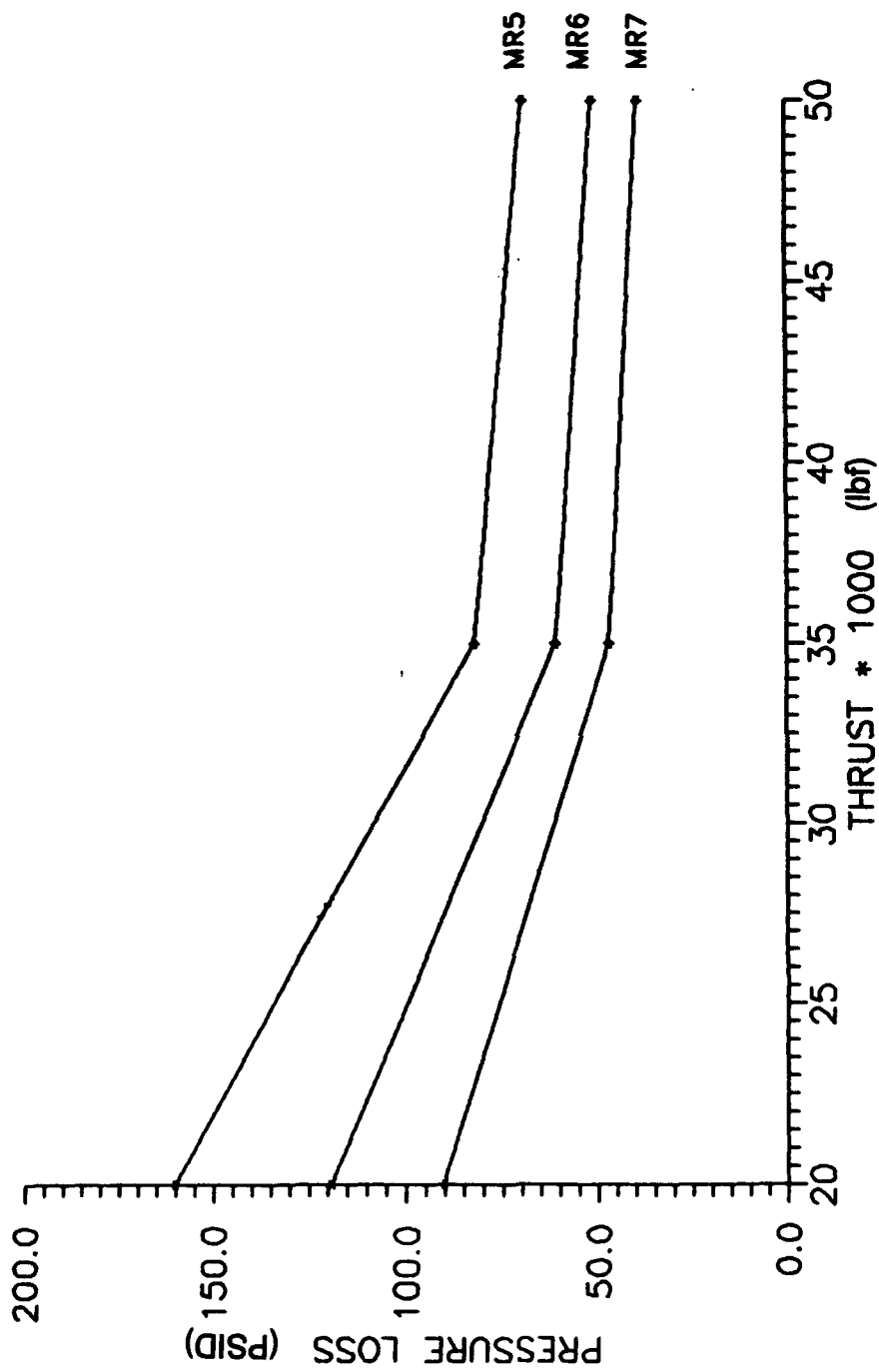


Figure A-18. Pressure Loss Cool Side Regenerator vs Thrust

## A.2, Design Methodology, (cont)

sufficient energy available in the hot  $H_2$  from the HEX to transfer to the cold  $H_2$  from the pump to result in the assumed baffle inlet temperature. The regenerator is then evaluated and sized to achieve the assumed baffle inlet temperature. The  $H_2$  pump discharge conditions are assumed to be the inlet conditions to the cold side of the regenerator.

The HEX and hydrogen regenerator geometries as determined in the analysis are given in Table A-VII.

### C. OXYGEN COOLED NOZZLE

The region of the nozzle that is regeneratively cooled with oxygen (area ratio of 28 to 635) is modeled using the SCALE computer code to predict the coolant pressure drop and the bulk temperature rise characteristics. The parameters defined in Table A-VIII are held constant throughout the analysis.

A preliminary power balance provided estimates of the required oxygen turbine inlet temperature and pressure. Coupling the temperature requirement with an estimate of the total energy available in the oxygen cooled portion of the nozzle results in an assumed oxygen inlet temperature to the nozzle of 610 R for all thrust levels. Since the pressure drop through the nozzle is typically low and the oxygen enthalpies are fairly insensitive to pressures in the range of this study, pressure effects are neglected in the estimate. The oxygen inlet pressure to the nozzle is assumed to be equal to the HEX O2 outlet condition. Figure A-19 summarizes the pressure drop variation with thrust for all components.

A channel geometry profile through the regeneratively cooled nozzle is determined assuming an  $MR = 6$  for each thrust level. The maximum channel depth profile (assuming a maximum allowable aspect ratio of 10) is determined using the design option of the SCALE program. The profile is then modified to reflect a maximum channel depth of 0.500 inches throughout the nozzle. Holding this cooling channel geometry profile constant at a given thrust level, the thermal and hydraulic characteristics at mixture ratios equal to 5 and 7 are then determined. The predictions are shown in Figures A-20 and A-21.

**Table A-VII**  
**H<sub>2</sub>/O<sub>2</sub> Hex Geometry**

	Thrust		
	20K lbf	35K lbf	50K lbf
Core Length (in.)	17.6	15.0	15.1
Core Weight (lbm)	58.8	87.1	125.
Total No. of Channels O <sub>2</sub>	966	1679	2392
Total No. of Channels H <sub>2</sub>	966	1679	2392

**H<sub>2</sub>/H<sub>2</sub> Regenerator Geometry**

	Thrust		
	20K lbf	35K lbf	50K lbf
Core Length (in.)	15.4	8.6	7.4
Core Weight (lbm)	41.08	39.73	48.2
Total No. of Channels H <sub>2</sub> – Hot	861	1491	2100
Total No. of Channels H <sub>2</sub> – Cold	861	1491	2100

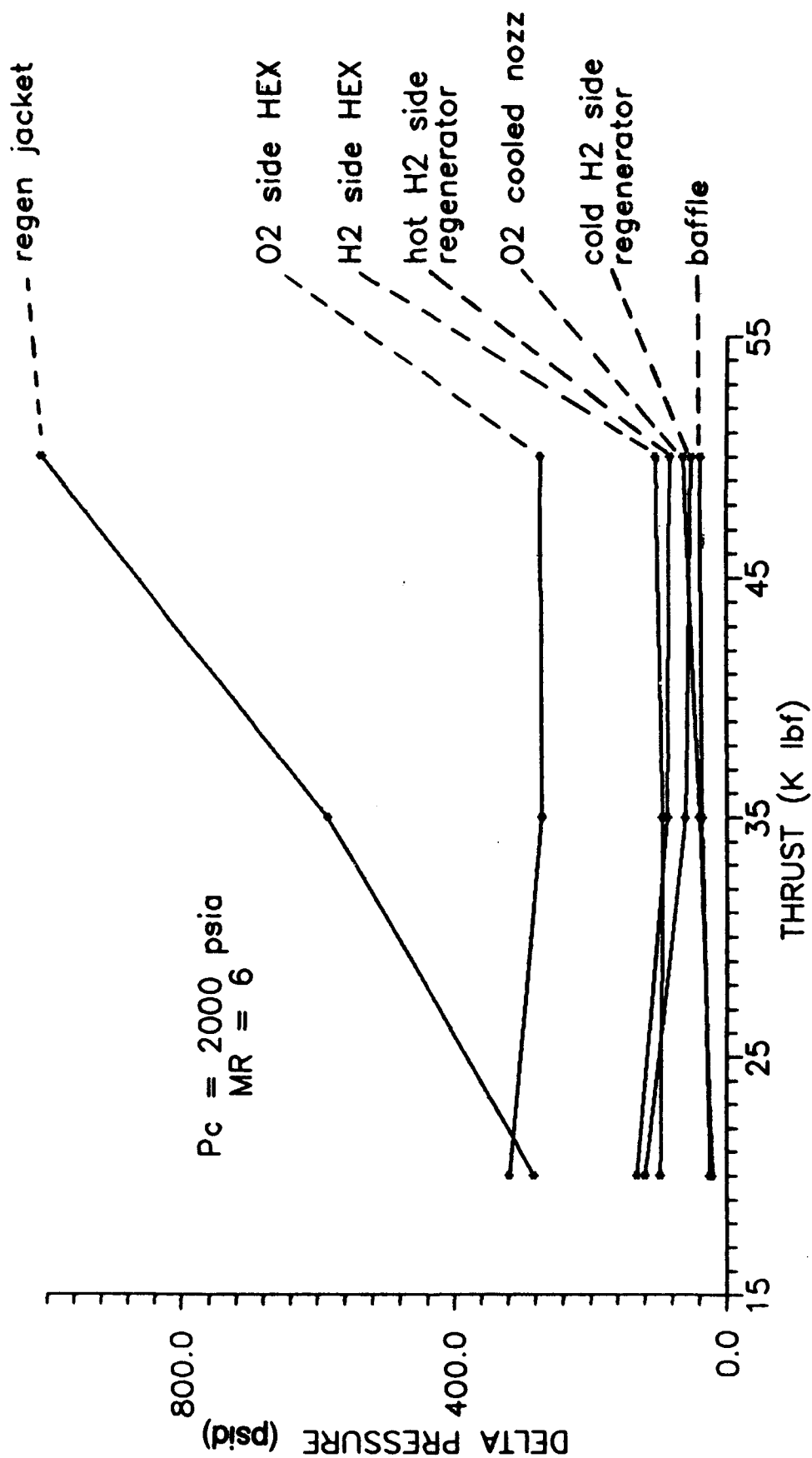


Figure A-19. Fluid Pressure Drop vs Thrust

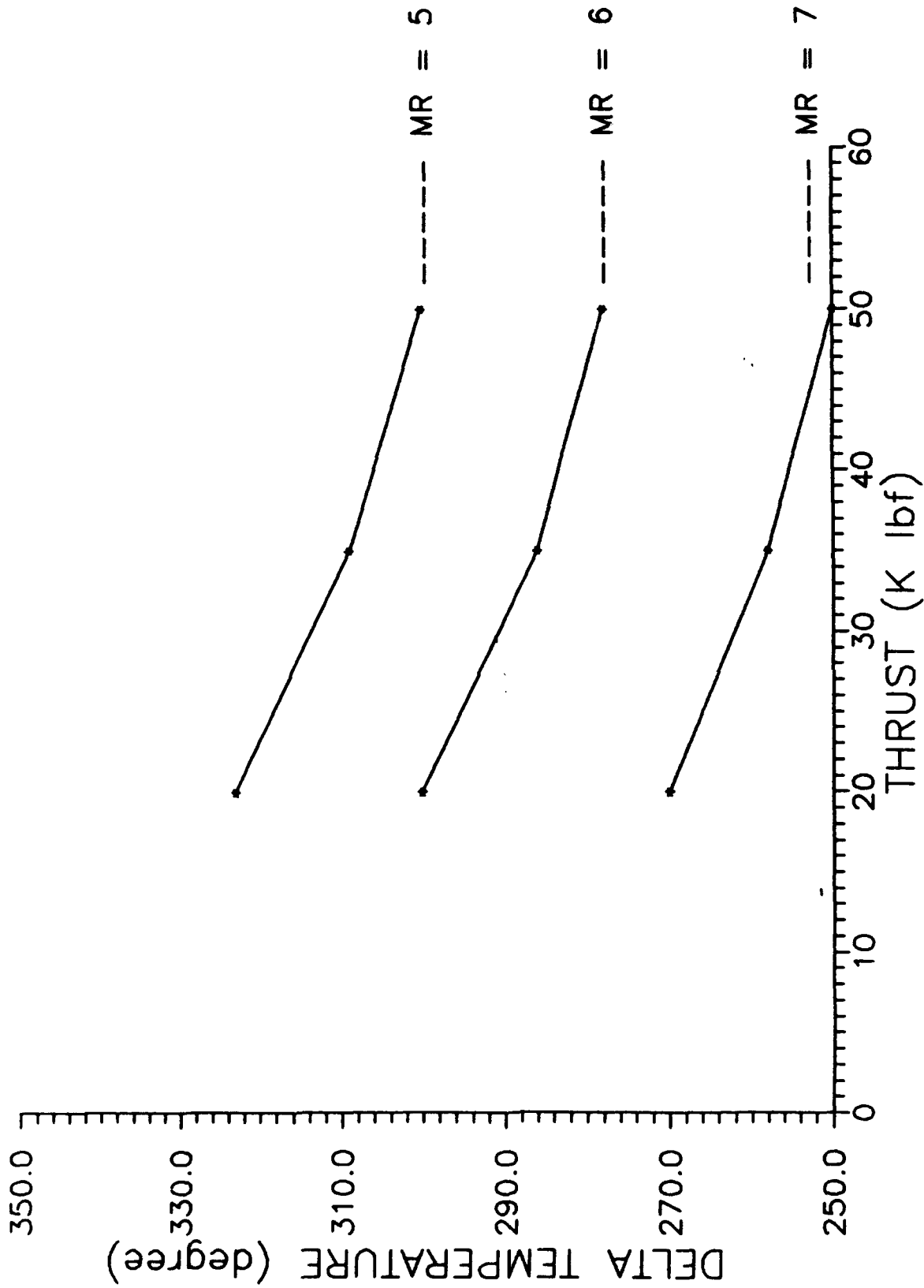


Figure A-20. Oxygen Cooled Nozzle 02 Delta Temperature vs Thrust

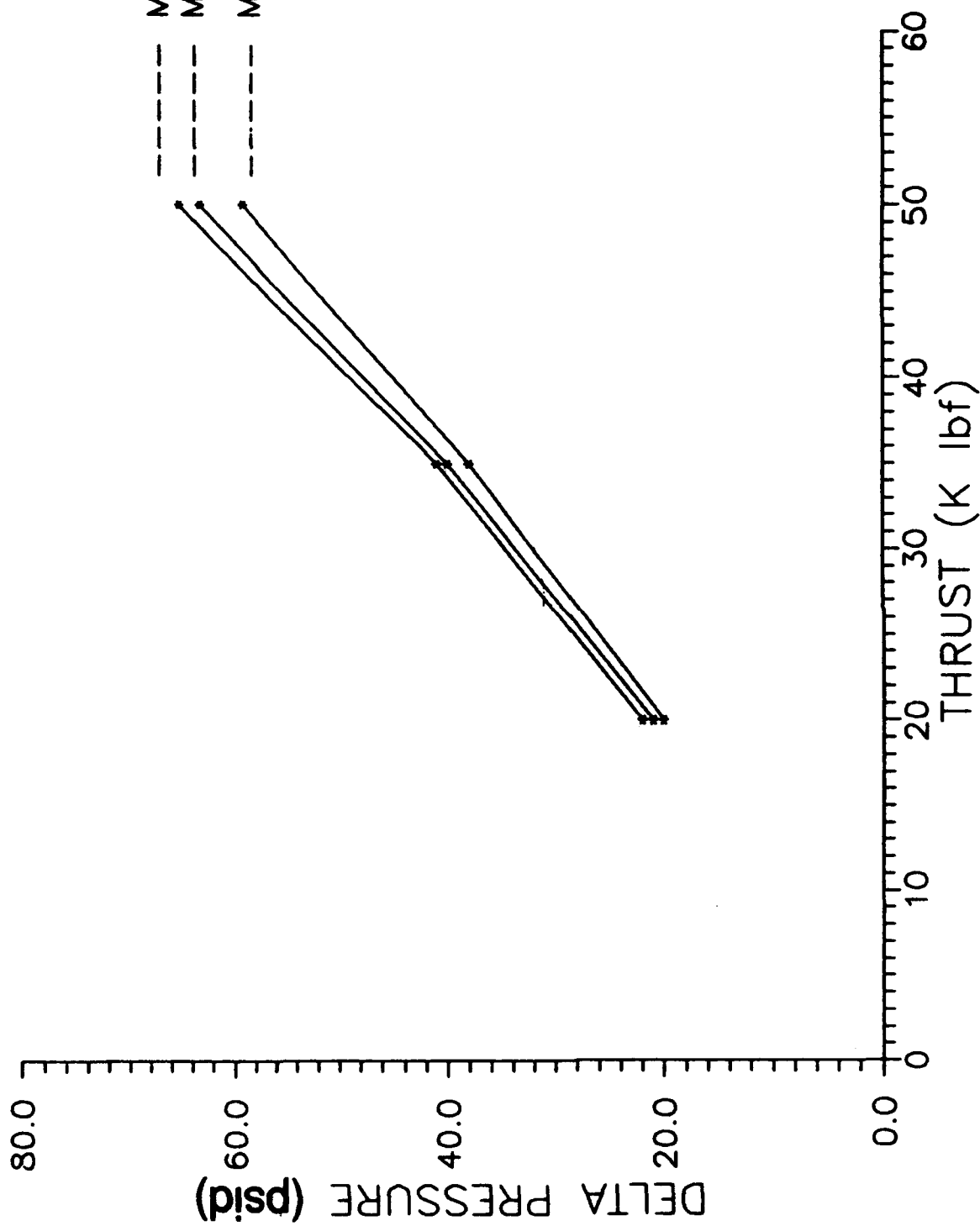


Figure A-21. Oxygen Cooled Nozzle O2 Pressure Drop vs Thrust

### A.3 BOUNDARY CONDITIONS

The Bartz equation is used to evaluate the gas-side heat transfer coefficient for the regeneratively cooled chamber and baffles:

$$Nu_f = 0.026 C_g(z) Re_f^{0.8} Pr_f^{0.4}$$

Symbols are defined in Section A.7. All properties are evaluated at the film temperature equal to the average of the wall temperature and the adiabatic wall temperature. All property and temperature data are obtained from the TRAN 72 computer program.

The 15.3 to 1 chamber contraction ratio assumed for all thrust levels in the present study is smaller than the near 17 to 1 value used in the 7.5K lbf design, however, the heat fluxes near the fore end of the barrel are assumed to be similar. Reference 3 asserts that gaseous hydrogen injectors often yield higher than nominal heat fluxes when the  $GH_2$  injection velocity exceeds the one dimensional isentropic chamber gas velocity. The injector designer states that this is the case with the OTV engine injector. Because the actual  $GH_2$  injection velocity used in this study is assumed to be the same as that of the 7.5K lbf engine design, the magnitude of the fore end heat flux should remain the same as well. However, the relative increase in  $C_g$  over the generic barrel value of 1.0 should be lower than in the 7.5K lbf engine study due to the smaller contraction ratio. The corrected barrel  $C_g$ 's are determined and compared to the generic barrel value of 1.0. The higher of the two is assumed. The resulting profile reflects a constant  $C_g$  value of 1.0 throughout the barrel. This infers that due to the smaller contraction ratio, the one-dimensional isentropic gas velocity has become sufficiently large to overpower the high fore end heat fluxes created by the injector element characteristics. The  $C_g$  profile from the aft end of the barrel to the end of the regeneratively cooled nozzle is maintained from the 7.5K lbf engine design. The complete profile is shown in Figure A-22.

The Hess and Kunz correlation (Ref. 4) is used to describe the forced convection heat transfer coefficients for hydrogen in the baffles, the regeneratively cooled chamber, the heat exchanger and the regenerator. This relationship is:

$$Nu_f = 0.0208 Re_f^{0.8} Pr_f^{0.4} \left( 1. + 0.01457 \frac{\mu_w \rho_b}{\mu_b \rho_w} \right)$$

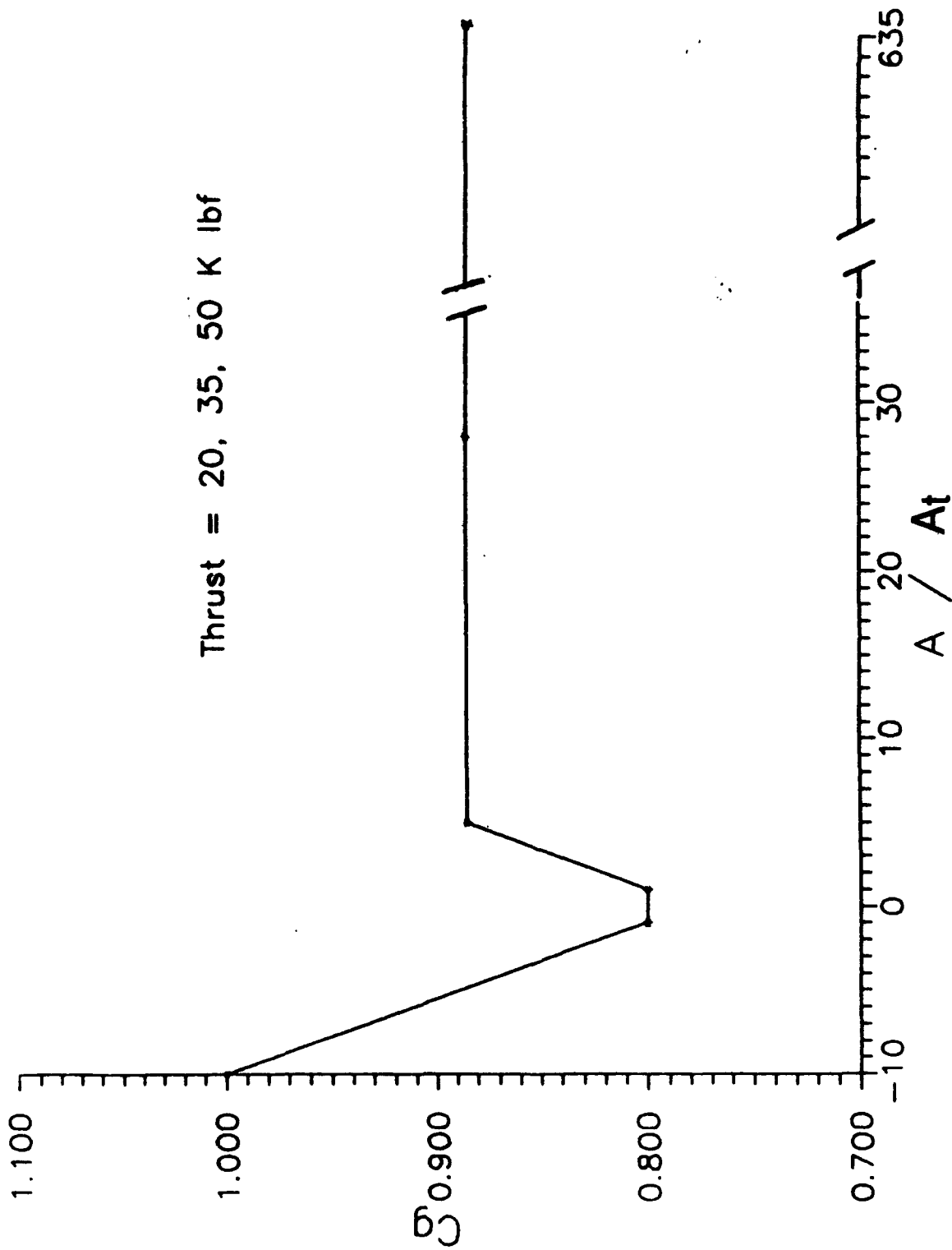


Figure A-22. Regeneratively Cooled Jacket and Baffles  $C_g$  vs Area Ratio

### A.3, Boundary Conditions, (cont)

The supercritical LOX correlation (Ref. 5) used to evaluate the convective heat transfer coefficients of oxygen is:

$$Nu_b = Nu_{ref} * (\rho_b / \rho_w)^{-.5} * (k_b / k_w)^{.5} * (c_p / c_{pt})^{2/3} * (P / P_{ct})^{-.2} * [1 + 2 / (1 / d)] \text{ where}$$
$$Nu_{ref} = .0025 * Re_b * Pr_b^{0.4}$$

The coolant pressure drop for a cooling channel within the regeneratively cooled chamber and baffle relates the exit static pressure to the inlet stagnation pressure. It is calculated as:

$$\Delta P_s = \Delta P_{inlet} + \Delta P_{fric} + \Delta P_{dyn}$$

One half of the dynamic head loss is assumed at the channel inlet to account for flow contraction.

The flow through the HEX and regenerator is assumed to be incompressible for the two components. This method results in a conservative pressure loss estimate when compared to a compressible pressure drop assumption.

The friction factor calculation (Ref. 6) used in all friction pressure loss evaluations is:

$$f = .0055 \left[ 1. + \left( 2.0E04 * \epsilon / D + 10^6 / Re \right)^{1/3} \right]$$

A roughness of 60.0 E-6 inches is assumed for the regeneratively cooled chamber, baffles, and nozzle and a roughness of 125.0 E-6 inches is assumed for the HEX and regenerator.

### A.4 DISCUSSION

#### A. GEOMETRY ALLOWABLES - ALL COMPONENTS

The maximum channel width to wall thickness for all components considers bending loads applied to fully-elastic hot walls and is described as:

#### A.4, Discussion, (cont)

$$\left| \frac{w}{tw} \right|_{\max} = \left| \frac{2 * F_{ty}}{\Delta P_{\max}} \right|^{1/2}$$

The maximum channel width to land width criteria used for all components considers tensile loads applied to fully elastic hot walls and is calculated as:

$$\left| \frac{w}{Land} \right|_{\max} = \left| \frac{(F)_{ty}}{\Delta P_{\max}} \right|$$

#### B. REGENERATIVELY COOLED CHAMBER

The geometric assumptions and general descriptions of the coolant channels in the regeneratively cooled chamber are summarized in Tables A-I and A-II. Table A-III describes the assumed hydrogen inlet conditions to the chamber.

The cooling channels in the chamber are assumed to be fabricated with a straddle mill rather than a constant width cutter. This method allows a smooth transition in increasing or decreasing channel width to minimize pressure loss. The channel sizes indicated in Table A-I are based on those used in the 7.5K lbf engine design with the exception of the channel and land widths at the throat and the land width in the chamber barrel section.

The channel width at the throat was increased and the land widths in the barrel were decreased from those values used in the 7.5K lbf engine design to decrease pressure drop. The channel width at the throat is increased to 0.011 inches rather than 0.010 inches used in the 7.5K lbf engine design. Because the total channel width center to center spacing is maintained from the earlier design, the land widths are decreased correspondingly to 0.010 inches from the 0.011 inches used previously. Coupling this assumption with the maximum 10 to 1 aspect ratio (channel depth/channel width) limit results in a channel flow area increase and flow velocity decrease of 21% at the maximum allowable channel depth. For the three thrust levels evaluated, the design of the channels in the throat region are, in general, geometrically limited and are therefore overcooled. The increase in flow area saves pressure drop. The maximum land width in the barrel was decreased from 0.040 inches used in the 7.5K lbf design to 0.025 inches.

#### A.4, Discussion, (cont)

Because the total number of channels is determined by the throat geometry, the decrease in barrel land width results in an increase in channel width of approximately 27%. Wall temperature control dictates the channel depth profile through the barrel, however the total coolant flow area is still larger with the 7.5K lbf engine assumption. The only constraint applied to the minimum land width definition is that the lands must provide structural support. Fabrication and weight issues were not considered.

The system schematic was changed to the parallel flow version with a 50/50 flow split occurring upstream of the regenerator (Figure A-23). The preliminary power balance was evaluated parametrically and a pump discharge pressure of 5500 psia was assumed. This pressure coupled with a low hydrogen inlet temperature of 90 R related to the new flow path significantly reduced the delta pressure through the chamber as compared to the series flow version of the dual propellant expander cycle.

The bulk hydrogen temperature rise and pressure drop versus thrust trends for the regeneratively cooled chamber are shown in Figures A-7 and A-8, respectively. Because the contraction ratio and the channel geometry at the throat remain constant for each thrust level evaluated, the amount of coolant flowrate per channel increases with the thrust level. This occurs because the throat and chamber diameters increase with the square root of thrust. An increase in hydrogen pressure drop and a decrease in bulk temperature rise as thrust increases is the result.

#### C. BAFFLES

The geometric assumption and general description of the coolant channels in the regeneratively cooled baffle are summarized in Tables A-I and A-II. The hydrogen inlet conditions are summarized in Table A-III.

The initial baffle material assumption differed from that of the 7.5K lbf design. The current effort started with a platinum alloy (Pt-ZGS) baffle rather than the NASA-Z baffle assumed in the earlier work. The NASA-Z baffle is limited to a 1050°F maximum gas-side wall temperature. In the previous study, the required hydrogen inlet temperature to the turbine was high (1000°R/540°F) and maintaining a wall temperature less than 1050°F at the coolant exit plane of the baffle was difficult.

## HYDROGEN CIRCUIT

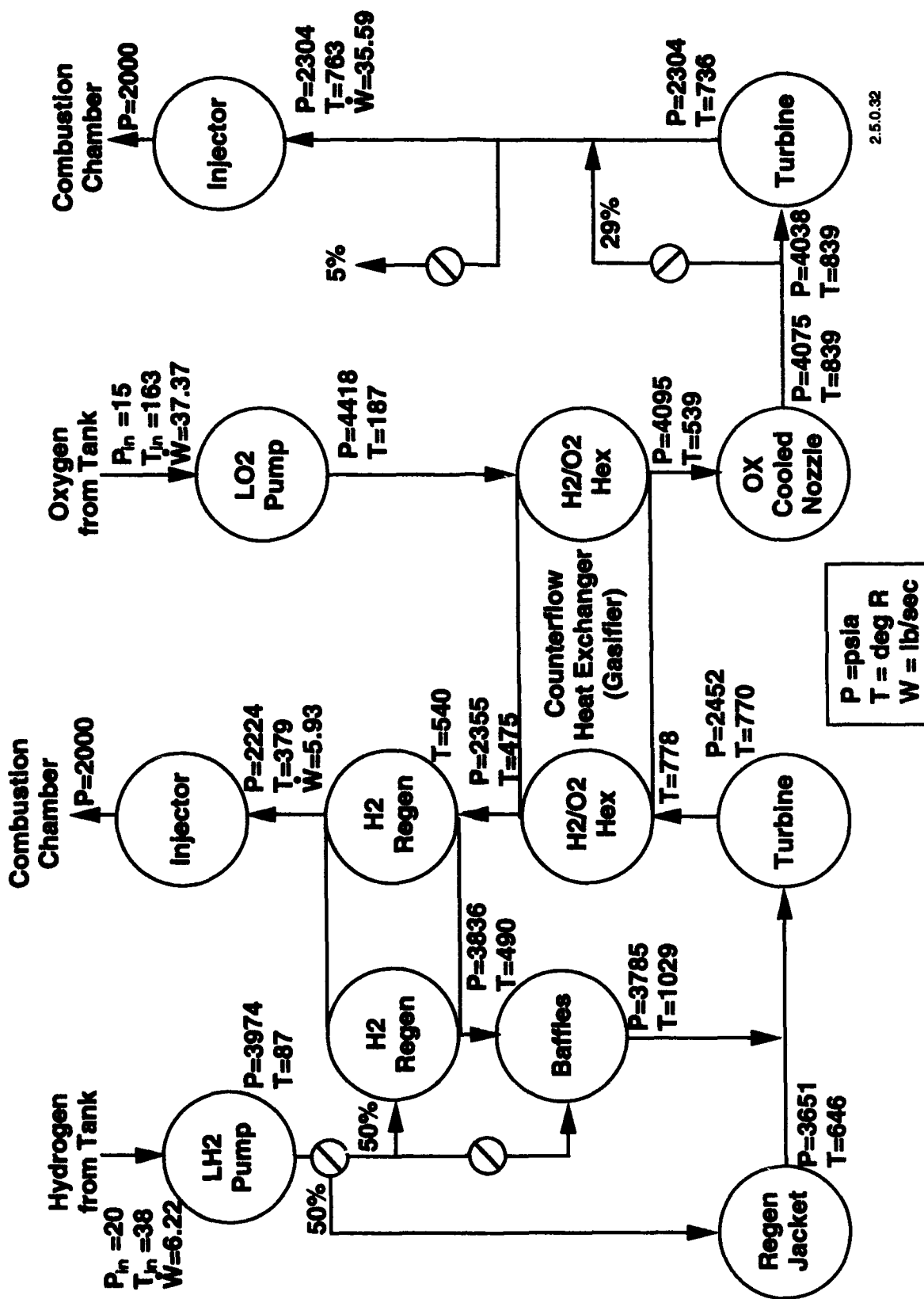


Figure A-23. Power Balance Results for 20K lbf Engine at MR = 6

#### A.4, Discussion, (cont)

Platinum was chosen as the baseline material for this effort because of its high thermal conductivity (similar to Nickel) and its high wall temperature capability (up to 2000°F). A later evaluation showed that copper alloy baffles could be used for all engine operations up to mixture ratios  $\leq 10.0$ .

The cooling channels in the baffle are assumed to be identical to those of the 7.5K lbf engine design; however, the core of the baffle is the only region evaluated; the tip and the corner regions are not analyzed for the present parametric study. The maximum baffle length is taken as either the length of the barrel section or 1/2 the chamber diameter, whichever is smaller. A baffle longer than the barrel section is not desirable in order to maintain a rectangular baffle shape and to prevent exposure to higher heat flux conditions associated with the convergent section. A baffle longer than 1/2 the barrel diameter was not considered because of combustion stability considerations. At the 20 and 35K lbf thrust levels, the combustion stability criteria defines the baffle length. Figure A-24 illustrates the resulting baffle lengths for the three thrust levels evaluated.

The selection of the baffle length affects the total heated surface area which, in turn, affects the turbine inlet temperature. Figure A-25 shows the bulk temperature rise trends for both the chamber and the baffle for the MR = 6 condition. As discussed in Section A.4B, the bulk temperature rise through the chamber goes down with thrust due to the relationship of heated surface area and H<sub>2</sub> flowrate to thrust. The H<sub>2</sub> through the baffle has the opposite trend, however. Because the number of coolant channels in the baffle are assumed to scale directly with thrust and the H<sub>2</sub> mass flux per channel remains constant for all thrust levels. The baffle length then becomes the parameter which differentiates the total heated surface area for the different thrust levels. Because baffle length increases as thrust goes up, so does the bulk temperature rise of the fluid. The turbine inlet temperature is a function of the delta temperature in both components. The sum of these temperature increases is very close for the 35 and 50K lbf thrust levels (963 and 960 R, respectively). At the 20K lbf thrust condition the resulting turbine inlet temperature is lower by approximately 68 degrees R due to the limited heated surface area. Figure A-26 shows the resulting turbine inlet temperature as a function of thrust.

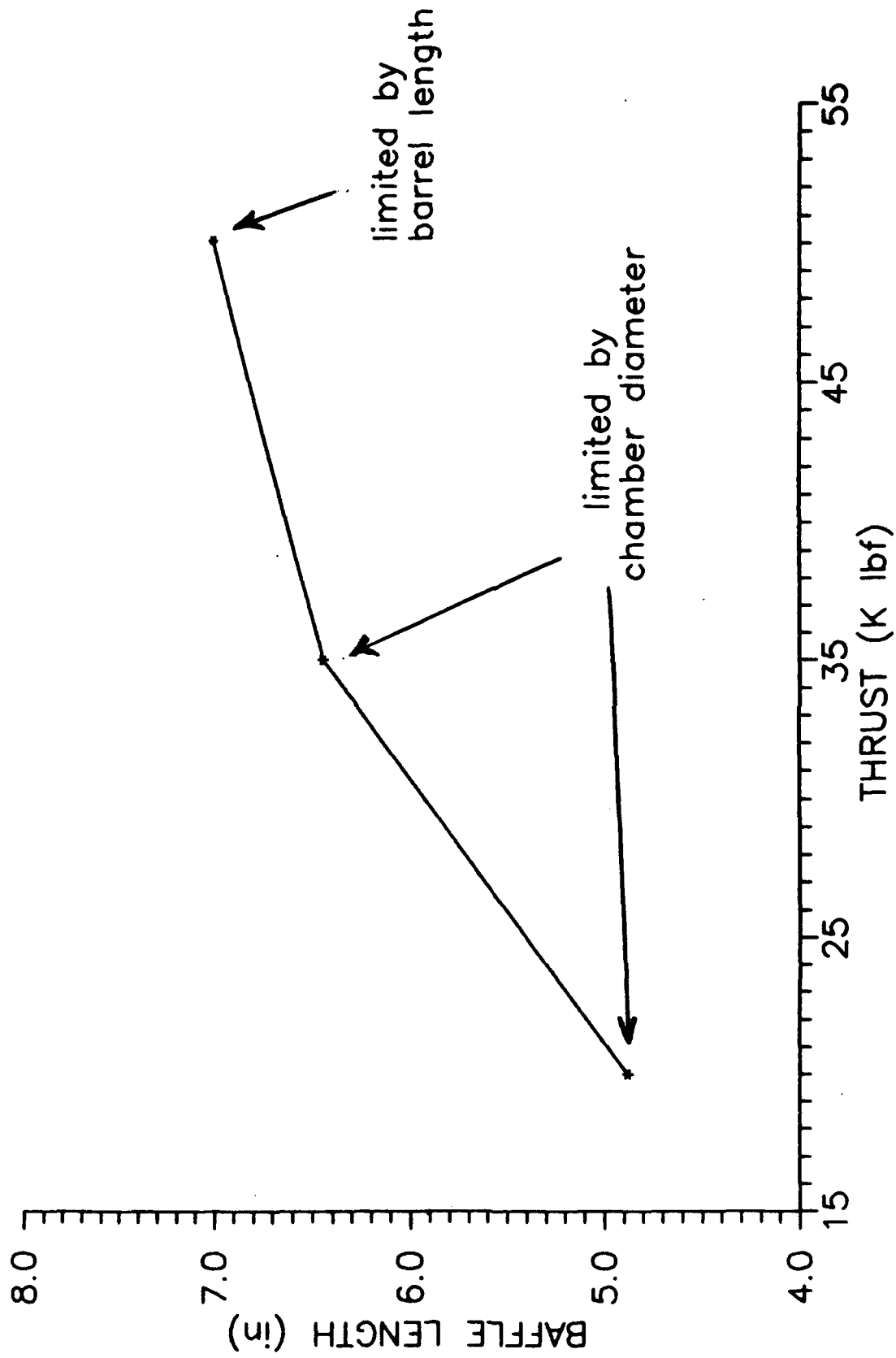


Figure A-24. Baffle Length vs Thrust

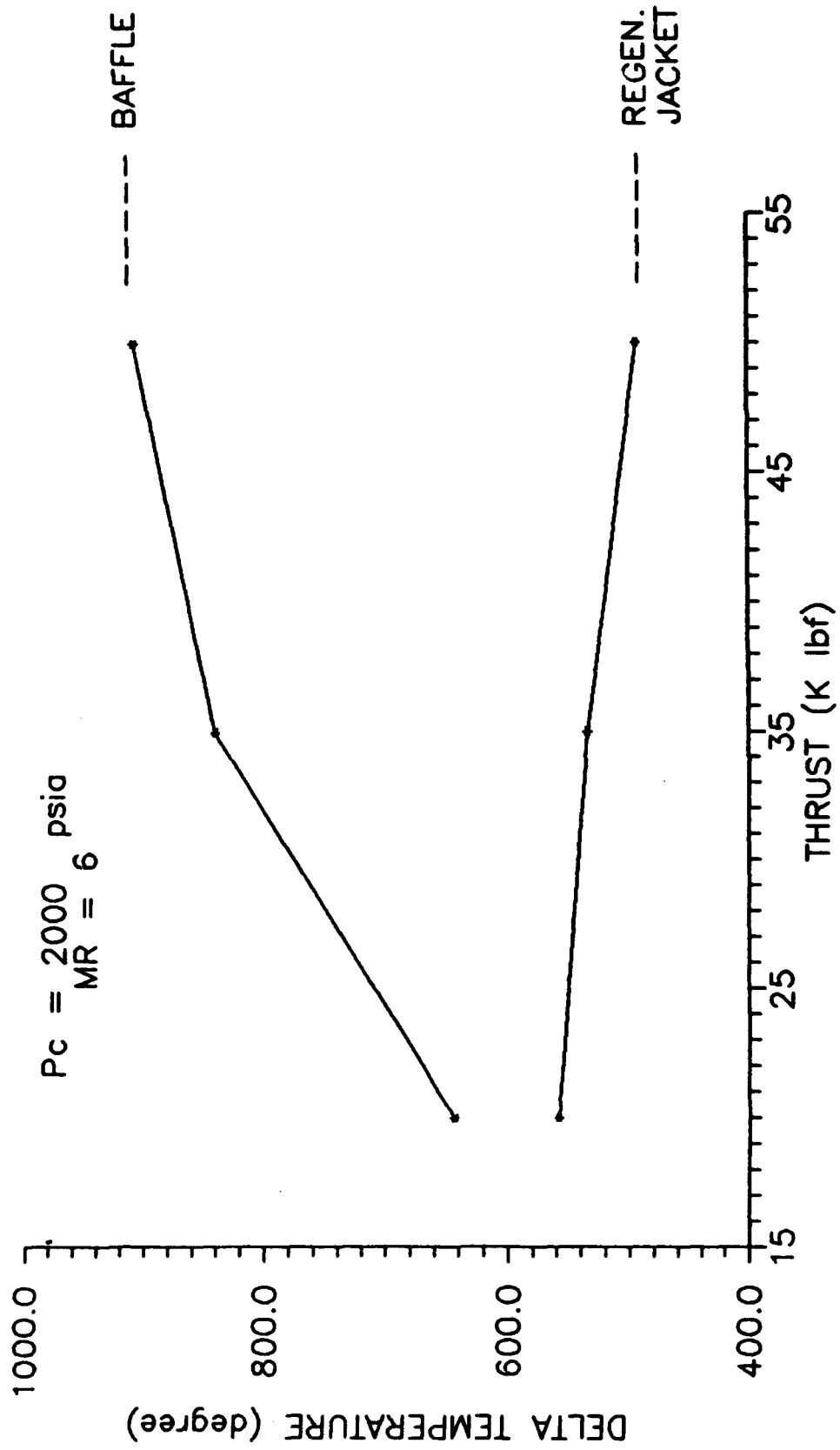


Figure A-25. Delta Temperature vs Thrust

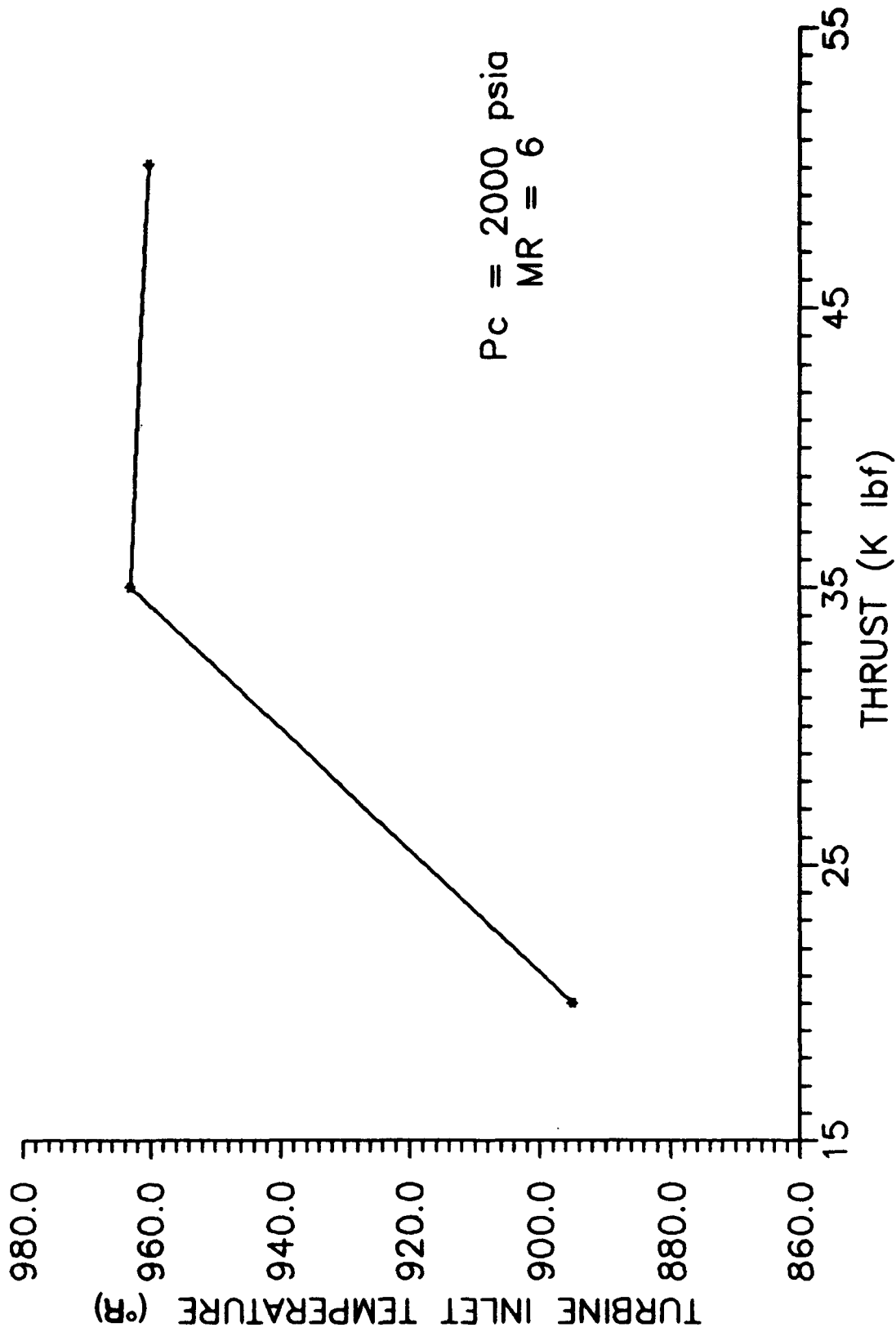


Figure A-26. Turbine Inlet Temperature vs Thrust

#### A.4, Discussion, (cont)

The pressure drop also increases with thrust. The losses are small compared to those of the chamber, however. An orifice directly downstream of the baffle is assumed to achieve the same exit pressure as that of the chamber. The Joule-Thompson effect is negligible for the pressure range of this study.

The bulk temperature rise and pressure drop versus thrust trends for the regeneratively cooled baffle for the MR = 5-7 range are shown in Figures A-9 and A-10, respectively.

#### D. HEAT EXCHANGER AND REGENERATOR

The divergences in pressure drop for the H<sub>2</sub> and O<sub>2</sub> in the HEX and the hot and cold H<sub>2</sub> in the regenerator are small at the three thrust levels evaluated. This is because the total number of fluid channels is assumed to increase directly with thrust to maintain a similar mass flux per channel throughout the thrust range. The differences in pressure drop for the fluids at the three thrust levels are attributable to the fluid inlet conditions and the overall length of the HEX or regenerator.

Because the hydrogen enthalpy is fairly insensitive to pressure for the pressure range of this study, the H<sub>2</sub> inlet temperature to the HEX is approximated as a 50/50 mixture of the fluid temperatures from the baffle and the regeneratively cooled chamber and a 6% loss across the turbine. The percent of turbine temperature loss was based on that assumed in the preliminary power balance using design curves supplied by the turbopump group.

$$T_{\text{Mixture}} = .94 * (.5 * T_{\text{Regeneratively Cooled chamber}} + .5 * T_{\text{Baffle}})$$

The HEX is sized to vaporize the oxygen prior to entering the O<sub>2</sub> cooled nozzle to achieve a turbine inlet temperature of 860 R (max) at a MR = 6 condition. The resulting hydrogen exit conditions are used as the inlet conditions to the hot side of the regenerator. A 25% bypass of H<sub>2</sub> around the HEX was assumed based on the optimum bypass determined in the 7.5K lbf analysis. The inlet temperature to the hot side of the regenerator is determined by:

#### A.4, Discussion, (cont)

$$T_{\text{Mixture}} = .75 * T_{\text{H2outHEX}} + .25 * T_{\text{H2inHEX}}$$

The inlet conditions for the HEX and the regenerator are listed in Tables A-IV and A-V, respectively. These conditions are given as a function of the thrust and mixture ratio.

The geometry and the dimensions for the HEX and the regenerator are listed in Tables A-VI and A-VII. The delta temperature trends for the O<sub>2</sub> and H<sub>2</sub> sides of the heat exchanger are shown in Figures A-11 and A-12, respectively. Figure A-13 shows the pressure loss across the HEX for the oxygen stream as a function of the thrust level. The inlet pressures and temperatures for all mixture ratios and thrust levels are assumed to be equal to the pump discharge conditions. The oxygen outlet temperature is constant throughout the thrust range for a given mixture ratio. Because the H<sub>2</sub> temperature at the HEX inlet is low at the 20K lbf thrust condition, the HEX is longer than at the higher thrust levels to compensate for the lower driving potential. The low temperature is due to the low chamber and baffle heated surface area to hydrogen flow rate ratio. A higher pressure drop at the lower thrust case results. The curves tend to flatten out beyond a thrust of 35K lbf due to the similarity in H<sub>2</sub> inlet temperature to the HEX.

Figure A-14 illustrates the HEX H<sub>2</sub> side pressure loss trends for the three mixture ratios. The H<sub>2</sub> delta pressure for thrusts from 20 to 35K lbf remains relatively constant, while at a thrust of 50K lbf losses increase. The pressure drops for the two lower thrust levels are similar because of the interaction of the HEX axial length and the H<sub>2</sub> inlet conditions. While the low thrust HEX is longer than that of the 35K lbf design, the lower H<sub>2</sub> dynamic pressure head (due to the higher H<sub>2</sub> inlet pressure and lower inlet temperature) compensates for the additional length. The H<sub>2</sub> inlet temperature and HEX lengths are similar for the 35 and 50K lbf thrust engines, however, the dynamic pressure head and total pressure loss for the 50K lbf design is higher due to the lower H<sub>2</sub> inlet pressure.

The temperature losses and gains as a function of the thrust level for the hot and cool hydrogen streams of the regenerator are depicted in Figures A-15 and A-16, respectively. At the 20K lbf level, in order to maintain the specified H<sub>2</sub> baffle inlet temperature of approximately 500°R, more energy is required to transfer from the hot to the cold H<sub>2</sub> to compensate for the reduced heated surface area per hydrogen flow rate in

#### A.4, Discussion, (cont)

the chamber and baffle. As a result, the temperature gain across the cool side and the temperature loss across the hot side of the regenerator are the highest at the 20K lbf condition.

The H<sub>2</sub> pressure drops across the hot and cool side of the regenerator as a function of the thrust level are depicted in Figures A-17 and A-18, respectively. Since the inlet temperature and pressure for the cool hydrogen stream is constant for all thrust levels and the required outlet H<sub>2</sub> temperature from the regenerator to the baffle is the highest at the lowest thrust level, the required regenerator length and the pressure loss of the cool H<sub>2</sub> is largest at the 20K lbf condition. The axial length of the regenerator also becomes the driving parameter in determining the pressure loss on the hot H<sub>2</sub> side of the regenerator even though the inlet pressure goes down as thrust goes up. Since the velocities of the hot H<sub>2</sub> through the regenerator channels are relatively low throughout the mixture ratio and thrust range, deviations in dynamic pressure head attributable to the different hot H<sub>2</sub> inlet pressures and temperatures are small.

#### E. OXYGEN COOLED NOZZLE

Table A-VIII summarizes the geometric assumptions for the coolant channels in the regeneratively cooled nozzle. The assumed inlet conditions are listed in Table A-III.

The cooling channels in the regeneratively cooled nozzle are assumed to be fabricated with a straddle mill cutter rather than a constant width cutter to minimize pressure drop. The assumptions for the cooling channel configuration do not reflect optimized values. They are, rather, based on maintaining reasonable ratios between channel width, land width, and gas-side wall thickness throughout the nozzle. Strength of both the gas-side wall and the land width are considered. The channel depth profile allowed for a maximum aspect ratio of 10 for channel widths less than or equal to 0.050 inches. As a comparison to the hydrogen cooled portion of the chamber, the maximum channel width in that region is 0.056 inches with a maximum allowable aspect ratio of 10. Rather than allow a maximum aspect ratio of 10 for the entire O<sub>2</sub> cooled nozzle region (the channel widths are assumed to be as large as 0.200 inches near the exit), the maximum allowable channel depth is set at 0.500 inches to represent a more reasonable total wall thickness. Due to the low coolant velocities in the region of the nozzle

**Table A-VIII  
Oxygen Cooled Nozzle  
Assumptions**

	Thrust (lbf)		
	<u>20K</u>	<u>35K</u>	<u>50K</u>
Coolant Inlet Area Ratio	28	28	28
Coolant Exit Area Ratio	635	635	635
Throat Area (in. <sup>2</sup> )	4.89	8.54	12.18
Total Flow Rate (lbs)	41.32	72.17	102.88
Maximum Channel Width (in.)	.200	.200	.200
Ratio of Channel Width to Land Width, max	2.0	2.0	2.0
Maximum Channel Depth (in.)	0.5	0.5	0.5
Single Bifurcation	Yes	Yes	Yes
Channel Width at Bifurcation (in.)	.100	.100	.100

#### A.4, Discussion, (cont)

affected by this prescription, the additional pressure drop penalty related to the maximum 0.500 inch channel depth assumption is negligible when compared to the pressure drop related to a maximum 10 to 1 aspect ratio maintained throughout the nozzle.

The resulting coolant delta temperature and pressure across the oxygen cooled nozzle are shown in Figures A-20 and A-21, respectively. The increase in pressure drop and decrease in bulk temperature rise with increasing thrust is similar to the trend seen for the regeneratively cooled chamber and is also attributable to the manner in which the surface area and propellant flow rate scale with thrust.

#### A.5 CONCLUSIONS

The thermal and hydraulic predictions were based on O<sub>2</sub> and H<sub>2</sub> pump exit conditions determined in a preliminary power balance and should be viewed as reference values. Adjustments in pressure drop for each component should be made if the pump discharge pressures for either the oxygen or hydrogen are altered from the reference values (discharge pressure of O<sub>2</sub> and H<sub>2</sub> are 5168 and 5500 psia, respectively) to account for density variations. Since the H<sub>2</sub> and O<sub>2</sub> enthalpies are fairly insensitive to pressure for the pressure range of this study, the thermal trends can be used directly assuming the same pump discharge temperatures (90°R for the H<sub>2</sub> pump and 188°R for the O<sub>2</sub> pump)

Of the five components evaluated, the regeneratively cooled chamber and the HEX are the limiting components for the system delta pressure on the H<sub>2</sub> and O<sub>2</sub> sides, respectively.

Prohibitively high H<sub>2</sub> pressure drops occur through the regeneratively cooled chamber when the 50/50 flow split (50% of the H<sub>2</sub> to the chamber and 50% to the baffle) is used and H<sub>2</sub> is preheated by the regenerator. When the coolant flow split is moved upstream of the regenerator and the H<sub>2</sub> to the chamber comes directly from the pump, the pressure drop through the chamber is substantially decreased. The higher density inlet hydrogen is predominantly attributable to the lower temperature. The difference in H<sub>2</sub> bulk temperature rise through the regeneratively cooled chamber for the parallel flow versus series flow is small, approximately 2%.

## A.5, Conclusions, (cont)

The  $H_2$  temperature at the inlet to the turbine reaches a peak value (963°R) at an engine thrust of 35K lbf thrust. The corresponding  $H_2$  pressure drop from the pump exit to the turbine inlet is approximately 590 psid. For the 50K lbf thrust condition, the  $H_2$  turbine inlet temperature is only slightly lower than that of the 35K lbf thrust case, but the pump-to-turbine delta pressure is nearly twice the 35K lbf thrust loss.

1. the total energy available to heat the hydrogen is not sufficient to obtain a system power balance for any chamber pressure or thrust level, it is recommended than an increase in chamber length ( $L'$ ) be considered. Because the baffle length is already limited due to combustion stability considerations ( $L_{baff} < 1/2 D_{barrel}$ ) for the 20K lbf and 35K lbf thrust engines, additional  $L'$  would provide more heated surface area only in the outer chamber's cylindrical section. For the 50K lbf thrust case the baffle length is currently limited by the length of the cylindrical barrel section. By increasing  $L'$ , additional surface area could be obtained in both the outer cylindrical section and the baffles. The additional pressure drop penalty would have to be considered, however.

The weights of the heat exchanger and regenerator could be reduced by allowing higher hydrogen pressure drops through the components. The pressure drop penalty on the hydrogen side of the heat exchanger and on both sides of the regenerator is small compared to that of the regeneratively cooled chamber (particularly at thrusts in the range of 35K lbf to 50K lbf); therefore, additional delta pressure would have a small effect on the hydrogen side of the system balance. Additional pressure drop on the oxygen side of the heat exchanger could also be investigated to reduce weight. No attempt was made to weight-optimize the HEX or hydrogen regenerator.

The  $O_2$  cooled nozzle is adequately cooled at the inlet area ratio of 28 and throughout the nozzle for a single pass of the oxygen. Mechanical design of the nozzle to accommodate the extendible/retractable section of the nozzle requires a pass-and-a-half flow design so that the collection manifold can be located away from the end of the cooled nozzle. The only penalty is a small increase in pressure drop due to loss in the 180° turn.

In summary, the parallel flow schematic has significantly improved the thermal margins for the dual expander cycle engine. There are no major thermal design limits for the required operating envelope.

## A.6 REFERENCES

1. Dommer, K.T., "OTV Regen-Cooling Jacket and Baffle Preliminary Design," ATC TAR 9985:008, 14 Jan. 1988.
2. Hayden, W.R., and Sabiers R., OTV Engine Preliminary Design Final Report, Contract NAS 3-23772, October 1988.
3. Ito, J.I., "A Physically Mechanistic Design Dependent Approach for Estimating Thermal Compatibility," ATC TAR 9980:2024, 21 Aug. 1987.
4. Hess, H.L., and Kunz, H.R., "A Study of Forced Convection Heat Transfer to Supercritical Hydrogen," ASME Paper 63-WA-205, 1963.
5. Spencer, R.G., and Rousar, D.C., "Supercritical Oxygen Heat Transfer," Contract NAS 3-20384, November, 1977.
6. Ewen, R.L., Calorimeter Chamber and Cooled Resonator Design, High Density Fuel Combustion and Cooling Investigation, Report No. TFD 9752:0185, Contract NAS 3-21030, ALRC,m 31 May 1978.

## A.7 NOMENCLATURE

$C_g$	Turbulent Pipe flow Correlation Coefficient
$C_p$	Specific Heat
$\bar{C}_f$	Integrated Average Specific Heat from $T_w$ to $T_b$
$d$	inside tube diameter
$D$	diameter
$f$	friction factor
$F_{ty}$	Yield Strength
$k$	Thermal conductivity
$L$	Length
$l$	Length from Start of Heated Tube to Temperature Measurement
$L'$	Axial length from injector to throat
$Land$	land width
$Nu$	Nusselt Number
$Nu_{ref}$	Reference Nusselt Number = $.0025 * Re_b * Pr_b^{.4}$
$P$	pressure
$Pr$	Prandtl Number
$Re$	Reynolds Number
$T$	Temperature
$tw$	Wall Thickness
$V$	Velocity
$W$	Channel Width

### Greek Letters:

$\mu$	dynamic viscosity
$\epsilon$	roughness
$\rho$	density

## A.7, Nomenclature, (cont)

### Subscripts:

b	Evaluated at bulk temperature
cr	Critical property
dyn	Dynamic
f	Evaluated at Film Temperature
fric	friction
H	Hydraulic
inlet	inlet
max	maximum
min	minimum
s	static
w	Evaluated at Wall Temperature

**APPENDIX B**  
**ADVANCED ENGINE POWER BALANCE**

**CONTENTS**

- B.1    Introduction**
- B.2    Power Balance At Mixture Ratio = 8**
- B.5    Power Balance At Mixture Ratio = 10**
- B.8    Power Balance At Mixture Ratio = 12**

## B.1 INTRODUCTION

This appendix contains power balance results at three mixture ratios outside of the normal operating range of  $MR = 6 \pm 1$ . This power balance work supports the Engine Variations subtask investigation of high mixture ratio operation. Balances at  $MR = 8$ , 10, and 12 were made at or very near to the maximum thrust point for the engine. A line connecting such points marks the high thrust boundary for the engine operating envelope. This maximum thrust limit is set by either the oxygen TPA maximum flowrate or by a design point temperature limit for the regeneratively cooled chamber or hydrogen cooled baffles. Another limit is set by available energy for the turbo-pumps. In general, high MR operation is both chamber wall temperature limited and hydrogen TPA energy limited before the oxygen flowrate limitation is effective. These power balances are supported by a detailed thermal design (see Appendix A) that confirms wall temperatures will be within design limits (800°F for the throat, 1050°F for all other copper surfaces) at these balance points.

2000 PSIA P<sub>L</sub>  
MR = 8

OTV ENGINE POWER BALANCE										Page 1
Off-Design Run	Oxidizer					Fuel				
	R	= 579.70 (in/deg R)	R	= 9205.00 (in/deg R)						
Tank Conditions	Pout	= 16.00 (psia)	Pout	= 20.00 (psia)						
	Tout	= 192.70 (deg R)	Tout	= 37.80 (deg R)						
	Heat	= -57.17 (BTU/°)	Heat	= -117.36 (BTU/°)						
	Rho out	= 71.17 (°/cuft)	Rho out	= 4.34 (°/cuft)						
Shut-off Valve	Pin	= 16.00 (psia)	Pin	= 20.00 (psia)						
	Pout	= 16.00 (psia)	Pout	= 19.88 (psia)						
	Delta P	= 0.04 (psi)	Delta P	= 0.14 (psi)						
	T	= 192.70 (deg R)	T	= 37.80 (deg R)						
	H	= -57.17 (BTU/°)	H	= -117.36 (BTU/°)						
	Rho in	= 71.17 (°/cuft)	Rho in	= 4.34 (°/cuft)						
	Rho out	= 71.17 (°/cuft)	Rho out	= 4.34 (°/cuft)						
	CdA	= 8.03000 (in <sup>2</sup> )	CdA	= 10.00000 (in <sup>2</sup> )						
Pump Conditions	Pin	= 37.90 (psia)	Pin	= 41.16 (psia)						
	Pout	= 3967.52 (psia)	Pout	= 3361.85 (psia)						
	Tin	= 192.70 (deg R)	Tin	= 38.08 (deg R)						
	Tout	= 194.34 (deg R)	Tout	= 61.37 (deg R)						
	Rho in	= 71.1917 (lb/ft <sup>3</sup> )	Rho in	= 4.3981 (lb/ft <sup>3</sup> )						
	Rho out	= 71.3460 (lb/ft <sup>3</sup> )	Rho out	= 4.5212 (lb/ft <sup>3</sup> )						
	Wdot	= 41.534 (lb/sec)	Wdot	= 3.192 (lb/sec)						
	Eff (hyd)	= 0.678	Eff (hyd)	= 0.640						
	Eff (mch)	= 1.000	Eff (mch)	= 1.000						
	N	= 47208.24 (rpm)	N	= 87177.85 (rpm)						
	HP	= 899.83 (HP)	HP	= 1911.18 (HP)						
	Q/N	= .0055487 (gpm/rpm)	Q/N	= .0061616 (gpm/rpm)						
Ox: Cool Side Heat Exchanger	Pin	= 3967.52 (psia)	Pin	= 3361.85 (psia)						
	Pout	= 3906.15 (psia)	Pout	= 3279.10 (psia)						
	Delta P	= 392.36 (psi)	Delta P	= 88.75 (psi)						
	Tin	= 184.34 (deg R)	Tin	= 61.37 (deg R)						
	Tout	= 625.57 (deg R)	Tout	= 398.16 (deg R)						
Fuel: Cool Side Regenerator	Delta T	= 441.22 (deg R)	Delta T	= 304.79 (deg R)						
	Min	= -42.26 (BTU/°)	Min	= 89.74 (BTU/°)						
	Heat	= 120.33 (BTU/°)	Heat	= 1282.67 (BTU/°)						
	Rho in	= 71.35 (°/cuft)	Rho in	= 4.52 (°/cuft)						
	Rho out	= 18.95 (°/cuft)	Rho out	= 1.34 (°/cuft)						
	Qdot	= 9750.08 (BTU/s)	Qdot	= 2293.40 (BTU/s)						
	Wdot	= 41.63 (°/sec)	Wdot	= 1.86 (°/sec)						
			% bypass	= 25.00						

OTV ENGINE POWER BALANCE

Oxidizer		Fuel	
Regen Jacket	Pin	= 3361.66 (psia)	
	Pout	= 3141.07 (psia)	
	Delta P	= 220.76 (psi)	
	Tin	= 81.37 (deg R)	
	Tout	= 714.37 (deg R)	
	Delta T	= 633.00 (deg R)	
	Min	= 88.74 (BTU/lb)	
	Max	= 2488.22 (BTU/lb)	
	Rho in	= 4.52 (lb/cuft)	
	Rho out	= 0.74 (lb/cuft)	
Baffles	Pin	= 3273.10 (psia)	
	Pout	= 3261.70 (psia)	
	Delta P	= 21.40 (psi)	
	Tin	= 314.24 (deg R)	
	Tout	= 1023.24 (deg R)	
	Delta T	= 709.00 (deg R)	
	Min	= 988.61 (BTU/lb)	
	Max	= 3558.69 (BTU/lb)	
	Rho in	= 1.61 (lb/cuft)	
	Rho out	= 0.55 (lb/cuft)	
Ox Nozzle Cooling	Pin	= 3606.16 (psia)	
	Pout	= 3671.74 (psia)	
	Delta P	= 35.41 (psi)	
	Tin	= 826.57 (deg R)	
	Tout	= 855.57 (deg R)	
	Delta T	= 29.00 (deg R)	
	Min	= 120.23 (BTU/lb)	
	Max	= 181.22 (BTU/lb)	
	Rho in	= 16.06 (lb/cuft)	
	Rho out	= 11.06 (lb/cuft)	
Back Pressure Valve	Pin	= 3671.74 (psia)	
	Pout	= 3671.71 (psia)	
	Delta P	= 0.03 (psi)	
	Tin	= 855.57 (deg R)	
	Tout	= 181.22 (deg R)	
	Delta T	= 674.35 (deg R)	
	Min	= 120.23 (BTU/lb)	
	Max	= 181.22 (BTU/lb)	
	Rho in	= 16.06 (lb/cuft)	
	Rho out	= 11.06 (lb/cuft)	

OTV ENGINE POWER BALANCE

	Oxidizer		Fuel	
Turbine Conditions	Pin	= 3871.71 (psia)	Pin	= 3141.06 (psia)
	Pout	= 2411.04 (psia)	Pout	= 2262.18 (psia)
	Wdot	= 38.186 (lb/sec)	Wdot	= 4.486 (lb/sec)
	Tin	= 865.67 (deg R)	Tin	= 868.61 (deg R)
	Tout	= 781.00 (deg R)	Tout	= 806.70 (deg R)
	Min	= 181.22 (BTU/lb)	Min	= 3013.86 (BTU/lb)
	Wdot	= 184.26 (BTU/lb)	Wdot	= 2776.77 (BTU/lb)
	Rho in	= 11.88 (lb/ft <sup>3</sup> )	Rho in	= 0.62 (lb/ft <sup>3</sup> )
	Rho out	= 8.93 (lb/ft <sup>3</sup> )	Rho out	= 0.48 (lb/ft <sup>3</sup> )
	Eff.	= 0.820	Eff.	= 0.912
	HP	= 667.64 (HP)	HP	= 1907.90 (HP)
	PR	= 1.481 (Pin/Pout)	PR	= 1.388 (Pin/Pout)
	U/Co	= 0.514 (fps/fps)	U/Co	= 0.907 (fps/fps)
Hot Side Heat Exchanger	Wheel dia	= 2.542 (in)	Wheel dia	= 3.090 (in)
	Wbypass	= 12.95	% bypass	= 13.43
	Pin	= 2262.18 (psia)	Pin	= 2262.18 (psia)
	Pout	= 2186.18 (psia)	Pout	= 2186.18 (psia)
	Delta P	= 76.00 (psi)	Delta P	= 76.00 (psi)
	Tin	= 815.78 (deg R)	Tin	= 815.78 (deg R)
	Tout	= 521.42 (deg R)	Tout	= 521.42 (deg R)
	Delta T	= 294.34 (deg R)	Delta T	= 294.34 (deg R)
	Min	= 2908.61 (BTU/lb)	Min	= 2908.61 (BTU/lb)
	Wdot	= 988.40 (BTU/lb)	Wdot	= 988.40 (BTU/lb)
	Rho in	= 0.48 (lb/ft <sup>3</sup> )	Rho in	= 0.48 (lb/ft <sup>3</sup> )
	Rho out	= 1.14 (lb/ft <sup>3</sup> )	Rho out	= 1.14 (lb/ft <sup>3</sup> )
	Qdot	= -6750.06 (BTU/s)	Qdot	= -6750.06 (BTU/s)
Gas Side Regenerator	Wdot	= 3.71 (lb/sec)	Wdot	= 3.71 (lb/sec)
	% bypass	= 25.00	% bypass	= 25.00
	Pin	= 2186.18 (psia)	Pin	= 2186.18 (psia)
	Pout	= 2104.18 (psia)	Pout	= 2104.18 (psia)
	Delta P	= 81.00 (psi)	Delta P	= 81.00 (psi)
	Tin	= 496.16 (deg R)	Tin	= 496.16 (deg R)
	Tout	= 316.84 (deg R)	Tout	= 316.84 (deg R)
	Delta T	= 179.32 (deg R)	Delta T	= 179.32 (deg R)
	Min	= 1443.12 (BTU/lb)	Min	= 1443.12 (BTU/lb)
	Wdot	= 981.32 (BTU/lb)	Wdot	= 981.32 (BTU/lb)
	Rho in	= 0.65 (lb/ft <sup>3</sup> )	Rho in	= 0.65 (lb/ft <sup>3</sup> )
	Rho out	= 1.10 (lb/ft <sup>3</sup> )	Rho out	= 1.10 (lb/ft <sup>3</sup> )
	Qdot	= -2283.46 (BTU/s)	Qdot	= -2283.46 (BTU/s)
Injector	Wdot	= 4.94 (lb/sec)	Wdot	= 4.94 (lb/sec)
	Pin	= 2104.18 (psia)	Pin	= 2104.18 (psia)
	Pout	= 2002.86 (psia)	Pout	= 2002.86 (psia)
	Tin	= 316.84 (deg R)	Tin	= 316.84 (deg R)
	Rho in	= 1.10 (lb/ft <sup>3</sup> )	Rho in	= 1.10 (lb/ft <sup>3</sup> )
	Rho out	= 1.06 (lb/ft <sup>3</sup> )	Rho out	= 1.06 (lb/ft <sup>3</sup> )
	Wdot	= 4.946 (lb/sec)	Wdot	= 4.946 (lb/sec)
	Drop	= 101.26 (psia)	Drop	= 101.26 (psia)
	Qdot	= 0.07823 (in <sup>2</sup> )	Qdot	= 0.07823 (in <sup>2</sup> )
	PG	= 2000.00 (psia)	PG	= 2000.00 (psia)
	DFed	= 3.88 (psia)	DFed	= 3.88 (psia)
	ERE	= 1.000	ERE	= 1.000
Combustion Chamber	Wdot	= 3.88 (lb/sec)	Wdot	= 3.88 (lb/sec)
	DFed	= 3.88 (psia)	DFed	= 3.88 (psia)
	ERE	= 1.000	ERE	= 1.000
	Wdot	= 3.88 (lb/sec)	Wdot	= 3.88 (lb/sec)
	DFed	= 3.88 (psia)	DFed	= 3.88 (psia)

$P_c = 1917 \text{ PSIA}$   
 $MR = 10$

OTV ENGINE POWER BALANCE										Page 1
Off-Design Run	Oxidizer				Fuel					
	R	= 579.70 (in/deg R)				R	= 9202.00 (in/deg R)			
Tank Conditions	Pout	= 15.00 (psia)				Pout	= 20.00 (psia)			
	Tout	= 162.70 (deg R)				Tout	= 37.60 (deg R)			
	Heat	= -67.17 (BTU/°)				Heat	= -117.35 (BTU/°)			
	Rho out	= 71.17 (g/cuft)				Rho out	= 4.34 (g/cuft)			
Shut-off Valve	Pin	= 15.00 (psia)				Pin	= 20.00 (psia)			
	Pout	= 15.00 (psia)				Pout	= 19.90 (psia)			
	Delta P	= 0.93 (psi)				Delta P	= 0.10 (psi)			
	T	= 162.70 (deg R)				T	= 37.60 (deg R)			
Pump Conditions	H	= -57.17 (BTU/°)				H	= -117.35 (BTU/°)			
	Rho in	= 71.17 (g/cuft)				Rho in	= 4.34 (g/cuft)			
	Rho out	= 71.17 (g/cuft)				Rho out	= 4.34 (g/cuft)			
	CdA	= 8.03000 (in^2)				CdA	= 10.00000 (in^2)			
Pump Conditions	Pin	= 37.90 (psia)				Pin	= 41.20 (psia)			
	Pout	= 4002.05 (psia)				Pout	= 2995.14 (psia)			
	Tin	= 162.70 (deg R)				Tin	= 36.10 (deg R)			
	Tout	= 184.71 (deg R)				Tout	= 70.00 (deg R)			
Fuel: Cool Side Regenerator	Rho in	= 71.1917 (lb/ft3)				Rho in	= 4.3371 (lb/ft3)			
	Rho out	= 71.3231 (lb/ft3)				Rho out	= 4.4549 (lb/ft3)			
	Wdot	= 43.674 (lb/sec)				Wdot	= 4.367 (lb/sec)			
	Eff (hyd)	= 0.676				Eff (hyd)	= 0.621			
Ox: Cool Side Heat Exchanger	Eff (mch)	= 1.000				Eff (mch)	= 1.000			
	N	= 48222.34 (rpm)				N	= 81085.51 (rpm)			
	HP	= 926.48 (HP)				HP	= 1174.24 (HP)			
	Q/N	= .0067087 (gpm/rpm)				Q/N	= .0068733 (gpm/rpm)			
Ox: Cool Side Heat Exchanger	Pin	= 4002.05 (psia)				Pin	= 2995.14 (psia)			
	Pout	= 3039.55 (psia)				Pout	= 2996.92 (psia)			
	Delta P	= 962.49 (psi)				Delta P	= 66.21 (psi)			
	Tin	= 184.71 (deg R)				Tin	= 70.00 (deg R)			
Fuel: Cool Side Regenerator	Tout	= 871.10 (deg R)				Tout	= 283.00 (deg R)			
	Delta T	= 486.39 (deg R)				Delta T	= 204.00 (deg R)			
	Min	= -42.09 (BTU/°)				Min	= 74.11 (BTU/°)			
	Heat	= 132.02 (BTU/°)				Heat	= 336.27 (BTU/°)			
Fuel: Cool Side Regenerator	Rho in	= 71.32 (g/cuft)				Rho in	= 4.45 (g/cuft)			
	Rho out	= 15.87 (g/cuft)				Rho out	= 1.92 (g/cuft)			
	Qdot	= 7630.52 (BTU/s)				Qdot	= 1281.62 (BTU/s)			
	Wdot	= 43.67 (g/sec)				Wdot	= 1.94 (g/sec)			
% bypass = 28.00										

QTV ENGINE POWER BALANCE			Page 2
	Oxidizer	Fuel	
Regen Jacket	Pin	= 2005.14 (psia)	
	Post	= 2707.43 (psia)	
	Delta P	= 197.71 (psi)	
	Tin	= 78.00 (deg R)	
	Tout	= 776.00 (deg R)	
	Delta T	= 697.00 (deg R)	
	Min	= 74.11 (BTU/d)	
	Heat	= 2076.71 (BTU/d)	
	Rho in	= 4.45 (d/cuft)	
	Rho out	= 0.62 (d/cuft)	
	Wdot	= 2.18 (d/sec)	
Baffles	Pin	= 2005.92 (psia)	
	Post	= 2023.20 (psia)	
	Delta P	= 19.72 (psi)	
	Tin	= 206.86 (deg R)	
	Tout	= 1002.35 (deg R)	
	Delta T	= 764.00 (deg R)	
	Min	= 849.67 (BTU/d)	
	Heat	= 3477.62 (BTU/d)	
	Rho in	= 1.90 (d/cuft)	
	Rho out	= 0.51 (d/cuft)	
	Wdot	= 2.18 (d/sec)	
Ox Nozzle Cooling	Pin	= 3609.66 (psia)	
	Post	= 3603.42 (psia)	
	Delta P	= 36.13 (psi)	
	Tin	= 871.16 (deg R)	
	Tout	= 851.10 (deg R)	
	Delta T	= 180.00 (deg R)	
	Min	= 192.62 (BTU/d)	
	Heat	= 100.09 (BTU/d)	
	Rho in	= 16.07 (d/cuft)	
	Rho out	= 11.94 (d/cuft)	
	Wdot	= 43.67 (d/sec)	
Back Pressure Valve	Pin	= 3603.42 (psia)	
	Post	= 3603.36 (psia)	
	Delta P	= 0.06 (psi)	
	Tin	= 851.10 (deg R)	
	Tout	= 851.10 (deg R)	
	Delta T	= 0.00 (deg R)	
	Min	= 100.09 (BTU/d)	
	Heat	= 11.94 (d/cuft)	
	Rho in	= 11.94 (d/cuft)	
	Rho out	= 11.94 (d/cuft)	
	GdA	= ..... (in^2)	
Back Pressure Valve	Pin	= 3603.42 (psia)	
	Post	= 3603.36 (psia)	
	Delta P	= 0.06 (psi)	
	Tin	= 851.10 (deg R)	
	Tout	= 851.10 (deg R)	
	Delta T	= 0.00 (deg R)	
	Min	= 100.09 (BTU/d)	
	Heat	= 11.94 (d/cuft)	
	Rho in	= 11.94 (d/cuft)	
	Rho out	= 11.94 (d/cuft)	
	GdA	= ..... (in^2)	

OTV ENGINE POWER BALANCE										Page 3
	Oxidizer					Fuel				
Turbine Conditions	Pin	= 3803.38	(psia)	Pin	= 2787.42	(psia)				
	Pout	= 2985.81	(psia)	Pout	= 2081.17	(psia)				
	Wdot	= 37.038	(lb/sec)	Wdot	= 3.847	(lb/sec)				
	Tin	= 851.10	(deg R)	Tin	= 888.17	(deg R)				
	Tout	= 773.23	(deg R)	Tout	= 831.82	(deg R)				
	Min	= 180.93	(BTU/°)	Min	= 3077.90	(BTU/°)				
	Hout	= 162.38	(BTU/°)	Hout	= 2881.33	(BTU/°)				
	Rho in	= 11.84	(g/cuft)	Rho in	= 0.54	(g/cuft)				
	Rho out	= 8.94	(g/cuft)	Rho out	= 0.44	(g/cuft)				
	Eff.	= 0.820		Eff.	= 0.808					
	HP	= 824.83	(HP)	HP	= 1178.38	(HP)				
	PR	= 1.510 (Pin/Pout)		PR	= 1.344 (Pin/Pout)					
	U/Co	= 0.515 (fps/fps)		U/Co	= 0.289 (fps/fps)					
Hot Side Heat Exchanger	Wheel dia	= 2.542	(in)	Wheel dia	= 3.090	(in)				
	%bypass	= 15.18		% bypass	= 11.92					
	Pin	= 2081.17	(psia)	Pin	= 2081.17	(psia)				
	Pout	= 2038.17	(psia)	Pout	= 2038.17	(psia)				
	Delta P	= 43.00	(psi)	Delta P	= 43.00	(psi)				
	Tin	= 839.18	(deg R)	Tin	= 839.18	(deg R)				
	Tout	= 187.86	(deg R)	Tout	= 187.86	(deg R)				
	Delta T	= 651.52	(deg R)	Delta T	= 651.52	(deg R)				
	Min	= 2887.14	(BTU/°)	Min	= 441.12	(BTU/°)				
	Hout	= 0.44	(g/cuft)	Hout	= 0.44	(g/cuft)				
	Rho in	= 1.88	(g/cuft)	Rho in	= 1.88	(g/cuft)				
	Rho out	= 1.88	(g/cuft)	Rho out	= 1.88	(g/cuft)				
	Qdot	= 7830.82	(BTU/s)	Qdot	= 7830.82	(BTU/s)				
Gas Side Regenerator	Wdot	= 3.12	(g/sec)	Wdot	= 3.12	(g/sec)				
	% bypass	= 25.00		% bypass	= 25.00					
	Pin	= 2038.17	(psia)	Pin	= 2038.17	(psia)				
	Pout	= 1980.17	(psia)	Pout	= 1980.17	(psia)				
	Delta P	= 58.00	(psi)	Delta P	= 58.00	(psi)				
	Tin	= 837.31	(deg R)	Tin	= 837.31	(deg R)				
	Tout	= 284.86	(deg R)	Tout	= 284.86	(deg R)				
	Delta T	= 72.78	(deg R)	Delta T	= 72.78	(deg R)				
	Min	= 1082.41	(BTU/°)	Min	= 1082.41	(BTU/°)				
	Hout	= 781.82	(BTU/°)	Hout	= 781.82	(BTU/°)				
	Rho in	= 1.02	(g/cuft)	Rho in	= 1.02	(g/cuft)				
	Rho out	= 1.26	(g/cuft)	Rho out	= 1.26	(g/cuft)				
	Qdot	= 1281.82	(BTU/s)	Qdot	= 1281.82	(BTU/s)				
Injector	Wdot	= 4.18	(g/sec)	Wdot	= 4.18	(g/sec)				
	Pin	= 1980.17	(psia)	Pin	= 1980.17	(psia)				
	Pout	= 1818.40	(psia)	Pout	= 1818.40	(psia)				
	Tin	= 284.86	(deg R)	Tin	= 284.86	(deg R)				
	Rho in	= 1.28	(g/cuft)	Rho in	= 1.28	(g/cuft)				
	Rho out	= 1.23	(g/cuft)	Rho out	= 1.23	(g/cuft)				
	Wdot	= 4.188	(lb/sec)	Wdot	= 4.188	(lb/sec)				
	Drop	= 81.77	(psia)	Drop	= 81.77	(psia)				
	CdA	= 0.87823	(in^2)	CdA	= 0.87823	(in^2)				
	PC	= 1817.00	(psia)	PC	= 1817.00	(psia)				
	DPac	= 3.53	(psia)	DPac	= 3.53	(psia)				
	ERE	= 1.000		ERE	= 1.000					
	F	= 19888.92	(lbf)	F	= 19888.92	(lbf)				
Combustion Chamber	PC	= 1817.00	(psia)	PC	= 1817.00	(psia)				
	DPac	= 3.53	(psia)	DPac	= 3.53	(psia)				
	ERE	= 1.000		ERE	= 1.000					
	F	= 19888.92	(lbf)	F	= 19888.92	(lbf)				

$P_c = 1550 \text{ psia}$   
 $MR = 12$

OTV ENGINE POWER BALANCE										Page 1
Off-Design Run										
	Oxidizer					Fuel				
	R	=	578.70 (in/deg R)	R	=	9202.00 (in/deg R)				
Task Conditions	Pout	=	15.00 (psia)	Pout	=	20.00 (psia)				
	Tout	=	162.70 (deg R)	Tout	=	37.80 (deg R)				
	Hout	=	-57.17 (BTU/lb)	Hout	=	-117.35 (BTU/lb)				
	Rho out	=	71.17 (lb/ft <sup>3</sup> )	Rho out	=	4.34 (lb/ft <sup>3</sup> )				
Shut-off Valve	Pin	=	15.00 (psia)	Pin	=	20.00 (psia)				
	Pout	=	15.00 (psia)	Pout	=	19.95 (psia)				
	Delta P	=	0.71 (psi)	Delta P	=	0.05 (psi)				
	T	=	162.70 (deg R)	T	=	37.80 (deg R)				
	H	=	-57.17 (BTU/lb)	H	=	-117.35 (BTU/lb)				
	Rho in	=	71.17 (lb/ft <sup>3</sup> )	Rho in	=	4.34 (lb/ft <sup>3</sup> )				
	Rho out	=	71.17 (lb/ft <sup>3</sup> )	Rho out	=	4.34 (lb/ft <sup>3</sup> )				
Pump Conditions	CdA	=	8.03000 (in <sup>2</sup> )	CdA	=	10.00000 (in <sup>2</sup> )				
	Pin	=	37.80 (psia)	Pin	=	41.25 (psia)				
	Pout	=	3207.78 (psia)	Pout	=	2312.98 (psia)				
	Tin	=	162.70 (deg R)	Tin	=	38.17 (deg R)				
	Tout	=	160.26 (deg R)	Tout	=	74.48 (deg R)				
	Rho in	=	71.1917 (lb/ft <sup>3</sup> )	Rho in	=	4.3338 (lb/ft <sup>3</sup> )				
	Rho out	=	71.2668 (lb/ft <sup>3</sup> )	Rho out	=	4.3102 (lb/ft <sup>3</sup> )				
	Wdot	=	38.128 (lb/sec)	Wdot	=	3.177 (lb/sec)				
	Eff (hyd)	=	0.977	Eff (hyd)	=	0.575				
	Eff (mch)	=	1.000	Eff (mch)	=	1.000				
	N	=	42765.89 (rpm)	N	=	70503.97 (rpm)				
	HP	=	648.13 (HP)	HP	=	722.13 (HP)				
	Q/N	=	.0058209 (gpm/rpm)	Q/N	=	.0046672 (gpm/rpm)				
Ox: Cool Side Heat Exchanger	Pin	=	3207.78 (psia)	Pin	=	2312.98 (psia)				
	Pout	=	2825.70 (psia)	Pout	=	2280.08 (psia)				
	Delta P	=	282.08 (psi)	Delta P	=	32.92 (psi)				
	Tin	=	160.26 (deg R)	Tin	=	74.48 (deg R)				
	Tout	=	376.44 (deg R)	Tout	=	193.17 (deg R)				
	Delta T	=	486.17 (deg R)	Delta T	=	118.70 (deg R)				
	Min	=	-45.10 (BTU/lb)	Min	=	44.91 (BTU/lb)				
	Hout	=	136.01 (BTU/lb)	Hout	=	-582.28 (BTU/lb)				
	Rho in	=	71.29 (lb/ft <sup>3</sup> )	Rho in	=	4.31 (lb/ft <sup>3</sup> )				
	Rho out	=	12.67 (lb/ft <sup>3</sup> )	Rho out	=	1.93 (lb/ft <sup>3</sup> )				
	Qdot	=	8906.51 (BTU/s)	Qdot	=	497.31 (BTU/s)				
	Wdot	=	38.13 (lb/sec)	Wdot	=	1.18 (lb/sec)				
Regenerator				% bypass	=	25.00				

QTV ENGINE POWER BALANCE			Page 2
	Oxidizer	Fuel	
Regen Jacket	Pin	= 2312.99 (psia)	
	Pout	= 2114.32 (psia)	
	Delta P	= 198.67 (psi)	
	Tin	= 74.48 (deg R)	
	Tout	= 831.48 (deg R)	
	Delta T	= 757.00 (deg R)	
	Hin	= 44.91 (BTU/lb)	
	Hout	= 2880.78 (BTU/lb)	
	Rho in	= 4.31 (lb/cuft)	
	Rho out	= 0.45 (lb/cuft)	
	Wdot	= 1.59 (lb/sec)	
Baffles	Pin	= 2280.06 (psia)	
	Pout	= 2270.18 (psia)	
	Delta P	= 9.87 (psi)	
	Tin	= 185.74 (deg R)	
	Tout	= 971.74 (deg R)	
	Delta T	= 806.00 (deg R)	
	Hin	= 387.74 (BTU/lb)	
	Hout	= 3355.66 (BTU/lb)	
	Rho in	= 2.25 (lb/cuft)	
	Rho out	= 0.41 (lb/cuft)	
	Wdot	= 1.59 (lb/sec)	
Ox Nozzle Cooling	Pin	= 2928.70 (psia)	
	Pout	= 2889.95 (psia)	
	Delta P	= 38.75 (psi)	
	Tin	= 876.44 (deg R)	
	Tout	= 826.44 (deg R)	
	Delta T	= 150.00 (deg R)	
	Hin	= 136.01 (BTU/lb)	
	Hout	= 174.79 (BTU/lb)	
	Rho in	= 12.67 (lb/cuft)	
	Rho out	= 9.96 (lb/cuft)	
	Wdot	= 38.13 (lb/sec)	
Back Pressure Valve	Pin	= 2889.95 (psia)	
	Pout	= 2889.92 (psia)	
	Delta P	= 0.03 (psi)	
	T	= 826.44 (deg R)	
	H	= 174.79 (BTU/lb)	
	Rho in	= 9.96 (lb/cuft)	
	Rho out	= 9.96 (lb/cuft)	
	CdA	= ..... (in^2)	
	Pin	= 2114.32 (psia)	
	Pout	= 2114.31 (psia)	
	Delta P	= 0.00 (psi)	
	T	= 901.81 (deg R)	
	H	= 3106.75 (BTU/lb)	
	Rho in	= 0.41 (lb/cuft)	
	Rho out	= 0.41 (lb/cuft)	
	CdA	= ..... (in^2)	

QTV ENGINE POWER BALANCE

		Oxidizer		Fuel	
Turbine Conditions	Pin	= 2689.82 (psia)	Pin	= 2114.31 (psia)	
	Pout	= 1986.90 (psia)	Pout	= 1639.70 (psia)	
	Wdot	= 26.636 (lb/sec)	Wdot	= 2.778 (lb/sec)	
	Tin	= 826.44 (deg R)	Tin	= 901.61 (deg R)	
	Tout	= 757.10 (deg R)	Tout	= 851.87 (deg R)	
	Min	= 174.79 (BTU/°)	Min	= 3108.76 (BTU/°)	
	Hout	= 159.34 (BTU/°)	Hout	= 2922.88 (BTU/°)	
	Rho in	= 8.98 (g/cuft)	Rho in	= 0.41 (g/cuft)	
	Rho out	= 7.67 (g/cuft)	Rho out	= 0.34 (g/cuft)	
	Eff.	= 0.919	Eff.	= 0.787	
	HP	= 645.26 (HP)	HP	= 722.06 (HP)	
	PR	= 1.466 (Pin/Pout)	PR	= 1.266 (Pin/Pout)	
Hot Side Heat Exchanger	U/Co	= 0.486 (fps/fps)	U/Co	= 0.280 (fps/fps)	
	Wheel dia	= 2.542 (in)	Wheel dia	= 3.080 (in)	
	bypass	= 22.53	% bypass	= 12.63	
	Pin	= 1839.70 (psia)	Pin	= 1839.70 (psia)	
	Pout	= 1616.70 (psia)	Pout	= 1616.70 (psia)	
	Delta P	= 24.00 (psi)	Delta P	= 24.00 (psi)	
	Tin	= 858.80 (deg R)	Tin	= 858.80 (deg R)	
	Tout	= 24.84 (deg R)	Tout	= 24.84 (deg R)	
	Delta T	= 833.96 (deg R)	Delta T	= 833.96 (deg R)	
	Min	= 2946.09 (BTU/°)	Min	= 2946.09 (BTU/°)	
	Hout	= 96.80 (BTU/°)	Hout	= 96.80 (BTU/°)	
	Rho in	= 0.84 (g/cuft)	Rho in	= 0.84 (g/cuft)	
Gas Side Regenerator	Rho out	= 5.27 (g/cuft)	Rho out	= 5.27 (g/cuft)	
	Qdot	= -8905.51 (BTU/s)	Qdot	= -8905.51 (BTU/s)	
	Wdot	= 2.27 (g/sec)	Wdot	= 2.27 (g/sec)	
	% bypass	= 25.00	% bypass	= 25.00	
	Pin	= 1616.70 (psia)	Pin	= 1616.70 (psia)	
	Pout	= 1588.70 (psia)	Pout	= 1588.70 (psia)	
	Delta P	= 32.00 (psi)	Delta P	= 32.00 (psi)	
	Tin	= 243.17 (deg R)	Tin	= 243.17 (deg R)	
	Tout	= 201.88 (deg R)	Tout	= 201.88 (deg R)	
	Delta T	= 41.28 (deg R)	Delta T	= 41.28 (deg R)	
	Min	= 683.96 (BTU/°)	Min	= 683.96 (BTU/°)	
	Hout	= 499.81 (BTU/°)	Hout	= 499.81 (BTU/°)	
Injector	Rho in	= 1.16 (g/cuft)	Rho in	= 1.16 (g/cuft)	
	Rho out	= 1.36 (g/cuft)	Rho out	= 1.36 (g/cuft)	
	Qdot	= -467.31 (BTU/s)	Qdot	= -467.31 (BTU/s)	
	Wdot	= 3.03 (g/sec)	Wdot	= 3.03 (g/sec)	
	Pin	= 1588.70 (psia)	Pin	= 1588.70 (psia)	
	Pout	= 1552.92 (psia)	Pout	= 1552.92 (psia)	
	Tin	= 201.88 (deg R)	Tin	= 201.88 (deg R)	
	Rho in	= 1.38 (g/cuft)	Rho in	= 1.38 (g/cuft)	
	Rho out	= 1.35 (g/cuft)	Rho out	= 1.35 (g/cuft)	
	Wdot	= 3.026 (lb/sec)	Wdot	= 3.026 (lb/sec)	
	Drop	= 30.79 (psia)	Drop	= 30.79 (psia)	
	CdA	= 0.67823 (in^2)	CdA	= 0.67823 (in^2)	
Combustion Chamber	PC	= 1850.00 (psia)	MR	= 12.00 (O/F)	
	Dpec	= 2.86 (psia)	Wdot	= 36.34 (lb/sec)	
	ERE	= 1.000	Dthroat	= 2.600 (in)	
		= 1.17		= 4	

## APPENDIX C

### CHUG STABILITY OF OTV 20K LBF ADVANCED ENGINE

#### CONTENTS

- C.1 Introduction
- C.2 Technical Discussion
- C.3 References

#### TABLES

- C-1 Hot Fire Data (Ref. 1)
- C-2 Hot Fire Data (Ref. 2)

#### FIGURES

- C-1 Injection Velocity/Effect of Throttling
- C-2 Data Plot - Ox Pressure Drop
- C-3 Data Plot - Fuel Pressure Drop

## C.1 INTRODUCTION

A study was performed to assess the potential for low frequency combustion instability, commonly known as "chug" arising from deep throttling of the advanced OTV engine.

The engine parameters used in the study include, a  $\text{GH}_2/\text{GO}_2$  system with 20,000 lbf thrust, a nominal mixture ratio of 6, chamber pressure of 2000 psia and a 20:1 throttling range. The injector is composed of Premixed I-Triplet elements. Some excellent sources of stability data for hot-fire testing of this injector are given as references (1) and (2). This element type was tested over a wide range of chamber pressures and mixture ratios and was never observed to chug. The evidence from reference (2) is especially compelling.

In the OTV series, only the 7500 lbf chamber has undergone detailed geometry characterization. The injector for that chamber was derived from the previous 3000 lbf injector by simply using more of the same size elements. If one assumes that same philosophy for the 20,000 lbf injector (using more of the same size injector elements), then the injector has already been demonstrated to be chug stable by virtue of the reference (1) program. If a larger size element must be used for the increased-thrust chambers in the series, then the chug stability margin must be inferred by analytical rationale until experimentally verified. The confidence level in the analytical rationale that predicts stability is very high.

## C.2 TECHNICAL DISCUSSION

It is generally understood that the low frequency combustion instability called chugging is a coupling between the propellant feed system and the initiation of combustion. The two most important variables characterizing the process are the injection  $\Delta P/P_c$  ratio and the combustion time lag.

In a system using liquid propellants, the time lag is dependent on many factors: The injection velocity, orifice size, the type of injector element, the atomization length, and the droplet vaporization rate. The typical situation is that an injector will be chug stable at full  $P_c$ , but as the engine is throttled down the injection  $\Delta P/P_c$  decreases,

## C.2, Technical Discussion, (cont)

the injection velocity decreases, and the combustion time lag increases and thus the injector becomes chug unstable. This is why throttling is a great concern for liquid propellants.

That is not the case for a system using gaseous propellants. In that situation, the propellant  $\Delta P/P_c$  ratio and combustion time lag are only a function of mixture ratio and propellant temperature. Since the gas density and mass flow rates are both linearly proportional to  $P_c$ , the injection velocity and combustion time lags will therefore be independent of  $P_c$ . This is illustrated in Figure C-1. This shows a plot of injection velocity as a function of  $P_c$  for a hypothetical OTV-type injector for two cases: the first with the gas being treated as incompressible (dashed lines on the plot), and the second being the actual density changes (solid lines). This shows that as the engine is throttled for the case of an incompressible (liquid) propellant, the injection velocity falls off with  $P_c$ . For the actual case of compressible flow, the injection gas velocity increases slightly with decreasing  $P_c$ . This is due solely to the fact that  $C^*$  decreases by 3 percent over that range of pressures. Otherwise, the curve would have been flat.

With gaseous propellants, the combustion time lag has no component due to atomization or vaporization, but there can be a component due to mixing. With some element types that have slow mixing characteristics, such as impinging like-on-like doublets or shear coaxes, this component may be enough to cause chugging, if designed with a low  $\Delta P$ . However, the element type under consideration for OTV (the pre-mix I-triplet) is such as to bring the time lag due to mixing to an absolute minimum. The impingement of fuel and oxidizer, and hence incipient combustion actually occurs within the injector face. So the propellants are already burning when they emerge from the injector.

There exist several sources of data on low frequency stability of this type of injector element under hot-fire conditions. These are listed above as references (1) and (2). The data from reference (1) is given as Table C-1, and data from reference (2) is given as Table C-2. Of particular note in Table C-2 are the tests numbered 122 and 115. both of these have mixture ratios are slightly less than that considered for OTV (5.4 and 5.6, respectively). The difference in chamber pressure with the two tests is 106 versus

**TABLE C-1**  
**HOT-FIRE DATA (REFERENCE 1)**

Stability Data  
For Single-Element Injectors, 1973

Test No.	Chamb.	MR	Pc (psia)	<u>DelP</u>	<u>DelP</u>	Stability
				Pc ox	Pc f	
135	-3	6.01	291	.182	.208	Stable
138		7.63	258	.181	.194	Stable
139		2.05	325	.410	.581	Stable
140		3.97	522	.227	.291	Stable
141		4.02	103	.217	.278	Stable
143		0.99	302	.707	1.159	Stable
144	-2	3.93	303	.226	.291	Stable
145		2.03	304	.438	.625	Stable
146		6.01	291	.166	.191	Stable
147		4.12	98	.221	.279	Stable
148	-1	3.94	317	.221	.283	Stable
149		2.06	329	.398	.569	Stable
150		3.90	524	.218	.283	Stable
151		5.99	290	.176	.203	Stable
152		4.14	103	.213	.270	Stable
153	-3	6.08	91	.185	.208	Stable
154		1.96	105	.420	.600	Stable

**TABLE C-2**  
**HOT-FIRE DATA (REFERENCE 2)**

Test No.	Date	Pc (psia)	POJ (psia)	PFJ (psia)	POJ-Pc (%)	PFJ-Pc (%)	MR	Ispvac (sec) c = 4.0	Dur (sec)	C* (ft/sec)
121	6/28/85	85	100	98	16	16	3.9	359	1.2	7,186
122	6/28/85	106	123	117	16	10	5.4	346	4.0	7,082
123	6/28/85	105	124	112	18	7	7.7	336	4.0	6,573
124	6/28/85	99	117	107	18	8	7.6	356	4.0	6,626
125	7/10/85	184	209	210	14	14	4.0	335	2.2	7,316
126	7/10/85	187	212	203	13	9	5.7	334	2.4	7,068
127	7/10/85	187	216	199	16	6	7.6	326	4.4	6,807
128	7/10/85	180	213	190	18	6	9.2	312	4.2	6,378
129	7/10/85	181	211	230	17	27	3.0	281	1.1	5,716
130	7/11/85	359	403	406	12	13	4.1	340	2.1	7,327
131	7/11/85	271	305	300	13	11	4.7	349	2.8	7,450
133	7/11/85	287	325	309	13	8	6.1	346	4.0	7,338
134	7/11/85	287	329	303	15	6	7.8	328	4.4	6,893
135	7/11/85	316	355	353	12	12	4.3	349	2.5	7,414

Key:

Pc Chamber Pressure  
 POJ Pressure Ox. Manifold  
 PFJ Injector  
 POJ-Pc Pressure Fuel Manifold  
 PFJ-Pc Injector  
 MR % Pressure Drop  
 Isp Oxygen Circuit  
 Dur % Pressure Drop  
 C\* Fuel Circuit  
 Mixture Ratio (O/F)  
 Specific Impulse  
 Test Duration  
 Characteristic  
 Exhaust Velocity

**TABLE C-2 (CONT.)**

Test No. 2459-120-A6-	F <sub>vac</sub> (lbs)	isp <sub>vac</sub> Meas (sec)	C+1 Meas (ft/sec)	Pc (psia)	MR	Dur (sec)	POJ (psia)	PFJ (psia)	$\frac{\Delta POJ-Pc}{Pc} \%$	$\frac{PFJ-Pc}{Pc} \%$	$\dot{w}_t$ lb/sec	Heat Flux Average Btu/in <sup>2</sup> -sec
140	227	362	7537	197	4.1	5.0	218	215	10	9	.6275	2.00
144	442	365	7707	390	4.4	4.6	427	419	9	7	1.2113	2.88
145	449	368	7656	391	5.84	5.0	430	408	10	5	1.2219	3.56
146	452	327	6802	393	8.3 <sup>2</sup>	5.0	440	404	12	3 <sup>3</sup>	1.3837	3.34
147	584	356	7552	517	6.16	4.5	568	540	10	5	1.6391	3.82
149	681	361	7864	620	4.13	3.2	676	673	9	9	1.8877	3.79
150	640	338	7488	588	5.23	2.6	642	625	9	6	1.8812	3.69
151	667	334	7214	601	6.51	2.6	659	628	10	5	1.9955	3.55
154	589	339	7314	530	7.49 <sup>2</sup>	3.5	584	548	10	3 <sup>3</sup>	1.7365	3.90
155	571	363	8005	526	5.4	4.2	572	553	9	5	1.5740	3.31

1 Not corrected for thermal effects.  
2 Fuel venturi possibly not sonic, questionable if and MR.  
3 Low  $\Delta P$  through injector fuel circuit due to cooling hole modifications  
larger  $C_dA \rightarrow$  smaller  $\Delta P$ .

Key:

F	Thrust
isp	Specific Impulse
C*	Characteristic
	Exhaust Velocity
Pc	Chamber Pressure
MR	Mixture Ratio (O/F)
Dur	Test Duration
POJ	Pressure Ox
	Manifold Injector
PFJ	Pressure Fuel
	Manifold Injector
$\frac{POJ-Pc}{Pc}$	% Pressure Drop
$\frac{PFJ-Pc}{Pc}$	Injector Ox Circuit
$\frac{PFJ-Pc}{Pc}$	% Pressure Drop
$\dot{w}_t$	Injector Fuel Circuit
	Total Flow Rate

TABLE C-2 (CONT.)

QTV 3X ICA  
COOLED THROAT  
HOT FIRE TEST SUMMARY

TEST NO.	POVI (psia)	POJ (psia)	TOVI (F)	PFVI (psia)	PFJ (psia)	TFVI (F)	INJECTION (lb/sec)	F WAC (lb)	PC (psia)	W <sub>o</sub> (lb/s)	U <sub>f</sub> (lb/s)	MR	INJ Cal-m (lb/sec)	Cal-m (lb/sec)	PFJ-Pc (Pc)	ISP (WAC)	CSIM (WAC)
108	1624	1150	101	1931	1134	91	1.40	1239	1046	2.437	0.379	4.6	0.1548	0.1595	9.912	8.412	305
109	1534	1129	102	2148	1135	83	1.40	1201	1018	2.406	0.417	3.8	0.1482	0.1505	10.902	11.498	304
110	1739	1174	95	1654	1128	88	1.40	1305	1054	2.642	0.497	5.8	0.1640	0.1662	11.172	6.822	309
111	820	576	97	1023	371	96	1.80	620	513	1.321	0.306	4.3	0.1539	0.1558	12.202	11.512	301
113	3225	2126	126	3745	2993	71	1.10	2263	1969	5.076	1.110	4.6	0.1744	0.1839	6.392	5.232	346
114	3655	2118	127	4183	2134	59	1.00	2444	1966	6.079	1.255	3.9	0.1616	0.1701	7.732	8.553	402
115	3403	2275	115	3329	2190	61	1.13	2464	2104	5.589	1.005	5.6	0.1751	0.1840	8.131	4.092	374

COOLANT CIRCUIT

TEST NO.	PLMRT (psia)	PLMFBI (psia)	TFM (F)	PCFI (psia)	TCFI (F)	PCFO (psia)	FILM (lb/sec)	DESIGNITY (lb/sec)	ICFB (F)	MLJ2 (lb/s)	MLJ2 desired (lb/s)	THROAT DEL P (psi)	THROAT DEL T (lb/s)	ENTHALPY IN (Btu/lb)	ENTHALPY OUT (Btu/lb)	HEAT LOAD (W/sec)
108	2771	2049	-345	1701	-324	1453	5.900	2.250	-54	0.337	0.481	240	270	253	1321	513
109	3275	3311	-355	1954	-375	1682	6.206	2.490	-85	0.390	0.537	274	290	246	1201	513
110	2408	2522	-342	1594	-314	1356	5.676	1.900	16	0.302	0.413	238	130	291	1504	533
111	1621	1450	-319	740	-276	610	5.057	0.760	-34	0.155	0.254	130	240	500	1305	275
113	4735	4651	-350	2550	-323	2168	7.100	2.890	-78	0.505	0.921	302	253	253	1232	912
114	4910	4026	-331	2381	-304	2018	7.336	2.450	-81	0.478	1.042	343	223	372	1220	915
115	4132	4181	-365	2662	-340	2200	7.020	3.330	-47	0.502	0.834	302	293	195	1355	948

Key:

Injector	-	Area Discharge	POVI	-	Pressure Ox. Venturi Inlet	PLMRT	-	LH <sub>2</sub> Run Tank Pressure
Cal-Ox	-	Coefficient Ox Inlet	POJ	-	Pressure Ox Manifold Injector	PLMFBI	-	LH <sub>2</sub> Flowmeter Inlet Pressure
Injector	-	Fuel Area Discharge	TOVI	-	Temp. Ox Venturi Inlet	TFM	-	Temp. Flowmeter Pressure
Cal-Fuel	-	Coefficient Fuel Inlet	PFVI	-	Pressure Fuel Venturi Inlet	PCTI	-	Pressure Cooled Throat Inlet
POJ-Pc	-	% Pressure Drop Oxidizer Circuit	PFJ	-	Pressure Fuel Manifold Injector	PCTO	-	Pressure Cooled Throat Outlet
PFJ-Pc	-	% Pressure Drop Fuel Circuit	TFVI	-	Temp. Fuel Venturi Inlet	TCTI	-	Temp. Cooled Throat Inlet
isp	-	Specific Impulse	F	-	Thrust	FMLH	-	Flowmeter Liquid Hydrogen
C*	-	Characteristic Exhaust Velocity	Pc	-	Chamber Pressure	TCTO	-	Temp. Cooled Throat Outlet
			W <sub>o</sub>	-	Ox Flowrate	WLMH <sub>2</sub>	-	Flowrate Liquid Hydrogen
			W <sub>f</sub>	-	Fuel Flowrate			
			MR	-	Mixture Ratio (O/F)			

## C.2, Technical Discussion, (cont)

2104 psia, respectively. This ratio corresponds to the 20:1 throttling range that is desired in the full-size hardware.

The normalized pressure drop ( $\Delta P/P_c$ ) is shown in Figures C-2 and C-3 for both the fuel and oxidizer circuits. The design  $\Delta P/P_c$  for the 7500 lbf OTV engine was 5% for the fuel and 9% for the oxidizer. This is well within the ranges shown from prior tests. As long as the detailed design for a 20,000 lbf chamber stays within this range of pressure drops, it should be stable.

## C.3 REFERENCES

1. "Investigation of Gaseous Propellant Combustion and Associated Injector/Chamber Design Guidelines", Contract No. NAS 3-14379, NASA-CR-121234, 31 July 1973.
2. "Orbital Transfer Vehicle 3000 lbf Thrust Chamber Assembly Hot-Fire Test Program", Interim Report, Contract No. NAS 3-23772-C.2.

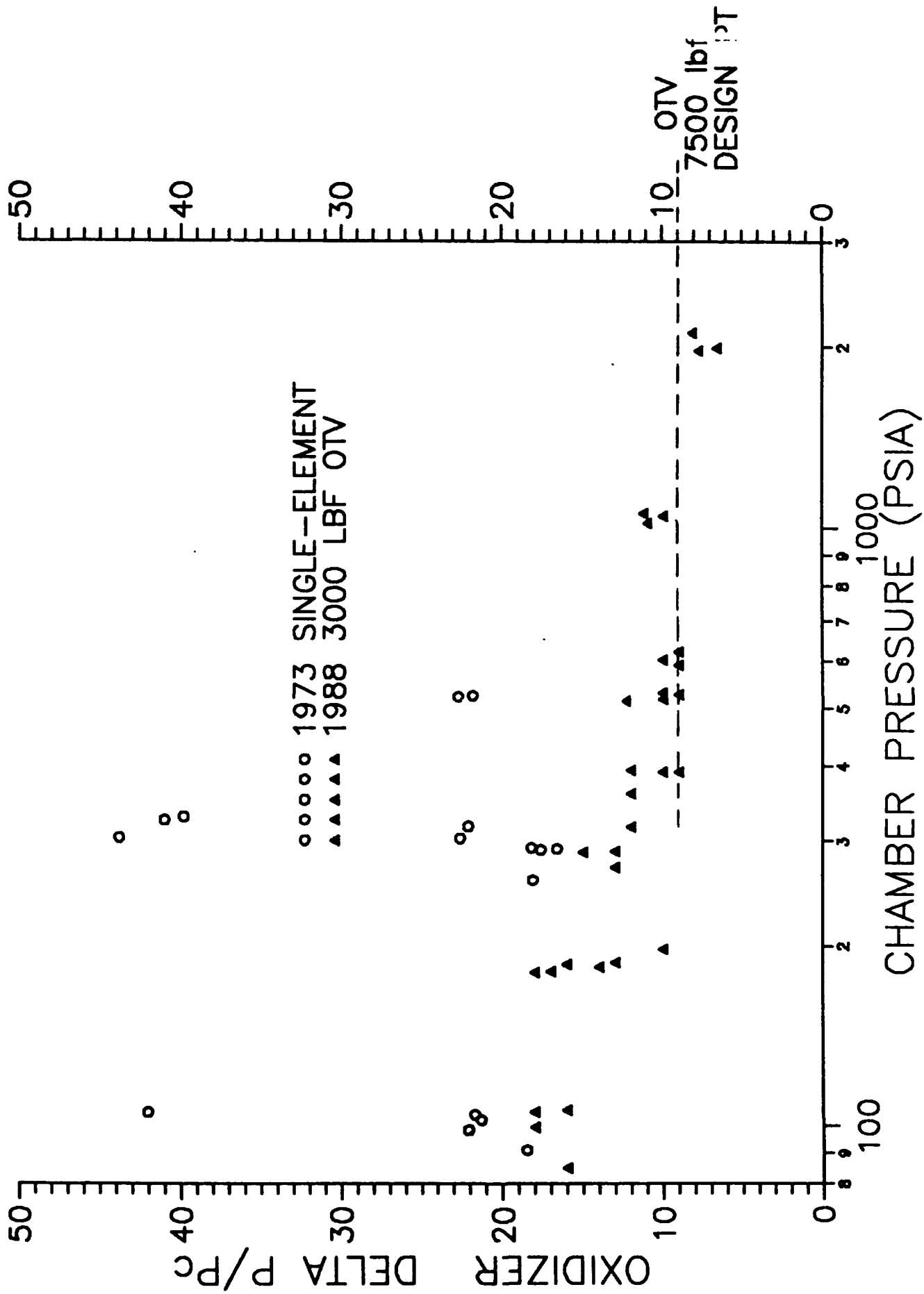


Figure C-2. Oxidizer Pressure Drop

